Final Program & Digest

2017 KSIC Autumn International Conference In Changwon City

November 30(Thusday) ~ December 1(Friday), 2017
CECO, Changwon, Korea

Supported by

Province of GyeongSangnam-do
Changwon City

Organized by

Korean Society of Industry Convergence (KISC)

Technically Co-sponsored by

The Korean Society of Industy Convergence (KSIC)
Institute of Control, Robotics and Systems (ICROS)
The Korean Society of Manufacturing Technology Engineers (KSMTE)
Korea Association of Robot Industry (KAR)
Gyeongnam Robot Industry Associaition (GRIA)
Gyeongnam Robot Land Foundation (GRF)
Artificial Life and Robotics (AROB)
Gyeongnam Convention & Visitors Bureau (GNCVB)

I. Welcome Messages

■□ Invitation Text □■

Sung-Hyun Han, Ph.D
General Chair of CICIRO 2017

Dear distinguished scholars, ladies and gentlemen, I feel very honored and privileged to welcome all the participants to Changwon city, Korea, for the 2017 international Conference on intelligent robot and convergence industry(CICIRO 2017). As the General Chair of the conference, I an very happy and honored to open the CICIRO2017 here in Changwon.

The CICIRO 2017 will bring together academicians and professionals from around the world to exchange ideas, discuss novel findings and new methods, reacquaint with colleagues, and broaden their knowledge. This conference covers a wide range of fields from robotics and intelligent control technology to convergence industry. Especially, many research papers on artificial intelligence, advanced mechatronics, smart factories, as well as technical fields such as intelligent robots, IT and NT, which are the core fields of the fourth industrial revolution, are presented in the 2017 Changwon International Intelligent Robotics Conference. This will greatly contribute to the establishment of policies to foster the nation's future new growth engine industry and local specialized industries.

It is our great honor to have world-class scholars as plenary and Invited lectures in CICIRO 2017. They are Prof. Balan Pillai(Helsingki Univ. Filand), Prof. Sung-Wan Kim(Seoul Nat'i Univ. Korea), Prof. Fumitoshi Matsuno(Kyoto Univ., Japan), Prof. Guoying Gu(Shanghai Jiao Univ., China), Prof. Ih-huck Song(Texas state Univ.,U.S.A) and Prof. Nguyen Chi hung(Hanoi Univ.,Vietnam). They will share their new theoretical results and thoughts on the fields of intelligent robotics, and convergence industry technology.

In addition, the 2017 International Intelligent Robotics Conference will provide a more efficient international industry-university cooperation network, and play a pivotal role in the development of the future new industry through international technology information exchange for advanced convergence industry.

Finally, I hope all of you who have visited the 2017 International Intelligent Robotics Conference will have good and rewarding time with the presentation of academic papers in Changwon. We sincerely hope that all the participants benefit from and have a fruitful time at CICIRO 2017 in Changwon city Korea.

Thank you very much.

■□ Welcoming Address □■

Welcome to the 2017 Changwon International Conference on Intelligent Robot and Convergence Industry (CICIRO). It is no coincidence that this conference is being held here, in the city of Changwon, the cradle of Korea's largest high-tech manufacturing industry. I warmly welcome all the specialists in the field, and leaders of industry, who have come from around the country and around the world to attend this event.

As you all know, we are on the brink of a Fourth Industrial Revolution. Its scope and complexity are all-embracing. This revolution is disruptive, transformative, and moving at immeasurable speed. It is pushing us all to innovate. The challenges and possibilities this revolution brings are immense. In response, global competition and collaboration are intensifying, with an undeniable trend toward development of advanced IT convergence technology.

In this light, this international conference seeks to provide vision and direction for new growth engines by introducing and discussing new technologies that can create new demand in robotics, convergence technologies, and high-tech manufacturing industries. This conference also seeks to promote more efficient network of international industry-university cooperation, as well as play a pivotal role in the development of future industries through international information exchange for the advancement of advanced manufacturing technology.

During this two-day event we will hear from many experts who will enlighten us on what is happening in the fields of artificial intelligence, advanced machines, mechatronics, and smart factories. Some will share their research on intelligent robots, IT, and network technology. These areas are all core to and drivers of the Fourth Industrial Revolution. We hope their contributions to this conference can assist in the establishment of policies that help foster new growth engines and local specialized industries.

Over these two days we have much to look forward to. And so, I hope you find your participation at CICIRO 2017, and your time in Changwon City, a rewarding and enjoyable experience.

The best to you all!

Thank you.

Park, Jae Kyu, Ph.D.
President, Kyungnam University

II. Conference Organization

A. Organizing Committee

General Chair :	Sung-Hyun Han, Kyungnam Univ., Korea
General Co-Chairs :	Ju-Jang Lee, KAIST,Korea Fumitoshi Matsuno, Kyoto Univ., Japan Sung-Wan Kim, Seoul Nat'l Univ., Korea J.M. Lee, Pusan Nat'l Univ., Korea
Organizing Co-Chairs :	In-Hyeok Song, Texas State Univ., USA Guoying Gu, Shanghai Jiao Tong Univ., China Young-Hoon Park, ADD, Korea Hee-Hyeol Lee, Waseda Univ., Japan Balan Pillai, Helsingki Univ., Finland Nguyen Chi Hung, Hanoi Univ., Vietnam
Program Co-Chairs :	Kang-Hyun Jo, Ulsan Univ., Korea Min-Cheol Lee, Pusan Nat'l Univ., Korea Kyung-Soo Kim, KAIST, Korea Jae-Sil Kim, Changwon Nat'l Univ. Korea Soo-hee Han, Postech, Korea Young-Im Cho, Gachon Univ., Korea
Regional Organizing Co-Chair :	Young-Jin Moon, Asan Hospital, Korea Kang-bak Park, Korea Univ., Korea Han-Sung Kim, Kyungnam Univ., Korea Kyung-Chang Lee, Pukyong Nat'l Univ., Korea Ho Lee, Kyungbuk Nat'l Univ., Korea
Regional Program Co-chair :	Jang-sik Park, Kyungsung Univ., Korea Won-gu Lee, Kyunghee Univ., Korea Sung-jun Park, chonnam Nat'l Univ., Korea Dang Bao Lam, Hanoi Univ., Vietnam Seok-Jo Go, Dongeui Institute of Technology, Korea
Publicity Chair :	Ha-Young Kim, Pusan National Univ., Korea Yang-Keun Jung, Shinla tech Co., Ltd., Korea
Finance Chair :	Young-Hwa Jeong, Daeho Tec., Korea Kyu-Hyun Jung, SEYOUNG INDUSTRY Co., Ltd.,Korea
General secretary :	Chul-Kyu Jin, kyungnam Univ., Korea

B. International Organizing Committee

Man Hyung Lee, Pusan National Univ., Korea
Hussein Abbass, Univ. of New South Wales, Australia
Hajime Asema, Tokyo Univ., Japan
Hideki Hashimoto, Chuo Univ., Japan
Mark A. Bedau, Reed College, United States
Malachy Eaton, Univ. of Limerick, Ireland
Joshua M. Epstein, The Johns Hopkins Univ., United States
Takayasu Fuchida, Kagoshima Univ., Japan
Adam Grzech, Wroclaw Univ. of Technology, Poland Maki K. Habib, The American Univ. in Cairo, Egypt
Yoshiteru Ishida, Toyohashi Univ. of Technology, Japan
David John Glyndwyr James, Coventry Univ., United Kingdom
Takashi Kohno, The Univ. of Tokyo, Japan
Man Hyung Lee, Pusan National Univ., Korea
Kenneth James Mackin, Tokyo Univ. of Information Sciences, Japan
Fumitoshi Matsuno, Kyoto Univ., Japan
Kaoru Mogushi, Juntendo Univ., Japan
Fusaomi Nagata, Tokyo Univ. of Science, Yamaguchi, Japan
Ken Naitoh, Waseda Univ., Japan
Masatoshi Nakamura, Research Institute of Systems Control, Japan Kazushi Nakano, The Univ. of Electro-Communications, Japan
Masanori Nishibori, International Univ. of Health and Welfare, Japan Nobuhiro Okada, The Univ. of Kitakyushu, Japan
Chintae Choi, RIST, Korea
Hyeungsik Choi, Korea Maritime Univ., Korea
Jae Weon Choi, Pusan Nat'l Univ., Korea
Kwan-ho Chun, Chungnam Univ., Korea
Carl Crane, Univ. of Florida, USA
Baocang Ding, Jiaotong Univ., China
Junping Du, Beijing Univ. of Sci. and Tech., China
Guangren Duan, Harbin Inst. of Tech., China
Yongsoon Eun, DGIST, Korea
Antonio Franchi, LAAS-CNRS, France
Anna Friesel, Technical Univ. of Denmark, Denmark
Li-Chen Fu, Nat'l Taiwan Univ., Taiwan
Toshio Fukuda, Nagoya Univ., Japan
Furong Gao, Hong Kong Univ. of Sci. and Tech., Hong Kong
Luis Gomes, Univ. Nova Lisbon, Portugal
Jerzy Świątek, Wroclaw Univ. of Technology, Poland
Yuichiro Taira, Sojo Univ., Japan
Charles E. Taylor, Univ. of California-Los Angeles, United States
Marion Oswald, Vienna Univ. of Technology, Austria
Steen Rasmussen, Univ. of Southern Denmark, Denmark
Thomas S. Ray, Univ. of Oklahoma, United States
Shinichi Sagara, Kyushu Institute of Technology, Japan
Katsunori Shimohara, Doshisha Univ., Japan
Hideyuki Suzuki, The Univ. of Tokyo, Japan
Reiji Suzuki, Nagoya Univ., Japan
Jian Chen, City Univ. of Hong Kong, Hong Kong
Kwang-Hyun Cho, KAIST, Korea
Kyoungrae Cho, Dong Seoul College, Korea
Toshio Tsuji, Hiroshima Univ., Japan
Masafumi Uchida, The Univ. of Electro-Communications, Japan
Fumio Uchikoba, Nihon Univ., Japan Shinjiro Umezu, Waseda Univ., Japan
Keigo Kunihito Yamamori, Univ. of Miyazaki, Japan
Kazuko Yamasaki, Tokyo Univ. of Information Sciences, Japan
Masao Yokota, Fukuoka Institute of Technology, Japan
Changshui Zhang, Tsinghua Univ., China
Kyung-Seok Byun, Mokpo Nat'l Univ., Korea

C. International Program Committee

Shyi-Ming Chen, National Taiwan Univ. of Science and Technology, Taiwan
Kazuyuki Aihara, The Univ. of Tokyo, Japan
Hiroshi Kinjo, Univ. of the Ryukyus, Japan
Kentarou Kurashige, Muroran Institute Technology, Japan
Yong Liu, Univ. of Aizu, Japan
Tomoharu Nakashima, Osaka Prefecture Univ., Japan
Trung Dung Ngo, Univ. of Prince Edward Island, Canada
Walter Nistico, Univ. of Dortmund, Germany
Harutoshi Ogai, Waseda Univ., Japan
Yangmin Li, Univ. of Macau, China
Der-Cherng Liaw, Nat'l Chiao Tung Univ., Taiwan
Myo Taeg Lim, Korea Univ., Korea
Fei Liu, Jiangnan Univ., China
Tao Liu, Dalian Univ. of Tech., China
Stefano Longo, Cranfield Univ., United Kingdom
Eric T. Matson, Purdue Univ., USA
Yoshifumi Morita, Nagoya Inst. of Tech., Japan
Shigeru Omatu, Osaka Institute of Technology, Japan Luigi Pagliarini, Technical Univ. of Denmark, Denmark
Rolf Pfeifer, Univ. of Zurich-Irchel, Switzerland
Mohd Rizon, Univ. of Malaysia Perlis, Malaysia
Peter S. Sapaty, National Academy of Sciences of Ukraine, Ukraine
Jeong Yon Sim, Kangnam Univ., Korea
Ken Sugawara, Tohoku Gakuin Univ., Japan
Mikhail Svinin, Kyushu Univ., Japan
Ivan Tanev, Doshisha Univ., Japan
Hiroshi Umeo, Osaka Electro-Communication Univ., Japan
Katsuji Uosaki, Fukui Univ. of Technology, Japan
Mutsumi Watanabe, Kagoshima Univ., Japan
Hidekazu Yanagimoto, Osaka Prefecture Univ., Japan
Ikuo Yoshihara, Univ. of Miyazaki, Japan
Yong Yu, Kagoshima Univ., Japan
Tao Zhang, Tsinghua Univ., China
Jordi Albo, La Salle – Ramon Llull Univ., Spain
Takaya Arita, Nagoya Univ., Japan
Nikos Aspragathos, Univ. of Patras, Greece
Juhoon Back, Kwangwoon Univ., Korea
Hyochoong Bang, KAIST, Korea
Young-bong Bang, Seoul Nat'l Univ., Korea
Pinhas Ben-Tzvi, George Washington Univ., USA
Young Jae Lee, Konkuk Univ., Korea
Donghai Li, Tsinghua Univ., China
Hongbo Li , Tsinghua Univ., China
Hyun Myung, KAIST, Korea
Nobuaki Nakazawa, Gunma Univ., Japan
Quang Hieu Ngo, Can Tho Univ., Vietnam
Quoc Chi Nguyen, Ho Chi Minh City Univ. of Tech., Vietnam
Yoshimasa Ochi, Nat'l Defense Academy, Japan
Yasuaki Ohataki, Kanagawa Inst. of Tech., Japan
Hyung-Soon Park, KAIST, Korea
Jaehyun Park, Inha Univ., Korea
Jong Hyeon Park, Hanyang Univ., Korea
Young Im Cho, The Univ. of Suwon, Korea
Mo-Yuen Chow, North Carolina State Univ., United States Yueyue Fan, Univ. of California-Davis, United States
Rintaro Haraguchi, Mitsubishi Electric Corporation, Advanced Technology R&D Center, Japan
Noriyasu Homma, Tohoku Univ., Japan
Dong Hyuk Cha, Korea Polytechnic Univ., Korea
Chwan Hsen Chen, Yuan Ze Univ., Taiwan

III. Local Information

A. Host Province, GyeongSangnam-do

The Best Investment location

Realize your dream in Gyeongsangnam-do where the perfect infrastructure awaits you!

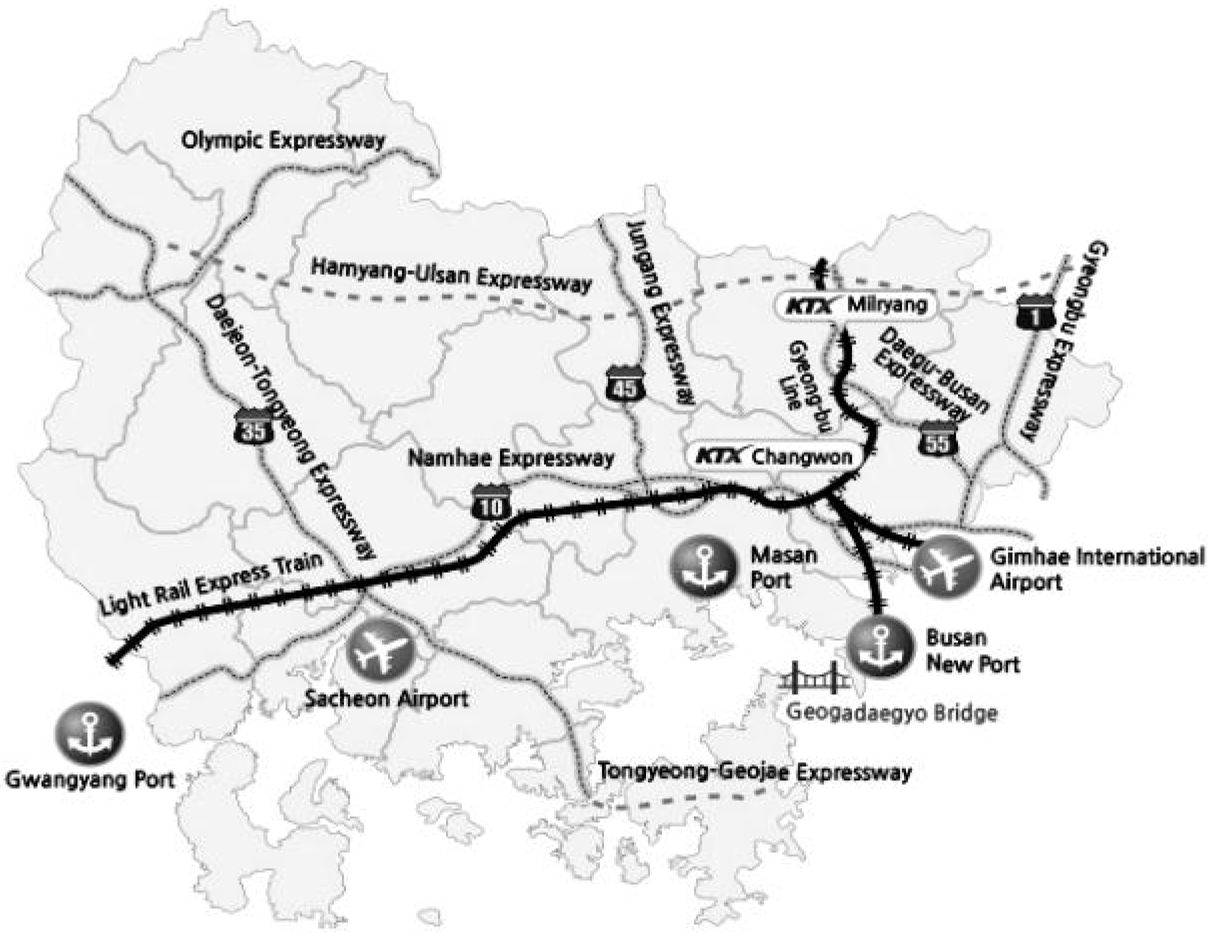

Airport
Gimhae International Airport and Sacheon Airport

Port
International ports (Busan Port, Gwangyang Port, and Masan Port)

Traffic Network
7 stations in expressway and 2 stations in KTX (Korea Train eXpress)

Industrial Complex
4,874 companies residing in 7 national industrial complexes and 158 General industrial complexes

Economic Zone
2 Free Economic Zones, 2 Foreign Investment Zones, and 1 Free Trade Zone

○ Gyeongnam

As of December 2012

Population	3.334 million (As of December 2013) ※ Number of foreigners registered: 69,126
Area	10,535㎢ (10.5% of Republic of Korea)
GRDP (Gross Regional Domestic Product)	KRW 95 trillion and 634.5 billion (the 3rd highest GRDP among all provinces of the Republic of Korea)
GRDP per capital	USD 26,134 (the 6th highest rate among all provinces of the Republic of Korea)
Economically active population	1.653 million (6.4% of entire economically active population in the Republic of Korea)
Total Enterprises / Number of Employees	242,123 Enterprises / 1,250,462 Employees
Trade Balance	Export: USD 51.9 billion (9.3% of entire export of the Republic of Korea) Import: USD 28.5 billion (5.5% of the entire import of the Republic of Korea)
Foreign-Invested Company	200 Companies Number of Employees: 28,762 / Production: USD 34,991 million Export: 20,724 million

B. Host City, Changwon City

Tourism environment

A multitude of transportation modes

City Tour Bus

The City Tour Bus takes the tourists to major attractions of the city on circular courses and 12 selective courses. Throughout the courses, all of the city tour buses will be accompanied by a guide to provide stories about major tourist spots

Nubija Bikes

Changwon, an active advocate of eco-friendly transportation, has introduced the bike lending program to promote the use of bikes. Tourists can get a one-day pass to use Nubija bikes.

Coastal Cruise

The Coastal Cruise departs from Masan Port Cruise Terminal (Pier 2) and sails to Dotseom Islet, Machang Bridge, Makgaedo Island, Namdo Island, Modo Island and back to Machang Bridge, providing panoramic sea views along the voyage

TRANSPORTATION

C. Changwon Exhibition Convention Center(CECO)

1. Superior Industrial Infrastructure

- The production base for global companies in high value-added industries including machinery, heavy industry, shipbuilding, aerospace, and robotics
- Arrangement for technical tour programs to companies that are relevant to conventions

2. EcoCity & Fantastic Tourist Resources

- Successfully holding prestigious environment conventions, RAMSAR COP 10
- A scenic and natural location
- UNESCO World Cultural Heritage(The Tripitaka Koreana)

3. Convention All-Inclusive Service

- State-of-the-art convention facilities
- Convention multi-functional complex (Hotel, Shopping&Entertainment facilities)
- Customizable menu and global level of service

4. Solid and Professional Support

- Thorough support from beginning to end
- Experienced professionals
- Arranging systematic financial support program with Gyeongnam Convention Bureau

5. Easy Access & Various Accommodations

- 30 minutes(by car) from Gimhae Int'l Airport
- Regular operation of KTX, high speed train, between Seoul and Changwon
- More than 10,000 rooms from luxurious hotels within 30 minutes from CECO

D. Transportation

1. Air Transportation

Incheon Int'l Airport → Kimhae(Busan) Airport (50min.) Kimhae(Busan) Airport → CECO (30~40 min.)	There are about 5 flights per day.
Kimpo Int'l Airport → Kimhae(Busan) Airport (50min.) Kimhae(Busan) Airport → CECO (30~40 min.)	There are about 30 flights per day with 1 hour intervals.

Incheon Int'l Airport	http://www.airport.kr/eng/
Kimpo Int'l Airport	http://www.airport.co.kr/mbs/gimpoeng/
Kimhae Int'l Airport	http://www.airport.co.kr/mbs/gimhaeeng/

2. Train(KTX : High Speed Train)

Seoul → Changwon : 2 Hours 50 Minutes
Station : Chanwon, Changwon Central, Masan(Within 15 Minutes from CECO)

KORAIL website	http://www.letskorail.com/ebizbf/EbizBfIndex_eng.do

3. Express Bus

Seoul(Gangnam Express Terminal or East Seoul Bus Terminal) → Changwon(5 hr)
Busan → Changwon(45 min.~1 hr)
(20 minute intervals from Sasang, Haeundae terminals)

IV. Program Schedule & Session Timetable

A. Program Schedule

☐ NOVEMBER 30th[THU.], 2017

<table>
<tr><td>13:00 ~ 14:00</td><td colspan="3">Registration</td></tr>
<tr><td>14:00 ~ 14:30</td><td colspan="3">Opening Ceremony</td></tr>
<tr><td rowspan="2">14:30 ~ 15:20</td><td>< Room 302 ></td><td colspan="2">< Room 301 ></td></tr>
<tr><td>Keynote Speech
Prof. BALAN PILLAI
Helsingki University, Finland</td><td colspan="2">Oral Session (I)</td></tr>
<tr><td rowspan="2">15:20 ~ 16:10</td><td>< Room 302 ></td><td colspan="2">< Room 301 ></td></tr>
<tr><td>Invited Lecture (T-I)
Prof. Ju-Jang Lee
KAIST, Korea</td><td colspan="2">Oral Session (II)</td></tr>
<tr><td>16:10 ~ 16:30</td><td colspan="3">Coffee Break Time</td></tr>
<tr><td rowspan="2">16:30 ~ 17:20</td><td>< Room 302 ></td><td colspan="2">< Room 301 ></td></tr>
<tr><td>Invited Lecture(T-II)
Prof. Han-Sung Kim
Kyungnam University, Korea</td><td colspan="2">Oral Session (III)</td></tr>
<tr><td rowspan="2">17:20 ~ 18:00</td><td>< Room 302 ></td><td colspan="2">< Room 301 ></td></tr>
<tr><td>Young Outstanding Reseacher
Prof. Moon-Hee Lee
Dong-Eui Institute of Technology, Korea</td><td>Poster Session (I)</td><td>Poster Session (II)</td></tr>
<tr><td>18:00 ~ 20:00</td><td colspan="3">Welcome Reception</td></tr>
</table>

□ DECEMBER 1st(FRI.), 2017

Time	Room 302	Room 301	Room 600A
9:00 ~ 9:50	Preparation and Registration		
9:50 ~ 10:30	< Room 302 > Invited Lecture(F-I) Prof. DANG BAO LAM Hanoi univ. of Science and Technology, Vietnam	< Room 301 > Invited Lecture(F-II) Prof. Kang-Hyun Jo University of Ulsan, Korea	
10:30 ~ 11:10	< Room 302 > Invited Lecture(F-III) Prof. Jang-Myung Lee Pusan National Univ., Korea	< Room 301 > Invited Lecture(F-IV) Prof. Young Jin Moon Asan Medical Center, Korea	
11:10 ~ 11:50	< Room 302 > Invited Lecture(F-V) Prof. Soo-Hee Han Pohang Univ. of Science and Technology, Korea	< Room 301 > Oral Session (I)	< Room 600A > Oral Session (II)
11:50 ~ 13:20	Lunch Time		
13:20 ~ 13:30	Opening Ceremony & Plenary Lecture		
13:30 ~ 14:10	< Room 302 > Plenary Lecture(F-I) Prof. Sung-Wan Kim Seoul National Univ., Korea	< Room 301 > Oral Session (III) / Oral Session (IV)	< Room 600A > Oral Session (V) / Oral Session (VI)
14:10 ~ 14:50	< Room 302 > Plenary Lecture(F-II) Prof. Fumitoshi Matsuno Kyoto Univ., Japan		
15:00 ~ 15:40	< Room 302 > Plenary Lecture(F-III) Prof. Guoying Gu Shanghai Jiao Tong Univ., China	< Room 301 > Poster Session (I) / Poster Session (II) / Poster Session (III)	
15:40 ~ 16:20	< Room 302 > Plenary Lecture(F-IV) Prof. In-Hyouk Song Texas State Univ.. USA	< Room 301 > Poster Session (IV) / Poster Session (V) / Poster Session (VI)	
16:20 ~ 17:00	< Room 302 > Invite Lecture(F-VI) Prof. Young-Im Cho Gachon University, Korea	< Room 301 > Poster Session (VII) / Poster Session (VIII) / Poster Session (IX)	
17:00 ~ 18:30	< Intelligent Robot Forum > Topic : Fourth Industrial Revoution and Intelligent Robot (Prof. Sung-Hyun Han) <Pannel Discussion> Pannel: Prof. Balan Pillai, Prof. Ju-Jang Lee, Prof. Dang Bao Lam, Prof. Jang-Myung Lee, Prof. Soo-Hee Han, Prof. Fumitoshi Matsuno, Prof. Guoying Gu, Prof. In-Hyouk Song, Prof. Sung-Hyun Han, Prof. Young-Im Cho, Prof. Young Jin Moon		
18:30 ~ 20:30	Banquit		

V. Keynote Speech

A. Keynote Speech I

November 30(THU) 14:30 ~ 15:20 **[Chair : Ju-Jang Lee]**

Professor BALAN PILLAI

Affiliation: Helsingki University, Finland

Title : ALGORITHM BASED SEMANTIC SYSTEM SET-UP FOR INTERNET

Abstract : The technological change can definitely put up an impact quickly; it always happens incrementally. The Uber and its concept - disrupted the taxi business overnight; though it wasn't likely before the Internet, high-speed mobile communications, Cloud computing, Big Data, distributed Storage and advanced Data Analytics enabled its platform. KPMG is investing a lot in cognitive technologies; counting IBM Watson to supercharge the audit capabilities. Are these all idiosyncrasies - not really! In the millennium, the telecommunications industry; is abuzz with megabits per minutes, gigabits, terabits and so. Those working in the forefront of the technologies involved; are getting used to the power of exponents, as major advances are happening in silicon, routing, switching, radio frequencies, and fiber optics.

Identified that the payer needs to know, no matter what has done at the Internet as communication to the public? The outcome of this spending on the Internet, at all, has to be massively sighted, smartly analyzed, synchronized, and evaluated. It should also cleverly rout with pragmatic impacts? This paper thereby process and address as to how that works seamlessly. There are several of them every second on the Net. An analyzing method is formed and called as Web Analytic. This tool is not any more new or narrative. However, this paper would show here; a new form of identification and interpretation in using the Semantic Infrastructure attached to it with Lambda Computer Modeling, then it becomes as novel diffusion. Most of the Web Analytic is associated with the Big Data players in the field, such as IBM, Google, Microsoft and few others. We may not go into details here. There are plenty of spaces to play a story rule. A genius process we have created as a novel proposition.

The doctrine is a thread to exigency. What is discussed here is bit dissimilar. Present concept is put under a patent-pending form. Fundamentally, a drive propels the system at the net in a flow-pattern. This is an all inclusive grid platform. The system would run from here yet again back-and-forth securely and between the systems-to-systems at the clouds.

Keywords : Idiosyncrasy, web analytic, grid platform, security, system, semantic infrastructure, ontology, clouds

Ⅵ. Plenary Lecture

A. Plenary Lecture I

December 1(FRI) 13:30 ~ 14:10 **[Chair : Ju-Jang Lee]**

Professor Sungwan Kim

Affiliation: Dept. of Biomedical Engineering Seoul National University College of Medicine Seoul, South Korea

Title : From Aerospace Engineering to BioMedical Engineering with Emphasis on Medical Robots

Abstract : Recent Research & Development (R&D) efforts on Medical Robots at Seoul National University (SNU) College of Medicine and SNU Hospital are presented. For surgical robot, two innovative ideas motivated from Aerospace technology are addressed. Those ideas are patented in the United States as well as South Korea. The several proto-types have been developed to demonstrate those feasibilities and those are getting surgeon’s attention now. Further, research outcomes are documented as journal articles. Then, rehabilitation robot is explained and the first proto-type, named as SNUExo, is described followed by mirror robot as well as Brain Machine Interface (BMI) based rehab robot. Various other robot- & aerospace- based technologies are also covered in this presentation.

B. Plenary Lecture II

December 1(FRI) 14:10 ~ 14:50 **[Chair : Jang-Myung Lee]**

Professor Fumitoshi Matsuno

Affiliation: Kyoto University, Japan

Title : Bio inspired robotic and its application to rescue and recovery

Abstract : Our lLaboratory has been engaged in two broad and connected areas of research that relate to each other and the human surroundings:; "“bBio-inspired Rrobotics"” and “"Rrescue Rrobotics."”. Living thingscreatures have been survived and been optimized by natural selection. An uUnderstanding of the functions of living things is very useful toin createing a new artificial robots. In our lab,. we are interested in analysis ofzing the beautiful skills and behaviors of living things, and we are trying to find solutions forto the following questions, among others: Why can a living snakes move without legs?, Why do quadrupedlegged living things change their gaitte patterns (for example, Walkwalk, Trottrot,

Gallop gallopfor a horse) due todepending on their moving speed of movement?, What is the mechanism of the flocking mechanism of huge numberbehaviors of birdss and fished?, How cando small ants buildproduce a big anthill?, Why can human beings can walk with two legs?, etc. Based on theour understanding of these phenomena, we can apply our knowledge to create of robots andto solve industrial problems in industry.

We believe that rescue robot systems Lisare another important application of robotic technology. When I was with During my time as an employee at Kobe University, I missed aone of my masters' student, Mr. Motohiro Kisoi, was killed byin the Great Hanshin-Awaji Earthquake on January 17, 1995. After Since this tragic event, I have been putting my heart into the development of useful rescue robot systems and creation of rescue engineering. WhenIn the Great East Japan Earthquake occurred in 2011, we dispatched and utilized grand the rescue robots KOHGA3 to inspection of damaged buildings inat Hachinohe and Aomori, and we dispatched underwater robots for to searching for bodies inat Minamisanriku, Miyagi, and Rikuzentakata in Iwate. My dream is to establish an international rescue robot team, like the popular TV show "Thunderbirds," withusing advanced robotic technologiesy. If we can dispatch rescue robots from Japan to disaster sites everywhere in the world for disaster response and recovery, it will be is a strong contribution to the world.

In this keynote speech I would like to introduce our research activities.

Biography : Fumitoshi Matsuno received the Dr. Eng. degree from Osaka University in 1986. In 1986 he joined the Department of Control Engineering, Osaka University. He became a Lecturer in 1991 and an Associate Professor in 1992, in the Department of Systems Engineering, Kobe University. In 1996 he joined the Department of Computational Intelligence and Systems Science, Interdisciplinary Graduate School of Science and Engineering, Tokyo Institute of Technology as an Associate Professor. In 2003 he became a Professor in the Department of Mechanical Engineering and Intelligent Systems, University of Electro-Communications, Tokyo. Since 2009, he has been a Professor in the Department of Mechanical Engineering and Science, Kyoto University. He holds also posts of the Vice-President of the Institute of Systems, Control and Information Engineers (ISCIE) and the Vice-President of NPO International Rescue System Institute (IRS). His current research interests lie in robotics, swarm intelligence, control of distributed parameter system and nonlinear system, and rescue support system in disaster. Dr. Matsuno received many awards including the Outstanding Paper Award in 2001, 2006 and 2017, Takeda Memorial Prize in 2001 and Tomoda Memorial Prize in 2017 from the Society of Instrument and Control Engineers (SICE), the Prize for Academic Achievement from Japan Society of Mechanical Engineers (JSME) in 2009, and the Best Paper Award in 2013 from Information Processing Society of Japan. He is a Fellow member of the SICE, the JSME, the Robotics Society of Japan (RSJ) and a member of the IEEE among other organizations. He served as a co-chair of IEEE RAS Technical Committee on Safety, Security, and Rescue Robotics (SSRR), an Editor-in-Chief of Journal of RSJ, an Editor of Journal of Intelligent and Robotic Systems, a chair of Steering Committee of SICE Annual Conference, a General Chair of IEEE SSRR2011 and IEEE/SICE SII2011, SWARM2015, SWARM2017 etc. He is an Editor of Journal of Robotics, an Associate Editor of Advanced Robotics, International Journal of Control, Automation, and Systems, etc. and on the Conf. Editorial Board of IEEE CSS.

C. Plenary Lecture III

December 1(FRI) 15:00 ~ 15:40 **[Chair : Sung-Wan Kim]**

Professor Guoying Gu

Affiliation: Institute of Robotics, School of Mechanical Engineering Shanghai Jiao Tong University

Title : Recent development of soft material robotics at SJTU

Abstract : Soft robotics based on soft functional materials is an emerging technology in the field of robotics, which makes the design, fabrication and control approaches for traditional rigid robots not applicable. In this talk, I will firstly introduce the state-of-the-art of soft robotics, and mainly present the recent achievements in our lab at SJTU, emphasizing the key points of working principle, key components and preliminary prototypes of different soft robots. Lastly, I will summarize the challenges and opportunities for the further studies in terms of mechanism design, manufacturing, dynamics modeling and control.

Brief CV : Guoying Gu received the Ph.D. degree in Mechatronic Engineering from Shanghai Jiao Tong University (SJTU), Shanghai, China, in 2006 and 2012, respectively.

He was a Visiting Scholar at Concordia University, Montreal, Canada, and National University of Singapore, Singapore. Supported by the Alexander von Humboldt Foundation, he was as a Humboldt Fellow at University of Oldenburg, Oldenburg, Germany. Since October 2012, he has worked at SJTU, where he is currently appointed as an Associate Professor. His research interests include soft robotics and high-precision motion control. He is the author or co-author of over 60 publications (including more than 40 SCI-indexed papers), which have appeared in journals, as book chapters and in conference proceedings.

Dr. Gu is a member of the IEEE and ASME. Now he severs as Associate Editor of International Journal of Advanced Robotic Systems. He has also severed for several international conferences as Associate Editor or a program committee member.

D. Plenary Lecture IV

December 1(FRI) 15:40 ~ 16:20 **[Chair : Kang-Hyun Jo]**

Professor In-Hyouk Song

Affiliation: Texas State University, USA

Title : Vertically Movable Gate Field Effect Transistor for Low-frequency Vibration Monitoring System

Abstract : The demand of MEMS products has gradually increased and replaced traditional sensors due to size, cost and integration convenience compared to traditional sensors. MEMS based sensors and actuators have been used in many applications including automobiles, display, and life science. As developing microfabrication technology, a variety of materials, such as polymer, metal, poly-silicon, etc., have been studied and employed for forming functioning devices. Among them, silicon (Si) wafer is still dominant in MEMS due to convenience of integration with electronics and excellent mechanical and electrical properties. The use of a Si microcomponent not only enables the integration of thousands of functioning electrical devices onto a single chip but also provides a means of interconnecting it with micromechanical components in an inexpensive manner. As an active sensing element, a suspended gate FET called a vertically movable gate field effect transistor (VMGFET), whose gate move in vertical direction to the plane of substrate, is presented. The gate structure of the VMGFET is formed with single crystalline silicon using a device layer of SOI wafer. In the presentation, the principle of VMGFET is introduced and the fabrication processes are discussed with the advantages of employment of SOI wafer. The electrical and mechanical characterizations of the fabricated VMGFET are presented for low-frequency vibration monitoring application.

Biography : Dr. In-Hyouk Song is an associate professor in Department of Engineering Technology at the Texas State Dallas. He received the M.S. and Ph.D. degrees in electrical engineering from Louisiana State University, Baton Rouge, in 2002 and in 2005, respectively. He had worked at National Research Council of Canada (CNRC – NRC) before joining Texas State University in 2010. His current research interests include MEMS sensors and actuators, including accelerometer, ultrasonic transducer, electrostatic actuators, and polymer based bio/chemical sensors.

VI. Invited Lecture

A. Invited Lecture I

November 30(THU) 15:20 ~ 16:10 **[Chair : Kang-Hyun Jo]**

Professor Ju-Jang Lee

Affiliation: Dept. of Electrical Engineering, KAIST

Title : Robust Fault-Tolerant Control for Underactuated Robot Manipulators

Abstract: This article addresses a robust fault-tolerant contol for underactuated robot manipulators faced with actuator failures and uncertainties. This paper deals with two control issues in manipulator contol fields, namely, the joint space control and Cartesian space control. For the joint space control of underactuated robot manipulators, a robust adaptive control scheme with fault tolerance is proposed using the brakes equipped at passive joints, in the presence of parametric uncertainty and external disturbances. The proposed joint control scheme has two control modes with a passive joint control and active joint control, and one braking mode to lock all passive joints at their desired set-points. In this case it is assumed that the passive joints do not have actuators but are equipped with brakes. For the Cartesian space control of robot manipulators with free-swining passive joints, a robust adaptive control scheme with fault tolerance is also proposed. This scheme is suitable for some joints with failed actuators and/or brakes as well as passive joints without actuators or brakes. In order to overcome the dynamic singularity problem for a nominal decoupling matrix (input matrix of the controller) used in the presented Cartesian contoller, a singularity-free Cartesian path planning is achieved via a computer simulation. The proposed joint and Cartesian space control schemes do not need a priori knowledge of the accurate dynamic parameters and the exact uncertainty bounds. To illustrate the feasiblity and robustness of the proposed control schemes, simulation studies are performed for a three-link planar robot manipulator with a passive joint, under parametric uncertainty and external disturbances.

◆ **Control of *nonholonomic underactuated* robot systems**

- Growing attention in recent years, and it has many practical application fields.

◆ **What is an *Underactuated Robot Manipulator* ?**

- Number of joint actuators < Number of total joints

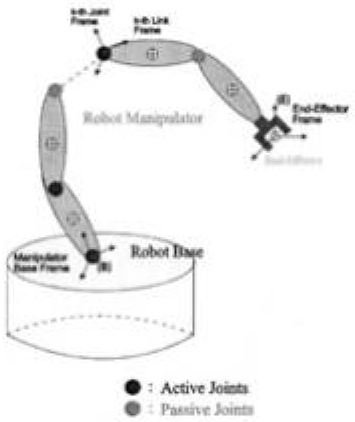

- Total joints (n) = Active joints (r) + Passive joints (p)
- Feature : 2nd-order nonholonomic constraints due to passive joints
- ***Active joints*** or ***Actuated joints*** *(r)* :
  - have their own actuators
- ***Passive joints*** or ***Unactuated joints*** *(p)* :
  - do *Not* have their own actuators

KAIST Ju-Jang Lee

B. Invited Lecture II

November 30(THU) 16:30 ~ 17:20 **[Chair : Kang-Hyun Jo]**

Professor Han Sung Kim

Affiliation: School of Mechanical Engineering

Kyungnam University, Korea

Title : Parallel Robot Technology and Applications

Abstract: Parallel robot manipulator has a moving platform connected to a fixed base by at least two serial kinematic chains called legs, comparing serial robot manipulator with a single kinematic chain. Since heavy actuators locate near or at the fixed base, a parallel robot has much smaller moving inertia than that of a serial robot counterpart and has high speed and high acceleration capabilities. Also, since external force and moment at the moving platform is supported by several legs, a parallel robot has large payload and high stiffness/mass ratio. Finally, since errors in actuators and parts are not accumulated and are distributed to several legs, a parallel robot has high accuracy. Perhaps best known is the six degrees-of-freedom Gough-Stewart platform with linear actuators and links that are only under tension and compression. It has the disadvantages of complex forward kinematics, a small workspace, and many components. Parallel manipulators with less than 6 DOF can alleviate these shortcomings. They typically cost less and are appropriate for various specific applications. The most common geometries provide 4-DOF (3 translational and 1 rotational DOF) such as a Delta parallel robot.

This plenary lecture is organized as follows. First, the characteristics of a parallel robot is explained comparing that of a serial robot. Second, main applications of parallel robots are introduced, which can maximize the advantages, such as high payload, high speed, high acceleration, high payload, high reliability, and high accuracy. Third, brief introductions to forward/inverse kinematics, Jacobian analysis, singularity analysis, dynamics analysis, and optimal design are given using the example of a Delta robot. Finally, several parallel robot

mechanisms developed at Robotics & Mechanism Design Lab in Kyungnam University are presented.

Biography: Han Sung Kim received the M.S. and Ph.D. degrees in Mechanical Engineering from Yonsei University, Korea in 1996 and 2000, respectively. Since March 2004, he has been working in School of Mechanical Engineering of Kyungnam University, Korea. Since his research interests include mechanism design, kinematics, parallel robot applications, and collaborative robots.

C. Invited Lecture III

December 1(FRI) 09:50 ~ 14:20 **[Chair : Soo-Hee Han]**

DANG BAO LAM

Affiliation: Hanoi university of Science and Technology (HUST)

Title : Robotics in Vietnam: brief review and a case study from HUST

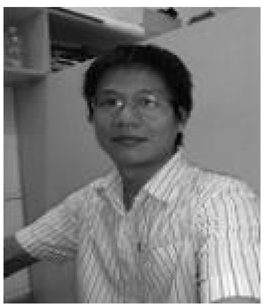

NGUYEN CHI HUNG

Affiliation: Hanoi university of Science and Technology (HUST)

Abstract:

- Overview of research, application and manufacture of robots in Vietnam in the beginning of 21stcentury

- SWOT analysis and growth forecast of robotics market in Vietnam to 2020

- Policies and solutions to develop robotics industry in Vietnam in the period up to 2020.

- VIEbot: a humanoid robot from cooperation between Hanoi university of Science and Technology and Vietnam Institute of Electronics, Informatics and Automation.

D. Invited Lecture IV

December 1(FRI) 09:50 ~ 14:20 **[Chair : Young-Jin Moon]**

Professor Kang Hyun Jo

Affiliation: University of Ulsan, Korea

Title : Vision based Intelligent Systems for Human Supportive Technology

Abstract : Computer vision technology has been investigated for decades to search out the theoretical and application topics. Therefore it is widely challenged to use in the different fields as the real application solutions nowadays. In the presentation, it is outlined and considered the status of Vision based Intelligent Systems research and its some application widely tackled in the ICT(information communication technology) fields. While the IoT based technology is widely spoken recently, the computer vision-based technology still is major technology to lead the hot issues in the artificial intelligence and its application because of its straight forward and intuitive understanding in the predefined domains and its neighboring coverage. Here these belonging contents will be discussed and shown with some examples like intelligent surveillance system, vision application to autonomous driving car systems and robotic application for human supportive technology. In the presentation, some of the current research topics are also introduced with the real application.

Biography : Kanghyun Jo received the BS degree from Busan National University and MS and Ph.D from Osaka University, in 1989, 1993, 1997, respectively. He worked in ETRI (Electro-Telecommunication Research Center) as a Post-Doc. Research Fellow during 1997-1998. Since March of 1998, he has been with University of Ulsan, as a Faculty member, now as a Professor, in charging of an Intelligent Systems Lab.

He had served as the vice dean of e-Vehicle Graduate Institute during 2007-2009 and continuously the vice dean of College of Engineering during 2009-2011. He experienced as visiting Professor/Researcher Kyushu University and KIST during 2005-2006 and also in Oregon State University during 2008-2009 and UC Riverside during 2013-2014.

He has been also serving as a director of many societies, like ICROS (Institute of Control, Robotics and Systems), KMMS (Korean Multimedia Society), SICE (Society of Instrumentation and Control Engineers, Japan), as well as IEEE IES. He is currently contributing as an editorial member for a few renowned international journals, such as IJCAS(International Journal of Control, Automation and Systems) and TCCI (Transactions on Computational Collective Intelligence) or a guest editor of IEEE TII(Transactions on Industrial Informatics).

By now he has made a variety of contributions for organizing conferences and other academic gatherings, ICIC (International Conference on Intelligent Computing, since 2006), ICCAS (International Conference on Control, Automation and Systems, since 2008), and ICCCI (International Conference on Computational Collective Intelligence, since 2010) as a steering member. He is currently serving as an AdCom member IEEE IES and managing IES Ulsan Chapter. He has published more than 200 peer-reviewed technical papers in the renowned journals, such as Springer Neurocomputing, IJCAS, IEEE Trans. Industrial Informatics and Trans. Industrial Electronics.

E. Invited Lecture V

December 1(FRI) 10:30 ~ 11:10 **[Chair : Balan Pillai]**

Professor Jang Myung Lee

Affiliation: Department of Electronics Engineering, Pusan National University, Korea

Title : Startup Time for Robots

Abstract: With the immerging technology of 4th industry innovation, it is time to make start up using the results of the robotics researches. It is definitely necessary to review several very successful robots in terms of technology and market to understand how the robotics has been changed with the current development of IT technologies. For this understanding, the basic component s of the intelligent robots have been discussed to see how they have been changed and in which direction they are required to be developed further, which may show the possible items for the start up. The robots are classified into five generations: 1.Industrial Robot, 2.Sensor-based Robot, 3.Intelligent Robot, 4.Self-energized Robot, and 5.Super-connected Robot. Currently, the 3rd generation robots are mostly mentioned and developed in the market. With the completion or success of the 3rd generation robots, the robotics industry will grow so rapidly that it pursues the 4th and 5th generation robots.

Bibliography: He is a Professor of Department of Electronics Engineering,Pusan National University, Koreasince 1992.Director for SPENALO National Robotics Research Center since 2009. Head of Division of Electrical &Electronics Engineering(2007 ~ 2010). The Ph.D. degree (1990) in ComputerEngineering from the University of Southern California, Los AngelesUSA. The MS and BS degrees from Seoul National University in Korea (1982, 1980). He served as a president of Korean Robotics Society in 2010, and served several years as a vice-president of ICROS, IEIE. Now he is serving as a CRB of Korea Research Foundation.

Research areas: His research interestsinclude Design of Robotic Control System, Factory Automation System Design,Sensor Integrated Manufacturing, Computer Communication, Robotics, Integrated Manufacturing Systems,Intelligent Control, Localization. He haspublished

101papers in international journals, such as IEEE Transcation on Industrial Electronics, Image and Vision Computing, IEEE/ASME Transactions on Mechatronics, etc(SCIindexed).

F. Invited Lecture VI

December 1(FRI) 10:30 ~ 11:10 **[Chair : Young-Im Cho]**

Professor Young Jin Moon

Affiliation: Department of Anesthesiology and Pain Medicine, Laboratory for Cardiovascular Dynamics, Asan Medical Center, University of Ulsan College of Medicine, Seoul, Korea.

Title : Hospital-initiated development of medical robots: Intervention and rehabilitation robots in Asan Medical Center

Abstract: In current development of medical robots, the role of clinicians and tight collaboration of clinicians and engineers have been considered very important. As such examples, four medical robots developed or being developed by Biomedical Engineering Research Center, Asan Institute for Life Sciences, Asan Medical Center (AMC) are presented. Firstly, an image-based needle insertion intervention robot has been developed in accordance with clinical unmet needs found by radiologists. The robot focuses on complete biopsy procedure including the task of tissue sampling, which is totally different from the existing needle insertion robots that handle only one needle. The second is robotic catheterization system used in cardiovascular interventions. To overcome limitation of the commercialized products for robotic arrhythmia ablation, AMC's research consortium has attempted to use information and big data such as ablation trajectories recorded by a mapping system and to give variable stiffness to robotic sheath that guides steering of a catheter. The two others are rehabilitation robots: one is a rehabilitation robot based on bio-signal such as electromyography and electrocardiography, and the other is an attempt to apply artificial intelligence to lower-limb rehabilitation. For the later, clinical big data is being collected from clinical trials performed by seven clinical institutions. As the examples in AMC have shown, clinicians' participation in development of medical robots is expected to be expanded more and more.

G. Invited Lecture VII

December 1(FRI) 11:10 ~ 11:50 **[Chair : Young-Im Cho]**

Professor Soo Hee Han

Affiliation: Department of Creative IT Engineering
Pohang University of Science and Technology,
Korea

Title : 3D mapping for localization of drones

Abstract : Drones are growing in popularity for their wide-ranging potential applications. The global drone market is expected to reach 5.5 billion dollar by 2020. While drones are popular and applied to a variety of areas, they have some rooms for improvement. Since drones are flown by operators and their batteries are also replaced or charged manually, it is a laborious and troublesome work to operate drones by hand for a long time. Additionally, we need to resolve some safety issues arising from communication interruption between an operator and a drone, and obstacle collision. In this regard, now is the time when an autonomous drone control system should be developed. In order to develop the autonomous drone control system, it is most important to achieve precise localization through 3 D perception technology. In this talk, we discuss how to construct high precision 3D maps for indoor and outdoor uses through LiDAR, composite sensors, and omnidirectional cameras. Indoor and outdoor localization systems based on composite 3D maps will be introduced together with real-time algorithms for aligning positions and directions among sensors, and estimating and compensating errors within sensors, with high precision GPS/INS integration technologies.

Biography : Soohee Han received his B.S. degree in electrical engineering from Seoul National University (SNU), Seoul, Korea in 1998. He received the M.S. and Ph.D. degrees in School of electrical engineering and computer science from Seoul National University, Seoul, Korea, in 2000 and 2003, respectively. From 2003 to 2007, he was a researcher at the Engineering Research Center for Advanced Control and Instrumentation of SNU. In 2008, he was a senior researcher at the robot S/W research center. From 2009 to 2014, he was with the Department of Electrical Engineering, Konkuk University, Seoul, Korea. Since 2014, he has been with the Department of Creative IT Engineering, POSTECH, Pohang, Korea. He is an associative editor of International Journal of Control, Automation, and Systems. He is a Senior Member of IEEE Control Society and has been serving as a member of IFAC TC 6.3(Power and Energy Systems). Dr. Han has published more than 150 international journal/proceeding papers. He has also authored 5 technical books. His main research interests are in the areas of autonomous vehicles, smart grid systems, electric vehicles, cyber physical energy systems, computer aided control system design, distributed control system, time delay system, and stochastic signal processing.

H. Invited Lecture IX

December 1(FRI) 16:20 ~ 17:00 **[Chair : Soo-Hee Han]**

Professor Young Im Cho

Affiliation: Faculty of Computer Engineering, Gachon University, South Korea

Title : Research of Intelligent IoT-Smart City Platforms

Abstract : Smart City platform have been developed in the city and national level. From Smart City, IoT is an important means to resolve current issues. Technical elements of the IoT is sensing, wired and wireless communications, network, service interfaces, big data, security etc.

Usually, Machine-to-Machine communications (M2M) is a phenomenon that has been proceeding quietly in the background. Current international standard was presented as a reference model in One M2M which is leading IoT. The four areas are IoT service-centric platform, data-centric platform, connectivity-centric platform, and device platform.

To avoid creation of competing M2M standards the 7 standards developing organizations, that publish telecom standards: TTC, ARIB (Japan), ATIS, TIA (USA), TTA (Korea) CCSA (China), ETSI (Europe) started the OneM2M Global Initiative to develop one globally agreed M2M Specification with initial focus on Service Layer. OneM2M aims to consolidate current M2M Service Layer standards activities such as ETSI TC M2M (Europe), TIA TR-50 (USA) and CCSA TC 10 (China), and to reduce standardization overlap and confusion and provide ongoing standards support to enhance interoperability, reduce market fragmentation, and improve security and reliability. (Ref: http://www.eclipse.org/proposals/technology.om2m/).

However, there is no international standardized IoT platform including data, service, connectivity and device, what is more there is no clear national standardized platform satisfy the reference model that is presented by oneM2M institute which is a leading organization to establish an international IoT standardized platform.

In this seminar, I am going to talk about some topics like following: IoT and Smart City basic, IoT International platform focusing on OneM2M reference model, components and model description for IoT platform. Thank you.

Biography: Professor Young Im Cho got bachelor's, master's, and doctoral degrees in Computer Science from Korea University in South Korea.She got Post-Doc. Degree at University of Massachusetts at 2000 in USA. Now she is Chiefs of AI and Smart City Laboratory at Gachon University, Korea-Kazakhstan ICT Cooperation Center and Intelligent Service Robot Automation System Society. She will be a Chief of Korea Intelligent and System Society from 2018. She was ex-committee member of National Information Strategy

Council under Korea President, and worked as a senior research at Samsung Electronics. She is a member of e-Government committee member in Korea Government. She was a visiting professor at Purdue University in USA from 2013 to 2014. She has published more than 300 publications including Journals, conferences. Also she has 13 text and reference books. She received a big medal from Korea Government at 2013, and 15 academic awards from academic societies. She is a member of more than 15 editorial boards of international journals and conferences. She is IEEE member, too. Her interesting areas are Artificial Intelligence, Smart City, Big data, Cloud Robot and e-Government and etc.

V. Young Outstanding Researcher

A. Young Outstanding Researcher

November 30(THU) 17:20 ~ 18:00 **[Chair : Seok-Jo Go]**

Professor Moon Hee Lee

Affiliation: Dong-Eui Institute of Technology, Korea

Title : Development and Application of Advanced Composite Materials

The development of composite materials has been accompanied by the development of metals, plastics and ceramics. Composite materials, which are materials to expand or replace existing materials, have been developed in the form of particle, fiber reinforcing or lamination structures, and are being applied to several industrial fields.

In the aerospace industry, the replacement of conventional aluminum and titanium alloys to carbon fiber-reinforced plastic composites (CFRRP) has been progressed to secure weight-saving with excellent mechanical property. This has been possible with decades of advancement in the mechanical properties of carbon fibers and cost-saving manufacturing processes of composite materials. In recent years, General Electrics (GE) Aviation has been expanding the application of composite materials to the development of a LEAP engine that uses a ceramic matrix composites (CMCs) instead of the conventional nickel-based superalloy as engine turbine components.

The application of composite materials in the energy field is also actively under consideration. In the design of International Thermonuclear Experimental Reactor (ITER), the application of silicon carbide fiber reinforced silicon carbide composites (SiCf/SiC) with excellent nuclear properties has been studied for the future fusion energy sources. On the other hand, after the earthquake in Fukushima, OECD / National energy agency (NEA) has been emphasizing the safety of nuclear facilities and countermeasure against the accident scenarios such as station-blackout (SBO) and loss-of-coolant-accidents (LOCAs). As part of the development of accident tolerant fuel (ATF), the studies on application of SiCf/SiC composite materials instead of conventional Zirconium alloys to nuclear fuel cladding materials are under review.

In the fields of electric/electronic components, the integration technology and high power electronic components in LED, hybrid/electric vehicle has a problem of heat generation during operation causes degradation of system efficiency and performance. In order to solve this problem, the design and material research for high performance electronic packaging has been under consideration of heat dissipation. In the materials field, metal matrix composites (MMCs) has being actively researched for high performance heat-sink. MMCs that can enhance not only the thermal conductivity but also coefficient of thermal expansion matching to the electronic substrate have been developed by reinforcing diamond powder, high thermal conductivity carbon fibers and carbon nanotubes in the conventional high thermal conductive copper or aluminum.

In the field of engine piston for automobiles, research on MMSs has also been actively carried out in order to improve the performance of conventional aluminum alloys. In order to achieve low density, high modulus and strength and suitable thermal expansion matching, attempts have been made to compose silicon carbide fibers, carbon nanotubes, or other ceramic fibers with conventional aluminum alloys.

In the recent development of the Industry 4.0, the role of the robotic system is much emphasized. In order to improve the performance of the robot system, such as weight- or energy-saving and operation in harsh environment, it is necessary to apply the materials based on the knowledge of various composites.

VII. Program Table

NOVEMBER 30th(THU.), 2017 [Oral Session]

Oral Session I [14:30 ~ 15:20] : Room 301

□ Oral Session I	Chair : Ehn-Joo Nah
14:30~14:40	**A Study on Autonomous Travelling Control of Direct Driving Robot with Two Driving** Min-Seong Kim1, Hyun-Woo Song2, Ehn-Joo Nah3, Sung-Hyun Han3
14:40~14:50	**A Precise Control of Robot Manipulator with Eight D.O.F Based on Digital Signal Process** Hyun-Woo Song1, Jae-Hyung Kim2, Min-Seong Kim3, Woo-Song Lee4, Yeon-Guk Noh5
14:50~15:00	**A Study on Robust Motion Control of Robot Arm Based on Neurel Network** Jae-Hyung Kim1, Min-Seong Kim2, Hyun-Min Kim3, Se-Han Lee4, Uhn-Joo Nah4, Sung-Hyun Han4
15:00~15:10	**A Flexible Control of Robot Hand Fingers with Six Joints** Dong-Hwa Jeong1, Min-Seong Kim2, Gi-Su Shin3, Se-Han Lee4
15:10~15:20	**A Stable Walking Motion Control of Humanoid Robot with 24 Joints** Hyun-Min Kim1, Min-Seong Kim2, Hyun-Woo Song3, Yang-Keun Jung4

Oral Session II [15:20 ~ 16:10] : Room 301

□ Oral Session II	Chair : Won-Sik Choi
15:20~15:30	**Surface type broaching machine forced vibration analysis under normal cutting operation condition based on finite element method** Pandu Sandi Pratama1, Destiani Supeno2, Jae-Young Byun2, Joong Soon Lee3, Jeong Hwan Jeong3, Won-Sik Choi2,#
15:30~15:40	**The Characteristics of 4Mhz NDT Ultrasonic Transducer for Weld Quality Inspection of Spot Welding Robot** Eon Uck Kang1, Pandu Sandi Pratama2, Jae Young Byun1, Eun Suk Lee1, Sung Won Chung1, Won Sik Choi1,#
15:40~15:50	**The red ginseng vinegar fermentation manufacturing using "Uinkin"** Se Ran Hwang, Destiani Supeno, Kwo Soon Hong, Chung Sung Won, Kwon Soon Goo, Park Jong Min, Kim Jong Soon, Won Sik Choi
15:50~16:00	**Improvement of the Life of the Electric Vehicle Carrier Reducer by the Finite Element Method** Jae Young Byun1, Pandu Sandi Pratama2, Eun Suk Lee1, Chun Suk Park3, Sung Won Chung1, Won Sik Choi1,#
16:00~16:10	**Characteristics of Jujube Cherry Tomato Fermentation** Destiani Supeno, Kwo Soon Hong, Chung Sung Won, Kwon Soon Goo, Park Jong Min, Kim Jong Soon, Won-Sik Choi

Oral Session III [16:30 ~ 17:20] : Room 301

□ Oral Session III	Chair : Pandu Sandi Pratama
16:30~16:42	**A Study on the tool for collecting insect pests from fruits trees** Ji-Hee Woo1, Destiani supeno1, Keefe Dimas haris sean1, En-Suk Lee1, Mi-kyung Nam1, Can-yeol Cha2, Yeong-jo Moon2, Won-Sik Choi1*
16:42~16:56	**Charactrtistics of Separation with Tofu and Tofu Container according to Water Temperature** Eun Suk Lee1, Jae Young Byeon, Mi Kyung Nam, Ji Hee Woo1, Na Kyung Kim2, Kang Sam Lee3, Won Sik Choi1,
16:56~17:08	**Fermentation system and characteristics of natural fermented vinegar using lotus and stems** Mi Kyung Nam1, Eun-Suk Lee 1, Ji Hee Woo1, Jae-Young Byeon1, Won-Sik Choi1*
17:08~17:20	**The change of plant and fluorescent lamp temperature in closed system cultivation** Dimas Harris Sean Keefe1, Jaeyoung Byun1, Pandu Sandi Pratama2, Jeongyeol Cho3, Wonsik Choi1,#

NOVEMBER 30th(THU.), 2017 [Poster Session]

Poster Session I [17:20 ~ 18:00] : Room 301

□ Poster Session I	Chair : In-Man Park
Poster 1	**A Orientation Control of Vertical Articulated Robot Manipulator Based on Servoing Feedback in Working Space** Hee-Jin Kim1, Woo-Song Lee2, Min-Seong Kim3, In-Man Park4 and Sung-Hyun Han5
Poster 2	**A Precise Position and Velocity Control of Vertical Type Robot Arm with Seven D.O.F** Min-Seong Kim1, Min-Hyuck Choi2, Jeong-Suk Kang3, Nam-Il Yoon3, Jong-Bum Won3, Sung-Hyun Han4
Poster 3	**A Stable Path Control of Robot Manipulator with 6 Joints for Forging Trimming Automation** Min-Seong Kim1, Jong-Hun Kim1, Sung-Hun Noh2, Gi-Su Shin3, Jeong-Suk Kang4, Jong-Bum Won4 and Sung-Hyun Han5
Poster 4	**A Study on Intelligent Control of Biped Robot for Smart Factory** Un-Tae Ha1, Min-Seong Kim2, Byung-Suk Yoon3, Jung-Eup Gye4, Jong-Gyo Jung5 and Sung-Hyun Han6
Poster 5	**A Study on Intelligent Motion Control of Humanoid Robot for Smart Factory** Min-Seong Kim1, In-Man Park2, Young-Hwa Jeong3, Sung-Hyun Han4

Poster Session II [17:20 ~ 18:00] : Room 301

□ Poster Session II	Chair : Yang-Geun Jeong
Poster 1	**AStudy on Motion Control of Humanoid Robot for Human-Robot Interaction** Min-Seong Kim1, Byeong-Gap Moon2, Kyu-Hyun Jung3, Myeong-Hwan Park4, Ju-Jang Lee5 and Sung-Hyun Han6
Poster 2	**A Study on Motion Control of Two Wheel Driving Mobile Robot by Voice Commend for Smart Factory** Gi-Hyun Kim1, Ho-Young Bae 2, Woo-Song Lee 3 and Sung-Hyun Han4
Poster 3	**A Study on Precise Control of Mobile Robot with Dual-Arm** Woo-Song Lee1 Ki-Young Ko2, Ho-Young Bae3, Mun-Keun Cho4, Ki-Hyun Kim5, and Sung-Hyun Han6
Poster 4	**A study on Robust Control for Working of Humanoid Robot** Min-Seong Kim1, Woo-Song Lee2, Hyun-Suk Sim3, Ho-Young Bae4, Sung-Hyun Han5
Poster 5	**A Study on walking Control of Biped Robot by Voice Command for FA** Yang-Geun Jeong1, Min-Seong Kim2, Yeon-Guk Noh3, and Sung-Hyun Han4

December 1st(THU.), 2017 [Oral Session]

Oral Session III [13:30 ~ 14:50] : Room 301

□ Oral Session III	Chair : Jang-myung Lee
13:30~13:46	**6 DOF Manipulator Technology in ROS Environment** Dong-eon Kim1, Dong-ju Park1, Ki-seo Kim1, Jin-hyun Park1 and Jang-myung Lee1*
13:46~14:02	**Edge Simplification Method for Stereo Images** Eun Kyeong Kim1, Hyunhak Cho2 Jongeun Park1 and Sungshin Kim1*
14:02~14:18	**Inverse Kinematic Analysis of 5 DOF Manipulator using Numerical method** Jin Gon Yoon 1, Sun Oh Park 1, Min Gyu Jung1 and Min Cheol Lee 1*
14:18~14:34	**Sliding Mode Control Of 2 Link Robotic Manipulator** Saad Jamshed1, Karam Dad1 and Min Cheol Lee1*
14:34~14:50	**Utilizing air pressure sensor for detecting of object** Jin-hyun Park1, Tae-eon Kim1, Ki-seo Kim1, Dong-eon Kim1, and Jang-myung Lee1*

Oral Session V [13:30 ~ 14:50] : Room 600A

□ Oral Session V	Chair : Kang-Hyun Jo
13:30~13:50	**Analysis of Traffic Sign Classification using Multiple Image Preprocessing Methods** Qing Tang1 and Kang-Hyun Jo2
13:50~14:10	**Exploiting Different Shape Features for Fall Action Classification** Sowmya Kasturi1 and Kang-Hyun Jo2
14:10~14:30	**Vehicle Contour Segmentation Using 3D Point Cloud** Yang Yu1, Laksono Kurnianggoro1, Kang-Hyun Jo2
14:30~14:50	**Human Pose Estimation from Images Using Convolution Neural Networks** Hoang Van Thanh1 and Kang-Hyun Jo2

December 1st(THU.), 2017 [Poster Session]

Poster Session I [15:00 ~ 15:40] : Room 301

□ Poster Session I — Chair : Woo-Song Lee

Poster 1	**A Study on the Path Planning and Control of Robot Manipulator with Six Joint for Molding and Forging Process Automation** Min-Seong Kim1, Geo-Seung Choi2, Byung-Seuk Yoon3, Jong-Bum Won4, Sung-Hyun Han5
Poster 2	**Intelligent Control of Mobile-Manipulator Robot by Voice Command for Smart Factory** Yang-Keun Jeong 1*, Min-Seong Kim 2, Hui-Jin Kim 3, Woo-Song Lee 4, Yeon-Guk Noh 5, Geo-Seung Choi 6, In-Man Park 7, Jang-Sik Park 8, and Sung-Hyun Han 9
Poster 3	**A Study on Robust Control of Robot Gripper Based on Pressure Sensors for Marking Automation Process** Min-Seong Kim 1, Jeong-Seok Kang 2, Jong-Dae Won 3, Sung-Hyun Han 4, Han-Sung Kim 4
Poster 4	**A Study on Accurate Motion Control of Mobile Robot with Dual-Arm** Yang-Geun Jeong 1, Gi-Su Shin 2, Min-Seong Kim 2, In-Man Park 3, Sung-Hyun Han 4

Poster Session I [15:00 ~ 15:40] : Room 301

□ Poster Session II — Chair : Hyun-Suk Sim

Poster 1	**A Real-Time Control for Precise Walking of Biped Robot** Jeong-Chul Moon 1, In-Man Park 2, Sung-Hyun Han 3
Poster 2	**A Robust Neural Network Control of Robot Manipulator for Industrial Application** Eun-Taek Ju 1, Woo-Song Lee 2, Sung-Hyun Han 3
Poster 3	**A Study on Grasping Control of Hand Fingers 12 Joints** Jae-Jong Kim 1, In-Man Park 2, Hyun-Suk Sim 3, Sung-Hyun Han 4
Poster 4	**A Study on Intelligent Control of Bipped Robot by Voice Command** Chang-Keun Oh 1, Woo-Song Lee 2, Sung-Hyun Han 3

December 1st(THU.), 2017 [Poster Session]

Poster Session II [15:00 ~ 15:40] : Room 301

□ Poster Session III Chair : Eun-Tae Ha

Poster 1	**A Study on Real-Time Control of Intelligent Robot with Three Wheel** Moon-Kuen Cho 1 , In-Man Park 2, Sung-Hyun Han 3
Poster 2	**A Study on Robust Control of Robot Manipulator for Industrial Application** In-Kyun Yoon 1 ,Woo-Song Lee 2, Sung-Hyun Han 3
Poster 3	**A Study on Robust Motion Control of Humanoid Type Robot for Cooperative Working** Ki-Young Ko 1 , Eun-Tae Ha 2, Sung-Hyun Han 3
Poster 4	**A Study on Stable Control of Intelligent Robot with Dual Arm for Cooperation working** Ho-Young Bae 1 , Yang-Keun Jeong 2 , Woo-Song Lee 3 , In-Man Park 4, Sung-Hyun Han 5

Poster Session III [15:00 ~ 15:40] : Room 301

□ Poster Session IV Chair : Yang-Geun Jeong

Poster 1	**A Study on Travelling Control of Humanoid Type Mobile Robot with Three Wheel** Se-Bin Park1, In-Man Park 2 and Sung-Hyun Han3
Poster 2	**A Travelling Control of Mobile Robot Based on Sonar Sensors** Jae-Sang Kim1 Yang-Keun Jeong2 Jong Bum Won3 and Sung-Hyun Han4
Poster 3	**A Precise Position Control of Robot Manipulator with Eight Joints** Taek-Jong Nam1 Yang-Keun Jeong2, Jong Bum Won3, Hyun-Cheol Lee4 and Sung-Hyun Han5
Poster 4	**A Stable Control of Legged Robot Based on Ultrasonic Sensor** Seong-Gyu Park1, Eun-Tae Ha2 and Sung-Hyun Han3

Poster Session IV [15:40 ~ 16:20] : Room 301

□ Poster Session V

Chair : In-Man Park

Poster 1	**A Study on Grasping Control of Robot Hand with 12 Joints** Chang-Young Lee1, Yang-Keun Jeong2 and Sung-Hyun Han3
Poster 2	**A Study on Intelligent Control of Humanoid Robot with Voice recognition** Min-Hwan Lee1, Woo-Song Lee 2 and Sung-Hyun Han3
Poster 3	**A Study on Robust Control of Articulated Robot Arm with Seven Joints** Hee-Jin Kim1, Sung-Cheol Jang2, and Sung-Hyun Han3
Poster 4	**A Study on Robust Control of Robotic Hand with 14 Joints for cooperate Working** Young-Tae Back1, Yang-Keun Jeong2 and Sung-Hyun Han3

Poster Session IV [15:40 ~ 16:20] : Room 301

□ Poster Session VI

Chair : Woo-Song Lee

Poster 1	**A Study on Robust Voice Control of Biped Robot for Cooperate working** Seong-Ju Choi1, Jong-Dae Won2, Woo-Song Lee 3, and Sung-Hyun Han4
Poster 2	**A Study on Stable Walking Control of Mobile Robot with Dual Arm** Hyung-Tae Lee1, Yang-Keun Jeong2, Woo-Song Lee3, In-Man Park4, and Sung-Hyun Han5
Poster 3	**A Study on Visual Feedback Control of Articulated Robot Arm with Seven Joints** Ki-Hyun Kim1 , Hyun-Suk Sim2 and Sung-Hyun Han3

A Study on Autonomous Travelling Control of Direct Driving Robot with Two Driving

Min-Seong Kim1, Hyun-Woo Song2, Ehn-Joo Nah3, Sung-Hyun Han3

[1] Department of Advanced Engineering., Kyungnam University, Changwon, 51767, Korea
(E-mail : kms21018@naver.com)
[2] Department of Mechatronics Engineering., Kyungnam University, Changwon, 51767, Korea
(E-mail : thgudn@naver.com)
[3] School of Mechanical Engineering, Kyungnam University, Changwon, 51767, Korea
(E-mail: uhnjoona@kyungnam.ac.kr/shhan@kyungnam.ac.kr)

Abstract : We Propose a new approach to the design and real implementation of wall following and fuzzy perception concept with a non-holonomic mobile robot named KU-DAWIN Robot. The main focus of this paper is obtaining a fuzzy perception of the environment in the design of each reactive behavior and solving the problem of behavior combination to implement a fuzzy behavior based control architecture. It should be remarked that, the proposed technique of the nonholonomic constraints are considered in the design of each behavior. Furthermore, in order to improve the capabilities of the intelligent control system and its practical applicability, teleoperation and planned behaviors, together with their combination with reactive ones, have been considered. Experimental results, of an application to control the KU-DAWIN Robot autonomous vehicle, demonstrate the robustness of the proposed method.

Keywords: Robot Navigation, Ultrasonic Sensor, Fuzzy Controller, Non-holonomic Mobile Robot

1. INTRODUCTION

Navigation is the process of determining and maintaining a path or trajectory to a goal destination. Autonomous mobile robots are required to navigate in more complex domains, where the environment is uncertain and dynamic. Autonomous navigation in these environments demands adaptation and perception capabilities. This paper describes improvements in the perception functions used in these kinds of robots. It should be noted that this is a nonholonomic vehicle with significant limitations in the reactive capabilities due to kinematic and dynamic constraints, and a few number of sensors and large blind sectors in between them, making autonomous navigation a nontrivial task. The methods presented in this paper have been conceived to deal with these limitations of conventional vehicles.

In addition, fuzzy perception can be used straightforward to perform the control of the mobile robot by means of fuzzy behavior-based scheme already presented in literature [2, 4, 7, 8, 10]. The main differences of the proposed approach with respect to other behavior based methods are: 1 - The nonholonomic constraints are directly taken into account in the behaviors. 2 - The fuzzy perception itself can be used both in the design of each reactive behavior and to solve the problem of blending behaviors.

Hence, the fuzzy behavior-based control scheme presented in this paper allows not only implement reactive behaviors but also teleoperation and planned behaviors, improving system capabilities and its practical application. Furthermore, in these behaviors, soft computing techniques play an important role to solve different problems.

2. Control Scheme

The following considerations are based on a mobile robot with the three degrees of freedom of planar movement, x, y and Θ (see Fig. 1). It is equipped with a ring of 12 ultrasonic sensors which are able to perceive vertical or nearly vertical planes. The number of sensors is irrelevant as long as there are no blind sectors between them. Θ refers to the orientation of this ring of sensors and not to the orientation of the robot itself, which is of no importance for the wall following algorithm. With $\dot{\phi}$ indicating the direction of movement the kinematics model of such a robot is described as follows:

$$dx = v\cos\phi dt;\ dy = -v\sin\phi dt;\ d\theta = \dot{\theta} dt \quad (1)$$

Since there is no modeling of the environment the absolute position of the robot does not matter. So there is no world frame used here and the kinematics model can be expressed instead as:

$$ds = v dt;\ d\phi = \dot{\phi} dt;\ d\theta = \dot{\theta} dt \quad (2)$$

The speed v, the angular speeds $\dot{\phi}$ and $\dot{\theta}$ are used as control variables of the robot and generated by the fuzzy controller.

Perception of each ultrasonic sensor i of the mobile robot is assigned a vector ki.Its direction equals the orientation of the sensor´s axis and its length is a function of the distance dimeasured by this sensor:

$$k_i = \frac{d_{\max} - d_i}{d_{\max} - d_{\min}} \tag{3}$$

where where dmin and dmax designate the shortestand longest distance respectively at which an object may be positioned to be reliably detected.kiis limited to 0 and 1 respectively

Since a vehicle with nonholonomic constraints cannot move itself in any direction at every time instant, it is interesting to weight the different perceptions according with the direction where the obstacle was detected. In other words, an obstacle is less important if it is placed at a location that cannot be reached by the mobile robot, but it is more dangerous if it is on a reachable position. This task can be accomplished by considering the perception angle (Θi) in the computation of the perception function

$$k_i = f(d_s, \theta_i) = sat_{0,1}\left(\frac{d_{\max}(\theta_i) - d_s}{d_{\max}(\theta_i) - d_{\min}(\theta_i)}\right) \tag{4}$$

where sat0,1(x) states for the saturation of x in the range [0, 1]. In this way, it is possible to assign different perceptions, i.e. different weights, to objects detected at the same distance relative to the mobile robot but at different directions. For example, perception function ki is obtained by using the nonlinear function $d_{\min}(\theta_i) = d_m(1-e) / (1-e\cos\theta_i)$, and $d_{\max} = n d_{\min}(\theta_i)$ (with n>1), in Eq. (4).

$$k_i = f(d_s, \theta_i) = sat_{0,1}\left(\frac{n d_m(1-e) - d_s(1-e\cos\theta_i)}{(n-1)d_m(1-e)}\right)$$

(5)

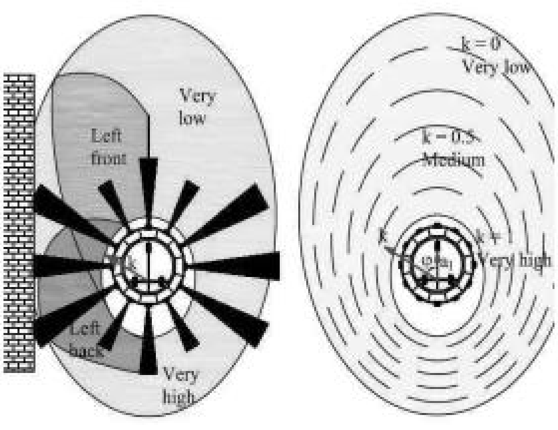

(a) (b)

Fig. 1 Ellipsoidal perception area

Furthermore, it is interesting to stress that the perception vector implies a fuzzy high level description of the environment, being independent of the type of range sensor used. So, it is possible to use different perception functions from Eq. 4 for each kind of sensor (laser, ultrasonic, infrared). Thus, sensor data fusion can be reduced to compute different vectors from the sensor measurements and to combine them to obtain the perception vector.

The previous perception can be updated as follows: consider a robot of arbitrary shape equipped with proximity sensors. Any such sensor may be located at a position U, with its axis pointing to the direction s (see Fig. 4). A frame r represents the robots position and orientation, x and Θ, respectively, with respect to the world reference system w. The velocity υ of the reference point and the angular velocity $\omega_{r/w} = \dot{\varphi}$ of the robot with respect to the fixed frame w, give the state of motion. Furthermore, the virtual perception coordinate system is assumed to be located at E, pointing to the direction of attention a1. Then, an object detected by a proximity sensor at a distance ds could be detected by a virtual sensor placed at E a distance d, and with an orientation Θ with respect to the vehicle's direction of attention a1.

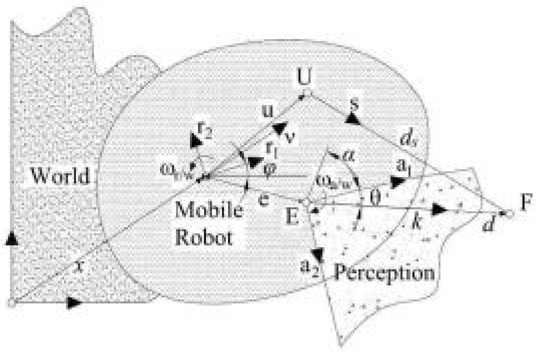

Fig.2 Updated perception

Now the virtual perception will be updated taking into account the robots motion as follows: considering a perception function k = f(d, Θ) and the corresponding inverse perception function, d = g(k, Θ), and carrying out some calculations, it can be shown that the derivatives of angle and length of the perception vector are given by (assuming $g \neq 0$ and $\partial g / \partial k \neq 0$).

$$\dot{\theta} = \frac{1}{g}\{(\dot{x} + \omega_{r/w} \times e)[r_1\cos(\alpha+\theta) - r_2\cos(\alpha+\theta)]\} - \omega_{r/w} - \omega_{a/r} \tag{6}$$

$$\dot{k} = \frac{-1}{\partial g/\partial k}\left\{(\dot{x} + \omega_{r/w} \times e)[r_1\cos(\alpha+\theta) - r_2\cos(\alpha+\theta)] + \frac{\partial g}{\partial \theta}\dot{\theta}\right\} \tag{7}$$

where $\omega_{r/w} = \dot{\alpha}$ is the angular velocity of the virtual perception coordinate system relative to the robot.

2.1 Obstacle avoidance procedures

The wall following method described is not only useful to execute an explicit instruction such as "follow that wall". It's also used to avoid an unexpected obstacle in a predefined movement or mission. While the robot is moving, unexpected obstacles or walls can appear and avoiding them is desired and then continues executing the rest of the plan. Taking all that into account the problem of the obstacle avoidance could be reduced to three main aspects presented detail below.

Start to avoid an unexpected obstacle: This part has been simplified to the robot by the planner. The planner makes the calculations to obtain the minimum distance between each particular movement in the known environment. The avoidance begins when one sensor detects an object nearer than the distance given by the planner.

How to avoid the obstacle: The avoidance of the obstacle consists of following the contour of the obstacle in the same way that has been explained before. The maximum speed of the following process will be the speed of the element movement (EM) that was in execution when the obstacle has been detected. That speed has been calculated as the maximum safe speed in the region of the environment by the planner.

Finish the avoidance of the obstacle: That part of the avoidance is the most complex part because of the multiple possibilities of movements and reasons for the finishing.

The avoidance can finish:

a) When the robot gets back to one of the EMs of the plan. (main case).

b) When a long time has elapsed from the beginning of the avoidance. (The obstacle covers all the rest of mission).

c) If the robot is very far from the point of the beginning of the avoidance. (The robot could go very far from its goal in the mission).

The cases (b) and (c) are easy to detect but the case (a) depends on the types of the movements of the robot in the mission. It's important to know that all of the calculations to detect the end of the avoidance have to be made as fast as possible to get the maximum time free in the CPU for the rest of processes (Position control, radio communications, avoidance, etc.). Then all of the types of movements possible are reduced to segments of lines and circumference's arcs.

2.2 Fuzzy Controller

Perception vector can be considered by means of fuzzy logic yielding a fuzzy description of the environment. This description of the environment can be easily used as input to a fuzzy controller to perform reactive navigation. Furthermore, it is also possible to compute different perception vectors from the virtual perception, and to use them to implement fuzzy controllers or behaviors which perform specific tasks taking into account nonholonomic constraints. The combination of the different behaviors, in a cooperative scheme, can be also easily done by means of fuzzy logic. In the following, a detailed description of the perception based fuzzy control system is performed, including implementation and combination of behaviors.

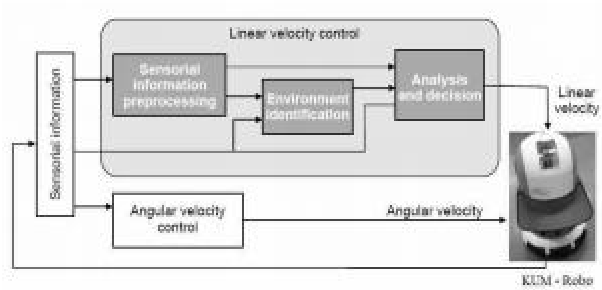

Fig. 3 Block diagram of control system

3. EXPERIMENTAL RESULTS

This section presents some experimental results of the proposed methods to the non-holonomic mobile robot KUM--Robo. The vehicle carries on-board a heterogeneous configuration of ultrasonic sensors. It is presented two kinds of experiment including general perception and application of fuzzy perception. All the experiments have been implemented in the KUM-Robo embed.

In this, instead of a typical ring of identical sonars, there are 12 sonars of three different types, placed at different locations (see Fig. 1a). Six of them are large-range sensors (0.6 – 3.0 m), four are mid-range (0.2 – 1.0 m), and the other two are of short-range (0.06 – 0.3 m). Furthermore, these ultrasonic sensors use a higher frequency and have a narrower sonar beam than the commonly used sonars in these kinds of applications. The sensors are arranged in a way that six of them cover the front part of the vehicle and the other four cover its lateral sides.

In these experiments, the virtual perception system was placed at the center of the robot's rear axle and the direction of attention a1 was kept parallel to the front wheel. The perception function used is given by Eq. 5, with n = 2; dm = 1.4, and e= 0.6.

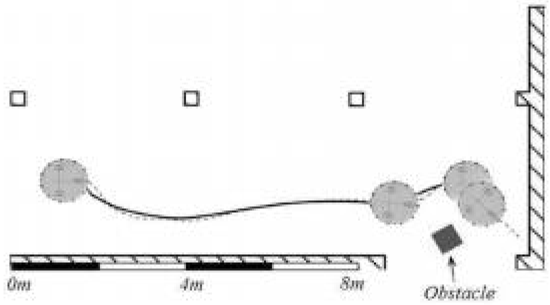

(a) Loss of perception while turning right

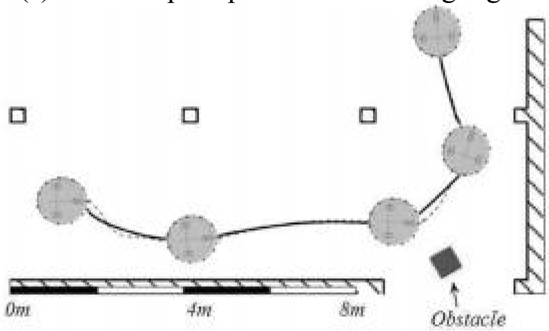

(b) With perception memory

Fig. 4 The differences result of perception's type

Fig. 4 shows an experiment with the same conditions but it was applied with differential perceptions.

Experiments result is shown in Fig. 11 where the robot has to navigate through a corridor which is partially obstructed by an obstacle. The robot starts at point A with corridor tracking behavior, since it has equal perception at both sides. As the robot moves on it detects free space to its left and changes its behavior smoothly to follow right wall. When entering the corridor it tries again to center itself in the corridor B until it encounters the obstacle at C and the obstacle avoidance behavior becomes dominant. The corridor is wide enough, i.e. the perception at both sides is sufficiently low that the turnaround behavior is not activated, so the robot tries to round the obstacle and, indeed, detects the passage between the obstacle and the wall. From this point on the robot is again guided mainly by the corridor tracking behavior until D.

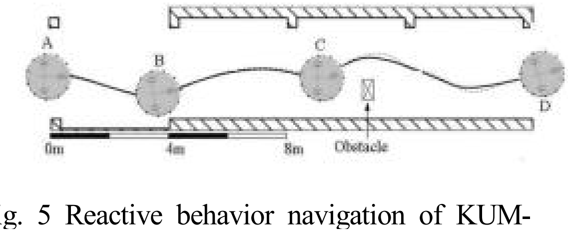

Fig. 5 Reactive behavior navigation of KUM-Robo

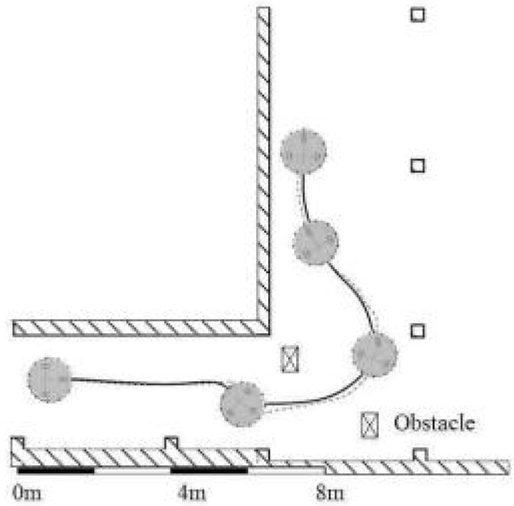

Fig. 5 Two – Obstacle avoidance behaviors

Finally, Fig. 6 shows the mobile robot in an autonomous behavior experiment avoiding two obstacles doing a right turn, to later on keep following a right wall. Note again the difficulties performing this experiment due to the features of the vehicle and the environment involved, making navigation a nontrivial task.

4. CONCLUSIONS

This work describes the design and real implementation of wall following and fuzzy perception concept with a non-holonomic mobile robot named KUM-Robo. The techniques to obtain a fuzzy perception of the environment in the design of each reactive behavior and solving the problem of behavior combination, to implement a fuzzy behavior based control architecture. It should be remarked that, at difference with other behavior based approaches, in the proposed technique the nonholonomic constraints are considered in the design of each behavior.

Furthermore, in order to improve the capabilities of the intelligent control system and its practical applicability, teleoperation and planned behaviors, together with their combination with reactive ones, have been considered. Experimental results, of an application to control the KUM-ROBO autonomous vehicle, demonstrate the robustness of the proposed method.

Reference

[1] G.A. Bekey, "Localization, Navigation, and Mapping", Autonomous Robots: From Biological Inspiration to Implementation and Control, The MIT press, pp 473-507, 2005.
[2] R.C. Luo, T.M. Chen, "Autonomous mobile target tracking system based on grey-fuzzy control algorithm," IEEE Trans. Ind. Electron. Vol. 47, No. 4, pp 920–931, 2000.
[3] J. Gasos, A. Rosetti, "Uncertainty repres entation for mobile robots: perception, modeling and navigation in unknown environments", J. of Fuzzy Sets and Systems, Vol. 107, No. 1, pp 1–24, 1999.
[4] I. Baturone, F.J. Moreno-Velo, S. San chez-Solano, A. Ollero, "Automatic design of fuzzy controllers for car-like autonomous robots", Fuzzy Systems, IEEE Trans. On Vol. 12, pp:447 – 465, 2004.
[5] R. Braunstingl, "Improving reactive naviga t ion using perception tracking", Robotics and Manufacturing, Recent Trends in Research and Applications, Vol. 6, pp 25-30, New York, 1996.
[6] J.J. Leonard, H.F. Durrant-Whyte, "Directed Sonar Sensing For Mobile Robot Navigation", Kluwer Academic Publishers, pp 147-155, 1992.
[7] A. Ollero, A. Garcia-Cerezo, J.L. Martinez, A. Mandow, "Fuzzy tracking methods for mobile robots", Prentice-Hall, pp 347-364, 1997.
[8] Ollero, G. Ulivi, F. Cuesta, "Fuzzy logic applications in mobile robotics", Kluwer Academic Publishers, pp. 301–324, 1999.
[9] A. Ollero, B.C. Arrue, J. Ferruz, G. Heredia, F. Cuesta, F. Lopez-Pichaco, C. Nogales, "Control and perception components for autonomous vehicle guidance. Application to the ROMEO vehicles", Control Engineering Practice, Vol. 7, No. 10, pp 1291-1299, 1999.
[10] Saffiotti, "Fuzzy logic in autonomous robot navigation: a case study", Handbook of Fuzzy Computation, pp 180–197, 1998.

A Precise Control of Robot Manipulator with Eight D.O.F Based on Digital Signal Process

Hyun-Woo Song[1], Jae-Hyung Kim[2], Min-Seong Kim[3], Woo-Song Lee[4], Yeon-Guk Noh[5]

[1] Department of Mechatronics Engineering., Kyungnam University, Changwon, 51767, Korea
(E-mail : thgudn@naver.com)
[2] Department of Advanced Engineering., Kyungnam University, Changwon, 51767, Korea
(E-mail : wogud1151@naver.com)
[3] Department of Advanced Engineering., Kyungnam University, Changwon, 51767, Korea
(E-mail : kms21018@naver.com)
[4] SUNJIN Technology Co., Ltd., Changwon, 82331, Korea
(E-mail: elflws@nate.com)
[5] SFNT Co., Ltd., Changwon, 631-821, Korea (ykno1339@naver.com)

Abstract : We describe a new approach to the design and real-time implementation of an adaptive controller for robotic manipulator based on digital signal processors in this paper. The Texas Instruments DSPs(TMS320C80) chips are used in implementing real-time adaptive control algorithms to provide enhanced motion control performance for dual-arm robotic manipulators. In the proposed scheme, adaptation laws are derived from model reference adaptive control principle based on the improved direct Lyapunov method. The proposed adaptive controller consists of an adaptive feed-forward and feedback controller and time-varying auxiliary controller elements. The proposed control scheme is simple in structure, fast in computation, and suitable for real-time control. Moreover, this scheme does not require any accurate dynamic modeling, nor values of manipulator parameters and payload. Performance of the proposed adaptive controller is illustrated by simulation and experimental results for robot manipulator consisting of dual arm with four degrees of freedom at the joint space and cartesian space.

Keywords Selceted keywords relevant to the subject

1. INTRODUCTION

At recent there are mach advanced techniques that are suitable for servo control of a large class of nonlinear systems including robotic manipulators (P.C.V. Parks, 1966; Y.K.Choi et al., 1986; Y.M.Yoshhiko, 1995). Since the pioneering work of Dubowsky and DesForges (1979), the interest in adaptive control of robot manipulators has been growing steadily (T. C. Hasi, 1986; D. Koditschck, 1983; A. Koivo et al., 1983; S. Nicosia et al., 1984). This growth is largely due to the fact that adaptive control theory is particularly well-suited to robotic manipulators whose dynamic model is highly complex and may contain unknown parameters. However, implementation of these algorithms generally involves intensive numerical computations (J. J. Craig, 1988; H. Berghuis et al., 1993).

Current industrial approaches to the design of robot arm control systems treat each joint of the robot arm as a simple servomechanism. This approach models the time varying dynamics of a manipulator inadequately because it neglects the motion and configuration of the whole arm mechanism. The changes in the parameters of the controlled system are significant enough to render conventional feedback control strategies ineffective. This basic control system enables a manipulator to perform simple positioning tasks such as in the pick-and-place operation. However, joint controllers are severely limited in precise tracking of fast trajectories and sustaining desirable dynamic performance for variations of payload and parameter uncertainties (R. Ortega et al., 1989; P. Tomei, 1991). In many servo control applications the linear control scheme proves unsatisfactory, therefore, a need for nonlinear techniques is increasing.

Digital signal processors (DSP's) are special purpose microprocessors that are particularly suitable for intensive numerical computations involving sums and products of variables. Digital versions of most advanced control algorithms can be defined as sums and products of measured variables, thus can naturally be implemented by DSP's. DSPs allow straightforward implementation of advanced control algorithms that result in improved system control. Single and/or multiple axis control systems can be controlled by a single DSP. Adaptive and optimal multivariable control methods can track system parameter variations. Dual control, learning, neural networks, genetic algorithms and Fuzzy Logic control methodologies are all among the digital controllers implementable by a DSP (N. Sadegh et al., 1990; Z. Ma et al., 1995). In addition, DSP's are as fast in computation as most 32-bit microprocessors and yet at a fraction of their prices. These features make them a viable computational tool for digital implementation of advanced controllers. High performance DSPs with increased levels of integration for functional modules have become the dominant solution for digital control systems. Today's DSPs with performance levels ranging from 5 to 5400 MIPS are on the market with price tags as low as $3 (P. Bhatti et al., 1997; T. H. Akkermans et al., 2001). In order to develop a digital servo controller one must carefully consider the effect of the sample-and-hold operation, the sampling frequency, the computational delay, and that of the quantization error on the stability of a closed-loop system (S. A. Bortoff, 1994). Moreover, one must also consider the effect of disturbances on the transient variation of the tracking error as well as its steady-state value (F. Mehdian et al., 1995; S. H. Han et al., 1996).

This paper describes a new approach to the design of adaptive control system and real-time implementation using digital signal processors for robotic manipulators to achieve the improvement of speedness, repeating precision, and tracking performance at the joint and cartesian space. This paper is organized as follows : In Section Ⅱ, the dynamic model of the robotic manipulator is derived. Section Ⅲ derives adaptive control laws based on the model reference adaptive control theory using the improved Lyapunov second method. Section Ⅳ presents simulation and experimental results obtained for a dual-arm robot. Finally, Section Ⅴ discusses the findings and draws some conclusions.

2. MODELING

The dynamic model of a manipulator-plus-payload is derived and the tracking control problem is stated in this section.

Let us consider a nonredundant joint robotic manipulator in which the n×1 generalized joint torque vector τ(t) is related to the n×1 generalized joint coordinate vector q(t) by the following nonlinear dynamic equation of motion

$$D(q)\,\ddot{q} + N(q,\dot{q}) + G(q) = \tau(t) \quad (1)$$

where $D(q)$ is the n×n symmetric positive-definite inertia matrix, $N(q,\dot{q})$ is the n×1 coriolis and centrifugal torque vector, and $G(q)$ is the n×1 gravitational loading vector.

Equation (1) describes the manipulator dynamics without any payload. Now, let the n×1 vector X represent the end-effector position and orientation coordinates in a fixed task-related cartesian frame of reference. The cartesian position, velocity, and acceleration vectors of the end-effector are related to the joint variables by

$$\begin{aligned} X(t) &= \Phi(q) \\ \dot{X}(t) &= J(q)\,\dot{q}(t) \\ \ddot{X}(t) &= \dot{J}(q,\dot{q})\,\dot{q}(t) + J(q)\,\ddot{q}(t) \end{aligned} \quad (2)$$

where Φ(q) is the n×1 vector representing the forward kinematics and J(q) = ⌈∂Φ(q)/∂q⌉ is the n×n Jacobian matrix of the manipulator.

Let us now consider payload in the manipulator dynamics. Suppose that the manipulator end-effector is firmly grasping a payload represented by the point mass ΔM_p.For the payload to move with acceleration $\ddot{X}(t)$ in the gravity field, the end-effector must apply the n×1 force vector $T(t)$ given by

$$T(t) = \Delta M_p\,[\,\ddot{X}(t) + g\,] \quad (3)$$

where g is the n×1 gravitational acceleration vector.

The end-effector requires the additional joint torque

$$\tau_f(t) = J(q)^T\,T(t) \quad (4)$$

where superscript T denotes transposition. Hence, the total joint torque vector can be obtained by combining equations (1) and (4) as

$$J(q)^T\,T(t) + D(q)\,\ddot{q} + N(q,\dot{q}) + G(q) = \tau(t) \quad (5)$$

Substituting equations (2) and (3) into equation (5) yields

$$\Delta M_p\,J(q)^T\,[J(q)\,\ddot{q} + \dot{J}(q,\dot{q})\,\dot{q} + g] + D(q)\ddot{q} + N(q,\dot{q}) + G(q) = \tau(t) \quad (6)$$

Equation (6) shows explicity the effect of payload mass ΔM_p on the manipulator dynamics. This equation can be written as

$$[D(q)+\Delta M_p\,J(q)^T J(q)]\,\ddot{q} + [N(q,\dot{q}) + \Delta M_p J(q)^T\,\dot{J}(q,\dot{q})\,\dot{q}] + [G(q)+\Delta M_p J(q)^T g] = \tau(t) \quad (7)$$

where the modified inertia matrix $[D(q)+\Delta M_p J(q)^T J(q)]$ is symmetric and positive-definite. Equation (7) constitutes a nonlinear mathematical model of the manipulator-plus-payload dynamics.

3. ADAPTIVE CONTROL SCHEME

The manipulator control problem is to develop a control scheme which ensures that the joint angle vector q(t) tracks any desired reference trajectory $q_r(t)$,where $q_r(t)$ is an n×1 vector of arbitrary time functions. It is reasonable to assume that these functions are twice differentiable, that is, desired angular velocity $\dot{q}_r(t)$ and angular acceleration $\ddot{q}_r(t)$ exist and are directly available without requiring further differentiation of $q_r(t)$. It is desirable for the manipulator control system to achieve trajectory tracking irrespective of payload mass ΔM_p.

The controllers designed by the classical linear control scheme are effective in fine motion control of the manipulator in the neighborhood of a nominal operating point P_o . During the gross motion of the manipulator, operating point P_o and consequently the linearized model parameters vary substantially with time. Thus it is essential to adapt the gains of the feedforward, feedback, and PI controllers to varying operating points and payloads so as to ensure stability and trajectory tracking by the total control laws. The required adaptation laws are developed in this section. Fig. 1 represents the block diagram of adaptive control scheme for robotic manipulator.

Nonlinear dynamic equation (7) can be written as

$$\tau(t) = D^*(\Delta M_p, q, \dot{q})\,\ddot{q}(t) + N^*(\Delta M_p, q, \dot{q})\,\dot{q}(t) + G^*(\Delta M_p, q, \dot{q})\,q(t) \qquad (8)$$

where D^*, $N^*$and G^* are n×n matrices whose elements are highly nonlinear functions of ΔM_p,q,and $\dot{q}$.

In order to cope with changes in operating point, the controller gains are varied with the change of external working condition.

This yields the adaptive control law

$$\tau(t) = [P_A(t)\,\ddot{q}_r(t) + P_B(t)\,\dot{q}_r(t) + P_C(t)\,q_r(t)] + [P_V(t)\,\dot{E}(t) + P_P(t)\,E(t) + P_I(t)] \qquad (9)$$

where $P_A(t)$, $P_B(t)$, $P_C(t)$ are feedforward time-varying adaptive gains, and $P_P(t)$ and $P_V(t)$ are the feedback adaptive gains, and $P_I(t)$ is a time-varying control signal corresponding to the nominal operating point term, generated by a feedback controller driven b y position tracking error E(t) defined as $q_r(t) - q(t)$.

The gains of adaptive control low in equation (9) are defined as follows:

$$P_A(t) = a_1[p_{a1}E + p_{a2}\dot{E}][\ddot{q}_r]^T + a_2\int_0^t [p_{a1}E + p_{a2}\dot{E}][\ddot{q}_r]^T dt + p_a(0) \qquad (10)$$

$$P_B(t) = b_1[p_{b1}E + p_{b2}\dot{E}][\dot{q}_r]^T + b_2\int_0^t [p_{b1}E + p_{b2}\dot{E}][\dot{q}_r]^T dt + p_b(0) \qquad (11)$$

$$P_C(t) = c_1[p_{c1}E + p_{c2}\dot{E}][q_r]^T + c_2\int_0^t [p_{c1}E + p_{c2}\dot{E}][q_r]^T dt + p_c(0) \qquad (12)$$

$$P_I(t) = l_2[p_{i2}E] + l_1\int_0^t [p_{i1}E]\,dt + p_i(0) \qquad (13)$$

$$P_P(t) = p_1[p_{p1}E + p_{p2}\dot{E}][E]^T + p_2\int_0^t [p_{p1}E + p_{p2}\dot{E}][E]^T dt + p_p(0) \qquad (14)$$

$$P_V(t) = v_1[p_{v1}E + p_{v2}\dot{E}][\dot{E}]^T + v_2\int_0^t [p_{v1}E + p_{v2}\dot{E}][\dot{E}]^T dt + p_v(0) \qquad (15)$$

where $[p_{p1}, p_{v1}, p_{c1}, p_{b1}, p_{a1}]$ and $[p_{p2}, p_{v2}, p_{c2}, p_{b2}, p_{a2}]$ are positive and zero/positive scalar adaptation gains, which are chosen by the designer to reflect the relative significance of position and velocity errors E and $\dot{E}$.

4. SIMULATION AND EXPERIMENT

This section represents the simulation results of the position and velocity control of a four-link robotic manipulator by the proposed adaptive control algorithm, as shown in Fig.2, and discusses the advantages of using joint controller based-on DSPs for motion control of a dual-arm robot. The adaptive scheme developed in this paper will be applied to the control of a dual-arm robot with eighth axes. Fig.2 represents link coordinates of the dual-arm robot.

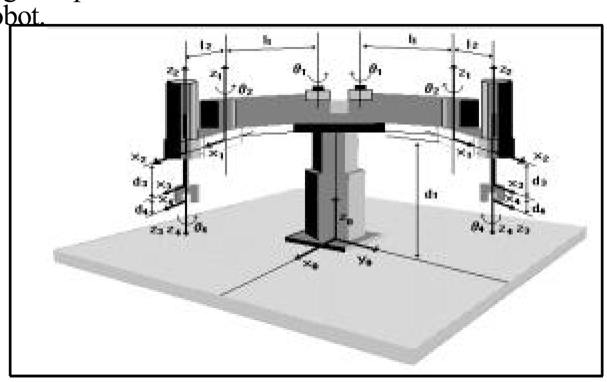

Fig.2. Link coordinates of dual-arm robot

Table Ⅰ Link parameters of robot.

Mass of link(kg)		Length of link(kg)		Inertia of link(kg)		Gear ratio of link	
m1	15.006 7	I1	0.35	I1	0.1538	r1	1/100
m2	8.994	I2	0.3	I2	0.0674	r2	1/80
m3	3.0	I3	0.175	I3	0.045	r3	1/200
m4	1.0	I4	0.007	I4	0.0016	r4	1/75
m5	15.06 7	I5	0.35	I5	0.1538	r5	1/100
m6	8.994	I6	0.3	I6	0.0674	r6	1/80
m7	3.0	I7	0.175	I7	0.045	r7	1/200
m8	1.0	I8	0.007	I8	0.0016	r8	1/75

Table Ⅱ Motor parameters of robot

Rotor inertia ($kg \cdot m^2$)		Torque constant (K m/a)		Back emf constant (V s/rad)		Amaturewinding resistance(ohms)	
Jm1	5.0031×10^{-5}	Ka1	21.4839×10^{-2}	Kb1	214.8592×10^{-3}	Ra1	1.5
Jm2	1.3734×10^{-5}	Ka2	20.0124×10^{-2}	Kb2	200.5352×10^{-3}	Ra2	4.2
Jm3	0.8829×10^{-5}	Ka3	20.0124×10^{-2}	Kb3	200.5352×10^{-3}	Ra3	9
Jm4	0.2256×10^{-5}	Ka4	17.6580×10^{-2}	Kb4	176.6620×10^{-3}	Ra4	20
Jm5	5.0031×10^{-5}	Ka5	21.4839×10^{-2}	Kb5	214.8592×10^{-3}	Ra5	1.5
Jm6	1.3734×10^{-5}	Ka6	20.0124×10^{-2}	Kb6	200.5352×10^{-3}	Ra6	4.2
Jm7	0.8829×10^{-5}	Ka7	20.0124×10^{-2}	Kb7	200.5352×10^{-3}	Ra7	9
Jm8	0.2256×10^{-5}	Ka8	17.6580×10^{-2}	Kb8	176.6620×10^{-3}	Ra8	20

B. Experiment

Fig. 3. Experimental set-up

The performance test of the proposed adaptive controller has been performed for the dual-arm robot at the joint space and cartesian space. At the cartesian space, it has been tested for the peg-in-hole tasks, repeating precision tasks, and trajectory tracking for B-shaped reference trajector. At the joint space, it has been tested for the trajectory tracking of angular position and velocity for a dual-arm robot made in Samsung Electronics Company in Korea. Fig.3 represents the experimental set-up equipment. To implement the proposed adaptive controller, we used our own developed TMS320C80 assembler software. Also, the TMS320C80 emulator has been used in experimental set-up. At each join to a dual-arm robot, a harmonic drive (with gear reduction ratio of 100 : 1 for joint 1 and 80 : 1 for joint 2) has been used to transfer power from the motor, which has a resolver attached to its shaft for sensing angular velocity with a resolution of 8096 (pulses/rev). Fig. 4 represents the schematic diagram of control system of dual-arm robot. And Fig. 5 represents the block diagram of the interface between the PC, DSP, and dual-arm robot.

The performance test in the joint space is performed to evaluate the position and velocity control performance of the four joints under the condition of payload variation, inertia parameter uncertainty, and change of reference trajectory.

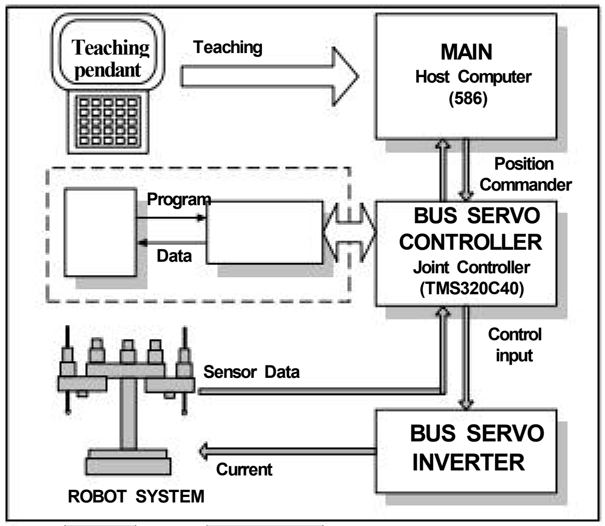

Fig. 4. The block diagram of the interface between the PC. DSP, and dual-arm robot.

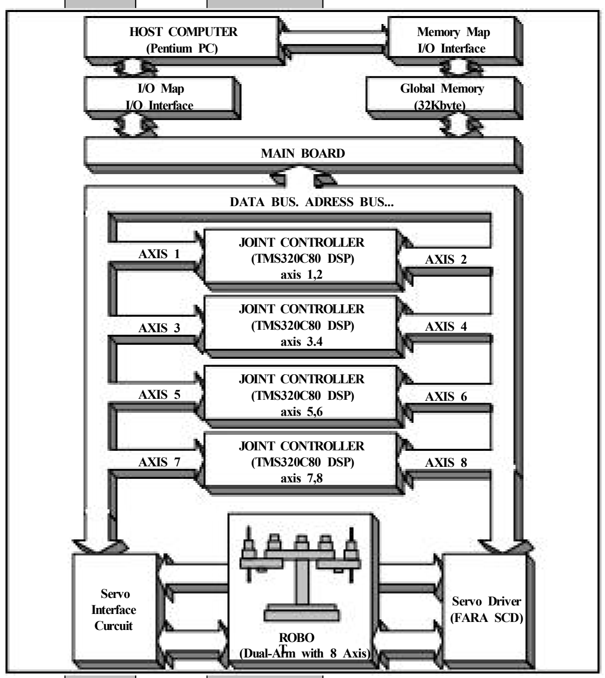

Fig. 5. The schematic diagram control system of dual-arm robot.

Fig.6 represents the B-shaped reference trajectory in the cartesian space. Fig. 7 shows the experimental results of the position and velocity control at the first joint with payload 4 kg and the change of reference trajectory. Fig. 8 shows the experimental results for the position and velocity control at the second joint with 4 kg payload. Fig.'s 9 and 10 show the experimental results for the position and velocity control of the PID controller with 4 kg payload. As can be seen from these results, the DSP-based adaptive controller shows extremely good control performance with some external disturbances. It is illustrated that this control scheme shows better control performance than the exiting PID controller, due to small tracking error and fast adaptation for disturbance.

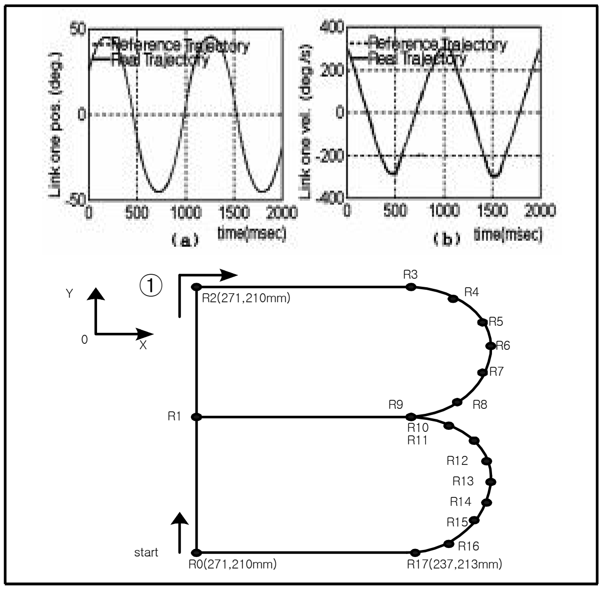

Fig. 6. The B shaped reference trajectory in the cartesian space.

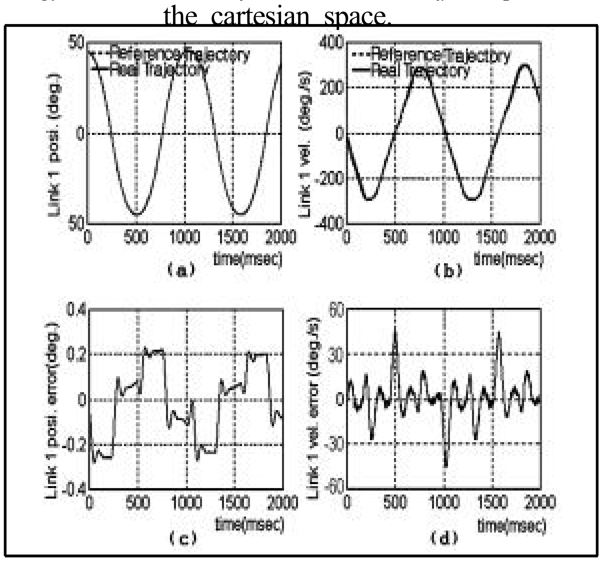

Fig. 7. (a)-(d) Experimental results for the position and velocity tracking of adaptive controller at the first joint with 4kg payload.

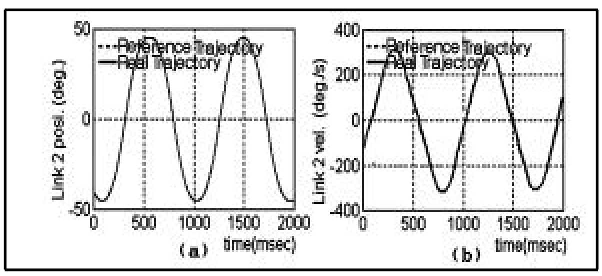

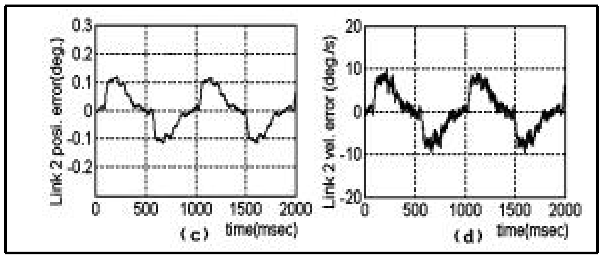

Fig. 8. (a)-(d) Experimental results for the position and velocity tracking of adaptive controller at the second joint with 4kg payload.

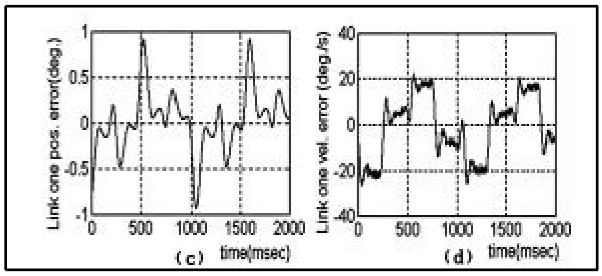

Fig. 9. (a)-(d) Experimental results of PID controller for the position and velocity tracking at the first joint with 4kg payload.

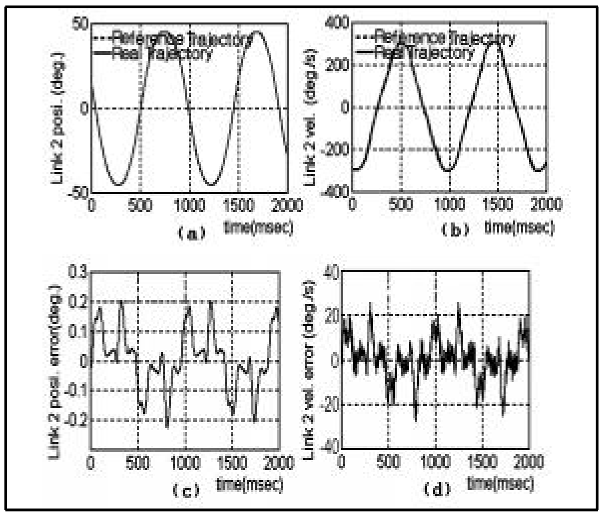

Fig. 10. (a)-(d) Experimental results of PID controller for the position and velocity tracking at the second joint with 4kg payload.

5. DISCUSSION AND CONCLUSIONS

A new adaptive digital control scheme is described in this paper using DSP(TMS320C80) for robotic manipulators. The adaptation laws are derived from the direct adaptive technique using the improved Lyapunov second method. The simulation and experimental results show that the proposed DSP-adaptive controller is robust to the payload variation, inertia parameter uncertainty, and change of reference trajectory. This adaptive controller has been found to be suitable to the real-time control of robot system. A novel feature of the proposed scheme is the utilization of an adaptive feedforward controller, an adaptive feedback controller, and a PI type time-varying control signal to the nominal operating point which result in improved tracking performance. Another attractive feature of this control scheme is that, to generate the control action, it neither requires a complex mathematical model of the manipulator dynamics nor any knowledge of the manipulator parameters and payload. The control scheme uses only the information contained in the actual and reference trajectories which are directly available. Futhermore, the adaptation laws generate the controller gains by means of simple arithmetic operations. Hence, the calculation control action is extremely simple and fast. These features are suitable for implementation of on-line real-time control for robotic manipulators with a high sampling rate, particularly when all physical parameters of the manipulator cannot be measured accurately and the mass of the payload can vary substantially. The proposed DSP-based adaptive controllers have several advantages over the analog control and the micro-computer based control. This allows instructions and data to be simultaneously fetched for processing. Moreover, most of the DSP instructions, including multiplications, are performed in one instruction cycle. The DSP tremendously increase speed of the controller and reduce computational delay, which allows for faster sampling operation. It is illustrated that DSPs can be used for the implementation of complex digital control algorithms, such as our adaptive control for robot systems.

REFERENCES

[1] P.C.V. Parks, July 1966, "Lyapunov Redesign of Model Reference Adaptive Control System," IEEE Trans. Auto. Contr., Vol. AC-11, No. 3, pp. 362-267.

[2] Y.K. Choi, M.J. Chang, and Z. Bien, 1986, "An Adaptive Control Scheme for Robot Manipulators." IEEE Trans. Auto. Contr., Vol. 44, No. 4, pp. 1185-1191.

[3] Y.M. Yoshhiko, June 1995, "Model Reference Adaptive Control for Nonlinear System with unknown Degrees, "In the proceeding of American Control Conference, pp.2505-2514, Seatle.

[4] S. Dubowsky, and D.T. DesForges, 1979, "The Application of Model Reference Adaptation Control to Robot Manipulators," ASME J. Dyn. Syst., Meas., Contr., Vol. 101, pp. 193-200.

[5] T.C. Hasi, 1986, "Adaptive Control Scheme for Robot Manipulators-A Review." In Proceeding of the 1987 IEEE Conference on Robotics and Automation, SanFransisco,CA.

[6] D. Koditschek, 1983, "Quadratic Lyapunov Functions for Mecanical Systems," Technical Report No. 8703, YaleUniversity,NewHaven,CT. A. Koivo and T. H. Guo, 1983, "Adaptive Linear Controller for Robot Manipulators." IEEE Transactions and Automatic Control, Vol. AC-28, pp. 162-171.

[7] S. Nicosia and P. Tomee, 1984, "Model Reference Adaptive Control Algorithm for Imdustrial Robots," Automatica, Vol. 20, No. 5, pp. 635-644.

[8] J. J. Craig, 1988, "Adaptive Control of Meduanical Manipulator," Addison-wesley. H. Berghuis, R.Orbega, and H.Nijmeijer, 1993, "A Robust Adaptive Robot controller," IEEE Trans., Robotics and Automation, Vol. 9, No. 6, pp. 825-830.

[9] R. Ortega and M.W. Spong, 1989, "Adaptive Motion Control of Rigid Robots: A Tutorial," Automatica, Vol. 25, pp. 877-888.

[10] P. Tomei, Aug. 1991, "Adaptive PD Controller for Robot Manipulators," IEEE Trans. Robotics and Automation, Vol.7, No.4.

[11] N. Sadegh and R. Horowitz, Aug. 1990, "An Exponentially Stable Adaptive Control Law for Robot Manipulators," IEEE Trans. Robotics and Automation, Vol. 9, No. 4.

[12] Z. Ma, J. shen, A. Hug, and K. Nakayama, October 1995, "Automatic optimum Order Assignment in Adaptive Filters," international conference on signal Processing Applications & Technology, Bostonpp.629-633.

[13] T. A. Lasky and T. C. Hsia, July 1994, "Application of a Digital Signal Processor in Compliant Control of an Industrial Manipulator," Proceedings of American Control Conference.

[14] K. Michael and P. Issa, June 1995, "Digital Signal Processor : A Control Element," In Proceedings of American Control Conference, Seatle, pp. 470-474.

[15] S. A. Bortoff, Feb. 1994, "Advanced Nonlinear Robotic Control Using Digital Signal Processing," IEEE Trans. Indust. Elect., Vol. 41, No. 1.

[16] F. Mehdian and M. Wirth, June 1995, "Adaptive Control of Robotic Manipulators Using DSPs," In Proceedings of American Control Conference, Seatle, pp.480-481.

[17] S. H. Han, J. Lee, D. Ahn, M. Lee, and K. Son, July 1996, "Implementation of Robust Adaptive Controller of Robotic Manipulator using DSPs, "In Proceedings of Eleventh International Conference on System engineering, Lasvegas, pp. 668-673.

[18] T. H. Akkermans and S. G. Stan, 2001, “Digital servo IC for optical disc drives”, Contr. Eng. Pract., vol. 9, no. 11, pp. 1245-1253.

A Study on Robust Motion Control of Robot Arm Based on Neurel Network

Jae-Hyung Kim[1], Min-Seong Kim[2], Hyun-Min Kim[3], Se-Han Lee[4], Uhn-Joo Nah[4], Sung-Hyun Han[4]

[1] Department of Advanced Engineering., Kyungnam University, Changwon, 51767, Korea
(E-mail : wogud1151@naver.com)
[2] Department of Advanced Engineering., Kyungnam University, Changwon, 51767, Korea
(E-mail : khm9153@nate.com)
[3] Department of Advanced Engineering., Kyungnam University, Changwon, 51767, Korea
(E-mail : kms21018@naver.com)
[4] School of Mechanical Engineering, Kyungnam University, Changwon, 51767, Korea
(E-mail: leesehan@kyungnam.ac.kr/uhnjoona@kyungnam.ac.kr/shhan@kyungnam.ac.kr)

Abstract : This paper presents two kinds of adaptive control schemes for robot manipulator which has the parametric uncertainties. In order to compensate these uncertainties, we use the neural network (NN) system that has the capability to approximate any nonlinear function over the compact input space. In the proposed control schemes, we need not derive the linear formulation of robot dynamic equation and tune the parameters. We also suggest the robust adaptive control laws in all proposed schemes for decreasing the effect of approximation error. To reduce the number of neural of network, we consider the properties of robot dynamics and the decomposition of the uncertainty function. The proposed controllers are robust not only to the structured uncertainty such as payload parameter, but also to the unstructured one such as friction model and disturbance. The validity of the control scheme is shown by computer simulations and experiment of dual-arm robot manipulator.

Keywords daptive tracking control, decomposition, neural network systems, robot dynamics, uncertainty.

1. INTRODUCTION

In the recent decade, increasing attention has been given to the tracking control of robot manipulators. Tracking control is needed to make each joint track a desired trajectory. A lot of research has dealt with the tracking control problem. Robots have to face many uncertainties in their dynamics, in particular structured uncertainty, such as payload parameter, and unstructured one, such as friction and disturbance. It is difficult to obtain the desired control performance when the control algorithm is only based on the robot dynamic model. To overcome these difficulties, in this paper we propose the adaptive control schemes which utilize a neural network as a compensator for any uncertainty. To reduce the error between the real uncertainty function and the compensator, we design simple and robust adaptive laws based on Lyapunov stability theory. In the proposed control schemes, the NN compensator has to see many neural because uncertainties depend on all state variables. To overcome this problem, therefore, we introduce the control schemes in which the number of neural of the NN compensator can be reduced by using the properties of robot dynamics and uncertainties. By computer simulations, it is verified that the NN is capable to compensate the uncertainties of robot manipulator.

2. ADAPTIVE CONTROL USING NEURAL NETWORK COMPENSATOR

The considered tracking problem is stated as follows: Knowing desired trajectories $q_d \in R^n, \dot{q}_d \in R^n$ with some or all the manipulator parameters unknown, determine a control law τ and a sliding surface $s = 0$ such that sliding mode occurs on the sliding surface, the tracking error $\tilde{q} = q - q_d$ has a prescribed transient response and it goes to zero asymptotically as $t \to \infty$.

A. Simple Adaptive Control Law

The sliding surface $s = 0$ is chosen as a hyperplane

$$s = \dot{\tilde{q}} + \Lambda \tilde{q} \quad (1)$$

where Λ is a positive-definite matrix whose eigenvalues are strictly in the right-half complex plane and $\tilde{q}$ is the tracking error vector.

If the sliding mode exists on $s = 0$, then from the theory of VSS, the sliding mode is governed by the following linear differential equation whose behavior is dictated by the sliding hyperplane design matrix Λ:

$$\dot{\tilde{q}} = -\Lambda \tilde{q} \quad (2)$$

$$\dot{q}_r(t) = \dot{q}_d(t) - \Lambda \tilde{q}(t) \quad (3)$$

Consider now the uncertainties of robot manipulator, (1) can be rewritten as

$$D(q)\ddot{q} + C(q, \dot{q})\dot{q} + G(q) + F(q, \dot{q}, t) = \tau \quad (4)$$

where $F(q, \dot{q}, t) = F_r(\dot{q}) + \tau_d$ However, in this paper, this uncertainty function vector has to be replaced by $F(q, \dot{q}, t)$ because it should represent not only friction and disturbance but also the payload variation, and D, C, G contain the payload parameter. So (4) can be rewritten as

$$D(q)\ddot{q}+C(q,\dot{q})\dot{q}+G(q)+F(q,\dot{q},\ddot{q},t)=\tau \quad (5)$$

In order to derive a control law and use a neural network with an adaptive mechanism, we let a Lyapunov function candidate be

$$V(t)=\frac{1}{2}\left(s^{T}Ds+\sum_{i=1}^{n}\tilde{\Theta}_i^{T}\Gamma_i\tilde{\Theta}_i\right) \quad (6)$$

Where $\tilde{\Theta}_i=\Theta_i^{*}-\Theta_i$, Θ^{*} is the j th column vector of the optimal parameter matrix Θ^{*} and Γ_i is a strictly positive real constant.

Differentiating $V(t)$ with respect to time yields

$$\dot{V}(t)=s^{T}D\dot{s}+\frac{1}{2}s^{T}\dot{D}s+\sum_{i=1}^{n}\tilde{\Theta}_i^{T}\Gamma_i\dot{\tilde{\Theta}}_i \quad (7)$$

$$=-s^{T}(D\ddot{q}_r+C\dot{q}_r+G+F-\tau)+\sum_{i=1}^{n}\tilde{\Theta}_i^{T}\Gamma_i\dot{\tilde{\Theta}}_i$$

Where $F(q,\dot{q},\ddot{q},t)$ is a completely unknown nonlinear function vector. Therefore, we replace $F(q,\dot{q},\ddot{q},t)$ by a Neural network $\hat{F}(q,\dot{q},\ddot{q}|\Theta)$. Let us define the control law as

$$\tau=D(q)\ddot{q}_r+C(q,\dot{q})\dot{q}_r+G(q)+\hat{F}(q,\dot{q},\ddot{q}|\Theta)-K_Ds \quad (8)$$

Where $K_d=diagK_i$, $i=1,2,\dots,n$ and

$$\hat{F}(q,\dot{q},\ddot{q}|\Theta)=\begin{bmatrix}\Theta_1^{T}\zeta(q,\dot{q},\ddot{q})\\ \Theta_2^{T}\zeta(q,\dot{q},\ddot{q})\\ \dots\\ \dots\\ \dots\\ \Theta_n^{T}\zeta(q,\dot{q},\ddot{q})\end{bmatrix} \quad (9)$$

Letting the optimal parameter matrix of the NN, we can define the minimum approximation error vector

$$w=F(q,\dot{q},\ddot{q},t)-\hat{F}(q,\dot{q},\ddot{q}|\Theta) \quad (10)$$

where $\tilde{\Theta}_i=\Theta_i^{*}-\Theta_i$ and $\zeta(q,\dot{q},\ddot{q})$ is a neural network basis function. Therefore, the adaptation laws are

$$\dot{\Theta}_i=-\Gamma_i^{-1}s_i\zeta(q,\dot{q},\ddot{q}),\ i=1,2,\dots n \quad (11)$$

Then

$$\dot{V}(t)=-s^{T}K_Ds-s^{T}w \quad (12)$$

$D(q)\ddot{q}+C(q,\dot{q})\dot{q}+G(q)+F_r(\dot{q})+\tau_d+c(q,\dot{q},\ddot{q},t)=\tau$ in Fig. 1.Because the term $s^{T}w$ is of the order of the minimum approximation error and from the universal approximation theorem, it is expected that w should be very small, i.e., $w\le\varepsilon$, if not equal to zero in the adaptive neural network system. The proposed control scheme is shown

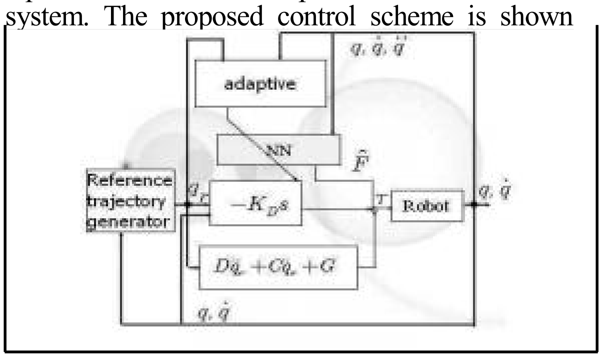

Fig. 1. the structure of the control systems

B. Robust Adaptive Control Law

Equation (12) contains the term $s^{T}w$; in this subsection, we propose the robust control law to reduce the approximation error. So we add a term to (12) as follows:

$$\tau=D(q)\ddot{q}_r+C(q,\dot{q})\dot{q}_r+G(q)+\hat{F}(q,\dot{q},\ddot{q}|\Theta)-K_Ds-W.sign(s) \quad (13)$$

Where

$$W=diag\left[w_{M1},w_{M2},w_{M3},\dots,w_{Mn}\right]$$
$$w_{Mi}\ge|w_i|,\ i=1,2,\dots,n$$

Now consider the Lyapunov candidate (6) as well as (11) and (13) and, after straightforward manipulation, we obtain the time derivative as follows:

3. NEURAL REDUCTION ALGORITHM

In Section 2, friction and disturbance can be represented by $F(\dot{q},t)$ and $F(q\dot{},q,t)$. But uncertainty of payload variation must be $F(q,\dot{q},\ddot{q},t)$. where we can represent

$$F(q,\dot{q},\ddot{q},t)=F_1(q,\dot{q},t)+F_2(q,\ddot{q},t) \quad (15)$$

and where

$$F_1(q,\dot{q},t)=c_c[C(q,\dot{q})\dot{q}]+c_G[G(q)]+F_r(\dot{q})+\tau_d \quad (16)$$
$$F_2(q,\ddot{q},t)=C_D[D(q)\ddot{q}]$$

The resulting control and adaptive laws are as follows:

$$\tau=D\ddot{q}_r+C\dot{q}_r+G+\hat{F}_1(q,\dot{q}\mid\Theta_1)+\hat{F}_2(q,\ddot{q}\mid\Theta_2)-K_Ds \quad (17)$$

$$\dot{\Theta}_{i1}=-\Gamma_i^{-1}s_i\zeta_i(q,\dot{q}),\ i=1,2,\dots n$$
$$\dot{\Theta}_{i2}=-\Gamma_i^{-1}s_i\zeta_i(q,\ddot{q}),\ i=1,2,\dots n \quad (18)$$

Now let a Lyapunov function candidate as

$$D(q)\ddot{q}+C(q,\dot{q})\dot{q}+G(q)+F_r(q,\dot{q}q,\dot{q},t)+\tau_d+C(q,\dot{q},\ddot{q},t)=\tau$$

$$V(t)=\frac{1}{2}\left(s^{T}Ds+\sum_{i=1}^{n}\tilde{\Theta}_{i1}^{T}\Gamma_i\tilde{\Theta}_{i1}+\sum_{i=1}^{n}\tilde{\Theta}_{i2}^{T}\Gamma_i\tilde{\Theta}_{i2}\right) \quad (19)$$

So

$$\dot{V}(t)=-s^{T}(D\ddot{q}_r+C\dot{q}_r+G+F-\tau)+\sum_{l=1}^{n}\tilde{\Theta}_{l1}^{T}\Gamma_l\dot{\tilde{\Theta}}_{l1}+\sum_{l=1}^{n}\tilde{\Theta}_{l2}^{T}\Gamma_l\dot{\tilde{\Theta}}_{l2} \quad (20)$$

Then, we let the minimum approximation errors to be as follows:

$$w_1=F_1(q,\dot{q},t)-\hat{F}(q,\dot{q}|\Theta_1^{*})$$
$$w_2=F_2(q,\ddot{q},t)-\hat{F}(q,\ddot{q}|\Theta_2^{*})$$

Substituting (17), (18), and (19) into (20), and after straightforward manipulation, we obtain the time derivative as follows:

$$\dot{V}(t)=-s^{T}K_Ds-s^{T}(w_1+w_2)$$

Therefore, the closed-loop system is stable. The robust control law is as follows

$$\tau=D\ddot{q}_r+C\dot{q}_r+G+\hat{F}_1(q,\dot{q}|\Theta_1)+\hat{F}_2(q,\ddot{q}|\Theta_2)-K_Ds-Wsign(s) \quad (21)$$

where

$$W=diag\left[w_{M1},w_{M2},w_{M3},\dots,w_{Mn}\right]$$
$$w_{Mi}\ge|w_l|,\ i=1,2,\dots,n$$

In Fig. 1, the structure of the neural

network, $\hat{F}$ is as follows:

$$\hat{F}(q,\dot q,\ddot q|\Theta) = \begin{bmatrix} \hat{F}_1(q,\dot q|\Theta_1) \\ \hat{F}_1(q,\dot q|\Theta_1) + \hat{F}_2(q,\ddot q|\Theta_2) \\ \vdots \\ \hat{F}_n(q,\dot q|\Theta_n) + F_n(q,\ddot q|\Theta_n) \end{bmatrix} \quad (22)$$

Therefore we use the structure of the neural network to compensate friction, disturbance and variation of payload as follows:

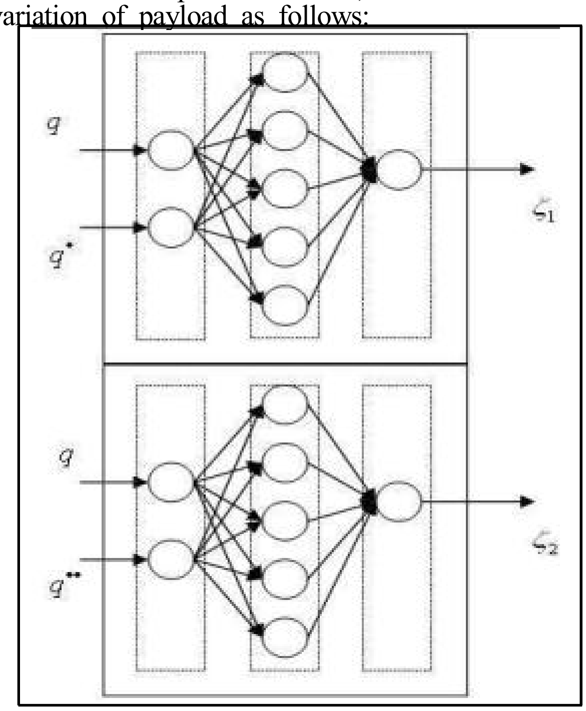

Fig. 2. The structure of a neural network compensating friction, disturbance and variation of payload

$$\hat{F}(q,\dot q,\ddot q|\Theta) = \hat{F}_1(q,\dot q|\Theta_1) + \hat{F}_2(q,\ddot q|\Theta_2)$$

4. SIMULATION and EXPERIMENT

4.1 Simulation

The model chosen for simulation is a two-link planar robot manipulator.

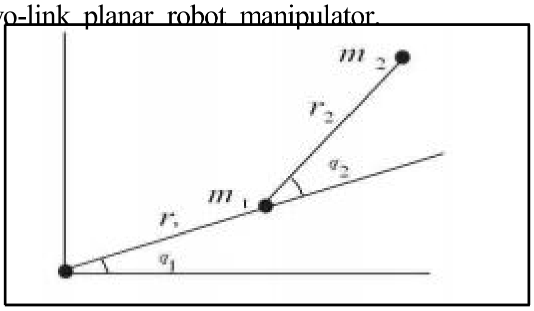

Fig. 3. Two-link planar robot manipulator

The dynamic equation can be derived by using the Euler－Lagrangian method as follows:

$$\begin{bmatrix} D_{11} & D_{12} \\ D_{21} & D_{22} \end{bmatrix}\begin{bmatrix} \ddot q_1 \\ \ddot q_2 \end{bmatrix} + \begin{bmatrix} -C_{12}\dot q_2 & -C_{12}(\dot q_1 + \dot q_2) \\ C_{12}\dot q_1 & 0 \end{bmatrix}\begin{bmatrix} \dot q_1 \\ \dot q_2 \end{bmatrix} + \begin{bmatrix} G_1(q_1,q_2) \\ G_2(q_1,q_2) \end{bmatrix} = \begin{bmatrix} \tau_1 \\ \tau_2 \end{bmatrix}$$

Figs. 4 and 5. show the simulation results of the case of all uncertainties, respectively.

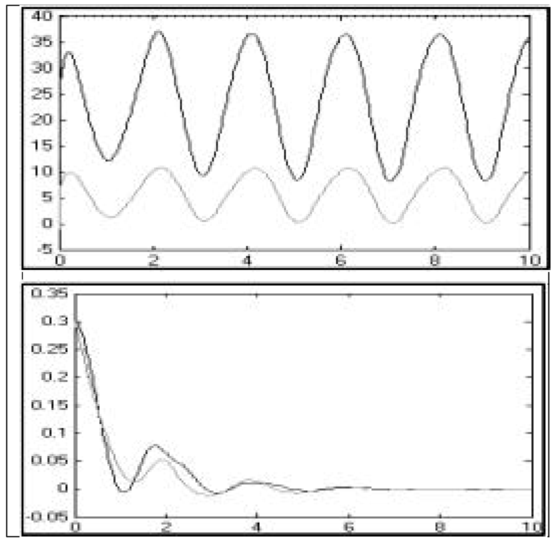

Fig. 4. The input torques τ_1, τ_2 and state errors of the joints in the case of all uncertainties using simple adaptive control

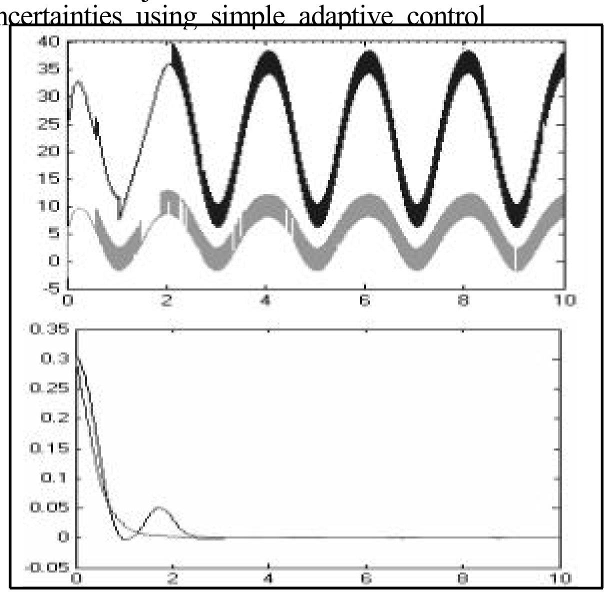

Fig. 5. The input torques τ_1, τ_2 and state errors of the joints in the case of all uncertainties using robust adaptive control

5.2 Experiment

We also apply real-time adaptive control based on neural network compensator to dual-arm robot.

The desired trajectories are

$$q_{1d} = q_{2d} = \frac{15\pi}{300\pi}\sin\left(\frac{2\pi}{3}t\right)$$

and the results of robust adaptive control are shown below

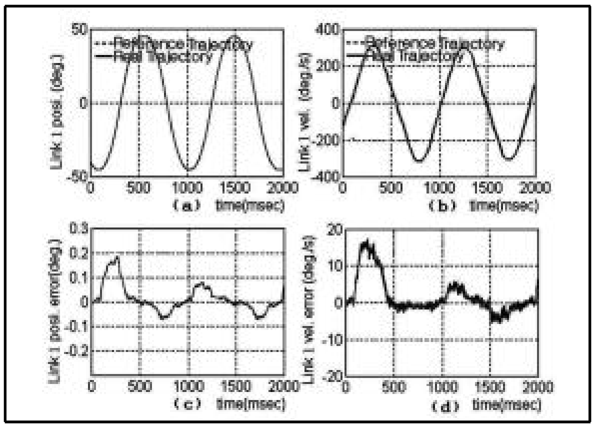

Fig. 6. (a)-(d) Experimental results for the position and velocity tracking of adaptive controller at the first joint.

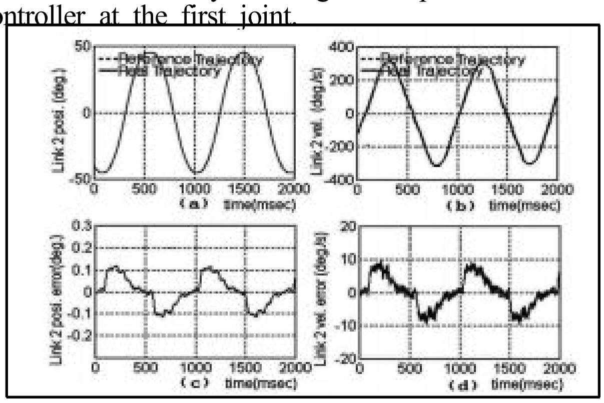

Fig. 7. (a)-(d) Experimental results for the position and velocity tracking of adaptive controller at the second joint.

5. CONCLUSIONS

In the results, we can see that the control objective is well accomplished and the neural network compensate the uncertainties. In all cases, robust control schemes are more effective than simple. The simulation and experimental results show that the neural network compensator - adaptive controller is robust to the payload variation, inertia parameter uncertainty, and change of reference trajectory.

REFERENCES

[1] G. Jumarie, "Tracking control of mechanical systems via sliding Lagrangian," J. Intell. Robotic Syst., vol. 13, pp. 181–199, 1995.

[2] C. Y. Su and T. P. Leung, "A sliding mode controller with bound estimation for robot manipulators," IEEE Trans. Robotics Automat., vol. 9, no. 2, pp. 208–214, 1993.

[3] J. E. Slotin and S. S. Sastry, "Tracking control of nonlinear systems using sliding surfaces, with application to robot manipulators,"Int. J. Contr., vol. 38, no. 2, pp. 465–492, 1983.

[4] J. J. E. Slotine and W. Li, Applied Nonlinear Control. Englewood Cliffs, NJ: Prentice-Hall, 1991.

[5] F. L. Lewis, C. T. Abdallah, and D. M. Dawson, Control of Robot Manipulators. London, U.K.: Macmillan, 1993.

[6] M. W. Spong, Robot Dynamics and Control. New York: Wiley, 1989.

[7] J. E. Slotine and W. Li, "On the adaptive control of robot manipulators," Int. J. Robotics Res., vol. 6, no. 3, pp. 49–59, 1987.

[8] W. C. Ham, "Adaptive nonlinear control of one-link flexible arm," in IEEE/RSJ Int. Conf. Intelligent Robots and Systems, vol. 1, Yokohama, Japan, 1993, pp. 3–7.

[9] "Adaptive control based on explicit model of robot manipulators," IEEE Trans. Automat. Contr., vol. 38, pp. 654–658, 1993.

A Flexible Control of Robot Hand Fingers with Six Joints

Dong-Hwa Jeong1, Min-Seong Kim2, Gi-Su Shin3, Se-Han Lee4

[1] Department of Amechnical Fusion Engineering., Kyungnam University, Changwon, 51767, Korea
(E-mail : dsds6859@naver.com)
[2] Department of Advanced Engineering., Kyungnam University, Changwon, 51767, Korea
(E-mail : kms21018@naver.com)
[3] ANY TOY CO. Ltd., Kyungnam University, Changwon, 51767, Korea
(E-mail : Shings@naver.com)
[4] School of Mechanical Engineering, Kyungnam University, Changwon, 51767, Korea
(E-mail: leesehan@kyungnam.ac.kr)

Abstract : Recently Manipulation capability is important for a robot. Interaction between a robot hand and objects can be properly controlled only is suitable sensors are available. Recently the tendency is to create robot hands more compact and high integrated sensors system, in order to increase the grasping capability and in order to reduce cabling through the finger, the palm and the arm. As a matter of fact, miniaturization and cabling harness represents a significant limitation to the design of small sized embedded sensor. Ongoing work is focusing on a flexible manipulation system, which consists of a dual flexible multi-fingered hand-arm system, and a dual active vision system.

Keywords hand controller, robot hand.

1. INTRODUCTION

Recently Manipulation capability is important for a robot. Interaction between a robot hand and objects can be properly controlled only is suitable sensors are available. In particular, information about the forces applied at the contact, the contact location, other indirect measurements, e.g. estimate of mass object, its inertia ellipsoid, or even non mechanical measurements, may play a crucial role to implement secure grasp and safe manipulation tasks. In the past two decades several robot hands and dexterous grippers have been developed. The major goals have been on one hand that of studying and implement newer mechanical solutions in order to increase miniaturization and dexterity, and, on the other, to investigate manipulation models and control techniques. At mechanical level study on dextrous grippers has mainly focused on the actuation and kinematics aspects. With very few exceptions (e.g. [7]-[9]), tendon actuated mechanisms, and their numerous variants, still represent an effective way to implement compact manipulators. Actuation of tendon based robot grippers poses various technical problems. Tendons coupling on one hand, friction and elasticity on the other, pose important problems for the control of tendon actuated mechanisms. However, the mechanical accuracy required to design a miniature (e.g. human sized) dextrous gripper, is by far less than an equivalent design based on gears or other stiff transmission mechanism. Recently the tendency is to create robot hands more compact and high integrated sensors system, in order to increase the grasping capability and in order to reduce cabling through the finger, the palm and the arm. As a matter of fact, miniaturization and cabling harness represents a significant limitation to the design of small sized embedded sensor.

The major contribution of this paper is to present the design of a fully integrated tactile and 3-axis force sensor, with embedded electronics. The approach adopted has been that of using low cost components available off-the-shelf, and to pursue a highly modular sensor design. The system is scalable and designed to be integrated on the supporting three-finger hand. In particular, two identical sensors are mounted on each finger, one for phalange. The structure of this paper is as follows. In section 2, the hand system design is described. Then, in section 3 the basics of the contact-sensing problem are discussed. The modular structure of the sensor is presented and detailed in sections 4. Conclusions & Result are finally discussed in section 5, 6.

2. HAND DESIGN

The mechanism of a flexible hand gripper requires the mass of the hand should be as low as possible. It is highly desirable that the hand weigh less than 1kg. Furthermore the low mass of the finger mechanism is desirable not only to achieve flexible motion but also for stable control.

Our philosophy about dynamic manipulation is maximization of the power and minimization of the mechanism. In particular four factors are important: (1)light weight, (2) high speed and high acceleration, (3) accuracy, (4) possibilities of flexible grasping. Fig. 1 shows the mechanical design of the hand, and Fig. 2

shows a scene of the Gripper control. We used three fingers, which is the minimum number to achieve a stable grasp. Each of fingers has 4 degrees of freedom (D.O.F); the hand system has 13 D.O.F included 1 D.O.F on the hand link. Note that the Joint 4 consists of the linear motor so that the finger tip can move as slide but other links just moving as rotate around a horizontal axis. In general a hand needs 9 D.O.F to move a target to any position and orientation. But our hand has 13 D.O.F so that the applications are very wide in the working environments, and the fingers are arranged so as to grasp the objects like circular and prismatic, etc. In order to achieve “lightning” high acceleration, we have developed a new actuator that allows a large current flow for a short time. Table 1 shows the specification for the actuator.

The finger has strain gauges at the joint 1 and joint 2 for force control. In addition a 6-axis force/torque sensor and a tactile sensor are mounted on each fingertip.

Table. 1. The specification of actuator

Motor type	Coreless DC Motors (Swiss MAXON Motor)
Operating Voltage [V]	12~16
Max. Holding torque [Kgf.cm]	38.5
Max. Speed [sec/60deg]	0.167
Weight [g]	66
Size [mm]	40 x 31 x 37
Gear Ratio	193
Position Resolution	1024
Operating Angle [deg]	300

The flexible motion imposes a heavy load on the finger mechanism. For this reason a simple mechanism should be used for reduction gear, transmission, etc. In most traditional hand systems a wire-driven mechanism is used. But this is not suitable for a lightweight mechanism, because it is large and complicated.

In our hand a newly developed small harmonic drive gear and a high-power mini actuator are fitted in each finger link and all of these parts are hidden in the plastic case. A harmonic drive gear has desirable properties for control such as no backlash and a high reduction rate.

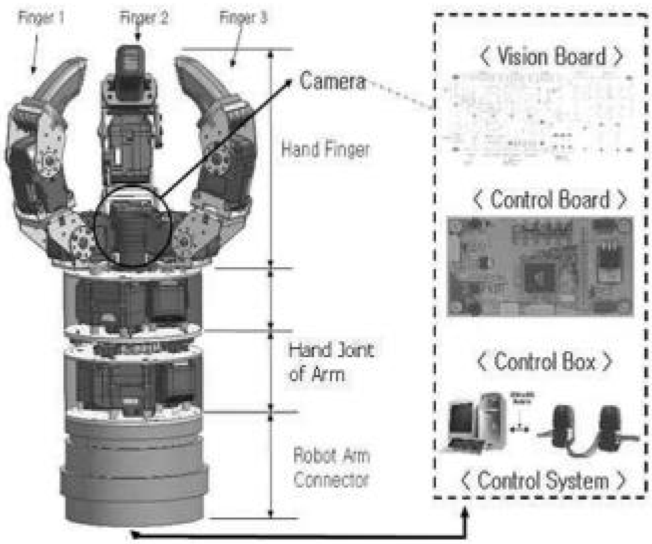

Fig. 1: Scene of the hand gripper control

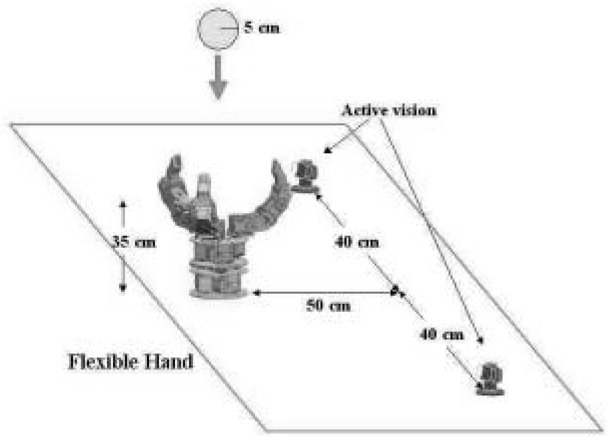

Fig. 2: Visual feedback control system

The hand system consists of a camera at the center position as shown in Fig. 1 or can be added the dual vision system, as shown in Fig. 2. Following the purpose of this paper; we discus about the system set up in Fig. 2. Vision is with a massive parallel vision system called column-parallel high-speed vision system [2].

Early image processing is performed in order to achieve segmentation of the image, extraction of the target area, and computation of the image moments. From these data, the position of the target is computed; each vision sensor is mounted on an active vision.

2.1 Force Sensor Design

Manipulation control requires in general some sort of feedback which could provide information about the interactions occurring during contact between the gripper and the grasped object. Assumptions must be made about the nature of the contact and, on the base of the selected contact models, it is possible to specify the nature of feedback required to properly control the interaction. Detailed contact mechanics models are in general too complex to be taken into account in real-time control applications. In practice, simplified lumped parameter models are usually considered, [4]. In the soft finger model it is assumed that also a torque, aligned with the normal to the surfaces in contact, arises. The model equations for these models are:

$$\begin{cases} f = p \\ m = q + c \times p \end{cases} \qquad (1)$$

Where p and q are the contact force and torque (for soft finger models only), c is the contact location, and f and m are the measured force and torque. Bicchi and Salisbury, [4], proposed procedures for computing p and q on the base of the measurements f and m. However a precise geometric model of the pressure (the robot finger) is required, and, except the case of simple geometries, the method is computationally intensive and critical for real-time implementation.

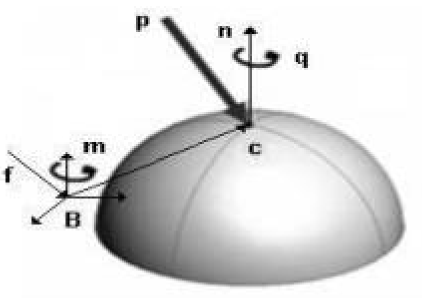

Fig. 3. Point of contact (q=0) and soft finger contact model.

A direct solution to the contact problem would be obviously possible if the contact location c would be directly measured. Therefore the availability of a direct force measurement and of the contact location allows directly to solve the point contact problem.

At system level the goal is to develop to an integrated tactile/force sensors with embedded electronics to be placed on the phalanges of three fingers. The relevant problems considered have been: choice of appropriate force transducers, pressure transducers for contact measurements, integrated electronic design.

As a force sensor, we have used the integrated micro force sensor LPM 562. This force sensor provides precise, reliable force sensing performance in a compact commercial grade package. The force sensor operates on the principle that the resistance of silicon implanted piezoresistors will increase when the resistors flex under an applied force. The load is applied to a stainless steel plunger transmitting force to the silicon sensing element. The sensor packaging incorporates a modular construction and use of innovative elastomeric technology and engineered molded plastics which allow for load capacities of 4500 grams overload. Detail specifications are shown in table 2.

The device consists of three strain sensitive thick-film resistors. A force applied to the interface stick produces a change of resistivity. Proper arrangement of the resistors in three Wheatstone bridges, and a simple decoupling amplifier, allow obtaining three voltages proportional to the applied force components. Digital potentiometers are used for self-calibration of the bridges and three instrument amplifiers provide appropriate signal conditioning before sampling.

Table. 2. The specifications of F/T sensor

No	Items	Specifications
1	Load Range	0-500 grams
2	Linearity	± 10 grams F.S.
3	Repeatability	± 10 grams
4	Material	Plastic Body
5	Temperature Range	53 to 104 °F
6	Output	0.024 mv/v/g
7	Bridge Resistance	5k ohms nominal
8	Excitation	5 Vdc
9	Safe Overload	4.500 grams

A. Tactile Sensor Transducer

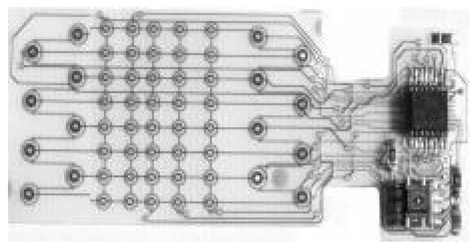

Fig. 4. The electrodes are etched on a flexible printed circuit board, are configured as a variable resolution 8 × 8 matrix (back side shown).

The tactile transducer is a matrix of 64 electrodes covered by a layer of pressure sensitive conductive rubber (PCR Co. Ltd.). The electrodes are etched on a flexible PCB substrate, fig. 4, in order to conform to a cylindrical surface. A thin elastic sheet covers the whole sensor and provides a mild preload useful to reduce noise. Pressure due to contacts produces changes of resistance among the electrodes. The geometry of the electrodes Fig. 4, has been defined with the goal of limiting the spurious currents that may occur across the various electrodes, and interfere with measurement, as discussed in [7].

B. Tactile Data Processing

Tactile data are sampled by the on-board MCU, with 10 bit resolution. Preliminary tests show an actual sensor resolution of 8 bit/taxel. Each tactile image consists of 64 taxels.

During contact, a number of adjacent taxels are subject to pressure. The analog output of the tactile sensor allows to measure the distribution of pressure over all the transducer. Therefore, we propose to compute the contact centroid [4], as

$$\hat{C} = \frac{\sum_{i=1}^{N}\sum_{j=1}^{N} x_{ij} \cdot p(x_{ij})}{\sum_{i=1}^{N}\sum_{j=1}^{N} p(x_{ij})} \qquad (2)$$

where $\hat{C}$ is the computed contact centroid, x_{ij} is the coordinate of the taxel and $p(x_{ij})$ the weight of this. As a matter of fact further geometric information about the distribution of the pressure during contact could be useful, although not directly relevant to point contact model solution. To this aim the pressure distribution is approximated as an ellipsoid, fig. 11, as follows:

$$E = \frac{\sum_{i=1}^{N}\sum_{j=1}^{N} (x_{ij}^{T} - \hat{C})(x_{ij} - \hat{C}) \cdot p(x_{ij})}{\sum_{i=1}^{N}\sum_{j=1}^{N} p(x_{ij})} \qquad (3)$$

Where E is a symmetric matrix who represent the ellipsoid. The approach used to compute and the associated approximate ellipsoid, is strongly based on the availability of an analog tactile sensor.

3. EXPERIMENT AND RESULTS

The main advantage of a multi-fingered hand is that it can grasp various objects by changing its shape. Several classifications of grasping have been proposed. In this proposal various grasps are classified into three large categories: a power grasp that passively resists arbitrary external forces exerted on the object, a precise grasp to manipulate the object, and an intermediate grasping which some fingers are used for a power grasp and the other fingers are used for a precise grasp.

We achieved these typical grasp types in our developed hand. Table. 3 shows the specification of robot hand and fig. 5 is some examinations of flexible gasping objects.

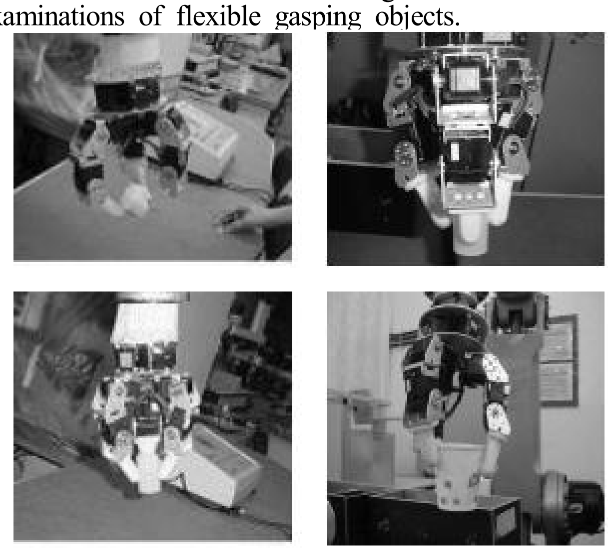

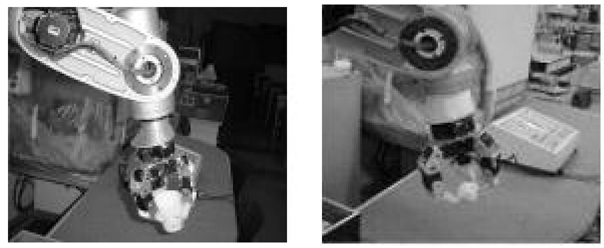

Fig. 5. The images of some catching examinations

Catching is one of the most important tasks for dynamic manipulation. In this section catching is shown using our flexible hand with a visual feedback controller. We used a rubber ball with radius of 5cm as a target, and we dropped it from about 1.2m in height. The speed of the falling ball is about 5.9m/s just before it hits the ground.

Table. 3. The specification of robot hand.

Total D.O.F	13
Weight [g]	600
Max. Speed at a finger tip [m/s]	3.2
Max. force at a finger tip [N]	26.5
Joint resolution [deg]	0.35

From various experimental trials, we have decided on the catching strategy shown in Fig. 5.

The catching tasks for the ball are:

- Approaching (0¸40ms)
- Locking (40¸50ms)
- Rebounding (50¸60ms)
- Holding (60ms¸).

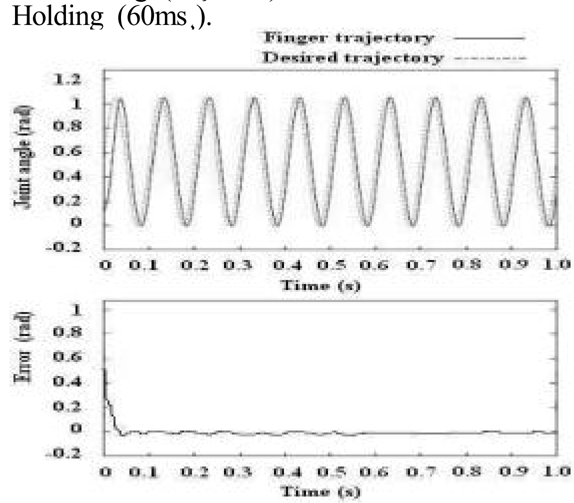

(a)Result for sine wave input trajectory

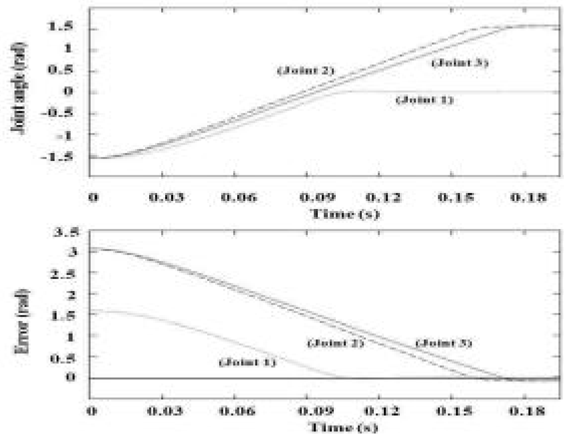

(b)Result for the step input trajectory
Fig. 6. Result of performance test for finger trajectory tracking

Fig. 6 shows the results when we changes the target position qo and Fig. 8 when we changes the distance d1 and d2, (X-Y axis, qo, d1 and d2 were defined in fig. 6.)

The success rate was more than 95% and tolerance of position error of the target was about ±1.5cm from the center of the palm.

Several types of failure modes were observed. The direction of a bounced ball depends on the coefficient of friction and restitution. It is difficult to know the accurate values of these parameters, but the errors in their measurement may be ignored if the speed of the fingertip is fast enough.

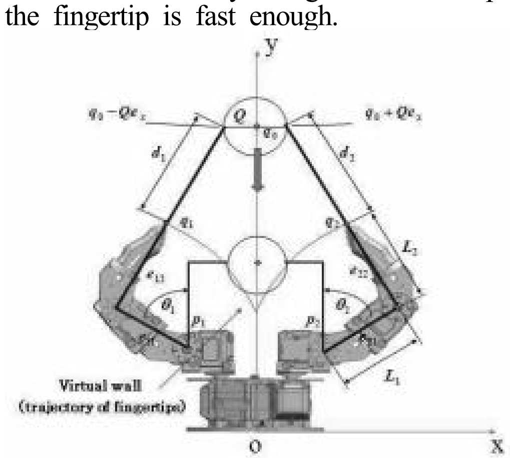

Fig. 7. Catching algorithm of grasping

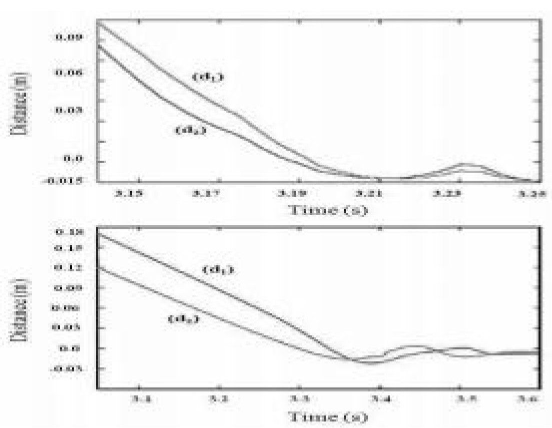

Fig. 7. Time response: Target Distance

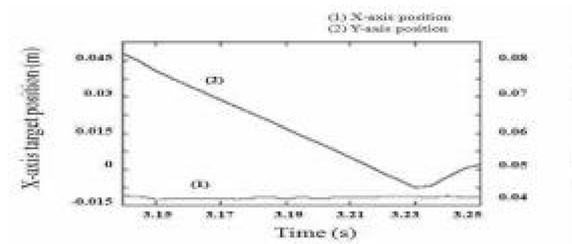

Fig. 8. Time response: Target Position

4. CONCLUSION

An integrated force and tactile sensor with embedded electronics has been presented in a lightweight flexible hand with 13 D.O.F, and the associated visual feedback control. The sensor consists of a three components commercial force sensor and of a custom matrix tactile sensor based pressure sensitive conductive rubber. The joint used of both tactile and force information allows the direct solution of the point contact problem. A technique to compute the contact centroid and a quadratic approximation of the pressure distribution during contact has been proposed. Ongoing work is focusing on a flexible manipulation system, which consists of a dual flexible multi-fingered hand-arm system, and a dual active vision system. In the future this new hand-arm system will be used for multi tasks.

The need for a robotic hand that works in the real world is growing. And such a system should be able to adapt to changes in environment. We think that the concept of a flexible hand system with real-time control implementation will become an important issue in robotic research.

REFERENCES

[1] T. Asfour, K. Berns and R. Dillmann, “The Humanoid Robot ARMAR”, Proc. of the Second International Symposium on Humanoid Robots (HURO´99), October 8-9, 1999, Tokyo, Japan

[2] T. Asfour, K. Berns, J. Schelling and R. Dillmann, “Programming of Manipulation Tasks of the Humanoid Robot ARMAR”, The 9th International Conference on Advanced Robotics (ICAR'99), 25-27 October, Tokyo, Japan

[3] S. Toyama, S. Hatae and S. Sugitani, “Multi-Degree of spherical ultrasonic motor”, Proc. ASME Japan/USA Sympo. Flexible Automation, 169, 1992

A Stable Walking Motion Control of Humanoid Robot with 24 Joints

Hyun-Min Kim[1], Min-Seong Kim[2], Hyun-Woo Song[3], Yang-Keun Jung[4]

[1] Department of Advanced Engineering., Kyungnam University, Changwon, 51767, Korea
(E-mail : khm9153@nate.com)
[2] Department of Advanced Engineering., Kyungnam University, Changwon, 51767, Korea
(E-mail : kms21018@naver.com)
[3] Department of Mechatronics Engineering., Kyungnam University, Changwon, 51767, Korea
(E-mail : thgudn@naver.com)
[4] Shinla Information Technology CO., Ltd., Changwon City,
51390, Korea (E-mail : shintech@hanmail.net)

Abstract : This paper deals with the stable walking for a humanoid robot, on uneven terrain, A humanoid robot necessitates achieving posture stabilization since it has basic problems such as structural instability. In this paper, a stabilization algorithm is proposed using the ground reaction forces, which are measured using FSR (Force Sensing Resistor) sensors during walking, and the ground conditions are estimated from these data. From this information the robot selects the proper motion pattern and overcomes ground irregularities effectively. In order to generate the proper angel of the joint. The performance of the proposed algorithm is verified by simulation and walking experiments on a 24-DOFs humanoid robot.

Keywords Force sensing resistor, fuzzy algorithm, humanoid robot, stabilization

1. INTRODUCTION

In this paper, a real-time walking stabilization method utilizing a fuzzy algorithm under uneven terrain is proposed. We focused most of our interest on landing phase. The ground reaction forces, measured by FSR sensors on the sole, are used to assess the ground condition and the robot posture. Simulation and experiment results for the proposed method are given in Section 3, followed by conclusions in the final section.

2. STABILIZATION

2.1 Walking pattern

Basically, a robot walks with the trajectory generated previously assuming even terrain. If different values from the expected sensor are measured during walking, the robot should be deployed using the stabilization algorithm. Fig.1 presents the walking algorithm.

When the robot is walking, it measures the ground reaction forces in real-time and utilizes them as inputs to the controller. When the control of the robot is interrupted by an unexpected situation or a unit step has ended, the new trajectory should be generated according to the changed situation. The newly verification based on the ZMP criterion. Once the stability of the trajectory is guaranteed, the robot becomes able to resume the walking.

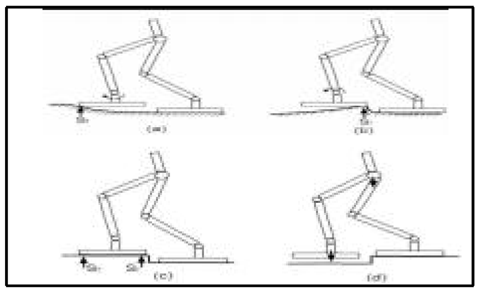

Fig. 1. The walking irregular ground condition.

2.2. Stabilization algorithm

In order to ensure that the robot walks stably, the motion should basically be stable and smooth. In addition, the robot must be able to detect approaching situations, and to control itself accordingly. When this control concept is applied, the robot is able to walk stably coping with unexpected external disturbances.

A robot can face unexpected situations during walking such as projecting ground, depressed ground, and projected ground as described in Fig.1.

3. EXPERIMENT AND RESULT

3.1 Humanoid robot and sensor system

The simulation is based on a humanoid robot. The robot has a height of about 950mm, a weight of roughly 35kg, and 24 DOFs. The robot determines a walking pattern using the ground reaction forces measured from the sole.

The robot measures these forces using FSR sensors fixed at the sole, and the obtained data is employed as the input of the stabilization algorithm. FSR sensors are generally used for measuring the dynamic force by the variation of resistance in the force or pressure acting on the surface. FSR sensors are economical, thin, light, and easy to use. In addition, Moving-Average Filter is applied to reduced influence of the disturbance by sensor noise. Equation (1) shows the Moving-Average Filter.

$$R(n) \quad \frac{\sum_{i=0}^{k} f(n-i)}{k} \tag{1}$$

In (1),,k, and R(n) are the raw sensor data at n time, orders of filter, and filtered data, respectively.
Four sensors are equipped at 4 corners of each foot. In order to minimize impact and deformation, and also to distribute repulsive power, the sole is composed of a bakelite plate and a rubber plate. The sensors are fixed between the two plates.

The robot walks according to a basic trajectory. In basic walking, a stride is 0.12m, velocity is 0.04m/s, and the ground is regarded as being flat. The robot steps on projected ground of 11mm in height with the tie if the swing leg. When the control algorithm is not applied, the sensor data is presented as given in Fig.2, The robot pushes the ground continuously, and the heel does not contact until the end of the stride.

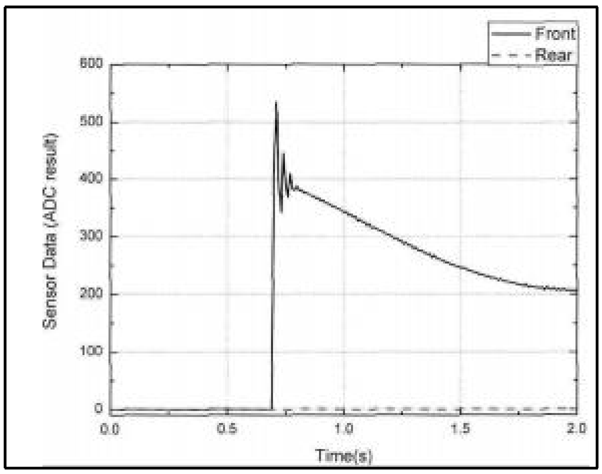

Fig. 2. FSR sensor data for uneven terrain

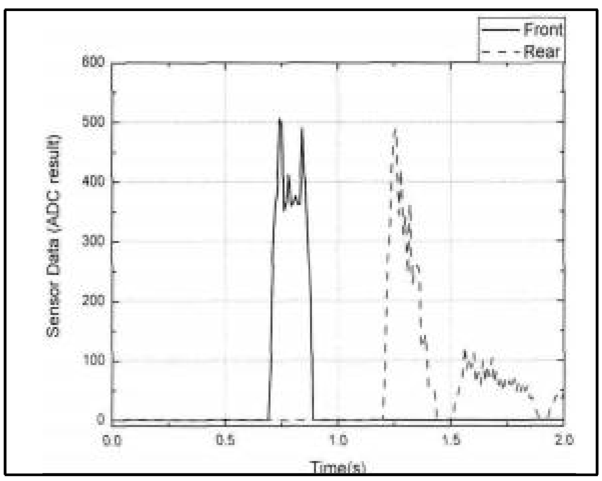

Fig. 3. Controller input for constant control.

4. CONCLUSION

This work was supported (National Robotics Research Center for Robot Intelligence Technology, Kyungnam University) by Ministry of Knowledge Economy under Human Resources Development Program for Convergence

REFERENCES

[1] M. Vukobratovic and D. Juricic, "Contribution to the synthesis of biped gait," IEEE Trans. on Bio-Medical Engineering, vol. 16,pp. 1-6, 1969.

[2] K. Nishiwaki, S. Kagami, Y. Kuniyoshi, M. Inaba, and H. Inoue, "Online generation of humanoid walking motion based on a fast generation method of motion pattern that follows desired ZMP," Proc. of IEEE/RSJ Int. Conf. on Intelligent Robots and System, vol. 3, pp. 2684-2689,2002.

[3] D. Djoudi and C. Chevallereau, "Stability analysis of a walk of a biped with control of the ZMP," Proc. of IEEE/RSJ Int. Conf. on Intelligent Robots and Systems, pp. 2461-2467, 2005..

2017 Changwon International Conference on Intelligent Robot and Convergence Industry (CICIRO 2017)
Nov. 30- Des. 1, 2017, Changwon Exhibition Convention Center(CECO), Changwon, Korea

Surface type broaching machine forced vibration analysis under normal cutting operation condition based on finite element method

Pandu Sandi Pratama1, Destiani Supeno2, Jae-Young Byun2, Joong Soon Lee3,
Jeong Hwan Jeong3, Won-Sik Choi2,#

[1] Live and Industry Convergence Research Institute, Pusan National University
[2] Dept of Bio-Industrial Machinery Engineering, Pusan National University2
[3] Korea Broach Manufacture Co., LTD

Abstract: A machine such as broaching machine are subjected to different loads and vibration. Due to this vibration there will be certain deformations which affect the performance of the machine in adverse manner. This paper proposed a vibration analysis of surface type broaching machine using ANSYS. In this research modal analysis was done to determine the natural frequency and vibration mode of structure and random vibration analysis was done to determine the structure response under random loading. With advancement in computation power, finite element analysis simulation is possible and become complement of experiment based analyses. The Finite Element Method (FEM) analysis is carried out to study the effect of vibration on the structure in order to ensure the safety. This work helps the machine developer make a better product at the early design stage with lower cost and faster development time. To do this, firstly, using CATIA, a CAD model is prepared. Secondly, the analysis is to be carried out using ANSYS 15. The modal analysis and random vibration analysis of the structure was conducted. The analysis shows that the proposed design was successfully shows the minimum deformation when the vibration was applied in normal condition.

Keywords: Surface type broaching machine, vibration analysis, cutting operation

1. INTRODUCTION

Broaching is a machining process that uses a toothed tool called a broach to remove material. In the broaching process, the work pieces was put on the material holder pushed by a hydraulic cylinder, and the broach tools were clamped stationary on the broach tool holder. The structural analysis is one of important step in the development process such as in [1~2]. In broaching machine, uneven force will lead the vehicles to the forced vibration. If the excitation vibration frequency and the resonance natural frequency of the frame structure is closed, the mechanical structure will produce local resonance and deformation. Therefore, the simulation related to the vibration analysis is needed in vehicle development process. In this research the modal analysis was performed to find out the natural frequency of the machine. Furthermore, the free vibration analysis was performed to understand the effect of vibration due to daily activities to the frame structure of the machine.

2. MATERIALAND METHOD

To analyzed the broaching machine structure, in this paper ANSYS program was used. The procedure of vibration analysis is as follows. Firstly, the 3D model of important component of the machine was created. Secondly, the model was simplified to obtained geometry model. Thirdly, the mesh of the model was generated. Fourthly, the materials properties were defined. The material for broaching machine is structural steel. Fifthly, the boundary condition was defined. Finally, solve the problem, visualized and read the results.

3. RESULTAND DISCUSSION

3.1 Modal Analysis

Modal analysis is a kind of linear analysis technology, used to determine the structure of the natural frequency and vibration mode. This paper uses Block Lanczos method to extract six order modal of chassis frame that have prestressed firstly. In modal analysis, the only effective load is zero displacement constraints, if in a certain degree of freedom (DOF) specifies a non-zero displacement constraints, the program will replace the degree of freedom by zero displacement constraints.

a. F=48.095 Hz

b. F=54.413 Hz

c. F=83.232 Hz

d. F=83.424 Hz

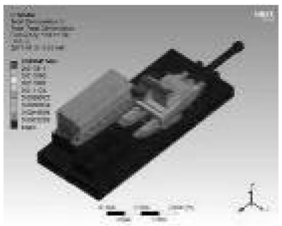

e. F=153.17 Hz

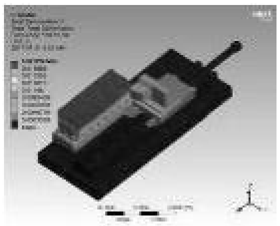

f. F=158.52 Hz

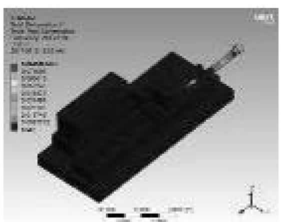

g. F=213.75 Hz

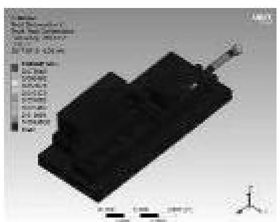

h. F=216.4 Hz

Fig. 1 Modal Analysis

3.2 Random Vibration Analysis

Random vibration analysis is used to determine the structure response under random loading. ANSYS uses the power spectral density (PSD) spectrum as random vibration analysis of the load input.

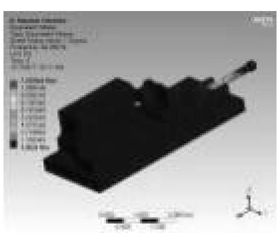

Fig. 2 Random vibration stress

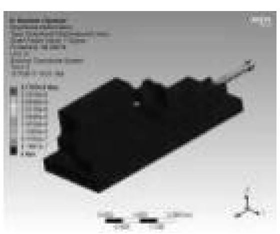

Fig. 3 Random vibration deformation

4. CONCLUSTION

In this research, natural frequency analysis and random vibration analysis was done to the surface type broaching machine. The simulation result show that the natural frequency value of the first order are among sensitive frequency value ranges which can be obtained from modal analysis. Modal analysis results show that the frame of 1 ~ 8 orders modal natural frequencies range are 48 ~ 216 Hz.

ACKNOWLEDGMENT

This work was supported by the Small and Medium Business Administration's, 2016 Technology Innovation and Development Project.

REFERENCES

[1] Wang G.S., Si J.P., Chen Y.Y., Guo L.N., and Zhao Y.N., *Structural Stability Analysis of Dump Truck Body Based on ANSYS*, Advanced Materials Research, Vol. 588, pp. 217-221, 2012.

[2] Si F.J.P., Wang G.S., and Ding X.L., *Analysis of Dump Truck Unloading Condition Based on ANSYS*, Advanced Materials Research, Vol. 548, pp. 724-729, 2012.

2017 Changwon International Conference on Intelligent Robot and Convergence Industry (CICIRO 2017)
Nov. 30- Des. 1, 2017, Changwon Exhibition Convention Center(CECO), Changwon, Korea

The Characteristics of 4Mhz NDT Ultrasonic Transducer for Weld Quality Inspection of Spot Welding Robot

Eon Uck Kang[1], Pandu Sandi Pratama[2], Jae Young Byun[1], Eun Suk Lee[1], Sung Won Chung[1], Won Sik Choi[1,#]

[1] Dept. of Bio-industrial Machinery Engineering, Pusan National University
[2] Life and Industry Convergence Research Institute Pusan National University

Abstract: Recently, automobile makers in Korea and abroad have tried to reduce the defect rate through weight reduction and precise welding inspection. In this study, a method to reduce the defect rate was proposed by using NDT (Non Destruction Testing) probes. The vertical scanning technique of A-SCAN was used for the purpose of efficient welding quality inspection. In addition, for efficient inspection, the ultrasonic signals generated by the single probe transducer, was reflected and received by pulse receiver and measured using oscilloscope. Before applying it to the arm of a robot, the relationship between the material thickness and the thickness of the probe according to the thickness of the probe was checked for the measurement. It was confirmed that measurement was possible at the probe-specific frequency suitable for the thickness of the material. We intend to improve the accuracy of the vertical scanning technique as A-SCAN in order to acquire data about the frequency range of the probe and to correlate the material and the thickness of the material with the appropriate frequency.

Keywords: NDT Ultrasonic Transducer, Weld Quality Inspection, Spot Welding Robot

1. INTRODUCTION

Light weight has recently become a hot topic for global auto's makers to improve fuel efficiency in automobiles. The main customers of the market are reducing fuel costs, preferring environmentally friendly hybrid cars, and approaching ways to reduce the weight of cars in the future, The purpose of this study is to investigate the effect of welding defect on steel - to - steel and steel - to - aluminum welded joints in order to lighten the existing steel The relationship between the material thickness and the natural frequency of the probe was investigated by analyzing the welding condition of the welded specimen according to the frequency characteristics of the NDT probe to efficiently detect the presence of weld defect.

2. METERIALAND METHOD

For this experiment, two kinds of samples were used for the test. The welded joints were welded to the welded joints of 3 mm × 2 specimens of SS440 and 1 mm × 2, respectively. An ultrasonic wave was generated while slowly moving the probe from the right side in the scanning direction to a welding nugget formed around the welding point. The size of the probe is 10mm x 10mm and the single-channel 4Mhz probe is constructed so that it can be inspected within 8mm of the welded area. The LeCroy oscilloscope confirms the amplitude intensity of the signal over time along the weld of the specimen. The scanning method was a linear scanning method of vertical type, and the ultrasonic signal was generated using the OLYMPUS 5077PR Pulser-Receiver. The output power of the pulse was set as manual input (pulse transmission signal), the set voltage was 100V and the frequency of the transducer was set to 5Mhz, and the amplification of the receiving input proceeded to + 10dB gain.

3. RESULTAND DISCUSSION

Fig. 1. A-SCAN was carried out with a 6T (mm) thick specimen welded. SS440 A-SCAN graph obtained by vertical scanning signal on 3mm × 2 pieces of 6mm specimen is shown in Fig 1. The time division unit is 10μSec and the cycle T is 15 ~ 20μSec. C, B, and A detection signals are confirmed. The first IP signals are the end of pulse transmission signals and are not reflected signals. The intensity of the amplitude is measured as a maximum of 72 mV, and the reflection signal of the second succeeding B and the A signal are gradually reduced and the amplitude converges. The defect flaw echo signal, can be expressed as crack in Fig. 2. After the fusion bonding of the welded specimen is completed, the point where the cracks or pores in the inside of the weld occur is echo. It was able to detect the position and detect the presence or absence of defects.

Experiments were carried out by varying the thickness of the material in 2mm specimens of SS440 1mm × 2. In Fig. 3. firstly. overlapping of the detected signals occurred. Secondly, the period of the amplitude of the reflected signal is too short and precise measurements are not made. We could trace the cause of this phenomenon as the cause of the frequency dependence of the signal returning to the material thickness and material according to the frequency.

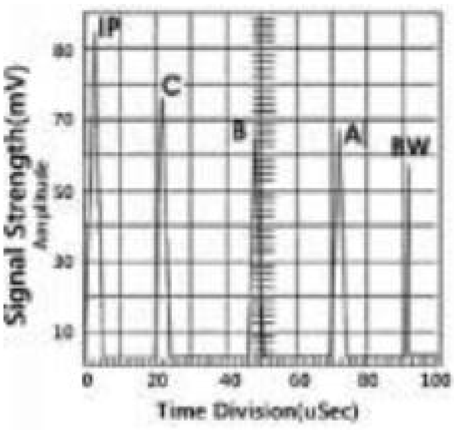

Fig. 1.A-SCAN Plotting

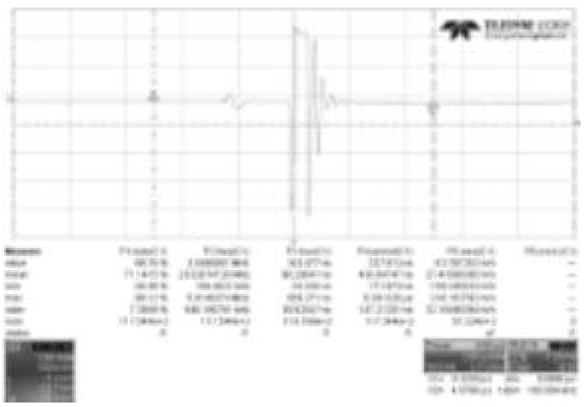

Fig. 2.Agraph plotting on before pulsing

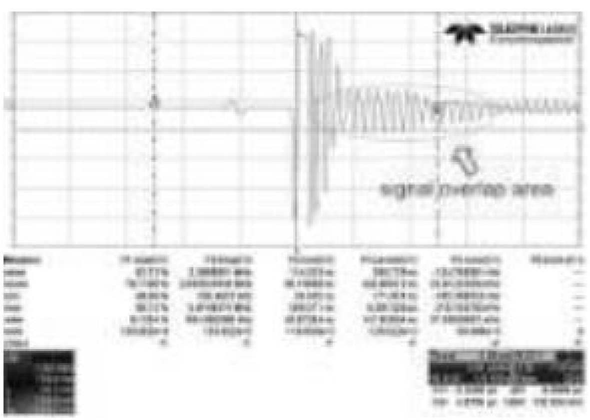

Fig. 3.Agraph plotting on after pulsing

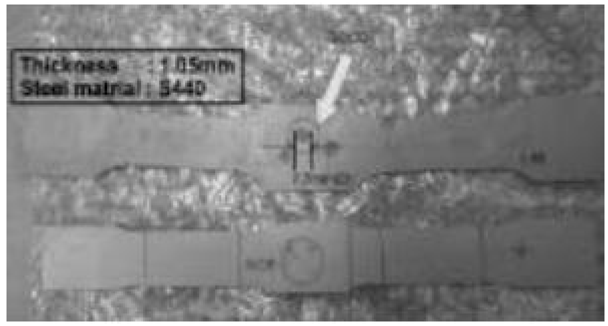

Fig. 4. Samples of SS440 for test

Fig. 5. Reducer after design change

4. CONCLUSTION

From this research, it can be obtained that there is a correlation between the frequency and the material thickness according to the results of the experiment with two specimens at the frequency of 4Mhz in the form of 100V bipolar square wave. It is also possible to estimate that the ultrasonic test signal is closely related to the material of the material as well as the relationship between the specimen thickness and frequency.

ACKNOWLEDGMENT

The results of this study were supported by the Ministry of Commerce, Industry and Energy in korea to develop a “64-channel C-SCAN wireless inspection system for the development and quality evaluation of lightweight body parts using R-FSSW technology” Project number R0005640)

REFERENCES

[1] Young Y. S., *Ultrasonic testing*, sang hakdang ISBN 978-89-6587-004-3 93560 PP 223-263, 2010.

[2] Kim J. K., *항공산업실부 경험으로 쓴 비파괴 검사*, 좋은땅, ISBN 979-11-5982-208-7 PP , 2016.

The red ginseng vinegar fermentation manufacturing using “Uinkin”

Se Ran Hwang, Destiani Supeno, Kwo Soon Hong, Chung Sung Won, Kwon Soon Goo, Park Jong Min, Kim Jong Soon, Won Sik Choi

Department of Bio-Industrial Machinery Engineering, Pusan National University

Abstract: Saponin is the most pharmaceutical active ingredients of the ginseng plant, it was called “Ginsenoside” which means the Glycoside of ginseng that composed glycosides and aglycones. The human body will absorb the saponin easily if these substrate was decomposed by active microorganism before consumption. Fermentation is the most convenient technique for this experiment, the fermentation product have some benefits for human body such as clearing the blood vessel, boost the human digestion system, fatigue recovery, prevention of diabetes, obesity, aging, and tumor. The experimental sampling was prepared by fresh Korean ginseng and red ginseng extract for the base ingredient. The concentrated of pure ginseng extract was addition to increase the saponin extract and the mix microbial powder was addition as starter to increase the fermentation efficiency. The purposed of this research was to study the vinegar fermentation process such as sugar content, pH and acidity development.

Keywords: red ginseng vinegar fermentation manufacturing , Uinkin

1. INTRODUCTION

Korean ginseng and red ginseng (*Panax ginseng* C. A. Meyer) has been know as medicinal plant with mysterious powers in the Orient, this plant have been known as the most valuable medicine of all medicinal herbs [1]. Red ginseng not only reinstates the body’s liveliness, decreases stress and fatigue, and elevates blood circulation, but also improves brain function. In addition, it enhances the activity of the immune system, maintains homeostasis, combats aging, and has proven beneficial against diabetes and cancers. It has been described that fermentation is an ideal process of biochemical alteration using microbial enzymes and microorganisms. Fermentation is conducted to improve the storage period, nutrition, and sensory characteristics related to foods [2].

2. METERIALAND METHODS

2.1 Sampling

Fresh Korean ginseng vinegar fermentation was prepared by 300g of fresh Korean ginseng, washed with tap water, added 400ml of water and blending into the liquid. Moreover, red ginseng vinegar fermentation was prepared using 46.15g red ginseng extract manufactured by Chongkundang Pharm’s company, South Korea and mix well in 900ml of water. The fermentation process were obtained for 70 days in 37℃. The initial sugar content or brix (%) was set in to 24% by manipulated sugar addition. The utilities and equipment that will be use for preparation such as fermentation jar, knife etc. were sterilize using hot water for 15 minute before used. Table 1. shows the ingredient and initial condition of fermentation process. Figure 1. shows the sample preparation for fresh Korean ginseng and red ginseng extract fermentation.

2.2 Instrument analysis

The pH level measurement was done using pH-meter (SATO, Japan). The device used is pH meter type sk-620PH, this device can measuring the pH with a value of 0-14. Sugar content in this research was measured using a refractometer type: Master-53M, capacity: 0.0-53%, ATAGO, Japan. Refractometer was designed to measure the refractive index of a solution. The Brix scale based on sucrose (sugar) and water solution. Total acidity of ginseng fermentation was measured using titration method, 1ml sample addition 0.1ml of phenolphthalein solution with sodium hydroxide until the sample solution change into purole color solution. The total acidity was expressed as percenty (%) of acetic acid contain in the sample per ml.

Table 1. The experimental ingredient and initial pH level and sugar content (%)

	Sample(g)	Salt(g)	Sugar(g)	Water(ml)	Microbial Powder(g)	Initial Brix(%)	Initial pH
Fresh Korean Ginseng (FKG)	300	3	234.36	900	6	34.3	6.39
Red Ginseng Extract (RGE)	46.15	3	197.9	900	6	24.1	6.5

3. RESULTAND DISCUSSION

The experimental preparation was done by using two different kind of ginseng, there are blending fresh Korean ginseng and pure red ginseng extract. Total acidity, and pH level were also slighly different at final fermentation process, 1.2%; 3.41pH for fresh Korea ginseng and 1.2%; 3.39pH for red ginseng extract (Figure 3.). The decrease in sugar content was caused by the degradation of sugar to alcohol during alcoholic fermentation by acid bacteria. The alcohol content in the sample was evaporate as a result of stirring process during fermentation process, the decrease in alcohol caused the acidity increase that proved by the decrease in pH value.

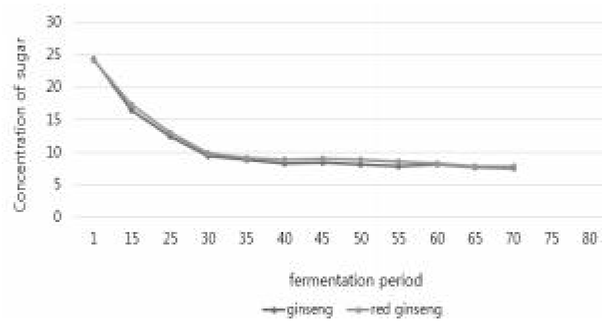

(a)

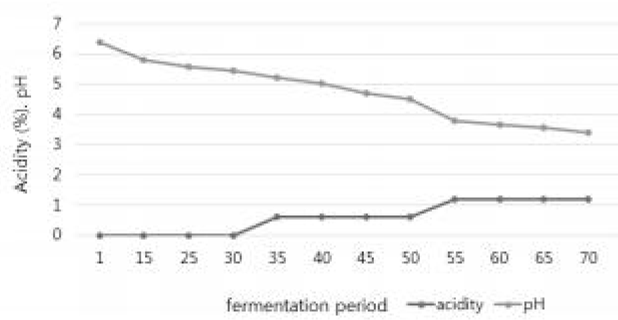

(b)

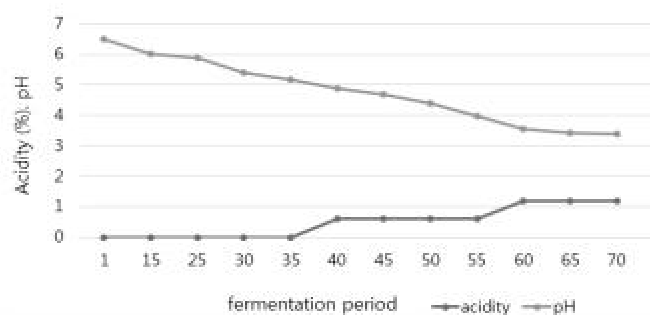

(c)

Fig. 3. Sugar content (%) development during fermentation period (a), total acidity (%) and pH development during fermentation period in Fresh Korean Ginseng (b) and Extract Red Ginseng

4. CONCLUSTION

Due to the experiment, the manufacturing of fresh Korean ginseng and red ginseng vinegar fermentation addition microbial powder as starter was possible. Sugar content was decreasing from ±24% to ±7.65% at 70 days of fermentation process, and total acidity, and pH level were also slighly different at final fermentation process, 1.2%; 3.41pH for fresh Korea ginseng and 1.2%; 3.39pH for red ginseng extract.

REFERENCES

[1] Kim, J. H., Kim, M. K., Wang, Hongtao, Lee, H. N., Jin, C. G., Kwon, W. S., Yang, D. C.. *Discrimination of Korean ginseng (Panax ginseng Meyer) cultivar Chunpoong and American ginseng (Panax quinquefolius) using auxin repressed protein gene*, J. Ginseng Res., Vol. 40, pp. 395-399, 2016.

[2] Christensen LP. *Ginsenosides chemistry, biosynthesis, analysis, and potential health effects*, Adv Food Nutr Res., Vol. 55, pp. 1-99, 2009.

2017 Changwon International Conference on Intelligent Robot and Convergence Industry (CICIRO 2017)
Nov. 30- Des. 1, 2017, Changwon Exhibition Convention Center(CECO), Changwon, Korea

Improvement of the Life of the Electric Vehicle Carrier Reducer by the Finite Element Method

Jae Young Byun[1], Pandu Sandi Pratama[2], Eun Suk Lee[1], Chun Suk Park[3], Sung Won Chung[1], Won Sik Choi[1,#]

[1] Dept. of Bio-industrial Machinery Engineering, Pusan National University
[2] Life and Industry Convergence Research Institute Pusan National University
[3] KEUNWOO TECH Co., Ltd.

Abstract: Electric vehicles have been increasingly used in agriculture to solve the problems of conventional powertrains. There are many favorable aspects to women or aged farmers and it is easy to change according to the requirements of farmers. However, there is a problem with the reducer breakage. In order to solve this problem, we study the gear reducer which is better than the existing one by improving the dimensions of each shaft. The reducer was disassembled to analyze the cause of the damage. In order to improve this, the material, structure of the reducer were changed. Structural analysis was carried out to confirm the stress occurs on the reducer. As a result of comparing the stresses before and after the design, it was found that the existing safety factor increased from 1.33 to 1.61. From this study, it can be seen that how to effectively improvement of the reducer strength is directly related to the improvement of the life of the gearbox.

Keywords: Electric Vehicle Carrier Reducer, Finite Element Method

1. INTRODUCTION

Electric vehicles carrier are increasingly used in many field such as industry, factories, marts, and leisure areas. It replaces the powertrain that have problems of noise and soot for transporting compost, fertilizer, seedlings and harvests required for field work. Also, unlike a power train, an electric vehicle is structurally simple and easy to use because it uses a battery. There are many benefits for women or aged farmers, and it is easy to add structures and functions according to the requirements of farmers. However, structure deformation caused by the friction and overload occurs in the speed reducer, affects shortening of the life of the gear. In this study, the gear dimension of the shaft are improved to develop the gear reducer suitable for the agriculture work.

2.ANALYSIS METHOD

2.1 Reducer shaft failure cause analysis

The broken gearbox was disassembled to guess the cause of the motor speed reducer defect. There was a case of abrasion due to abrasion of the contact part of the shaft and the gear box. Deterioration of the shaft occurs due to external influence. As a result, 6 kinds of indications were found out due to discoloration, grease scattering, grease deterioration, discoloration of the assembly due to internal deterioration, and wear of the first gear. Therefore, it is presumed that the overload of the first stage gear causes noise and abrasion and malfunction due to the second reduction gear.

2.2 Improvement of reducer

Based on the estimates in Section 2.1 above, some improvements are considered when the reducer is required to be improved. First, the tooth width of existing shafts 3 and 4 was increased to improve gear wear. Secondly, the material was changed from SCM440 to SCM415 for the purpose of preventing failure. Finally, for the purpose of removing the notch where stress concentration occurs, the right angle cutting is changed to round cutting when the pinion is machined.

2.3 Comparison of safety factors through structural analysis

In order to compare the data before and after improvement of the reducer, the reducer was disassembled and reversed. The design was changed by applying the proposed reduction gear reducer according to the estimation of the damage of the reducer. Then, each drawing was assembled through CATIA V5R21 and structural analysis was performed with ANSYS R15.0.

3. RESULTAND DISCUSSION

As a result of comparing the stresses before and after the modification, the maximum stress applied to the gearbox before the change is 1.773e9Pa and the maximum stress applied after the change is 1.4465e9Pa. A stress reduction of 0.327e9Pa was observed. The calculation of the safety factor can be done by dividing the material stress at the maximum stress. Comparing the safety factors, the safety factor is increased from 1.33 to 1.61.

Fig. 1. Reducer before design change

Fig. 2. Reducer after design change

4. CONCLUSTION

In this study, the effective improvement of the gearbox was researched to solve the damage of the electric car reducer of field farming. We reverse engineered the existing product and dismantled the broken gear box to estimate the cause. The contents of the study are as follows.

1. It is estimated that the cause of the reduction gear failure is the deterioration and damage caused by the transition to anothershaftduetotheabrasionoftheprimarygearduetothe badinfluenceofthefield.
2. The safety factor of 1.61, which is higher than the safety factor of 1.33, has appeared due to improvement of design of reducer.

It was found that how effectively the modification of the contact part of the reducer is directly related to the improvement of the life of the gearbox, and it is found that it is effective to extend the life by improving the safety factor through design modification.

ACKNOWLEDGMENT

This work was supported by Korea Institute of Planning and Evaluation for Technology in Food, Agriculture, Forestry(IPET) through Agriculture, Food and Rural Affairs Research Center Support Program, funded by Ministry of Agriculture, Food and Rural Affairs(MAFRA)(716001-7)

REFERENCES

[1] Yoshihiro Fujisawa, Masaharu Komori, *Surface finishing method for tooth flank of heat-treatedsurface-hardened small gears using a gear-shaped tool composed ofalumina- fiber-reinforced plastic*, Precision Engineering, Vol.39, pp 234-242, 2015.

2017 Changwon International Conference on Intelligent Robot and Convergence Industry (CICIRO 2017)
Nov. 30- Des. 1, 2017, Changwon Exhibition Convention Center(CECO), Changwon, Korea

Characteristics of Jujube Cherry Tomato Fermentation

Destiani Supeno, Kwo Soon Hong, Chung Sung Won, Kwon Soon Goo,
Park Jong Min, Kim Jong Soon, Won-Sik Choi
Department of Bio-Industrial Machinery Engineering, Pusan National University

Abstract: This study was done to investigate the behavior of jujube cherry tomato during fermentation and to investigate the effect of sugar content and effective microbial addition during fermentation. In this research, semi-mature tomato that contain low initial sugar content (±6.2°Bx) and average pH ± 4.97 were used as fermentation material. Six fermentation condition such as TFA1 (Sugar content: 25%); TFB1 (Sugar content: 25%, EM: 2g); TFC1 (Sugar content: 30%); TFD1 (Sugar content: 30%, EM: 2g); TFE1 (Sugar content: 35%); TFF1 (Sugar content: 35%, EM: 2g) were prepared. The fermentation period was done at 192 hours in 25°C room temperature. The pH, acidity, sugar content and microbial growth were observed during fermentation process. The experimental result shows that in the end of fermentation the lowest pH obtained from TFB1, the sugar content is reduced during fermentation, the highest acidity percentage obtained from TFE1, and the highest colony form unit obtained from TFD1.

Keywords: Jujube Cherry Tomato Fermentation

1. INTRODUCTION

Tomato is the world's largest vegetable crop, because it is wide spread production and special nutritive value. This fruit are the most widely consumed fresh fruit in the world. It is containing significant amount of carotenoids (Lycopene and Beta-carotene), several polyphenols (Caffeic and Chlorogenic acid), rutin, naringenin and rich source of vitamin A and C. In addition, tomatoes also contains a trace elements such as selenium, copper, manganese, iron, phosphorus and zinc that act as cofactors for antioxidant enzymes [1]. Fermentation technologies have a potential for stimulating development in the food industry especially in tomato processing considering their low cost, scalability, minimal energy and infrastructural requirements and the wide consumer acceptance of fermented products [2]. The purpose of this research was to study the characteristic of tomato fermentation and to investigate the effect of sugar content and effective microbial addition during fermentation.

2. METERIALAND METHOD

2.1 Sampling preparation

In this study, jujube cherry tomato was obtained from Sacheon city, South Gyeongsang Province, South Korea. The initial sugar content is ±6.2°Bx and pH ±4.97. The granulated sugar were used in this research was produced by Beksul, CJ co., ltd, South Korea. Effective microbial (EM) powder (Hwang Se Ran EM, South Korea) contains various microbial spore. The samples were prepared for six condition; TFA1 (Sugar content: 25%); TFB1 (Sugar content: 25%, EM: 2g); TFC1 (Sugar content: 30%); TFD1 (Sugar content: 30%, EM: 2g); TFE1 (Sugar content: 35%); TFF1 (Sugar content: 35%, EM: 2g). 300g of tomato and ingredient in each treatment were blending with 300ml of drinking water. The fermentation period was done after 192 hours. The pH level and sugar contents were monitored in every 12 hours during fermentation period.

2.2 Instrumental analysis

Measured pH level was done by pH meter (SATO, Japan). The device used is pH meter type SK620PH, this device can measuring the pH with a value of 0-14. Sugar content in this research was measured using a refractometer type: Master-53M, capacity: 0.0-53%, ATAGO, Japan. The number of microbial in the colony were determining using plate counting analysis using MRS medium.The samples was prepared with 1-3 dilution (x1, x10, 100, 1000).

3. RESULTAND DISCUSSION

Fermentation proceeds satisfactorily when the pH of the mash has been adjusted to a pH of 3.0 to 4.5, which is a favorable pH for the yeast growth. As the concentration of the total solids decreases, the pH increases (Fig. 1). The experimental result in Fig. 2 shows that the titratable acidity is increased during fermentation process. The maximum result obtained from TFE1. The changes in pH and acidity must be due to changes in concentration of the sugars (Fig. 3) and organic acids. In this research as shown in Fig. 4 the highest colony form unit obtained from the 30% and 2g EM addition

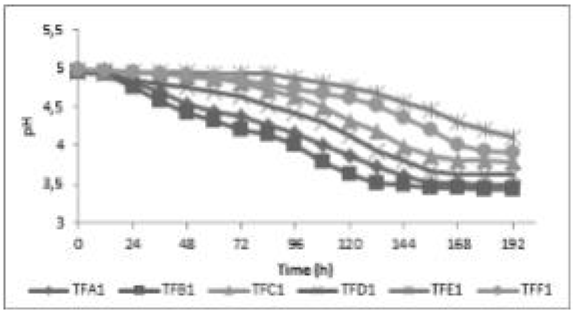

Fig. 1. The pH development obtained from tomato fermentation in 25°C room temperature

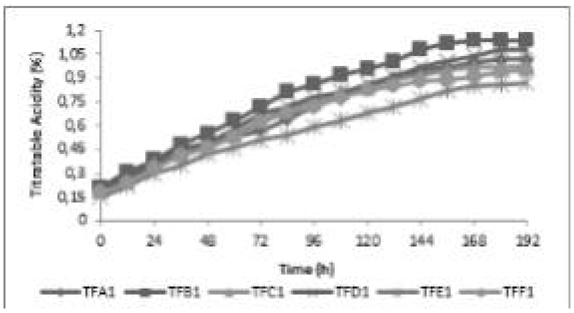

Fig. 2. The titratable acidity development obtained from tomato fermentation in 25°C room temperature

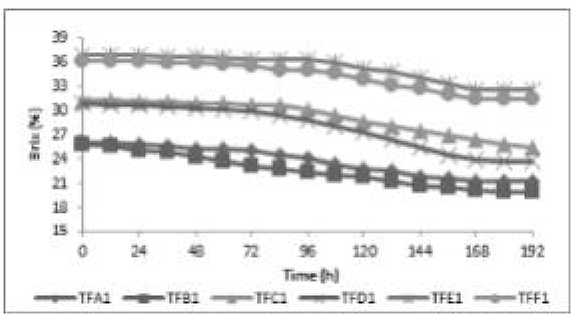

Fig. 3. The sugar content development obtained from tomato fermentation in 25°C room temperature

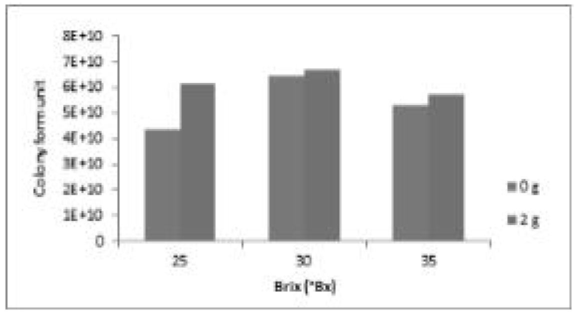

Fig. 4. CFU final amount depends on concentration of sugar content

4. CONCLUSTION

In this research, the behavior of jujube cherry tomato during fermentation and the effect of sugar content and effective microbial addition during fermentation were investigated. The experimental result shows that in the end of fermentation the lowest pH obtained from TFB1, the sugar content is reduced during fermentation, the highest acidity percentage obtained from TFE1, and the highest colony form unit obtained from TFD1.

REFERENCES

[1] B. R. and T. G. Josephine Nirmala Many, *Study on Tomato Wine Production and Optimization*, IOSR J. Environ. Sci. Toxicol. Food Technol., vol. 8, no. 1, pp. 97–100, 2014.

[2] R. Rolle and M. Satin, *Basic requirements for the transfer of fermentation technologies to developing countries,* Int. J. Food Microbiol., vol. 75, no. 3, pp. 181–187, 2002.

2017 Changwon International Conference on Intelligent Robot and Convergence Industry (CICIRO 2017)
Nov. 30- Des. 1, 2017, Changwon Exhibition Convention Center(CECO), Changwon, Korea

A Study on the tool for collecting insect pests from fruits trees

Ji-Hee Woo[1],Destiani supeno[1],Keefe Dimas haris sean[1],En-Suk Lee[1],Mi-kyung Nam[1],
Can-yeol Cha[2],Yeong-jo Moon[2],Won-Sik Choi[1]*
[1] Department of Bio-Industrial Machinery Engineering, Pusan National University,
[2] Hansol Farming Co. Ltd.

Abstract: Tree branches control and insect prevention are the critical thing when growing fruit. If the branches and pests are not controlled, they affect the growth and quality of the fruit. The string is used to manage the tree branches and controlling the insect, but the usage of the string is weak. The string could not reduce the growth of insect and branch. Due to the weakness of the string, pesticides were sprayed by drone. This method causes dangerous environmental pollution. Thus, this research was conducted to analyze a structure of the tool that could control the tree branches and insect. The tool was analyzed by Ansys R15.0. The sample of this tool is nylon. The frame safety factor of the sample is 13.062, and the hook safety factor is 20.912. Base on the data, the nylon safety factor values are higher than 1. this value showed that the product is safe if the material is nylon.

Keywords: Selected keywords relevant to the subject.

1. INTRODUCTION

Tree branches control and Pest prevention are most important for fruit growing. Fruit trees branches, when flowering period, were managed well to maintain the flower in the branches. the amount of flowers have correlation with the number of fruit and the quality of fruit. In addition, Pest insect trapping equipment is installed for pest prevention, but this tool has several disadvantage, for example the price is high, the usage and effectiveness are low. moreover, drones are used on farms that is caused environmental problems by spraying too much insecticide. Therefore, this study was consucted to develop a fixed tools that can kill the pests of fruit trees and holding the tree branches. the tool, pesticides, insecticides, and adhesives can be processed and used for 365 days regardless of the season. There is a hole in the top and bottom of the tool to catch pests in all directions. At the same time it is a good product with the ability to hold the tree by connecting the line to the outside of the tool. Therefore, in this study, structural analysis was performed using pest trap raw materials before production.

2. METERIALAND METHOD

2.1 Selection of materials

Composite Polypropylene, nylon, and ABS are the material that produce by some company. in this experiment, the nylon was used as a sample to analyse the product. The hook part was analyzed using stainless steel material. All boundary conditions were simulated at 100N.

2.2 Comparison of safety factors through structural analysis

An important part of the pest harvesting tool was produced in 3D model, The entire pest collection tool model specification was made with a width of Ø126mm and a height of 50mm. This modeling is based on Inventor 2017. As an analysis program, structural analysis was performed using Ansys R15.0.

3. RESULTAND DISCUSSION

The results of the analysis of the tool for insect trapping are shown in Fig.1 and Fig.2. The maximum stress applied to the entire frame is 82,737 MPa, The maximum stress applied to the hook portion was 6.3501e7 Pa. The stress of the frame was 6.3339e6 Max, and the stress of the hook was 9.8983e6 Max. 1The safety factor was calculated by Yield Strength / Equivalent stress. The safety factor values are higher than 1. this value showed that the product is safe if the material is nylon.

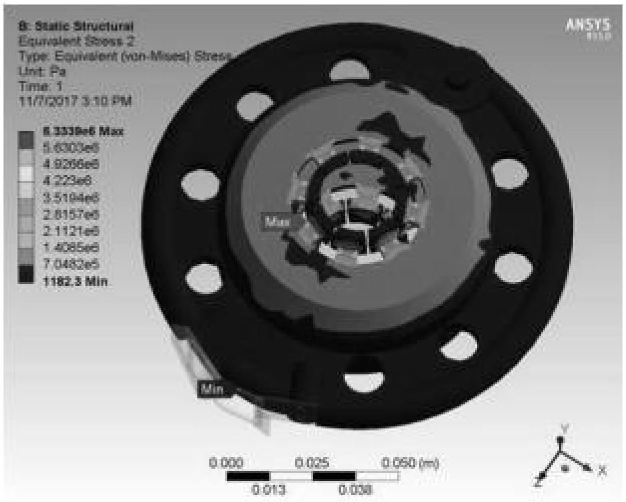

Fig. 1. Von-Misses stress occurred at frame

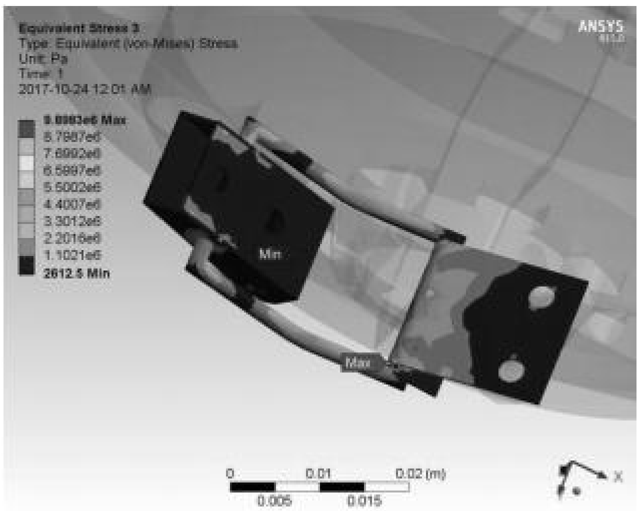

Fig. 2. Von-Misses stress occurred at hook

4. CONCLUSTION

In this study, the structural analysis of the tool for insect trapping was used to investigate the safety factor of nylon sample. As a result, the safety factor of the frame using nylon is 20.912. The safety factor of the hook was 20.912. Therefore, this value showed that the product is safe if the material is nylon because the safety factor values are higher than 1.

ACKNOWLEDGMENT

This paper is funded from the projects of Growth Technology Development by small&medium business Technology development management system center.

REFERENCES

[1] Y.H Kwon, H.S Park. *Distributed Structural Analysis Algorithms for Large-Scale Structures based on PCG Algorithms*, Journal of the Computational Structural Engineering Institute of Korea, Vol.12, No.3, 1999.

Charactrtistics of Separation with Tofu and Tofu Container according to Water Temperature

Eun Suk Lee[1], Jae Young Byeon, Mi Kyung Nam , Ji Hee Woo[1], Na Kyung Kim[2], Kang Sam Lee[3], Won Sik Choi[1]

Dept. of Bio Industrial Machinery Engineering, Pusan National University[1]

Bio Health Institute[2]

Dept .of Slow Food Inc[3]

Abstract: In this study, tofu is characterized by the fact that the beans are completely boiled. It is rich in nutrients because the nutrients of the beans are kept alive as they are stored without removing the beans. Especially ash, carbohydrate, vitamin k1, and niacin. It is rich in dietary fiber and has a fine-grained network structure. Compared to regular tofu, the texture is soft and sour and resilient The nutritional components of soybeans were reformed into tofu. The nutritional value of soybeans is not transformed, so it not only savors fresh taste, but also preserves its melting texture. It is a tofu that can absorb the nutrients of the whole body because the ingredients of soybeans are not destroyed. In this study, we investigated the optimum temperature for the best frozen tofu by checking the constant temperature of 600 ㎛ soybean powder in boiling water, diluted with water, and cooling the soymilk in the cooler. Then, the amount of natural mineral coagulants removed with arsenic was administered in different amounts. The next step in the process, hot water, is to measure the temperature of the best volume of the tofu clot to find the peak of the best tofu taste. And the separation phenomenon of tofu with the temperature during sterilization was investigated.

Keywords: Tofu and Tofu Container, Water Temperature

1. INTRODUCTION

Tofu is one of the processed foods that have been cooked using soybeans in Korea, China and Japan since ancient times.Tofu is high in moisture content, high digestibility, and other grains contain a small amount of amino acids containing arsinic sulfur.Therefore, tofu is a nutritional food with a lot of protein. It is known that it contains saponin, isoflavone, phytate, phytosterol, protease and inhibitor which have a lot of unsaturated fatty acid and have physiological activity such as anticancer, antioxidant and effect. Tofu products made from soybeans include general tofu, soya bean curd, soybean curd, soybean curd, soybean curd, and so on. In general tofu, proteins are extracted from soybean and removed from beans. Then, coagulant is added to produce a product by coagulation of protein. In the case of soybean, soybean, soybean and soybean, protein extraction process is the same as that of general tofu. And the production steps thereafter are somewhat different. Since general tofu is produced by extracting only the water-soluble protein of soybean, it is a food having a high loss of other water-soluble components and insoluble proteins contained in soybean.However, the soybean micropowder is used in the frontal part, and the process of removing the beans and the immersion process for a long time are omitted, so that the tofu can be produced in a short time. In this study, tofu is characterized by its ability to produce soluble protein, insoluble protein, fiber and other nutrients without loss.

2. Material and Method

2.1 Manufacturing process of tofu

In this study, we used Soybean Soybean Powder from Kangwon Province. The coagulant was used to make arsenic-free natural minerals. The tofu container was made of polypropylene (PP) and the machine was made for the frontal part, and the tofu was made during the frontal part manufacturing process. The process of manufacturing the tofu is as shown in Fig. 1 and takes more than an hour.

In the manufacturing process, the soybean powder is mixed with the soybean powder, stirred at a certain temperature, and then steamed. Then, the soybean curd coagulant is added, and the coagulant and the boiled soybean are put through the automatic machine. do. The storage temperature of the sterilization process was closely observed and compared with that of the well container in the tofu container after refrigerated storage.

Stirring + middling + moxibustion	Mineral + soy milk	Packing	Sterilization + refrigerated
			

Fig 1.Manufacturing of tofu

2.2 The principle of protein coagulation

Originally, water and protein are not mixed. The surfactant protects the protein particles, which causes water and protein to mix. Surfactants consist of hydrophilic and non-hydrophilic groups.
In the case of protein, it is a non-water-related off-peak season, so that the surfactant around the protein is adhered to a low-water period and becomes a colloidal state. At the outermost surface, a hydrophilic group is formed on the surface, which is well mixed with water. At this time, when a strong electrolyte such as a mineral is attached, the electrolyte ions attack the hydrophilic group of the colloid, thereby destroying the structure of the colloid. At this time, the protein which was protected by the surfactant was coagulated by using the principle that it was exposed to the aqueous solution and could not be dissolved and fell into the precipitate.

3. Result and Discussion

Through the clotting principle of protein, it was found that the tofu was not falling well in the tofu container when the tofu was manufactured through the tofu manufacturing process. As a result, The temperature of the hot water was set at 40 ° -75 ° and the temperature of the cold water was set at 10 ° -12 °, The duration of the separation of the tofu box and tofu was measured between 3 and 15 minutes. As a result, we could see that the warm water was well separated.

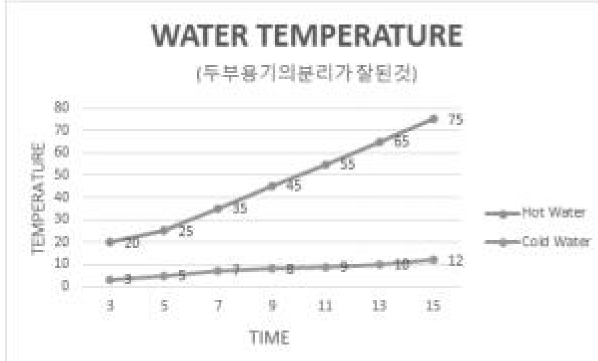

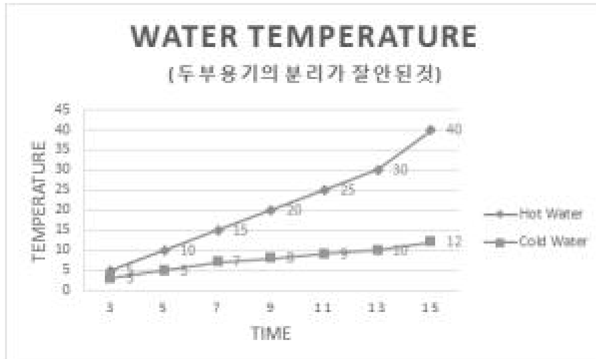

Fig 2. Separation of tofu container according to temperature change

4. Conclusion

A study on the separation characteristics of tofu and tofu containers according to water temperature,
When the tofu did not come off the container well, it was found that the tofu was not separated from the container when the temperature of the hot water was 40 ° or less and the time was less than 10 minutes. When the temperature of the hot water was 75 °, it was found that the tofu was separated from the container when the temperature was maintained at 12 ° for 15 minutes.

Acknowledgment

This paper is funded from the projects of Ministry of Agriculture, Food and Rural Affairs.

REFERENCES

[1] Coagulation and Characterization of Soybean Powder Particles
[2] Characterization of Soy Protein by Coagulant Mixing
[3] Development of domestic soybean curd using arsenic-free water
[4] Coagulation Characteristics of Soy Protein by Coagulant Mixture

Fermentation system and characteristics of natural fermented vinegar using lotus and stems

Mi Kyung Nam[1],Eun-Suk Lee [1], Ji Hee Woo[1], Jae-Young Byeon[1],Won-Sik Choi[1*]

Dept. of Bio Industrial Machinery Engineering, Pusan National University[1]

Abstract: The lotus is a perennial plant that is native to southern Asia and northern Australia. The lotus is a clean and noble plant that grows in the mud, and at the end of autumn, the end of the lotus grows. The leaf is a circular shield, and bloom is at the end of a long peduncle that emerges from the water around July to August. There are 4 to 5 calyx pieces, the fruit is called rice, It is used for edible or medicinal purposes along with the rootstock of the ground. The roots, petiole and fruit of the lotus are used as flowers for food, and the leaves are used as astringents and hemostats. The root is used as a tonic, the fruit is used as a treatment for gynecological diseases or as a tonic, and the water with the roots is good for mouth inflammation and tonsillitis, and the root of the root is good for the treatment of pulmonary tuberculosis, And seeds are used to reinforce the tusks, rootstocks contain asparagine, arginine, lecithin and many starches. The part used for medicine is roots, leaves, stamens, young sprouts, and contains excellent ingredients that help to strengthen the energy and to restore fatigue. In this study, we observed the process of making natural fermented vinegar using the lotus collected from the northwestern part of Milyang city. In the fermentation room at 35 ℃, 3 different control groups with different sugar contents were made, Fermentation was carried out for 90 days and sugar content, pH and alcohol content were measured.

Keywords: lotus and stems, Fermentation system

1. INTRODUCTION

The scientific name of lotus is nelumbo nucifera gaertnfh, whose origin is Egypt, India and is the most produced in China. Lotus is a perennial aquatic herb that grows in a pond and grows in paddy fields and fields. The rhizome is thick and stretched sideways with many nodes and white, with a cavity in the middle. Leaves come out of the roots, petioles are 1 ~ 2m long, come out on the water, and are round shields with a diameter of about 40cm. Flowers bloom in July and August, white and red, with yellow and blue lotus flowers. A flower stalk emerges from the roots and a 15-20 cm flower blooms at the end of the stem. Calyx is 4-5 pieces and yellowish and small. Petals are elliptical in several, fruit (ovary) is elliptical with nuts, and it is black. In this study, we tried to make natural fermented vinegar using lotus and date. Nowadays, western foods and instant food, high protein, high fat, and foods containing food additives are widespread, and modern fermented vinegar is considered to be a necessary health food for modern people. The organic acids such as citric acid and acetic acid which are abundant in vinegar smooth the energy metabolism in the body and help the decomposition of lactic acid and waste products which are the fatigue substances of our body not only to accelerate the recovery of fatigue but also to cause the diseases such as arteriosclerosis and thrombosis It prevents the formation of lipids and prevents arteriosclerosis.

In addition, as blood circulation improves, it removes stain and dullness, and elasticity and gloss are also made. In this way, the process of making lotus flower natural fermented vinegar and solid natural fermented vinegar was observed by combining a combination of the good efficacy and the pure action of vinegar.

2. Materials and Experiments

2.1 Lotus, fermentation materials

The experimental materials used in this study were flowers and ages of Paeoniae, which are produced in the northwestern part of Milyang city, Gyeongsangnam - do. The strains used for fermentation were Uinkin-Weissella koreensis BSS10, Lactobacillus salivarius SW709, Lactobacillus brevis BSS04, Lactobacillus casei BSS05, Lactobacillus strains purchased from Busan.Korea, which were developed by Daejeon Research Institute, Korea. plantarum HS729, Lactobacillus sakei MG521 Leuconostoc citreum BSS07, Leuconostoc mesenteroides SY1118, Streptococcus thermophilus BSS08, Saccharomyces cerevisiae BSS01, Bacillus subtilis BSS09, and Bacillus subtilis BSS11. White sugar was used for the sugar, tap water was purified from the jar for one day, Shinan - silver salt was used, and a glass bottle was used for the fermentation vessel.

pH meter (pH-250L, NeoMet,ISTEK)		**SEM pocket-refractometer-(ATAGO,Japan)**	
Fermentation chamber		**Glass bottle**	
Fig.1 Equipment for fermentation			

2.2 Fermentation system of lotus

In this study, we experimented with three kinds of control group with different lotus sugar content.

The first lotus (100g) was soaked with a brush to remove the aphid by immersing it in the activated yeast activity solution, washing it with tap water three times, and finely ground it in a blender so that the lotus component could be well leached. In the fermentation process, 630 g of white sugar, 2 ts, and 2 ts were added to the disinfected glass bottle, and the sugar content was 31.2 brix. The second lotus (100g) was put in the same manner as the first one with 410g of white sugar. At that time, sugar content was 24brix. The third lotus was put in the same manner as the first one with 240g of sugar. At this time, brix was 14.6brix. We also made three control groups with varying degrees of sugar. The first age is the same as the lotus. After finely chopping 3cm, the mixture was finely ground in a blender, and 545g of white sugar, 2ts, and 1ts of salting were put in a sterilized glass bottle. Its sugar content was 31.5brix. In the second generation, 545 g of white sugar was put in a glass bottle in the same manner as the first one. At that time, sugar content was 24brix. In the third generation, 180g of white sugar, white sugar, was put in a glass bottle in the same manner as the first one. The sugar content of this was 14.6brix. The lotus and the age were well stirred, and the lid was covered. The sugar content, Ph and alcohol content were measured in the chamber of 35 ° C until alcohol fermentation. After 30 days of fermentation, when alcohol fermentation was sufficiently performed, the mallow and liquid were separated using a cotton swab, and 300 ml of bottled water was added to the undiluted lotion solution and the aged root solution, and acetic acid fermentation was carried out in a chamber. However, the third lotus with low sugar content and the third age did the second fermentation without singer. As time went on, thin film began to form. Stir with the well-disinfected wooden sticks, and if you wake up the cottage, the bacteria of the air in the air will enter the vinegar.

3. Results and discussion

The fermentation process until the vinegar was observed by making three kinds of control lotions for 100 days of lotus and age. In order to proceed with alcohol fermentation, samples were taken at 10 ℃ intervals in a fermentation room at 28 ℃, and after 30 days of alcohol fermentation, alcohols were separated from the lotus and fermented fermented mushrooms and the alcohol was transferred to a new glass bottle which was sterilized. Samples were taken at intervals of 10 days and measured. The results are shown in the following figure.

<Brix>

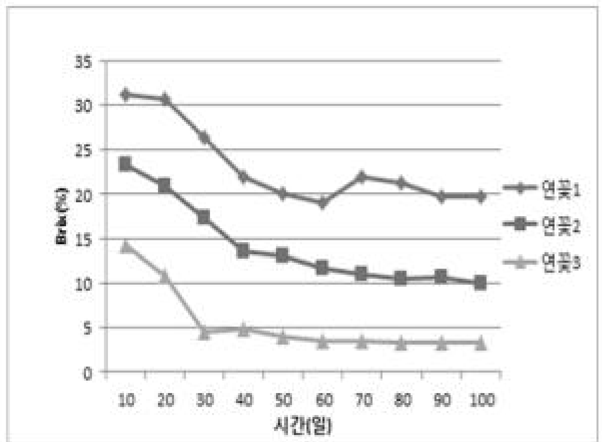

<pH>

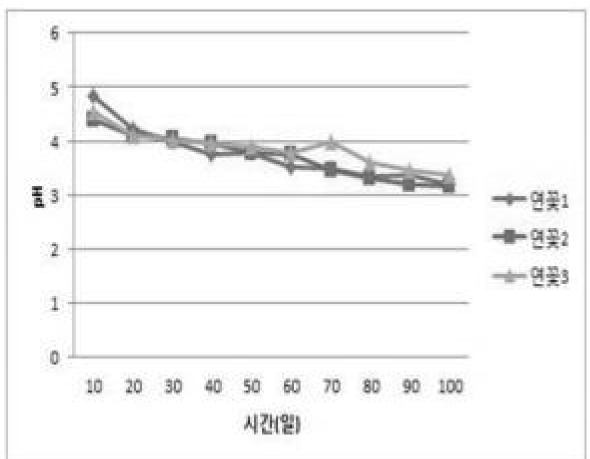

4. Conclusion

In this study, we tried to maximize the efficiency of the fermented vinegar by combining the excellent characteristics of lotus flower and date and obtained the following conclusions.

1) The sugar content gradually decreased as the date of fermentation elapsed.

2) The change of pH was 3 ~ 4 and it was found that the fluctuation of the change was not severe.

3) As the fermentation progressed, the color of the lotus changed from transparent yellow to brown, and the color of the ages changed from green to brown.

REFERENCES

[1] Park Won-seok "Microbiology and fermentation change the world" (2013)

[2] Jung, Dong-Hyo "Functionality of Fermented Foods" (2012)

[3] Now "Natural Vinegar Making Notes" (2014)

[4] Park Kook Moon "Enzymes and Health" (2013)w

2017 Changwon International Conference on Intelligent Robot and Convergence Industry (CICIRO 2017)
Nov. 30- Des. 1, 2017, Changwon Exhibition Convention Center(CECO), Changwon, Korea

The change of plant and fluorescent lamp temperature in closed system cultivation

Dimas Harris Sean Keefe[1], Jaeyoung Byun[1], Pandu Sandi Pratama[2],
Jeongyeol Cho[3], Wonsik Choi[1,#]

Dept. of Bio-industrial Machinery Engineering, Pusan National University[1]
Live and Industry Convergence Research Institute, Pusan National Universit[2]
Luxus. Co. Ltd[3]

Abstract: Growing plant in the factory with closed system cultivation, lamp light is used to change sunlight. The plant performs better growth under blue, red or blue-red lamplight. This research was conducted to determine the thermal change of plant and different lamp in the closed system cultivation. This system was applied to grow lettuce under blue, red, white and blue and red light. The plant and the lamp, every 30 minutes, were measured by Giltron Gt3000 temperature gun and FLIR thermal camera. The result showed that the white lamp had the higher temperature among the color of the lamp. The blue, red, and red-blue lamp temperature had the same temperature with room temperature. The plant temperature did not affect significantly by the lamp temperature. Due to the temperature of the blue, red, and red-blue light fluorescent lamp, this result could be used then to determine the effect of fluorescent lamp spectrum on the morphology of plant.

Keywords: plant and fluorescent lamp

1. INTRODUCTION

Light is the most important factor in the plant growth. Supplemental lights, nowadays, is used in the greenhouse. Okamoto (1996), Drozdova et al. (2001), and Chung et al. (2010) reported that growing plant by various lights provided better growth performances. The quality of spectrums on the light was adjusted to ensure optimal spectrum during planting time. However, Lamp involves the greenhouse environment like temperature. many types of lamps could be use for substituting sun light but, the most lamp that is used for growing plant is High Pressure Sodium (HPS) and Light Emitting Diode (LED). In this paper, fluorescent lamp was considered to cultivate lettuce on closed system greenhouse. the different color of lamp was prepared to determine the heat change of lamp and plant.

2. Materials and Method

This research was conducted in the bio industry machinery laboratory at Pusan National University. The different color of fluorescent lamp used in the research were white, blue, red and blue-red. The lamp was provided by Lexus Co. Ltd, South Korea which substituted the sun for growing plant. Lettuce was used in this research as testing plant. Four lamp color treatments were set in the greenhouse. Under each light, five lettuce was planted in the growing pot. The lamp and the plant were measured by Temperature Gun and FLIR thermal camera every 30 minutes.

3. Results and discussion

Plant, in many previous research, growth better under white light than mix light (blue and red light). Lettuce is the tested plant that observed with all variable measurement such as photosynthesis rate, shoot weight, leaf area, and leaf number being the same with and without green. However, the thermal variable of the plant is conducted in small number. The different lamp color and plant temperature were tested in this research. Blue light lamp, red light lamp, white lamp, and mix Blue and red) light lamp temperature raised 41.7℃, 41.5℃, 42.6℃, 34.1℃, 45.5℃, and 43.3℃. Moreover, the plant temperature increased with the lamp temperature.

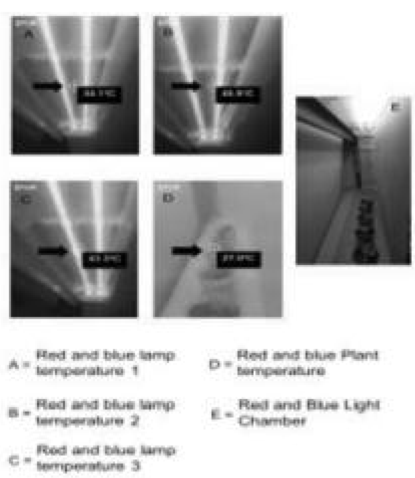

Fig. 1. Blue and Red Light Lamp

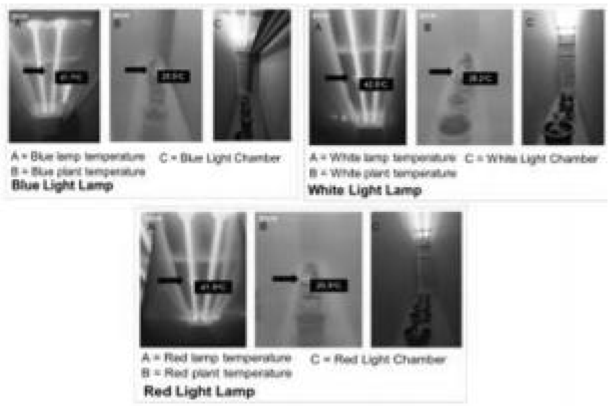

Fig. 2. Blue Light Lamp, White Light lamp, and Red Light Lamp

4. Conclusion

The fluorescent lamp that used in this research showed that the temperature of the lamp and the plant have an excellent control of temperature. The highest temperature of the lamp is 31.1 Celsius degrees, and the highest temperature of the plant is 24.8 Celsius degrees. These findings could be used then to design the spectrum of the fluorescent lamp to support plant growth, especially in the soilless cultivation, closed system method, and horticulture system.

REFERENCES

[1] J.P. Chung, C.Y. Huang, T.E. Dai.“Spectral effects on embryogenesis and plantlet growth of Oncidium ‘Gower Ramsey’", Sci. Hortic., 124, pp. 511-516, 2010.

[2] I.S. Drozdova, V.V. Bondar, N.G. Bukhov, A.A. Kotov, L.M. Kotova, S.N. Maevskaya, A.T. Mokronosov "Effects of light spectral quality on morphogenesis and source–sink relations in radish plant" Russ. J. Plant Physiol., 48, pp. 415-420, 2001.

[3] K. Okamoto, T. Yanagi, S. Takita, M. Tananka, T. Higuchi, Y. Ushida, H. Watamabe. "Development of plant growth apparatus using blue and red as artificial light source", Acta Hortic., 440, pp. 111-116, 1996.

2017 Changwon International Conference on Intelligent Robot and Convergence Industry (CICIRO 2017)
Nov. 30th~ Dec. 1st, 2017, Changwon Exhibition Convention Center(CECO), Changwon City, Korea

A Orientation Control of Vertical Articulated Robot Manipulator Based on Servoing Feedback in Working Space

Hee-Jin Kim[1], Woo-Song Lee[2], Min-Seong Kim[3], In-Man Park[4] and Sung-Hyun Han[5]

[1]M.S Course, Manigement & Industry Graduate School
Kyungnam University, 51767, Korea
(E-mail : jizhen79@nate.com)
[2] SUNJIN Technology Co., Ltd., Changwon, 82331, Korea
(E-mail: elflws@nate.com)
[3] Department of Advanced Engineering., Kyungnam University, Changwon, 51767, Korea
(E-mail : kms21018@naver.com)
[4] Intem Co., Ltd., Changwon City, 51565, Korea
(E-mail:intem237@hanmail.net)
[5] School of Mechanical Engineering, Kyungnam University, Changwon, 51767, Korea
(E-mail: shhan@kyungnam.ac.kr)

Abstract: This study presents how it is effective to use many features for improving the accuracy of the position control for vertical type articulated robot. Some rank conditions, which relate the image Jacobian, and the control performance are derived. It is also proven that the accuracy is improved by increasing the number of features. Effectiveness of the redundant features is verified by the real time experiments on a Robot manipulator with seven joint.

Keywords: Visual Feedback Control, Redundant Feature, Feature-Based Path Planning, Real-Time Control

1. INTRODUCTION

This paper presents a method to solve this problem by using a binocular stereo vision. The use of stereo vision can lead to an exact image Jacobian not only at around a desired location but also at the other locations. The suggested technique places a robot manipulator to the desired location without giving such prior knowledge as the relative distance to the desired location or the model of an object even if the initial positioning error is large. This paper deals with modeling of stereo vision and how to generate feedback commands. The performance of the proposed visual feedback system was evaluated by the simulations and experiments and obtained results were compared with the conventionalmethods.

There are mainly two ways to put the visual feedback into practice. One is called look-and-move and the other is visual feedback. Visual feedback is the fusion of results from many elemental areas including high-speed image processing, kinematics, dynamics, control theory, and real-timecomputing.

2. PATH PLANNING

The origin of the world frame is located at a certain point in the world.

Now let ${}_I p = ({}_l x, {}_l y)$ and ${}_r p = ({}_r x, {}_r y)$ be the projections onto the left and right images of a point p in the environment, which is expressed as ${}^c p = ({}^c x\ {}^c y\ {}^c z)^T$ in the camera frame. Then the following equation is obtained (see Fig. 1).

$$ {}^l x\, {}^c z = f({}^c x + 0.5d) \quad (1\text{-a})$$

$$ {}^r x\, {}^c z = f({}^c x - 0.5d) \quad (1\text{-b})$$

$$ {}^l y\, {}^c z = f\, {}^c y \quad (1\text{-c})$$

$$ {}^r y\, {}^c z = f\, {}^c y \quad (1\text{-d})$$

Suppose that the stereo correspondence of feature points between the left and right images is found. In the visual feedback, we need to know the precise relation between the moving velocity of camera and the velocity of feature points in the image, because we generate a feedback command of the manipulator based on the velocity of feature points in the image.

This relation can be expressed in a matrix form which is called the image Jacobian. Let us consider n feature points $p_k (k = 1, \cdots, n)$ on the object and the coordinates in the left and right images are ${}^l p_k ({}^l x_k, {}^l y_k)$ and ${}^r p_k ({}^r x_k, {}^r y_k)$, respectively. Also define the current location of the feature points in the image ${}_I p$ as

$$ {}_I p = ({}_l x_1\ {}_r x_1\ {}_l y_1\ {}_r y_1 \cdots {}_l x_n\ {}_r x_n\ {}_l y_n\ {}_r y_n)^T \quad (2)$$

where each element is expressed with respect to the virtual image frame Σ_p.

First, to make it simple, let us consider a case when the number of the feature points is one. The relation between the velocity of feature point in image ${}_I \dot{p}$ and the velocity of camera frame ${}^c \dot{p}$ is given as

$$^I\dot{p} = J_{Ic}\,{}^c\dot{p} \tag{3}$$

where J_{Ic} is the Jacobian matrix which relates the two frames. Now let the translational velocity components of camera be $\dot{x}$, $\dot{y}$ and $\dot{z}$ and the rotational velocity components be w_x, w_y, w_z then we can express the camera velocity V as

$$V = [\dot{x}\ \dot{y}\ \dot{z}\ w_x\ w_y\ w_z]^T = [v\ \ {}^cw_c]^T \tag{4}$$

Then the velocity of the feature point seen from the camera frame ${}^c\dot{p}$ can be written

$${}^c\dot{p} = \frac{d\,{}^cp}{dt} = \frac{d}{dt}\,{}^cR_w({}^wp - {}^wp_c) = {}^cR_w\{-{}^ww_c \times ({}^wp - {}^wp_c)\} + {}^cR_w({}^w\dot{p} - {}^w\dot{p}_c) \tag{5}$$

where ${}^cR_w$ is the rotation matrix from the camera frame to the world frame and ${}^wp_c$ is the location of the origin of the camera frame written in the world frame. As the object is assumed to be fixed into the world frame, ${}^w\dot{p} = 0$. The relation between ${}^c\dot{p}$ and V is

$${}^c\dot{p} = {}^cR_w\{-{}^ww_c \times ({}^wp - {}^wp_c)\} - {}^cR_w\,{}^w\dot{p}_c = -{}^cw_c \times {}^cp - {}^c\dot{p}_c = \begin{bmatrix} -w_y\,{}^cz + w_z\,{}^cy - v_x \\ -w_z\,{}^cx + w_x\,{}^cz - v_y \\ -w_x\,{}^cy + w_y\,{}^cx - v_z \end{bmatrix} \tag{6}$$

Therefore, substituting Eq. (6) into Eq. (3), we have the following equation.

$$^I\dot{p} = J_{Ic}\,{}^c\dot{p} = JV \tag{7}$$

In Eq. (7) matrix J which expresses the relation between velocity ${}^I\dot{p}$ of the feature point in the image and moving velocity V of the camera is called the image jacobian.

From the model of the stereo vision Eq. (1), the following equation can be obtained.

$$2\,{}^cx\,({}^lx - {}^rx) = d\,({}^lx + {}^rx) \tag{8}$$

$${}^cy\,({}^lx - {}^rx) = {}^ly\,d = {}^ry\,d \tag{9}$$

$${}^cz\,({}^lx - {}^rx) = f\,d \tag{10}$$

Above discussion is based on the case of one feature point. In practical situation, however, the visual feedback is realized by using plural feature points. When we use n feature points, image Jacobian $J_1, \cdots, J_n$ are given from the coordinates of feature points in the image. By combining them, we express the image Jacobian (J_{im}) as

$$J_{im} = [\,J_1 \cdots J_n\,]^T \tag{11}$$

Then, it is possible to express the relation of the moving velocity of the camera and the velocity of the feature points even in the case of plural feature points, that is,

$$^I\dot{p} = J_{im}V \tag{12}$$

where we suppose that the stereo and temporal correspondence of the feature points are found.

In the case of the monocular, the image Jacobian J has the following form.

$$J = f\begin{bmatrix} -\frac{1}{^cz} & 0 & \frac{^cx}{^cz^2} & \frac{^cx\,^cy}{^cz} & -\frac{1+{}^cx^2}{^cz} & \frac{^cy}{^cz} \\ 0 & -\frac{1}{^cz} & \frac{^cy}{^cz^2} & \frac{1+{}^cy^2}{^cz} & -\frac{^cx\,^cy}{^cz} & -\frac{^cx}{^cz} \end{bmatrix} \tag{13}$$

The x , y and z axes of the coordinate frames are shown in Fig. 1.

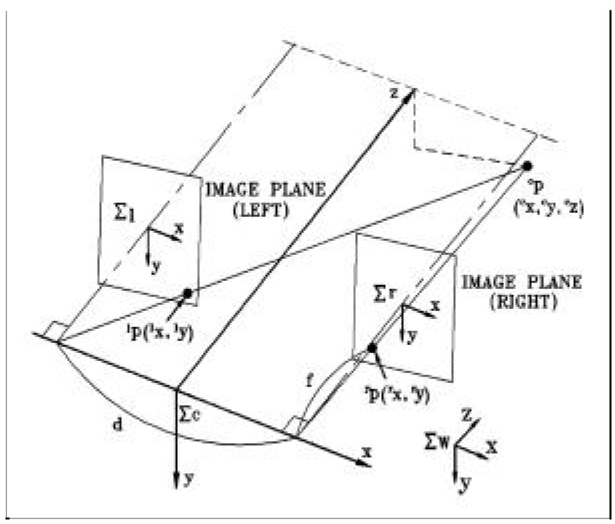

Fig. 1 The coordinates system of vision model.

3. EXPERIMENTS

We have compared the visual feedback using the monocular vision with that using the stereo vision by the experiment.

The error between the desired location and the current location of the feature points in cases of the monocular and stereo visions are shown in Fig. 2.

Two stereo images were taken and transformed to the binary images in the real time and in parallel by two image input devices and the coordinate of the gravitational center of each feature point was calculated in parallel by two transporters. We gave the stereo correspondence of the feature point in the first sampling. However, the stereo and temporal correspondence of the feature points in the succeeding sampling was found automatically by searching a nearby area where there were the feature points in the previous sampling frame. The coordinates of the feature points were sent to a transporter for motion control and it calculated a feedback command for the robot. The result was sent to the robot controller by using RS-232C, and the robot was controlled by a velocity servo system in thecontroller.

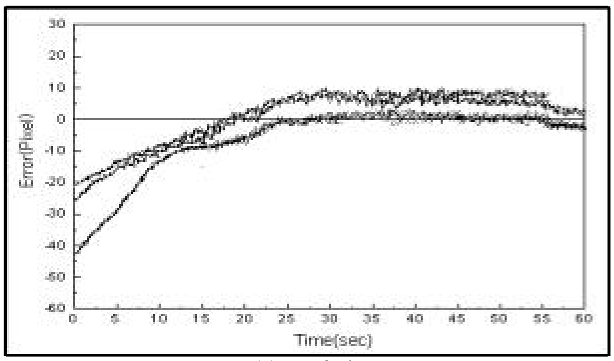

(a) Left image

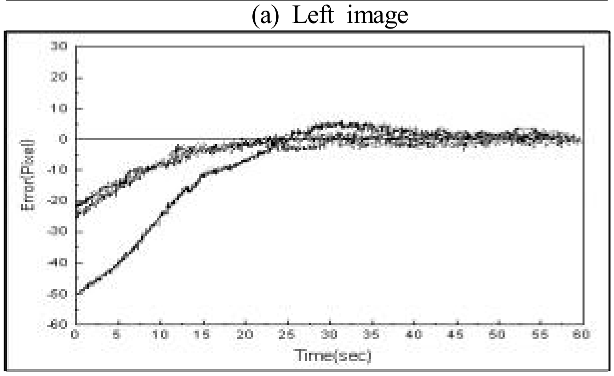

(b) Right image

Fig. 2. Position error in x and y axes.

The sampling period of visual feedback was about 50 *m*sec . Details were 16 *m*sec for taking a stereo image, about 1*m*sec for calculating the coordinates of the feature points, 3*m*sec for calculating feedback command, about 16 *m*sec for communicating with the robot controller. If we send a feedback input to the robot controller without using RS-232C, the faster visual feedback can be realized.

The desired location was $(0,0,550)^T$ *mm* and the desired orientation in Euler angle, (↗,❑ ,▱) ■ (0, 0, 0) degree and the initial error was $(55,55,55)^T$ *mm* for translation. The other parameters were the same as in the simulation. The error of current and desired location of the feature points are shown in Fig. 5. From these experimental results, we can see that the manipulator converges toward a desired location even if the calibration is not precise.

4. CONCLUSION

We have proposed a new technical of visual feedback with the stereo vision to control the position and orientation of an assembling robot with respect to an object. The method overcomes the several problems associated with the visual feedback with the monocular vision. By using the stereo vision, the image Jacobian can be calculated at any position. So neither shape information nor desired distance of the target object is required. Also the stability of visual feedback is illustrated even when the initial error is very large.

ACKNOWLEDGEMETN

This study was performed by project of the robot business belt construction enterprise.

REFERENCES

[1] Chaumette, F., Rives, P., and Espiau, B., "Positioning of a robot with respoect to an object, tracking it and estimating its velocity by visual servoing," In *Proceedings of the IEEE International Conference on Robotics and Automation*, pp. 2248-2253, 1991.

[2] Bernard, E., Francois, C., and Patrick, R., "A new approach to visual servoing in robotics," *IEEE Transactions on Robotics and Automation*, pp. 313-326, 1992.

[3] Weiss, L. E., Sanderson, A. C., and Neuman, C. P., "Dynamic sensor-based control of robots with visual feedback," *IEEE Journal of Robotics and Automation*, pp. 404-417,1987.

[4] Hashimoto, K., Kimoto, T. Edbine, T.,and Kimura, H., "Manipulator control with image-based visual servo," In *Proceedings of IEEE International Conference on Robotics and Automation*, pp. 2267-2272, 1991.

[5] Hashimoto, K., Edbine, T., and Kimura, H., "Dynamic visual feedback control for a hand-eye manipulator," In *Proceedings of the IEEE/RSJ International Conference on Intelligent Robots and Systems*, pp. 1863-1868, 1992.

A Precise Position and Velocity Control of Vertical Type Robot Arm with Seven D.O.F

Min-Seong Kim[1], Min-Hyuck Choi[2], Jeong-Suk Kang[3],
Nam-Il Yoon[3], Jong-Bum Won[3], Sung-Hyun Han[4]
[1] Department of Advanced Engineering, Graduate School Kyungnam University,
Changwon, 51767, Korea (kms21018@naver.com) * Corresponding author
[2] School of Mechanical Engineering, Kyungnam University,
Changwon, 631-701, Korea (shhan@kyungnam.ac.kr)
[3]SMEC Co., Ltd., Gimhae, 50969, Korea(jskang@esmec.com/yni@esmec.com/won@esmec.com)
[4] School of Mechanical Engineering, Kyungnam University,
Changwon, 631-701, Korea (shhan@kyungnam.ac.kr)

Abstract: We describe a new approach to the design and real-time implementation of an adaptive controller for robotic manipulator based on digital signal processors in this paper. The Texas Instruments DSPs(TMS320C80) chips are used in implementing real-time adaptive control algorithms to provide enhanced motion control performance for dual-arm robotic manipulators. In the proposed scheme, adaptation laws are derived from model reference adaptive control principle based on the improved direct Lyapunov method.
Keywords: Adaptive Control, Dual-Arm Robot, Real Time Control, Real-Time Implementation

1. INTRODUCTION

This paper describes a new approach to the design of adaptive control system and real-time implementation using digital signal processors for robotic manipulators to achieve the improvement of speedness, repeating precision, and tracking performance at the joint and cartesian space.

2. MODELING

The dynamic model of a manipulator-plus-payload is derived and the tracking control problem is stated in this section.

Let us now consider payload in the manipulator dynamics. Suppose that the manipulator end-effector is firmly grasping a payload represented by the point mass M_p. For the payload to move with acceleration $\ddot{X}(t)$ in the gravity field, the end-effector must apply the n×1 force vector $T(t)$ given by

$$T(t) = M_p [\ddot{X}(t) - g] \quad (1)$$

where g is the n×1 gravitational acceleration vector.

The end-effector requires the additional joint torque

$$\tau_f (t) = J(q)^T T(t) \quad (2)$$

where superscript T denotes transposition. Hence, the total joint torque vector can be obtained by combining equations (1) and (4) as

$$J(q)^T T(t) + D(q) \ddot{q} + N(q, \dot{q}) + G(q) = \tau (t) \quad (3)$$

Substituting equations (2) and (3) into equation (4) yields

$$M_p J(q)^T [J(q) \ddot{q} + \dot{J}(q, \dot{q}) \dot{q} - g] + D(q) \ddot{q} + N(q, \dot{q}) + G(q) = \tau (t) \quad (4)$$

3. SIMULATION AND EXPERIMENT

This section represents the simulation results of the position and velocity control of a four-link robotic manipulator by the proposed adaptive control algorithm, as shown in Fig.1, and discusses the advantages of using joint controller based-on DSPs for motion control of a dual-arm robot. The adaptive scheme developed in this paper will be applied to the control of a dual-arm robot with eighth axes. Fig.1 represents link coordinates of the dual-arm robot.

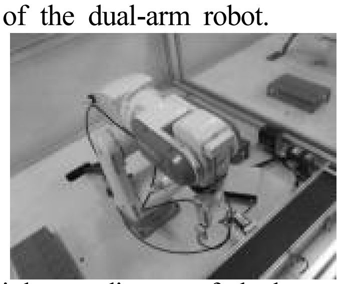

Fig.1. Link coordinates of dual-arm robot

4. CONCLUSION

The proposed DSP-based adaptive controllers have several advantages over the analog control and the micro-computer based control. This allows instructions and data to be simultaneously fetched for processing. Moreover, most of the DSP instructions, including multiplications, are performed in one instruction cycle.

REFERENCES

[1] M. Vukobratovic and D. Juricic, "Contribution to the synthesis of biped gait," IEEE Trans. on Bio-Medical Engineering, vol. 16,pp. 1-6, 1969

2017 Changwon International Conference on Intelligent Robot and Convergence Industry (CICIRO 2017)
Nov. 30th~ Dec. 1st, 2017, Changwon Exhibition Convention Center(CECO), Changwon City, Korea

A Stable Path Control of Robot Manipulator with 6 Joints for Forging Trimming Automation

Min-Seong Kim[1], Jong-Hun Kim[1], Sung-Hun Noh[2], Gi-Su Shin[3], Jeong-Suk Kang[4], Jong-Bum Won[4] and Sung-Hyun Han[5]

[1] Department of Advanced Engineering, Graduate School Kyungnam University, Changwon, 51767, Korea (kms21018@naver.com/ kimjh4750@naver.com) * Corresponding author

[2] YoungChang Robotech Co., Ltd., Gimhae, 50969, Korea(giosugo@naver.com)

[3] ANY TOY CO. Ltd., Kyungnam University, Changwon, 51767, Korea (E-mail : Shings@naver.com)

[4] SMEC Co., Ltd., Gimhae, 50969, Korea(jskang@esmec.com/won@esmec.com)

[5] Department of Mechanical Engineering, Kyungnam University, Changwon, 51767, Korea (shhan@kyungnam.ac.kr)

Abstract: We describe a new approach to the design and real-time implementation of an adaptive controller for robotic manipulator based on digital signal processors in this paper. The Texas Instruments DSPs(TMS320C80) chips are used in implementing real-time adaptive control algorithms to provide enhanced motion control performance for vertical type robotic manipulators. In the proposed scheme, adaptation laws are derived from model reference adaptive control principle based on the improved direct Lyapunov method

Keywords: : Adaptive Control, Dual-Arm Robot, Real Time Control, Real-Time Implementation

1. ROBOT MODELING DYNAMICS

The dynamic model of a manipulator-plus-payload is derived and the tracking control problem is stated in this section.

Let us now consider payload in the manipulator dynamics. Suppose that the manipulator end-effector is firmly grasping a payload represented by the point mass M_p. For the payload to move with acceleration $\ddot{X}(t)$ in the gravity field, the end-effector must apply the n×1 force vector $T(t)$ given by

$$T(t) = M_p [\ddot{X}(t) - g] \qquad (1)$$

where g is the n×1 gravitational acceleration vector.

The end-effector requires the additional joint torque

$$\tau_f(t) = J(q)^T T(t) \qquad (2)$$

2. SIMULATION AND EXPERIMENT

This section represents the simulation results of the position and velocity control of a four-link robotic manipulator by the proposed adaptive control algorithm, as shown in Fig.1, and discusses the advantages of using joint controller based-on DSPs for motion control of a dual-arm robot. The adaptive scheme developed in this paper will be applied to the control of a vertical type robot with seven axes. Fig.1 represents link coordinates of the vertical type robot.

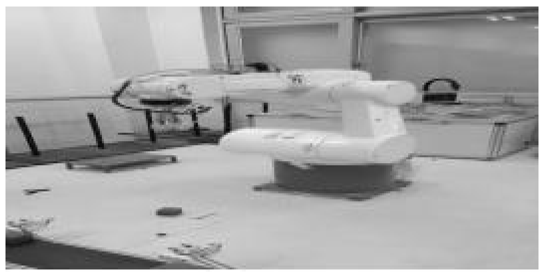

Fig. 1 link coordinates of the vertical type robot.

3. CONCLUSION

The proposed DSP-based adaptive controllers have several advantages over the analog control and the micro-computer based control. This allows instructions and data to be simultaneously fetched for processing. Moreover, most of the DSP instructions, including multiplications, are performed in one instruction cycle.

4. ACKNOWLEDGEMENT

This study was performed by project of the robot business belt construction enterprise. And supported by the Ministry of Trade, Industry and Energy. (R0004565)

REFERENCES

[1] P.C.V. Parks, July 1966, "Lyapunov Redesign of Model Reference Adaptive Control System," IEEE Trans. Auto. Contr., Vol. AC-11, No. 3, pp. 362-267.

[2] Y.K. Choi, M.J. Chang, and Z. Bien, 1986, "An Adaptive Control Scheme for Robot Manipulators." IEEE Trans. Auto. Contr., Vol. 44, No. 4, pp. 1185-1191.

A Study on Intelligent Control of Biped Robot for Smart Factory

Un-Tae Ha[1], Min-Seong Kim[2], Byung-Suk Yoon[3], Jung-Eup Gye[4], Jong-Gyo Jung[5] and Sung-Hyun Han[6]

[1] PhD. Course, Graduate School Kyungnam University, Changwon, 51767, Korea (euntha@hanmail.net) * Corresponding author

[2] Department of Advanced Engineering, Graduate School Kyungnam University, Changwon, 51767, Korea (kms21018@naver.com)

[3] Doosan Heavy Industries & Construction Co., Ltd., Changwon, 51711, Korea (rtrshbaek@hanmail.net)

[4] Ministry of Trade, Industry & Energy Office of Strategic R&D Planning, Sejong, 30118, Korea(jekeh66@naver.com)

[5] KAVAS Co., Ltd., Changwon, 630-812, Korea (jongkyo@kavas.co.kr)

[6] Department of Mechanical Engineering, Kyungnam University, Changwon, 51767, Korea (shhan@kyungnam.ac.kr)

Abstract: We present a new technology for real-time walking of a humanoid robot. A humanoid robot necessitates achieving stabilization for real time walking since it has basic problems such as structural stability. In this paper, a robust control algorithm for stable walking is proposed based the ground reaction forces, which are measured using force sensors during walking, and the environmental conditions are estimated from these situation. From this information the robot selects the proper motion and overcomes ground irregularities effectively. In order to generate the proper angel of the joint. The performance of the proposed algorithm is verified by simulation and experiments for a 20-DOFs humanoid robot.

Keywords: Stable walking, Control algorithm, Humanoid robot, Robust walking

1. INTRODUCTION

This paper proposes an obstacle avoidance architecture allowing walking humanoid robots to walk safely around in factory and home environment.

A main technological target of the proposed robot (Model:V-HUR) is to autonomously explore and wander around in home environments as well as to communicate with humans.

2. ROBOT CONTROLSYSTEM

The main board of the CPU receives the resulting disparity image as a digital video signal. The stereo control parameters can be set between the main CPU and the 8bit CPU on board through a special serial communication link.

The vision system (mentioned above) receives image from the two CCD cameras. These parameters are useful for computing 3D range data. The disparity is calculated for each pixel in the left image by searching for the corresponding pixel in the right image. An additional reliability image is calculated following criteria to reject results on above conditions.

3. EXPERIMENT

Firstly, the disparity is converted into 3D range data using the parameters from camera calibration and then a Hough transformation is applied to all data points. Apply the *randomized Hough transformation* selects sets of data points from which the surface parameters can be directly computed and records the result in a table. If many-data sets yield the same parameters, a high score for these parameters is obtained.

Fig. 1 The humanoid robot

4. CONCLUSION

The autonomous mobility for the humanoid robot V-HUR in the home environment is realized base on the development of a small stereo vision system, the recognition of floor and obstacles using plane extraction.

REFERENCES

[1] D. Pagac, E. Nebot and H. Durrant-Whyte, "An evidential approach to map-building for autonomous vehicles," IEEE Transactions on Robotics and Automation, 14(4), 623-629, 1998.

A Study on Intelligent Motion Control of Humanoid Robot for Smart Factory

Min-Seong Kim1, In-Man Park2, Young-Hwa Jeong3, Sung-Hyun Han4

[1] Department of Advanced Engineering., Kyungnam University, Changwon, 51767, Korea (E-mail : kms21018@naver.com)
[2] Intem Co., Ltd., Changwon City, 51565, Korea (intem237@hanmail.net)
[3] Daeho Technology Korea Co., Ltd., 513983, Korea (yhjung@daehoteck.co.kr)
[4] Department of Mechanical Engineering, Kyungnam University, Changwon, 51767, Korea (shhan@kyungnam.ac.kr)

Abstract: We present a new technology for real-time walking of a humanoid robot. A humanoid robot necessitates achieving stabilization for real time walking since it has basic problems such as structural stability. In this paper, a robust control algorithm for stable walking is proposed based the ground reaction forces, which are measured using force sensors during walking, and the environmental conditions are estimated from these situation. From this information the robot selects the proper motion and overcomes ground irregularities effectively. In order to generate the proper angel of the joint. The performance of the proposed algorithm is verified by simulation and experiments for a 20-DOFs humanoid robot

Keywords: Stable Walking, Control Algorithm, Humanoid Robot, Robust Walking

1. INTRODUCTION

This paper proposes an obstacle avoidance architecture allowing walking humanoid robots to walk safely around in factory and home environment.

A main technological target of the proposed robot (Model:V-HUR) is to autonomously explore and wander around in home environments as well as to communicate with humans.

2. SYSTEM MODELING

The main board of the CPU receives the resulting disparity image as a digital video signal. The stereo control parameters can be set between the main CPU and the 8bit CPU on board through a special serial communication link.

The vision system (mentioned above) receives image from the two CCD cameras. These parameters are useful for computing 3D range data. The disparity is calculated for each pixel in the left image by searching for the corresponding pixel in the right image. An additional reliability image is calculated following criteria to reject results on above conditions. After block matching has been carried out, the matching score is calculated by interpolating scores near the highest peak.

The sharpness of this peak corresponds to the available texture around this pixel and thus can be used as a reliability value for the disparity calculation. If there are other peaks with similar matching scores then the disparity computation is ambiguous and the reliability is set to a low value. (The matching score is compared with neighboring scores).

3. EXPERIMENT

Firstly, the disparity is converted into 3D range data using the parameters from camera calibration and then a Hough transformation is applied to all data points. Apply the *randomized Hough transformation* selects sets of data points from which the surface parameters can be directly computed and records the result in a table. If many data sets yield the same parameters, a high score for these parameters is obtained.

Although applying floor detection methods, obstacles and regions the robot can walk on can be found. However, in general it is difficult to decide from a single observation with a limited field of view, the action the robot should carry out next. We follow this notion and introduce a terrain map where all observations and motions are integrated.

4. CONCLUSION

The autonomous mobility for the humanoid robot V-HUR in the home environment is realized base on the development of a small stereo vision system, the recognition of floor and obstacles using plane extraction.

The terrain is represented in a robot centric coordinate system without making any structural assumptions about the surrounding world. And the representation of a terrain map based on these observations, robot motion, and the generation of a walking path on the terrain map

REFERENCES

[1] D. Pagac, E. Nebot and H. Durrant-Whyte, “An evidential approach to map-building for autonomous vehicles,” IEEE Transactions on Robotics andAutomation, 14(4), 623-629, 1998.

A Study on Motion Control of Humanoid Robot for Human-Robot Interaction

Min-Seong Kim[1], Byeong-Gap Moon[2], Kyu-Hyun Jung[3],
Myeong-Hwan Park[4], Ju-Jang Lee[5] and Sung-Hyun Han[6]
[1] Department of Advanced Engineering, Graduate School Kyungnam University, Changwon, 51767, Korea (kms21018@naver.com)
[2] KWANGJIN PRECISION Co., Ltd., Changwon, 51220, Korea (kkj362@naver.com)
[3] SEYOUNG INDUSTRY Co., Ltd., Changwon, 51211, Korea (sysky25@naver.com)
[4] ROBOT VALLEY Co., Ltd., Changwon, 51572, Korea (mhpark01@korea.com)
[5]KAIST, Daejun, 34141, Korea(jjlee@ee.kaist.ac.kr)
[6] Department of Mechanical Engineering, Kyungnam University, Changwon, 51767, Korea (shhan@kyungnam.ac.kr)

Abstract: This paper deals with the stable walking for a biped robot, on uneven terrain, A biped robot necessitates achieving posture stabilization since it has basic problems such as structural instability. In this paper, a stabilization algorithm is proposed using the ground reaction forces, which are measured using FSR (Force Sensing Resistor) sensors during walking, and the ground conditions are estimated from these data. From this information the robot selects the proper motion pattern and overcomes ground irregularities effectively. In order to generate the proper angel of the joint. The performance of the proposed algorithm is verified by simulation and walking experiments on a 24-DOFs biped robot.

Keywords: Force sensing resistor, Fuzzy algorithm, Biped robot, Stabilization

1. INTRODUCTION

In this paper, a real-time walking stabilization method utilizing a fuzzy algorithm under uneven terrain is proposed. We focused most of our interest on landing phase. The ground reaction forces, measured by FSR sensors on the sole, are used to assess the ground condition and the robot posture. Simulation and experiment results for the proposed method are given in Section 3, followed by conclusions in the final section.

2. WALKING PATTEN

Basically, a robot walks with the trajectory generated previously assuming even terrain. If different values from the expected sensor are measured during walking, the robot should be deployed using the stabilization algorithm. Fig.1 presents the walking algorithm.

When the robot is walking, it measures the ground reaction forces in real-time and utilizes them as inputs to the controller. When the control of the robot is interrupted by an unexpected situation or a unit step has ended, the new trajectory should be generated according to the changed situation.

3. BIPED ROBOT AND SYSTEM

The robot walks according to a basic trajectory. In basic walking, a stride is 0.12m, velocity is 0.04m/s, and the ground is regarded as being flat. The robot steps on projected ground of 11mm in height with the tie if the swing leg. When the control algorithm is not applied, the sensor data is presented as given in Fig.2, The robot pushes the ground continuously, and the heel does not contact until the end of the stride.

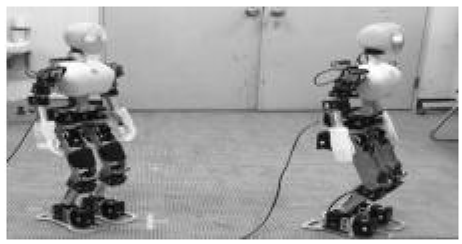

Fig. 1 The biped robot for cooperative working.

4. CONCLUSION

This paper described a real-time control technology to implement the walking of a biped robot on uneven terrain. It was assumed that the ground condition on the basis of ground reaction forces measured sensors on the soles of the feet during walking. The robot could maintain balanced walking through control of the ankle joints using a fuzzy algorithm.

REFERENCES

[1] M. Vukobratovic and D. Juricic, "Contribution to the synthesis of biped gait," IEEE Trans. on Bio-Medical Engineering, vol. 16,pp. 1-6, 1969

AStudy on Motion Control of Two Wheel Driving Mobile Robot by Voice Commend for Smart Factory

Gi-Hyun Kim1, Ho-Young Bae 2, Woo-Song Lee 3 and Sung-Hyun Han4

[1] Doosan Heavy Industries & Construction Co., Ltd., Changwon, 51711, Korea
(E-mail: kihyeon.kim@doosan.com)
[2] V-Mac Company Co., Ltd. Changwon, 50850, Korea (E-mail: sswq1r@hanmail.net)
[3] SUNJIN Technology Co., Ltd., Changwon, 82331, Korea
(E-mail: elflws@nate.com)
[4] School of Mechanical Engineering, Kyungnam University,
Changwon, 631-701, Korea (E-mail: shhan@kyungnam.ac.kr)

Abstract: In this paper, we describe an voice recognition control technology for Mobile robot system which can robustly recognize voice by adults and children in noisy environments. We evaluate the performance of robot control system in a communication robot placed in a real noisy environment. Voice is captured using a wireless microphone. To suppress interference and noise and to attenuate reverberation, we implemented a multi-channel system consisting of an outlier-robust generalized side-lobe canceller technique and a feature-space noise suppression using criteria. Voice activity periods are detected based end-point detection

Key words: Robust voice recognition, Side-lobe canceller, navigation system

1. INTRODUCTION

To make mobile robot communication natural, it is necessary for the robot to recognize voice even while it is moving and performing gestures. For example, a robot's gesture is considered to play a crucial role in natural mobile robot communication [1-3]. In addition, robots are expected to perform tasks by physical actions to make a presentation. If the robot can recognize human interruption voice while it is executing physical actions or making a presentation with gestures, it would make the robot more useful.

Each kind of robot motion or gesture produces almost the same noises every time it is performed. By recording the motion and gesture noises in advance, the noises are easily estimated. By using this, we introduce a new method for VRCS under robot motor noise. Our method is based on three techniques, namely, multi-condition training, maximum-likelihood linear regression[5], and missing feature theory. These methods can utilize pre-recorded noises as described later. Since each of these techniques has advantages and disadvantages, whether it is effective depends on the types of motion and gesture. Thus, just combining these three techniques would not be effective for voice recognition under noises of all types of motion and gestures. The result of an experiment of isolated word recognition under a variety of motion and gesture noises suggested the effectiveness of this approach.

2. CONTROLSCHEME

The proposed robot system has three wheels; two driven wheels fixed at both sides of the mobile robot and one castor attached at the front and rear side of the robot. The ultrasonic sensors are mounted around of the mobile robot in middle layer for the detection of obstacles with various heights. In this study, a sonar array composed of 16 ultrasonic sensors cannot be fired simultaneously due to cross talk. Instead, we adopt a scheduled firing method where sensors are activated in sequence of $\{s_1, s_{12}, s_2, s_{11} \ldots\}$. The arrangement of the ultrasonic sensors in upper layer and the sensors are marked as dots in the figure. The distances e_j $(j = 1, 2, \ldots 12)$ from the origin of the robot frame {R} to obstacles detected by the sensor s_j, can be defined as $e_j = ♎_j + R_r$. Here, R_r is the radius of the robot and the $♎_j$, is the range value measured by the sensor s_j .

A local map is introduced to record the sensory information provided by the 16 sonar sensors with respect to the mobile robot frame $\{R\}$. Sector map defined locally at the current mobile robot frame is introduced. Then, the obstacle position vector se'_j with respect to the frame $\{R\}'$ can be calculated by

$$Se_j \; \text{🖬} \begin{pmatrix} \cos♎❑ & \sin♎❑ & 0 & \text{📭}\sin♎❑ \;/❑_p \\ \text{📭}\sin♎❑ & \cos♎❑ & 0 & (1\text{📭}\cos♎❑)/❑_p \\ 0 & 0 & 1 & 0 \\ 0 & 0 & 0 & 1 \end{pmatrix} \quad (1)$$

where se_j denotes the obstacle position vector defined at the frame $\{R\}$. When the mobile robot is located at a point $0'$. the distance value $se'_j = \| se'_j \|$ from the origin of the frame $\{R\}'$ to the obstacle and angle $s\varphi'$ can be calculated by Eq.(1) . Here, $\|.\|$ denotes Euclidean norm.

The local map defined at the frame $\{R\}'$ is newly constructed by using the previous local map defined at the frame $\{R\}$ as follows:

$$Se_n \leftarrow Se_{j,n} = INT\left(\frac{se_j}{\sigma}\right) + \frac{N}{2} \; ; \; j = 1,2,...,N \qquad (2)$$

Where $\leftarrow$ and INT denote the updating operation and integer operation, respectively. Here, se_n, denotes the distance value of n sector and N represents the number of the sector. If the range values obtained by sensors when the mobile robot is located at a point o' are e_j = (j = 1,2 ,... 12) , the new local map is partially updated as follows : $se_j \leftarrow e_j$, j = 1,2 .... 12. The maximum range of the sonar sensor is set to be $\Omega_{max} = \Omega_{max} - R_r$. Any return range which is larger than is ignored.

The primitive behaviors may be divided as follows: goal-seeking behavior, ball-following behavior, keep-away behavior, free space explorer and emergency stop, etc. The output of a primitive behavior is defined by the vector.

$$u(t) = (v(t), \omega(t))^T = (v(t), w(t), T_{ms})^T \qquad (3)$$

where t and T_{ms} denote the time step and the sampling time, respectively. Here, T denotes the transpose and $\omega(t)$ denotes the angular velocity of the robot.

We will divide the primitive behaviors into two basic: avoidance behavior and goal-seeking behavior.

The avoidance behavior is used to avoid the obstacles irrespective of the goal position, while the goal-seeking behavior is used to seek the goal position irrespective of obstacle location. Design of each behavior proceeds in following sequences; (A) fuzzification of the input/output variables, (B) rule base construction through reinforcement learning, (C) reasoning process, (D) defuzzification of output variables.

In order for the mobile robot to arrive at the goal position without colliding with obstacles, we must control the mobile robot motion in consideration of the obstacle position X_{oi}, = (x_{oi}, y_{oi}) , the mobile robot position X = (x , y) and its heading angle θ with respect to the world coordinate frame $\{W\}$ shown in Fig. 1.

In order to avoid the increase in the dimension of input space, the distance values d_i , (i = 1.2,3,4) are defined by

$$d_1 = \min(se_1, se_2, se_3)$$
$$d_2 = \min(se_4, se_5, se_6) \qquad 4a \qquad (4)$$
$$d_3 = \min(se_7, se_8, se_9) \qquad 4b$$
$$d_4 = \min(se_{10}, se_{11}, se_{12})$$

$\phi_m(-\pi \le \phi_m \le \pi)$ denotes the orientation of a sector with the shortest range. We choose the input variables for avoidance behavior as ϕ_m and $d_i = \| X_{0i} - X \|$,(i = 1,2,3,4) for goal-seeking behavior as heading angle difference ψ and distance to goal $z = \| X_g - X \|$. The input linguistic variables d_i, ψ, ϕ_m and z are expressed by linguistic values (VN, NR, FR), (NB, NM, ZZ, PS, PM, PB), (LT, CT, RT) and (VN, NR, FR, VF), respectively Their membership functions are expressed as shown in fig. 1.

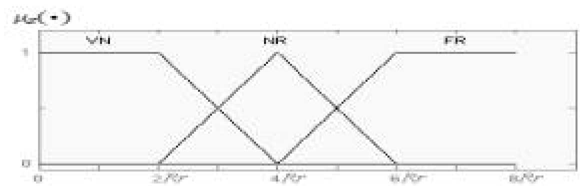

(a) The distance value

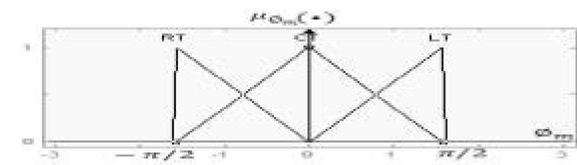

(b) The orientation of the sector with the shortest range value

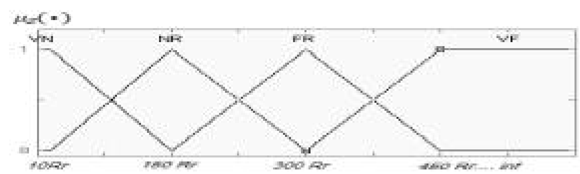

(c) The distance to goal position

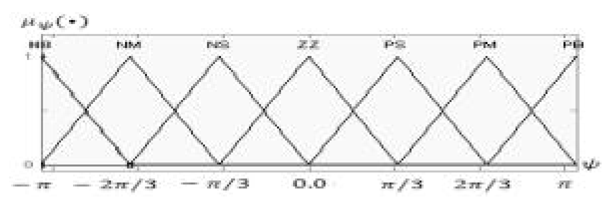

(d) The heading difference

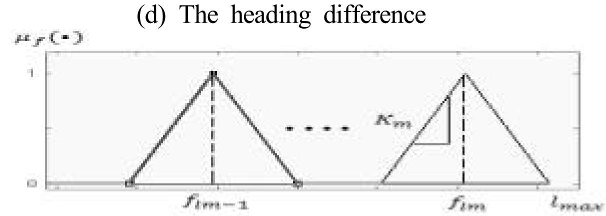

(e) The linear velocity of mobile robot for the k-th behavior

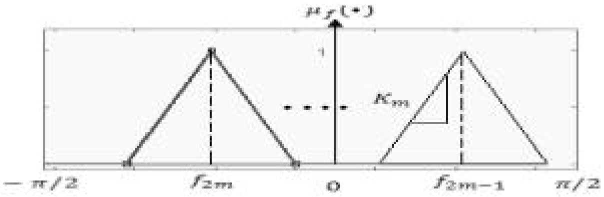

(f) The incremental steering angle for k-th behavior
Fig. 1 The membership functions of the input-output variables

3. EXPERIMENTS

The proposed robot has the maximum travel speed of 0.6 m/s and the maximum steering rate of 3.0rad/sec. Experiments are performed in an indoor with the first experiment for voice recognition without objects and second experiment for both of them: voice recognition and obstacles avoidance. The first experimental space is approximately 9.0m by 1,5m wide, and the second experimental space is approximately 14m by 2.4m wide. Since this environment is too simple to test the performance of the overall system, several polygon obstacles were randomly placed in the path of the mobile robot navigation.

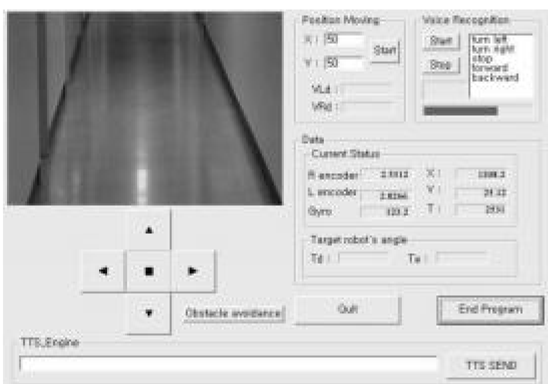

Fig. 4. Voice recognition interface

Through a series of the navigation experiments, it was observed that the heading angle error is a serious problem to the proposed robot depend on dead reckoning The large heading angle error almost resulted from the uncertain parameters when the mobile robot changes its direction Even if the wheel slippage occurs, the true position and heading angle of the mobile robot could be updated by two beacon pairs and consequently the mobile robot could arrive at the given goal position while avoiding the obstacles.

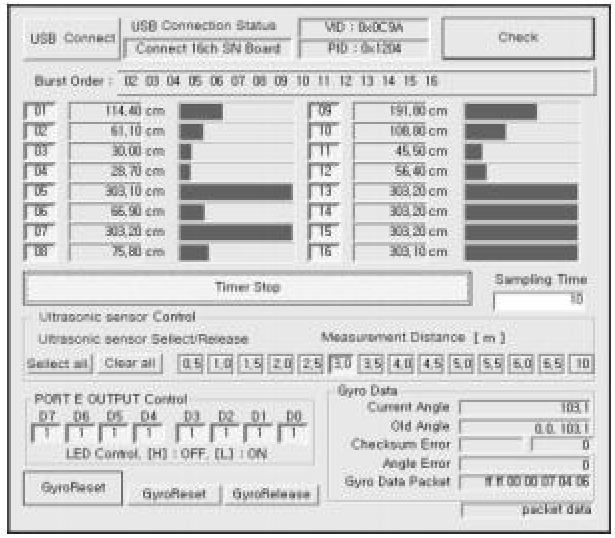

Fig. 3. Obstacle detection using ultraasonic sensors

4. CONCLUSIONS

This paper proposed the integration of robust voice recognition and navigation system capable of performing autonomous navigation in unknown environments. In order to evaluate the performance of the overall system, a number of experiments have been undertaken in various environments.

REFERENCES

[1] M. Blanchet, J. Boudy, and P. Lockwood, “Environment adaptation for speech recognition in noise,” in Proc. of EUSIPCO-92, vol. VI,1992, pp. 391–394.
[2] R. P. Lippmann, E. A. Martin, and D. B. Paul, “Multi-style training for robust isolated-word speech recognition,” in Proc. of ICASSP-87. IEEE, 1987, pp. 705–708.
[3] J. Barker, M. Cooke, and P. Green, “Robust asr based on clean speech models: An evaluation of missing data techniques for connected digit recognition in noise,” in Proc. of Eurospeech-2001. ESCA, 2001, pp. 213–216.
[4] P. Renevey, R. Vetter, and J. Kraus, “Robust speech recognition using missing feature theory and vector quantization,” in Proc. Of Eurospeech-2001. ESCA, 2001, pp. 1107–1110.

2017 Changwon International Conference on Intelligent Robot and Convergence Industry (CICIRO 2017)
Nov. 30th~ Dec. 1st, 2017, Changwon Exhibition Convention Center(CECO), Changwon City, Korea

A Study on Precise Control of Mobile Robot with Dual-Arm

Woo-Song Lee[1] Ki-Young Ko[2], Ho-Young Bae[3], Mun-Keun Cho[4],
Ki-Hyun Kim[5], and Sung-Hyun Han[6]

[1] SUNJIN Technology Co., Ltd., Changwon, 82331, Korea
(E-mail: elflws@nate.com)
[2] Doosan Heavy Industries & Construction Co., Ltd., Changwon, 51711, Korea
(kiyoung.ko@doosan.com)
[3] V-Mac Company Co., Ltd. Changwon, 50850, Korea
(E-mail: sswq1r@hanmail.net)
[4] Doosan Heavy Industries & Construction Co., Ltd., Changwon, 51711, Korea
(E-mail: kihyeon.kim@doosan.com)
[5] ATM Korea Co., Ltd, Gumi, 642-820 Korea
(E-mail: pjm8927@naver.com)
[6] School of Mechanical Engineering, Kyungnam University,
Changwon, 631-701, Korea (E-mail: shhan@kyungnam.ac.kr)

Abstract: The main focus of this paper is obtaining a fuzzy perception of the environment in the design of each reactive behavior and solving the problem of behavior combination to implement a fuzzy behavior based control architecture. It should be remarked that, the proposed technique of the nonholonomic constraints are considered in the design of each behavior. Furthermore, in order to improve the capabilities of the intelligent control system and its practical applicability, teleoperation and planned behaviors, together with their combination with reactive ones, have been considered.

Keywords: Real-Time control, Sensor, Fuzzy Controller, Non-holonomic

1. INTRODUCTION

The real-time trajectory control is the process of determining and maintaining a path or trajectory to a goal destination. Autonomous mobile robots are required to navigate in more complex domains, where the environment is uncertain and dynamic. Autonomous navigation in these environments demands adaptation and perception capabilities. This paper describes improvements in the perception functions used in these kinds of robots. It should be noted that this is a nonholonomic vehicle with significant limitations in the reactive capabilities due to kinematic and dynamic constraints, and a few number of sensors and large blind sectors in between them, making autonomous navigation a nontrivial task. The methods presented in this paper have been conceived to deal with these limitations of conventional vehicles.

In addition, fuzzy perception can be used straightforward to perform the control of the mobile robot by means of fuzzy behavior-based scheme already presented in literature. The main differences of the proposed approach with respect to other behavior based methods are: 1 - The nonholonomic constraints are directly taken into account in the behaviors. 2 - The fuzzy perception itself can be used both in the design of each reactive behavior and to solve the problem of blending behaviors.

Hence, the fuzzy behavior-based control scheme presented in this research allows not only implement reactive behaviors but also teleoperation and planned behaviors, improving system capabilities and its practical application. Furthermore, in these behaviors, soft computing techniques play an important role to solve different problems.

2. CONTROLSCHEME

The following considerations are based on a mobile robot with the three degrees of freedom of planar movement, x, y and θ. It is equipped with a ring of 12 ultrasonic sensors which are able to perceive vertical or nearly vertical planes. The number of sensors is irrelevant as long as there are no blind sectors between them. θ refers to the orientation of this ring of sensors and not to the orientation of the robot itself, which is of no importance for the wall following algorithm. With ♐🕮indicating the direction of movement the kinematics model of such a robot is described as follows:

dx 🖬 *v*cos♐*dt*; *dy* 🖬 📭*v*sin♐*dt*; *d*❑ 🖬❑🕮*dt* (1)

Since there is no modeling of the environment the absolute position of the robot does not matter. So there is no world frame used here and the kinematics model can be expressed instead as:

$$ds = v\,dt;\quad d\gamma = \dot{\gamma}\,dt;\quad d\theta = \dot{\theta}\,dt \tag{2}$$

The speed v, the angular speeds $\dot{\gamma}$ and $\dot{\theta}$ are used as control variables of the robot and generated by the fuzzy controller.

Perception of each ultrasonic sensor i of the mobile robot is assigned a vector ki. Its direction equals the orientation of the sensor´s axis and its length is a function of the distance di measured by this sensor:

$$k_i = \frac{d_{max} - d_i}{d_{max} - d_{min}} \tag{3}$$

where dmin and dmax designate the shortest and longest distance respectively at which an object may be positioned to be reliably detected. ki is limited to 0 and 1 respectively

Since a vehicle with nonholonomic constraints cannot move itself in any direction at every time instant, it is interesting to weight the different perceptions according with the direction where the obstacle was detected. In other words, an obstacle is less important if it is placed at a location that cannot be reached by the mobile robot, but it is more dangerous if it is on a reachable position. This task can be accomplished by considering the perception angle (θi) in the computation of the perception function

$$k_i = f(d_s, \theta_i) = sat_{0,1}\left(\frac{d_{max}(\theta_i) - d_s}{d_{max}(\theta_i) - d_{min}(\theta_i)}\right) \tag{4}$$

where sat0,1(x) states for the saturation of x in the range [0, 1]. In this way, it is possible to assign different perceptions, i.e. different weights, to objects detected at the same distance relative to the mobile robot but at different directions. For example, perception function ki is obtained by using the nonlinear function

$d_{min}(\theta_i) = d_m(1-\mu) / (1-\mu\cos\theta_i)$, and $d_{max} = n\,d_{min}(\theta_i)$ (with n>1), in Eq. (4).

$$k_i = f(d_s, \theta_i) = sat_{0,1}\left(\frac{n d_m(1-\mu) - d_s(1-\mu\cos\theta_i)}{(n-1)d_m(1-\mu)}\right) \tag{5}$$

Furthermore, it is interesting to stress that the perception vector implies a fuzzy high level description of the environment, being independent of the type of range sensor used. So, it is possible to use different perception functions from Eq. 4 for each kind of sensor (laser, ultrasonic, infrared). Thus, sensor data fusion can be reduced to compute different vectors from the sensor measurements and to combine them to obtain the perception vector.

The previous perception can be updated as follows: consider a robot of arbitrary shape equipped with proximity sensors. Any such sensor may be located at a position U, with its axis pointing to the direction s

A frame r represents the robots position and orientation, x and θ, respectively, with respect to the world reference system w. The velocity υ of the reference point and the angular velocity $\omega_{r/w} = e_r\dot{\theta}$ of the robot with respect to the fixed frame w, give the state of motion. Furthermore, the virtual perception coordinate system is assumed to be located at E, pointing to the direction of attention a1. Then, an object detected by a proximity sensor at a distance ds could be detected by a virtual sensor placed at E a distance d, and with an orientation θ with respect to the vehicle's direction of attention a1.

Now the virtual perception will be updated taking into account the robots motion as follows: considering a perception function k = f(d, θ) and the corresponding inverse perception function, d = g(k, θ), and carrying out some calculations, it can be shown that the derivatives of angle and length of the perception vector are given by (assuming g ≠ 0 and $\partial g/\partial k \neq 0$).

$$\dot{\theta} = \frac{1}{g}\left(\dot{x} + \omega_{r/w} \times e\right) \cdot e_{r1}\cos(\ldots) - \ldots e_{r2}\cos(\ldots) - \ldots - \omega_{r/w} - \omega_{a/r} \tag{6}$$

$$\dot{k} = \frac{1}{\partial g/\partial k}\left(\left(\dot{x} + \omega_{r/w} \times e\right) \cdot e_{r1}\cos(\ldots) - \ldots e_{r2}\cos(\ldots) - \frac{\partial g}{\partial \theta}\dot{\theta}\right) \tag{7}$$

where $\omega_{r/w} = \dot{\theta}$ is the angular velocity of the virtual perception coordinate system relative to the robot.

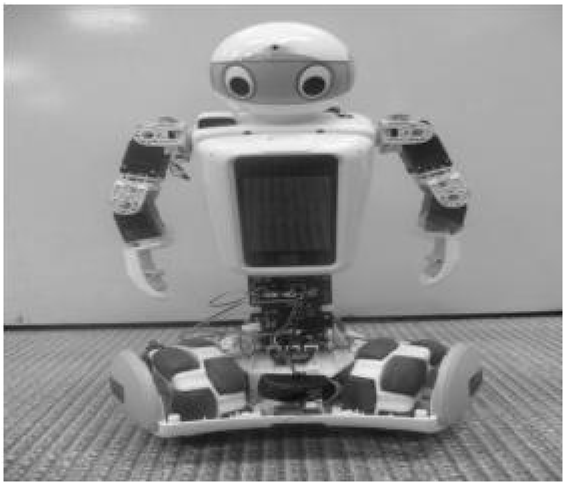

Fig. 1. The mobile robot with dual-arm

3. EXPERIMENTS

We have performed experimental results of the proposed methods to the mobile robot ROBO-N. The vehicle carries on-board a heterogeneous configuration of ultrasonic sensors. It is presented two kinds of experiment including general perception and application of fuzzy perception. All the experiments have been implemented in the ROBO-N embed.

In this, instead of a typical ring of identical sonars, there are 12 sonars of three different types, placed at different locations. Six of them are large-range sensors (0.5–2.5m), four are mid-range (0.3–1.0m), and the other two are of short-range (0.06–0.5m). Furthermore, these ultrasonic sensors use a higher frequency and have a narrower sonar beam than the commonly used sonars in these kinds of applications. The sensors are arranged in a way that six of them cover the front part of the vehicle and the other four cover its lateral sides.

Experiments result is shown in where the robot has to navigate through a corridor which is partially obstructed by an obstacle. The robot starts at point A with corridor tracking behavior, since it has equal perception at both sides. As the robot moves on it detects free space to its left and changes its behavior smoothly to follow right wall. When entering the corridor it tries again to center itself in the corridor B.

4. CONCLUSIONS

We propose a new approach to control of mobile robot of trajectory following and fuzzy perception concept with a nonholonomic mobile robot.

Experimental results, of an application to control the autonomous vehicle, demonstrate the robustness of the proposed method.

REFERENCES

[1] R. Braunstingl, “Improving reactive navigation using perception tracking”, *Robotics and Manufacturing, Recent Trends in Research and Applications*, Vol. 6, pp 25-30, New York, 1996.

[2] J.J. Leonard, H.F. Durrant-Whyte, “Directed Sonar Sensing For Mobile Robot Navigation”, Kluwer Academic Publishers, pp 147-155, 1992.

[3] A. Ollero, A. Garcia-Cerezo, J.L. Martinez, A. Mandow, “Fuzzy tracking methods for mobile robots”, Prentice-Hall, pp 347-364, 1997.

[4] Ollero, G. Ulivi, F. Cuesta, “Fuzzy logic applications in mobile robotics”, Kluwer Academic Publishers, pp. 301–324, 1999.

A study on Robust Control for Working of Humanoid Robot

Min-Seong Kim[1], Woo-Song Lee[2], Hyun-Suk Sim[3], Ho-Young Bae[4], Sung-Hyun Han[5]

[1] Department of Advanced Engineering, Graduate School Kyungnam University, Changwon, 51767, Korea (kms21018@naver.com/ kimjh4750@naver.com) * Corresponding author

[2] SUNJIN Technology Co., Ltd., Changwon, 82331, Korea (elflws@nate.com)

[3] DongSan Tech Co., Ltd., 52061, Korea(hs8388@dscast.co.kr)

[4] V-Mac Company Co., Ltd. Changwon, 50850, Korea (sswq1r@hanmail.net)

[5] School of Mechanical Engineering, Kyungnam University, Changwon, 631-701, Korea (shhan@kyungnam.ac.kr)

Abstract: This paper deals with the stable walking for a biped robot, on uneven terrain, A biped robot necessitates achieving posture stabilization since it has basic problems such as structural instability. In this paper, a stabilization algorithm is proposed using the ground reaction forces, which are measured using FSR (Force Sensing Resistor) sensors during walking, and the ground conditions are estimated from these data. From this information the robot selects the proper motion pattern and overcomes ground irregularities effectively. In order to generate the proper angel of the joint. The performance of the proposed algorithm is verified by simulation and walking experiments on a 24-DOFs biped robot.

Keywords: Force sensing resistor, fuzzy algorithm, biped robot, stabilization

1. INTRODUCTION

In this paper, a real-time walking stabilization method utilizing a fuzzy algorithm under uneven terrain is proposed. We focused most of our interest on landing phase. The ground reaction forces, measured by FSR sensors on the sole, are used to assess the ground condition and the robot posture. Simulation and experiment results for the proposed method are given in Section 3, followed by conclusions in the final section.

2. WALKING PATTERN

Basically, a robot walks with the trajectory generated previously assuming even terrain. If different values from the expected sensor are measured during walking, the robot should be deployed using the stabilization algorithm. Fig.1 presents the walking algorithm.

When the robot is walking, it measures the ground reaction forces in real-time and utilizes them as inputs to the controller. When the control of the robot is interrupted by an unexpected situation or a unit step has ended, the new trajectory should be generated according to the changed situation. The newly verification based on the ZMP criterion. Once the stability of the trajectory is guaranteed, the robot becomes able to resume the walking.

3. BIPED ROBOT AND SENSOR SYSTEM

The robot walks according to a basic trajectory. In basic walking, a stride is 0.12m, velocity is 0.04m/s, and the ground is regarded as being flat. The robot steps on projected ground of 11mm in height with the tie if the swing leg. When the control algorithm is not applied, the sensor data is presented as given in Fig.2, The robot pushes the ground continuously, and the heel does not contact until the end of the stride.

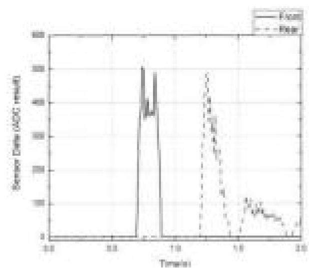

Fig. 1 Controller input for constant control.

4. CONCLUSION

This paper decribed a real-time control technology to implement the walking of a biped robot on uneven terrain. It was assumed that the ground condition on the basis of ground reaction forces measured sensors on the soles of the feet during walking. The robot could maintain balanced walking through control of the ankle joints using a fuzzy algorithm

REFERENCES

[1] M. Vukobratovic and D. Juricic, "Contribution to the synthesis of biped gait," IEEE Trans. on Bio-Medical Engineering, vol. 16,pp. 1-6, 1969

A Study on walking Control of Biped Robot by Voice Command for FA

Yang-Geun Jeong[1], Min-Seong Kim[2], Yeon-Guk Noh[3],
and Sung-Hyun Han[4]

[1] Shinla Information Technology CO., Ltd., Changwon City, 51390, Korea (E-mail : shintech@hanmail.net)
[2] Department of Advanced Engineering., Kyungnam University, Changwon, 51767, Korea (E-mail : kms21018@naver.com)
[3] SFNT Co., Ltd., Changwon, 631-821, Korea (ykno1339@naver.com)
[4] Department of Mechanical Engineering, Kyungnam University, Changwon, 51767, Korea (shhan@kyungnam.ac.kr)

Abstract: Generally, it is possible to control the walking information based on the biped robot's own postures, because a type of motion and gesture produces almost the same pattern of noise every time. In this paper, we describe an voice recognition control technology for biped robot system which can robustly recognize voice by adults and children in noisy environments. We prove the performance of robot control system in a communication robot placed in a real noisy environment. Voice is captured using a wireless communication.

Keywords: Robust voice recognition, Side-lobe canceller, navigation system

1. INTRODUCTION

Each kind of robot motion or gesture produces almost the same noises every time it is performed. By recording the motion and gesture noises in advance, the noises are easily estimated. By using this, we introduce a new method for VRCS under robot motor noise. Our method is based on three techniques, namely, multi-condition training, maximum-likelihood linear regression, and missing feature theory. These methods can utilize pre-recorded noises as described later. Thus, just combining these three techniques would not be effective for voice recognition under noises of all types of motion and gestures. The result of an experiment of isolated word recognition under a variety of motion and gesture noises suggested the effectiveness of this approach.

2. CONTROLSCHEME

The proposed robot system has three wheels; two driven wheels fixed at both sides of the mobile robot and one castor attached at the front and rear side of the robot. The ultrasonic sensors are mounted around of the mobile robot in middle layer for the detection of obstacles with various heights. In this study, a sonar array composed of 16 ultrasonic sensors cannot be fired simultaneously due to cross talk. Instead, we adopt a scheduled firing method where sensors are activated in sequence of $\{s_1, s_{12}, s_2, s_{11} \ldots\}$. The arrangement of the ultrasonic sensors in upper layer and the sensors are marked as dots in the figure. The distances e_j $(j = 1, 2, \ldots 12)$ from the origin of the robot frame {R} to obstacles detected by the sensor s_j, can be defined as $e_j =$ ♎$_j + R_r$. Here, R_r is the radius of the robot and the ♎$_j$, is the range value measured by the sensor s_j .

The primitive behaviors may be divided as follows: goal-seeking behavior, ball-following behavior, keep-away behavior, free space explorer and emergency stop, etc. The output of a primitive behavior is defined by the vector.

3. EXPERIMENTS

The proposed robot has the maximum travel speed of 0.55 m/s and the maximum steering rate of 3.0rad/sec. Experiments are performed in an indoor with the first experiment for voice recognition without objects and second experiment for both of them: voice recognition and obstacles avoidance.

Through a series of the navigation experiments, it was observed that the heading angle error is a serious problem to the proposed robot depend on dead reckoning The large heading angle error almost resulted from the uncertain parameters when the mobile robot changes its direction Even if the wheel slippage occurs, the true position and heading angle of the mobile robot could be updated by two beacon pairs and consequently the mobile robot could arrive at the given goal position while avoiding the obstacles.

4. CONCLUSION

This paper proposed the integration of robust voice recognition and navigation system capable of performing autonomous navigation in unknown environments. In order to evaluate the performance of the overall system, a number of experiments have been undertaken in various environments.

REFERENCES

[1] M. Blanchet, J. Boudy, and P. Lockwood, "Environment adaptation for speech recognition in noise," in Proc. of EUSIPCO-92, vol. VI,1992, pp. 391–394.

[2] R. P. Lippmann, E. A. Martin, and D. B. Paul, "Multi-style training for robust isolated-word speech recognition," in Proc. of ICASSP-87. IEEE, 1987, pp. 705–708.

2017 Changwon International Conference on Intelligent Robot and Convergence Industry (CICIRO 2017)
Nov. 30th~ Dec. 1st, 2017, Changwon Exhibition Convention Center(CECO), Changwon City, Korea

A Study on the Path Planning and Control of Robot Manipulator with Six Joint for Molding and Forging Process Automation

Min-Seong Kim[1], Geo-Seung Choi[2], Byung-Seuk Yoon[3], Jong-Bum Won[4] and Sung-Hyun Han[5]

[1] Department of Advanced Engineering., Kyungnam University, Changwon, 51767, Korea (E-mail: kms21018@naver.com)

[2]SAMHYUN CO. Ltd., Changwon, 51398, Korea (E-mail: gschoi@samhyun.co.kr)

[3]Dongmyeongjeong-gi Co., Ltd., Changwon, 51561, Korea (E-mail : bsyoon@naver.com)

[4] SMEC co., Ltd. Gimhae City, 50969, Korea (Tel : +82-10-4582-8264; E-mail :won@esmec.com)

[5]School of Mechanical Engineering, Kyungnam University, Changwon, 51767, Korea (Tel: +82-10-3585-5111; E-mail: shhan@kyungnam.ac.kr)

Abstract: In this study, we proposed robust control schemes for robot system which has the parametric uncertainties in forging process. In order to compensate these uncertainties, we use the neural control algorithm that has the capability to approximate any nonlinear model over the precise input space. In the proposed control schemes, it is not necessary to drive the linear formulation of robot dynamic equation and tune the parameters. We also suggest the robust adaptive control laws in all proposed schemes for decreasing the effect of approximation error. To reduce the number of neural of network, we consider the properties of robot dynamics and the decomposition of the uncertainty function. The proposed controllers are robust not only to the structured uncertainty such as payload parameter, but also to the unstructured one such as friction model and disturbance. The reliability of the control scheme is shown by computer simulations and experiment of robot manipulator with 6 axis in forging process.

Keywords: Robust control, decomposition, neural network, robot dynamics, uncertainty .

1. INTRODUCTION

To overcome these difficulties, in this paper we propose the adaptive control schemes which utilize a neural network as a compensator for any uncertainty. To reduce the error between the real uncertainty function and the compensator, we design simple and robust adaptive laws based on nonlinear stability method. In the proposed schemes, the compensator has to see many neural because uncertainties depend on all state variables. To overcome this problem, therefore, we introduce the control schemes in which the number of neural of the NN compensator can be reduced by using the properties of robot dynamics and uncertainties.

2. PATH PLANNING AND CONTROL

A robot manipulator is defined as an open kinematic chain of rigid links. Each degree of freedom of the manipulator is powered by independent torques. Using the Lagrangian formulation, the equations of motion of an -degree-of-freedom manipulator can be written as

$$D(q)\ddot{q}+C(q,\dot{q})\dot{q}+G(q)+F_r(\dot{q})+\tau_d=\tau \quad (1)$$

where $q\in R^n$ is the generalized coordinates; $D(q)\in R^{n\times n}$ is the symmetric, bounded, positive-definite inertia matrix; vector $C(q,\dot{q})\dot{q}\in R^n$ presents the centripetal and Coriolis torques; $\tau_d\in R^n$, $G(q)\in R^n$, $F_r(\dot{q})\in R^n$ and $\tau\in R^n$ represent the gravitational torques, friction, disturbance, and applied joint torques, respectively.

The robot model (2) is characterized by the following structural properties.

This property is utilized in this paper in order to reduce the number of neural in the neural network compensator.

The considered tracking problem is stated as follows: Knowing desired trajectories $q_d\in R$, $q^n_d\in R^n$, with some or all the manipulator parameters unknown, determine a control law τ and a sliding surface $s=0$ such that sliding mode occurs on the sliding surface, the tracking error $\tilde{q}=q-q_d$ has a prescribed transient response and it goes to zero asymptotically as $t\to\infty$.

A. Simple Adaptive Control Law

The sliding surface $s=0$ is chosen as a hyperplane

$$s=\dot{\tilde{q}}+\Lambda\tilde{q} \quad (5)$$

where Λ is a positive-definite matrix whose eigenvalues are strictly in the right-half complex plane and $\tilde{q}$ is the tracking error vector.

If the sliding mode exists on $s=0$, then from the theory of VSS, the sliding mode is governed by the following linear differential equation whose behavior is dictated by the sliding hyperplane design matrix Λ :

$$\dot{\tilde{q}}=-\Lambda\tilde{q} \quad (6)$$

Obviously, the tracking error transient response is then determined entirely by the eigenvector structure of the matrix Λ .

In order to derive the sliding mode control law, which forces the motion of the error to be along the sliding surface $s=0$, a vector of self-defined reference variables is introduced for the succinct formula expression in the sequel, that is,

$$\dot{q}_r(t)=\dot{q}_d(t)-\Lambda\tilde{q}(t) \quad (7)$$

Consider now the uncertainties of robot manipulator, (1) can be rewritten as

$$D(q)\ddot{q} + C(q,\dot{q})\dot{q} + G(q) + F(q,\dot{q},t) = \tau \quad (8)$$

Where $F(q,\dot{q},t) = F_r(q) + \tau_d$. However, in this paper, this uncertainty function vector has to be replaced by $F(q,\dot{q},\ddot{q},t)$

So (9) can be rewritten as

$$D(q)\ddot{q} + C(q,\dot{q})\dot{q} + G(q) + F(q,\dot{q},\ddot{q},t) = \tau \quad (9)$$

we let a Lyapunov function candidate be

$$V(t) = \frac{1}{2}\left(s^T D s + \sum_{i=1}^{n} \tilde{\theta}_i^T \Gamma_i \tilde{\theta}_i\right) \quad (10)$$

Where $\tilde{\theta}_i = \theta^*_i - \hat{\theta}_i$, θ^* is the j th column vector of the optimal parameter matrix θ^* and Γ_i is a strictly positive real constant.

Differentiating $V(t)$ with respect to time yields

$$\dot{V}(t) = s^T D\dot{s} + \frac{1}{2} s^T \dot{D} s + \sum_{i=1}^{n} \tilde{\theta}_i^T \Gamma_i \dot{\tilde{\theta}}_i$$

$$= -s^T(D\ddot{q}_r + C\dot{q}_r + G + F - \tau) + \sum_{i=1}^{n} \tilde{\theta}_i^T \Gamma_i \dot{\tilde{\theta}}_i \quad (11)$$

Where $F(q,\dot{q},\ddot{q},t)$ is a completely unknown nonlinear function vector. Therefore, we replace $F(q,\dot{q},\ddot{q},t)$ by a Neural network $\hat{F}(q,\dot{q},\ddot{q}\,|\,\theta)$ .Let us define the control law as

$$\tau = D(q)\ddot{q}_r + C(q,\dot{q})\dot{q}_r + G(q) + \hat{F}(q,\dot{q},\ddot{q}\,|\,\theta) - K_D s \quad (12)$$

Where $K_D = diag(K_i)$, $i = 1, 2, \ldots, n$.

3. EXPERIMENT AND RESULTS

We also apply real-time adaptive control based on neural network compensator to dual-arm robot shown in figs. 1. Because the characteristics of two arms are the same, so we show the results into one arm is enough.

Fig. 1. Experimental set-up

All the algorithm calculation is calculated by Matlab and Simulink matlab on host computer and push into dual-arm robot which is shown in the Fig. 2. The desired trajectories are

$$q_{1d} = q_{2d} = 15\pi \sin\left(\frac{2\pi}{300\pi} t - \frac{2\pi}{3}\right)$$

and the results of robust adaptive control are shown below

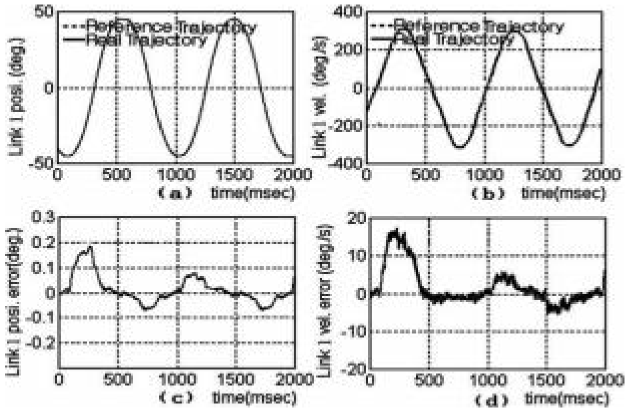

Fig. 2. (a)-(d) Experimental results for the position and velocity tracking of adaptive controller at the first joint.

4. CONCLUSIONS

In this paper, we have illustrated that the control objective is well accomplished and the neural network compensate the uncertainties. In addition, the proposed control technology needs to apply to robot manipulators include more joints, for forging process automation.

ACKNOWLEDGEMENT

This study was performed by project of the robot business belt construction enterprise..

REFERENCES

[1] J. E. Slotin and S. S. Sastry, “Tracking control of nonlinear systems using sliding surfaces, with application to robot manipulators,” Int. J. Contr., vol. 38, no. 2, pp. 465–492, 1983.
[2] J. J. E. Slotine and W. Li, Applied Nonlinear Control. Englewood Cliffs, NJ: Prentice-Hall, 1991.
[3] F. L. Lewis, C. T. Abdallah, and D. M. Dawson, Control of Robot Manipulators. London, U.K.: Macmillan, 1993.
[4] M. W. Spong, Robot Dynamics and Control. New York: Wiley, 1989.
[5] W. C. Ham, “Adaptive nonlinear control of one-link flexible arm,” in IEEE/RSJ Int. Conf. Intelligent Robots and Systems, vol. 1, Yokohama, Japan, 1993, pp. 3–7.
[6] “Adaptive control based on explicit model of robot manipulators,” IEEE Trans. Automat. Contr., vol. 38, pp. 654–658, 1993.

6 DOF Manipulator Technology in ROS Environment

Dong-eon Kim[1], Dong-ju Park[1], Ki-seo Kim[1],Jin-hyun Park[1]and Jang-myung Lee[1*]
[1] Department of Electronic Engineering, Pusan national University
Busan, Republic of Korea ({dongeon1696, djpark1696, Jinhyun1696,kiseo1696, jmlee}@pusan.ac.kr)

Abstract: The grasping pose of the dual-arm has been determined depending upon the shape of the objects which is identified by the pan/tilt camera. For the stable grasping of the object, an operability index of the dual-arm robot (OPIND) has been defined by using the current values applied to the motors for the given grasping pose. When analyzing the motion of a manipulator, the manipulability index of both arms has been derived from the Jacobian to represent the relationship between the joint velocity vector and the workspace velocity vector, which has an elliptical range representing easiness to work with.

Keywords: OPIND, 6 DOF Manipulator Technology, ROS Environment, Dual-arm Robot.

1. INTRODUCTION

Because of complication and diversification of industrial sites, the demand for multi-product small-volume production increases and accordingly it is the right time for intelligentialization of various robot manipulators. Especially, an optimal path of the manipulator is necessary to realize efficient work and a stable grasping method is required under the optimal posture which is generated according to the conditions of objects[1~4]. In order to intelligently control the above manipulator, we are trying to develop a dual-arm robot system that is used for manufacturing and service robots in ROS environment. ROS is a robotic operating system for development of robot applications. It provides necessary libraries, various development and debugging tools. In this paper, kinematic analysis of a 10- D.O.F. dual-arm robot is presented. In the inverse kinematics system, each joint angle is calculated according to the given elbow coordinates, end point coordinates, and tool tip orientation[5~8]. In addition, for compliance control, the manipulability index of the dual-arm robot is defined by using the current value applied to the motor and it is indicated as OPIND(operability index of the dual-arm robot). When analyzing the motion of the manipulator, the easiness of operation is indicated by an ellipse with the operability index of both arms derived from the Jacobian showing the relationship between the joint velocity vector and the workspace velocity vector. Using this, the speed and force of each joint required for the robot to move in any specific directions and to any positions is approximately the same as the that in actual movement[9~11]. Simulation was carried out through RVIZ provided by ROS. We created reference trajectory for robots and compared the result under the application of OPIND with that under the unapplied state when the robot was operating[12,13].

2. SYSTEM CONFIGURATION

The system configuration is shown in Fig. 1 below.

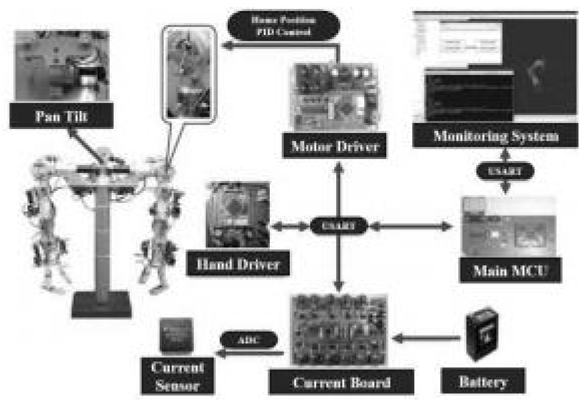

Figure. 1 System Configuration Block Diagram

The Dual-Arm robot uses 4 Maxon DC motors and 5000 resolution incremental encoders. The hand part of the robot is composed of a Dynamixel motor. Refer to Table 1 below for the motor specifications.

Figure. 2 3-DOF Finger Hand

Figure 2 is a photograph of the hardware used in the robot's hand. It is possible to measure the current value inside the motor and the force is measured by using a pressure sensor at the tip of the finger.

3. OPIND(OPERABILITY INDEX OF THE DUAL-ARM ROBOT)

In this paper, OPIND(operability index of the dual-arm robot) is defined as the operability index of both arms. The greater the size of the operability ellipse derived from the Jacobian matrix of the tool, the less the speed and force requirements of each joint to obtain the desired speed and force of the tool tip. Also, as the ellipse is closer to the sphere, the closer to the sphere, the speed and force of each joint required to move the tool to any arbitrary or specific direction position becomes almost equal to the speed and force of each joint that is required during actual movement. Operational ellipses can be derived from a Jacobian that represents the relationship between the velocity vector of the joint and the workspace velocity vector when analyzing the motion of the manipulator. On the other hand, the work given to the robot follows the path made by the continuous value of the position and the direction of the tool end.

$$X = f(\theta)$$
$$\dot{X} = J(\theta)\dot{\theta} \qquad (1)$$

Equation (1) shows the relationship between the position of the tool tip and the azimuth angle, the angular velocity of the joint, and the velocity ($\dot{\theta}$) of the tool tip.

$$\|\dot{\theta}\|^2 = \dot{\theta}_1^2 + \dot{\theta}_2^2 + \cdots + \dot{\theta}_n^2 \le 1, \qquad (2)$$

Expressions in the joint velocity space using $\dot{X}$ and $J(\theta)$ are as shown in Eq. (2), and if they are converted into velocities in the Cartesian coordinate space,

$$\|\dot{\theta}\|^2 = \dot{\theta}^T\dot{\theta} = \dot{X}^T(J^{-1})^T J^{-1}\dot{X}$$
$$= \dot{X}^T(JJ^T)^{-1}\dot{X} \le 1 \qquad (3)$$

This is as shown above. In addition, this paper shows the volume of the operational ellipse assuming that there is no excess degree of freedom.

$$M(\theta) = |\det J(\theta)|, \qquad (4)$$

Equation (4) represents a measure of the ability of the end device to move in all directions, usually at the current position. That is, when the operability index value approaches 0, the value of each joint for moving to an arbitrary coordinate can not be obtained by Expression (1), which means that the manipulator falls into the trouble of the singularity. By using this principle, the point where the operability index becomes zero is determined as the position of the singular point, and a method of avoiding the singularity for the coordinated control of the two - arm robot is studied and applied.

The relationship of each joint speed to the rectangular coordinates for both arms is as follows.

$$Left\ ARM:\ \dot{X}_1^T(J_1J_1^T)^{-1}\dot{X}_1 \le 1$$
$$Right\ ARM:\ \dot{X}_2^T(J_2J_2^T)^{-1}\dot{X}_2 \le 1 \qquad (5)$$

Using the inverse kinematics, the position and azimuth of each joint are determined, and the OPIND for the various movement paths is calculated from the coordinates on the predetermined plane. We then calculated the cumulative mean of the OPINDs by summing the successive values and performed an optimal path planning to increase the efficiency so that the OPIND converges to zero and does not fall into singularity.

4. EXPERIMENT

The position of the end-effector is controlled by forward kinematics and inverse kinematics using different markings at each joint position of the two-arm robot shown in Fig. 3, and the target object is gripped using a robot hand of three degrees of freedom. When the gripped object was moved to the desired target point, the current data of each joint was analyzed.

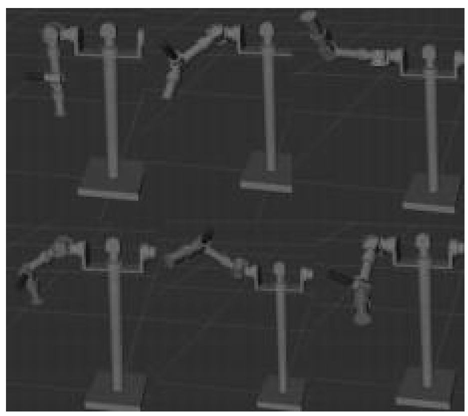

Figure. 3 Visualization in RViz environment

Figure 4 shows the visualization in the RViz environment for the simulation. The simulation environment is configured according to the actual robot using the 3D drawing. The simulation environment was constructed by applying the actual motor specifications and the OPIND applied state and the non - applied state were compared using the current value when the robot was operated on the simulation.

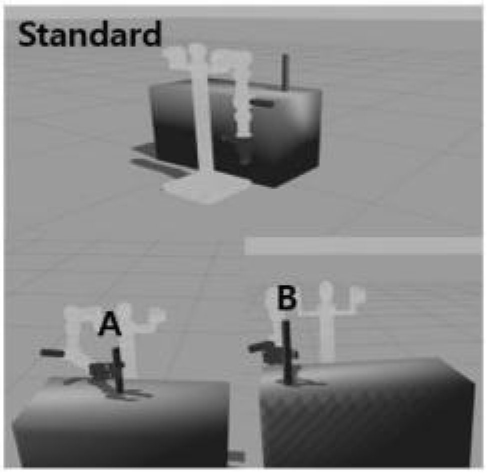

Figure. 4 Simulation path (Standard → A → B)

Figure 5 shows a simulation using a robot. It shows the state at the starting position and the state at the target point when simulating. In Figure 5, the above picture shows the initial state before operation. By applying the proposed OPIND algorithm, the arm moves to the starting point A, and then the object is held and moved to the target point B side.

Here, the current of the motor according to the time is shown. Figure 6 through Figure 9 show the simulation results of the simulation without the algorithm and the simulation with the algorithm.

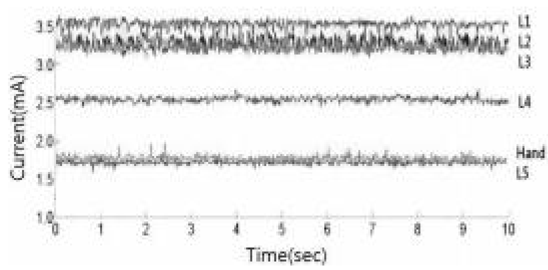

Figure. 5 Motor current graph of left arm before OPIND application

In the simulation, the actual motor specifications and performance are applied. Fig. 5 is a graph showing the motor current data when the left arm is moved to the target point without the algorithm applied. L1, L2, and L3 represent the joints corresponding to the shoulders, L4 is the joint corresponding to the elbow, and L5 is the joint shown for the rotation of the elbow. Hand represents the measured current of the 3-DOF robot hand. The closer you are to the shoulder joints, the more current is consumed due to the weight.

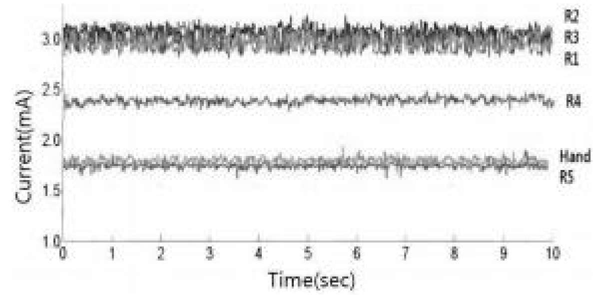

Figure. 6 Motor current graph of right arm before OPIND application

Figure 6 is a graph of the right arm measured without the algorithm applied. Likewise, R1, R2, and R3 are joints representing the shoulder, R4 is the joint that exits the elbow, and R5 is the joint that represents the rotation of the elbow. Hand also shows the current of the 3-DOF robot hand attached to the right as in the left. Figure 8 also shows that the current value of the motor corresponding to the shoulder joint is large.

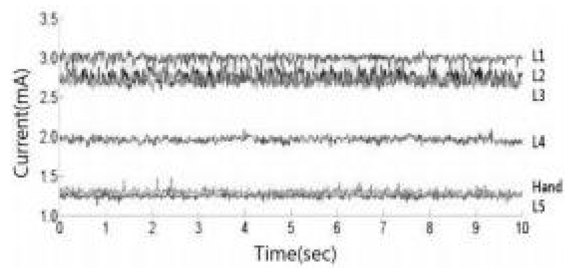

Figure. 7 Motor current graph of left arm after OPIND application

Fig. 7 is a graph showing the motor current of the left arm which is moved to the target point while the OPIND is applied. OPIND was applied to avoid the singularity, and the motor current value data was output through the simulation. This indicates that the robot has moved using a path that takes a small load because the motor does not fall into the trouble of the singularpoint.

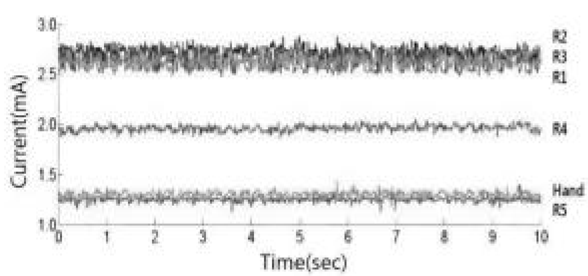

Figure. 8 Motor current graph of right arm after OPIND application

Fig. 8 shows the motor current in the right arm with OPIND applied. It shows that the robot has moved by using a path that takes less load on the motor because it does not fall into the trouble of singular point.

Figure 9 and Figure 8 show that moving the path by avoiding the singularity indicates that the load on the motor is low and that the path is optimized for the load.

5. CONCLUSION

In order to meet the demand of intelligentization of multi - purpose robot manipulator, a dual - arm robot system was developed in the ROS environment. Using the amount of consumed electric power to numerically evaluate the stability of a dual-arm robot, we created a cost function for each posture and proposed an optimal working posture accordingly.

Next, we will attach a 3-Finger hand to the manipulator and grasp various shapes of objects, We plan to analyze the optimum grasping position and pattern by estimating force distribution using compliance control.

ACKNOWLEDGMENT

This research is based upon work supported by the Ministry of Trade, Industry & Energy(MOTIE, Korea) under Industrial Technology Innovation Program. No.10073147

REFERENCES

[1] Panagiotis K. Artemiadis, Pantelis T.Katsiaris and Kostas J, Kyriakopoulos, “A biomimetic approach to inverse kinematics for a redundant robot arm.”

[2] C. Ott, O. Eiberger, W. Friedl, B. Bauml, U. Hillenbrand, C. Borst, A. Albu-Schaffer, B. Brunner, H. Hirschmuller, S. Kielhofer, R. Konietschke, M. Suppa, T. Wimbock, F. Zacharias, and G. Hirzinger, “A humanoid two-arm system for dexterous manipulation,” In IEEE-RAS Int. Conf. on Humanoid Robots, pp.276-283, Dec, 2006.

[3] M. Gharbi, J. Cort´es, T. Sim´eon, “A sampling-based path planner for dual-arm manipulation”, Proceedings of the 2008

[4] A. Miller, S. Knoop, H. Christensen, and P. Allen, Automatic grasp planning using shape primitives”, in IEEE International Conference on Robotics and Automation, Vol.2, pp.1824-1829, 2003.

[5] Gregory Z. GrudiE and Peter D. Lawrence, “Iteratice Inverse Kinematics with Manipulator,” Proceedings of the IEEE Transactions on Robotics and Automation, VOL.9, NO.4, pp 476-483,August, 1993.

[6] K. L. Doty, C. Melchiorri, E. M. Schwartz,and C. Boonivento, “Robot manipulability”, IEEE Trans. On Robotics and Automation, Vol.11, No.3, pp.462-468, 1995.

[7] C. Eitner, Y.Mori, K. Okada, and M. Inaba, “Task and vision based online manipulator trajectory generation for a humanoid robot”, In Humanoid Robots, 2008. Humanoids 2008. 8th IEEE-RAS International Conference on, pp.293-298, Dec. 2008

[8] S. H. Lee and J. M. Lee, “Task-oriented dual-arm manipulability and its application to configuration optimization”, IEEE Trans. 27th Conf. Decision and Control, pp.2253-2260, 1988.

[9] C. S. Park, H. U. Ha and J. M. Lee, “Optimal Trajectory Planning for Cooperative Control of Dual-arm Robot”, Journal of Institute of Control, Robotics and Systems, Vol.16, No.9, pp.891-897, September, 2010.

[10] C. S. Park, H. U. Ha, J. B Son. J. M. Lee “Optimization of Dual-Arm Configurations for Efficient Handling of objects”, Korea Robotics Society, 2011.Jun, pp. 130-140.

[11] H. Chen and J. M. Lee, "Path Planning of 5-DOF Manipulator Based on Maximum Mobility," International Journal of Precision Engineering and Manufacturing, ISSN 2234-7593, Vol.15, Iss. 1, pp 45-52 52, January 2014.

[12] Y. S. Kim, J. B. Song, “Real-time Robot Arm Operating Software using ROS and Xenomai”, The Korean Society of Mechanical Engineers, 2015. NOV,pp. 3614-3615.

[13] C. R. Kim, I. H. Kim, T. H. Kim, “Xenomai-based Embedded Controller for High-Precision, Synchronized Motion Application”, KOREA INFORMATION SCIENCE SOCIETY, 2015. March, pp.173-182.

2017 Changwon International Conference on Intelligent Robot and Convergence Industry (CICIRO 2017)
Nov. 30th~ Dec. 1st, 2017, Changwon Exhibition Convention Center(CECO), Changwon City, Korea

Edge Simplification Method for Stereo Images

Eun Kyeong Kim[1], Hyunhak Cho[2] Jongeun Park[1] and Sungshin Kim[1]*
[1] Department of Electrical and Computer Engineering, Pusan National University, Busan, 46241, Korea ({kimeunkyeong, acacia13, sskim}@pusan.ac.kr)
[2] Department of Interdisciplinary Cooperative Course: Robot, Pusan National University, Busan, 46241, Korea (darkruby1004@pusan.ac.kr)

Abstract: Image segmentation is important technology in image analysis. Image segmentation can be implemented by edge detection. However, edge detection yields the substantial complex image because some technology is very sensitive. Therefore, this paper proposes the method of edge elimination for image segmentation. To that end, we consider color information and disparity image. The concepts of the proposed method are as follows: Pixels have similar color in an object; The value of disparity bears a close parallel to other disparity values of same object. As experimental results, the proposed method can eliminate the unnecessary edge.

Keywords: Edge Detection, Edge Elimination, Image Segmentation, Stereo Images.

1. INTRODUCTION

Image analysis is the research field which extracts the necessary information in the image. C. Kim et al [1] shows that, in case of image analysis, image segmentation is necessary to classify and recognize objects. Image segmentation considers the brightness of pixels in an object is similar and objects are separated by brightness discontinuity.

K. S Fu et al [2] shows that image segmentation is related to thresholding. Thresholding is done by considering the brightness information of pixels. However, it is difficult to segment objects because of similar intensity of lights, less amount of information. Therefore, to segment an image effectively, we consider the edge image. Edge represents relatively distinct boundary. However, the edge image is sensitive. So, it is necessary to eliminate the unnecessary edges on the edge image. To implement this idea, we consider color and disparity map in case of stereo images. Color and disparity map is used for distinguishing objects. Because an object has similar color and disparity.

The rest of this paper is as below. Section 2 explains edge detector. Section 3 describes the proposed method. Section 4 shows the experimental results. Finally, Section 5 discusses conclusions and future works.

2. EDGE DETECTOR

Boundary extraction is valuable because the image can be analyzed by using only boundary information. Oh [2] shows that edge maintains the information which describes the objects and the situation in the image. And the edge image needs less memory because the edge image is binary image. By linking edges such as lines and curves, the edge images can be used for matching and recognition.

Edge is the point changing the features such as brightness, color, or texture of an image. So, the algorithm of edge detection calculates the change, it decides edge at the point which has large changes. To calculate the change, differentiation is used.

D. Scharstein et al [3] provides some examples for stereo images. Fig. 1. is included in database of D. Scharstein. Fig. 1. shows the edge images by several methods of edge detection. Fig. 1(a). is applied Roberts operator. It is two by two matrix. Fig. 1(b). is applied Prewitt operator. Its operator considers upper and lower rows when the differential value of x-direction is calculated. It contains smoothing effect. Fig. 1(c). is applied Sobel operator. It gives weights to adjacent pixels. Lastly, Fig. 1(d). is applied Canny operator. This algorithm has disadvantages: sensitive, and the problem of finding optimal parameter. Sensitive makes difficulty of analyzing the image because of complexity. Therefore, we select the canny edge detector, and then the edge image is re-processed by eliminating edges for obtaining clear boundary. This process is done by considering color and disparity map as mentioned above.

3. THE PROPOSED METHOD

To detect edge effectively, this paper proposes the method to eliminate edge, which is already extracted, by

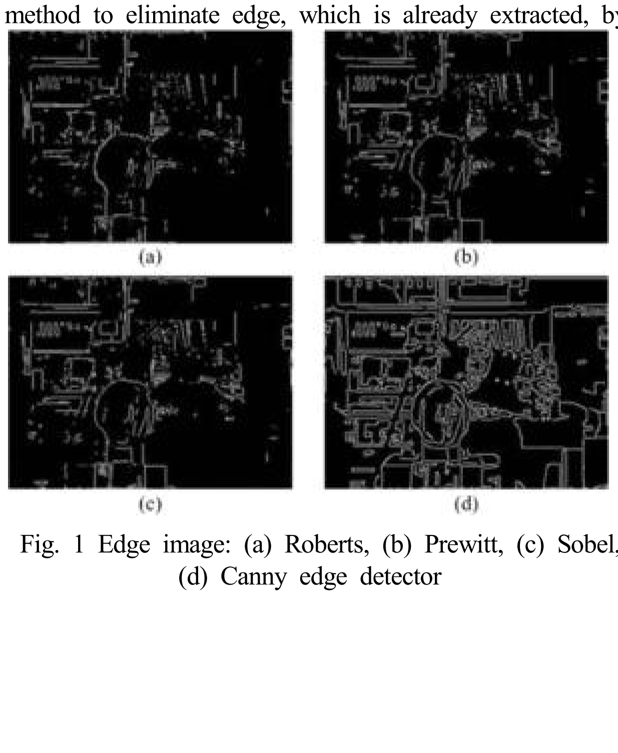

Fig. 1 Edge image: (a) Roberts, (b) Prewitt, (c) Sobel, (d) Canny edge detector

using color information and disparity map. E. K. Kim et al [4] shows that disparity map is related to the depth information in case of stereo images. The proposed method is as below.

First, we load the target image. And this target image is processed such as detecting edge and separating color space. Edge image can be obtained by smoothing, calculating gradient magnitude and non-maximum suppression. And target image is separated with respect to RGB color space. It helps the image segmentation effectively. We assume that an object has similar color in its overall surface. This feature is used for the image segmentation.

Next, the corresponding image is loaded. If the target image is the left image, the corresponding image is the right one. By using the target image and the corresponding image, disparity map is generated.

Based on the edge image, R, G, B component images, and disparity map, the decision process is followed. These things listed above is the input of the decision process. Through the decision process, we eliminate the edge which are already extracted. Finally, the result image can be obtained.

4. EXPERIMENTALRESULTS

Experiments are carried out according to the process mentioned above. The target images are provided by H. Hirschmüller et al [5]. It is difficult to find the difference between R, G, and B component image. So, we consider the similarity together with R, G, and B component. This concept is related to the similarity of pixels in an object. After edge detection and the separation of color space, using the disparity, edge is eliminated by the decision process. An experimental result is shown in Fig. 2. Fig. 2(a). is edge image by Canny edge detector. And Fig. 2(b). represents edge image by the proposed method.

As an experimental result, the proposed method can delete unnecessary edge which is located in an object. However, the edge is remained in case of an object has complex texture. In the future work, we consider texture features to eliminate edge effectively. In case of Fig. 4., there is a rope which is mixed from blue and orange. To delete edge in a rope, the texture features will be considered.

5. CONCLUSION

This paper proposed the method for effective edge detection in case of stereo images. Stereo images have the unique information which is called disparity. It is related to depth information. We assume the value of disparity is similar with the value of disparity of neighborhood. Based on this concept, we combine color and disparity information for detecting edge effectively. Color information is used because the pixels are similar with neighborhood in an identical object. As experimental results, the proposed method can detect edge more effective than traditional method.

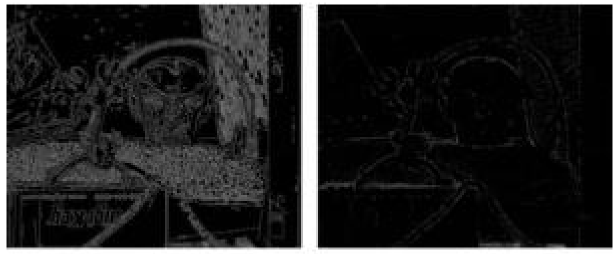

Fig. 2. Experimental result: (a) Edge image by canny edge detector, (b) Edge image by the proposedmethod

In the future work, we will detect and delete edge information by considering the relationship between adjacent pixels.

ACKNOWLEDGEMENT

This work was supported by BK21PLUS, Creative Human Resource Development Program for IT Convergence and was supported by the MOTIE (Ministry of Trade, Industry & Energy), Korea, under the Industry Convergence Liaison Robotics Creative Graduates Education Program supervised by the KIAT (N0001126) and was supported by the Technology Innovation Program(10073147, Development of Robot Manipulation Technology by Using Artificial Intelligence) funded By the Ministry of Trade, Industry & Energy(MOTIE, Korea)

REFERENCES

[1] C. Kim, H. Jeong, and H. Yang, *Digital Image Processing through MATLAB*, Life and Power Press, 2016.

[2] K. S. Fu, R. C. Gonzales, and C. S. LeeR. C. Baker and B. Charlie, *Robotics: Control, Sensing, Vision, and Intelligence*, McGrawHill, 1987.

[3] D. Scharstein, and R. Szeliski, “A taxonomy and evaluation of dense two-frame stereo correspondence algorithms,” *International Journal of Computer Vision*, Vol. 47, No. 1-3, pp. 7-42, 2002

[4] E. K. Kim, H. Cho, H. Lee, S. A. Wibowo, and S. Kim, “Improvement of disparity map using loopy belief propagation based on color and edge,” *Journal of Korean Institute of Intelligent Systems*, Vol. 25, No, 5, pp. 502-508, 2015

[5] H. Hirschmüller, and D. Scharstein, “Evaluationof cost functions for stereo matching,” *IEEE Conference on Computer Vision and Pattern Recognition*, pp. 1-8, 2007.

Inverse Kinematic Analysis of 5 DOF Manipulator using Numerical method

Jin Gon Yoon [1], Sun Oh Park [1], Min Gyu Jung[1] and Min Cheol Lee [1]*
[1] Departmentof Mechanical Engineering, Pusan National University,
Busan, 46241, Korea ({y1k1000, sunoh425, youadeul, mclee}@pusan.ac.kr)* Corresponding author

Abstract: This paper present a system configuration and inverse kinematics solution using inverse jacobian method for single 5 DOF manipulator as a basic study on a dual arm robot. Inverse kinematics can be obtained by geometric method, algebraic method, and numerical method using inverse jacobian. In case of geometric and algebraic method, the mathematical computation becomes more difficult as the axis increases. Therefore, the inverse kinematic analysis of the 5 DOF manipulator was performed using the numerical method and the behavior of manipulator was confirmed on the MATLAB simulation. However, it was impossible to get solution at the point where singularity occurred. In hence, we will solve the singularity problem and then apply it to the real system in the future.

Keywords: Inverse kinematics, Manipulator, Numerical method.

1. INTRODUCTION

In many case, manipulators are often used to produce and automate a variety of products while maintaining good quality in industrial field.

Low degree of freedom manipulator is suitable for simple and repetitive tasks, but it is impossible to process and assemble complex shaped product. To overcome these drawbacks, YASKWA(Japan), DLR(Germany), and KIMM(Korea) are constantly developing high DOF dual arm robot and demand for such robots is also increasing[2].

In this paper, we introduce the system configuration and kinematic analysis method of a single 5 DOF manipulator as a basic research on dual arm robot. Robot system consists of computer, manipulator and MMC(Multi-Motion Control) board to perform digital input/output. MATLAB was used for kinematic analysis.

2. SYSTEM CONFIGURATION

Robot system consists of host PC, servo driver, robot arm and MMC board. The host PC gives the command to manipulator using MMC board that communicate with PC though PCI bus.

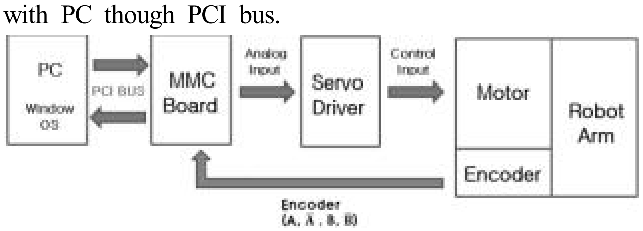

Fig. 1. System configuration

Fig 1 presents system configuration for motion control of robot arm.

We can give a position command using Visual C program that calculate voltage value to actuate each motor. Then MMC board get digital command though PCI bus and convert digital signal to analog signal. Analog signal is amplified by servo driver and finally DC motor get proper voltage value.

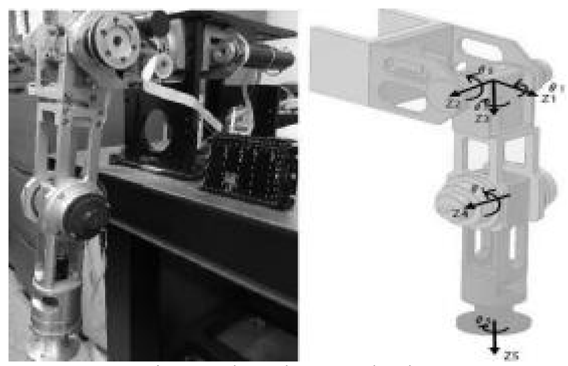

Fig. 2. The robot arm hardware

Fig 2 present the robot arm hardware (left) and axis of each motor (right).

3. INVERSE KINEMATICS

3.1 D-H parameter

Table 2. The table of D-H parameter

Joint	θ (°)	D (m)	α (°)	a (m)
1	* θ_1	0	-90	0
2	* θ_2	0	90	0
3	* θ_3	0.2	-90	0
4	* θ_4	0	90	0
5	* θ_5	0.29	0	0

*: rotation angle

Θ is rotation of z-axis, D is distance of z-axis, α is rotation of x-axis, a is distance of x-axis.

The following equation can be derived using DH parameter.

$$T = \begin{bmatrix} R_0^n & O_0^n \\ \mathbf{0} & 1 \end{bmatrix} \quad (1)$$

T is equivalent to multiplying a matrix from axis 1 to axis n of D-H parameter. is R_0^n 3x3 matrix rotation value and O_0^n 3x1 matrix position value.

3.2 5 DOF jacobian solution

Jacobian can be expressed as

$$J = \begin{bmatrix} J_v \\ J_w \end{bmatrix} \quad (2)$$

Jacobian can be represented by 3 position value J_v (dx,dy,dz) and 3 rotation angle J_w (∂x, ∂y, ∂z).

$$J_w = [\rho_1 z_0 \;\; \rho_2 z_1 \;\; \cdots \;\; \rho_n z_{n-1}] \quad (3)$$

$$J_v = \frac{\partial o_0^n}{\partial q_i} = z_0^{i-1} \times (O_0^n - O_0^{i-1}) \quad (4)$$

$$z_0 = \begin{bmatrix} 0 \\ 0 \\ 1 \end{bmatrix}, z_1 = R_0^1 z_0, \cdots, z_5 = R_4^5 z_4 = R_1^5 z_0 \quad (5)$$

Jacobian J_w, J_v are expressed as above equation [3]. ρ_i is equal to 1 if joint i is revolute and 0 if joint i is prismatic. We can get jacobian using above equation.

$$J = \begin{bmatrix} z_0 \times (o_5 - o_0) & z_1 \times (o_5 - o_1) & \cdots & z_5 \times (o_5 - o_4) \\ z_0 & z_1 & \cdots & z_5 \end{bmatrix} \quad (6)$$

Since the 5 DOF jacobian is a 6x5 matrix, it is difficult to directly obtain the inverse jacobian. Therefore, inverse jacobian was obtained by following method.

$$J \times J^{-1} = \mathrm{I} \quad (7)$$

$$J|J^T(JJ^T)^{-1}| = \mathrm{I} \quad (8)$$

$$J_{5\times6}^{-1} = J_{5\times6}^T \, (J_{6\times5} J_{5\times6}^T)^{-1} \quad (9)$$

$$d\theta_{5\times1} = J_{5\times6}^{-1} \, dX_{6\times1} \quad (10)$$

As using (9) equation, we can get the inverse jacobian even though it is not a square matrix. Finally, we can find each angle using (10) equation.

3.3 Experiment

The initial position value and the target position value are given as

$$\text{Initial position} \begin{bmatrix} x \\ y \\ z \\ \emptyset_n \\ \emptyset_o \\ \emptyset_a \end{bmatrix} = \begin{bmatrix} 0 \\ 0 \\ 0.49 \\ 0 \\ 0 \\ 0 \end{bmatrix} \quad (11)$$

$$\text{Target position} \begin{bmatrix} x \\ y \\ z \\ \emptyset_n \\ \emptyset_o \\ \emptyset_a \end{bmatrix} = \begin{bmatrix} 0.31 \\ 0.25 \\ 0.27 \\ 60 \\ 30 \\ 120 \end{bmatrix} \quad (12)$$

The unit of x,y,z is [m], and the unit of $\emptyset_n, \emptyset_o, \emptyset_a$ is [degree]. T can be obtained from the equation (12).

$$T = \begin{bmatrix} -0.424 & -0.648 & 0.643 & 0.31 \\ 0.765 & 0.127 & 0.631 & 0.25 \\ -0.484 & 0.759 & 0.434 & 0.27 \\ 0 & 0 & 0 & 1 \end{bmatrix} \quad (13)$$

The following results can be obtained by using the equation [2-10].

$$\text{Target angle} \begin{bmatrix} \theta_1 \\ \theta_2 \\ \theta_3 \\ \theta_4 \\ \theta_5 \end{bmatrix} = \begin{bmatrix} 0.52 \\ 0.78 \\ 0.63 \\ 0.39 \\ 0.53 \end{bmatrix} \quad (14)$$

The unit of θ_i is [rad].

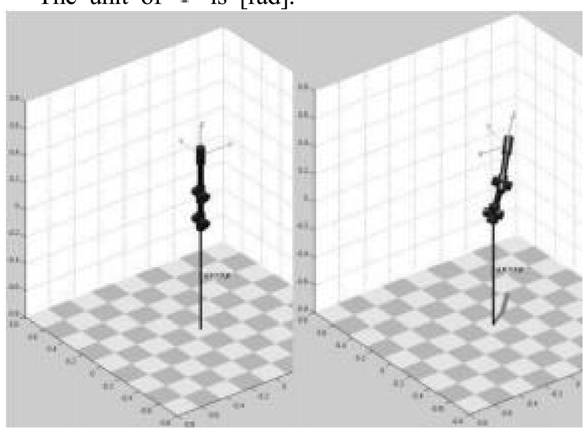

Fig. 3. Initial position (left) and final position (right) of manipulator

4. CONCLUSION

The result show that inverse kinematics can be obtained by using inverse jacobian and can be calculated relatively more easily than other methods.

Once we input desired target position value, we can obtain the corresponding target angle value of each joint, which means we can approach desired position by controlling motors of each joint.

However, the weak point of this method is that singularity occurs when the inverse jacobian becomes zero. In the future, a solution of avoiding singularity will be applied to the equation and experiment will be implemented to real physics system.

ACKNOWLEDGMENT

This research was supported by the Ministry of Trade, Industry & Energy and the Korea Evaluation Institute of Industrial Technology (KEIT) with the program number of "10038660", the MOTIE (Ministry of Trade, Industry & Energy), Korea, under the Industry Convergence Liaison Robotics Creative Graduates Education Program supervised by the KIAT (N0001126), and the Technology Innovation Program(10073147, Development of Robot Manipulation Technology by Using Artificial Intelligence) funded By the Ministry of Trade, Industry & Energy(MOTIE, Korea).

REFERENCES

[1] Hwan-Wook Je (2009), "A Study of the Collision Detection of Robot Manipulator without Torque Sensor" *Proceedings of International Joint Conference, Fukuoka International Congress Center*, Japan, Aug 18-21, 2009, pp.4468-4471

[2] Hyun Hee Kim (2016), "SMCSPO Based Reaction Force Estimation for 7 DOF Robot Arm, Proceedings of 16th International Conference on Control", *Automation and Systems (ICCAS 2016), HICO*, Gyeongju, Korea, Oct. 16-19. 123-145, 1989.

[3] Mark W. Spong, Seth Hutchinson, and M. Vidyasagar(2004), *Robot Dynamics andControl*

Sliding Mode Control Of 2 Link Robotic Manipulator

Saad Jamshed[1], Karam Dad[1] and Min Cheol Lee[1]*
[1] Department of Mechancial Engineering, Pusan National University,
Busan,46241, Korea ({saadjamshed93, karamdadkallu}@gmail.com, mclee @pusan.ac.kr))* Corresponding author

Abstract: In this research a simulation of sliding mode control on 2 link robotic manipulator has done. Sliding mode control (SMC) a robust control is used to track desired trajectory. Design of Sliding Mode Control and results of simulation has shown in this paper.

Keywords: Sliding Mode Control (SMC), Robust Control.Perturbation

1. INTRODUCTION

Accurate trajectory tracking is challenging topic in robotic manipulator control. This is due to nonlinearities and input coupling present in robotic arm. This paper is concerned with the control of two degree of freedom robot manipulator using sliding mode control so that actual trajectory tracks desired trajectory as close as possible despite of highly nonlinear and coupled dynamics.. Simulation study has been done in Matlab/Simulink environment. The result shows that Sliding Mode Control (SMC) produce better response in presence of uncertainty.

2. Dynamic & Control of 2 Links Robotic Manipulator

2.1 Dynamic

Dynamical equation of 2 link robotic manipulator using lagrangian approach

M(q)q’’+N(q,q’)q’+F(q’)+G=T (1)

M=mass of link, N=centripetal and coriolis force and centripetal force, F=frictional forces, G=gravity term, T=torque applied.

We take centripetal, friction and gravitational forces as disturbance or perturbation.

M1(q’’)+N1(q,q’)+F1(q’)+G1=T1 (2)

M2(q’’)+N2(q,q’)+F2(q’)+G2=T2 (3)

2.2 Sliding Mode Control

SMC is robust control used to control non linear system.SMC has 2 phase reaching phase and sliding phase as shown in fig 1.

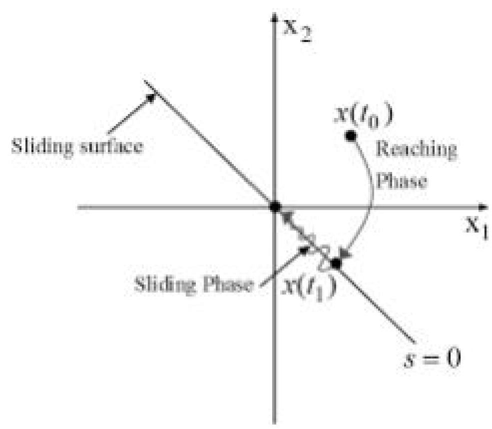

Fig.1 Sliding phase and reaching phase of SMC.

S=e’+ce (4)

e=error between trajectories c=constant

e=xd-x (5)

SMC consist of 2 control switching control and equivalent control switching control move system states to sliding surface (reaching phase) and equivalent control help states to remain on sliding surface in the presence of uncertainty.

When sliding mode begins sliding equation become

S’=-Ksat(s)+Pert (6)

Where,

S’S<0

K>Pert

Sat is smooth switching function force states to move on sliding surface

3.Simulation SMC Of Robotic Manipulator

Simulation of 2 link robotic manipulator has done on simmechanics a robotic model is import fom solid works to simmechanics.Fig 2 shows the simmechanics model of 2 link robotic manipulator. Fig 3 and fig 4 shows the result of 2ndlink of roboticmanipulator.

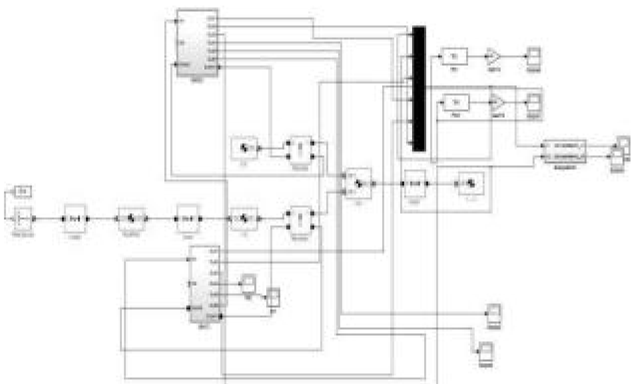

Fig.2Simmechanics model of 2 link robotic manipulator.

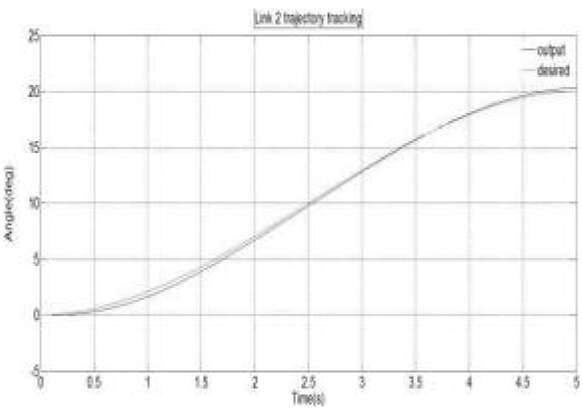

Fig3.Trajectory tracking of link2 of robotic manipulator..

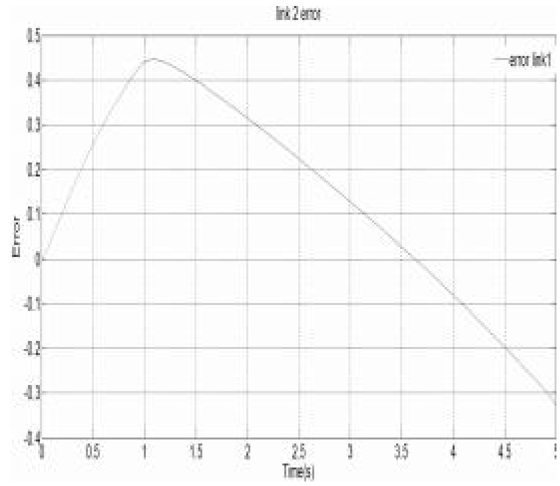

Fig4.Link 2 trajectory tracking error.

REFERENCES

[1] Manjeet and Pooja khatri, "Trajectory Control Of 2 Link Robotic Manipulator using PID" *Golden Research Thoughts*, Vol. 3,Issue .5,ISSN 2231-5063

[2] Professor Min Cheol Lee "Sliding Mode Control "*Lectures.*

[3] Unniversita'Delgi Studi Di Calgiari "Quick Introduction to Sliding Mode Control".*Lecture*

Utilizing air pressure sensor for detecting of object

Jin-hyun Park[1], Tae-eon Kim[1], Ki-seo Kim[1], Dong-eon Kim[1], and Jang-myung Lee[1]*
[1] Department of Electronic Engineering, Pusan national University
Busan, Republic of Korea ({Jinhyun1696, taeeon7379, kiseo1696, dongeon1696, jmlee}@pusan.ac.kr)

Abstract: In this paper, we propose a grasping force measurement method with a pressure sensor attached to a fingertip for grasping force control of a finger robot. We used Robotiz's 3Finger robot. For the application of the air pressure sensor, after inserting the air pressure sensor inside the fingertip of the finger-robot and sealing it, the air pressure is measured using the pressure during grasping. It is shown that the grasping force measurement is possible based on the measured air pressure. The validity is verified by comparing the data with the force sensor which is widely used for grasping force measurement.

Keywords: Utilizing air pressure sensor, 3 Finger-robot, Grasp method.

1. INTRODUCTION

Recently, the utilization of mechanized robots has been increased in all industrial fields, and robot technologies that can replace human abilities have been studied extensively. Researches on the gripping force measurement and control technology of grippers for picking up objects have also been actively conducted.

The gripping force measurement can be performed by using various sensors such as force sensor, tactile sensor, and load cell. In the case of the force sensor which is most used, there is a large difference in sensing depending on the attachment area of the gripper, and it is difficult to apply the correct sensor in the curved structure. Tactile sensor has a disadvantage of high price and load cell also has high price and largevolume.

In this paper, we propose a gripping force measurement method using a flexible material such as air pressure sensor and human skin.

2. BODY

For the verification of this paper, ROBOTIS 3Finger gripper, Interlink force sensor (FSR402) and BOSCH air pressure sensor (BMP180) were used.

First, ROBOTIS's 3Finger gripper consists of 3 MX-28 Dynamixel and frame as shown in Figure. 1, and it controls the Dynamixel by daisy-chain method using ROS package in Linux OS. The 3Finger gripper of ROBOTIS company was chosen because it is not a general 2JAW GRIPPER but a 3DOF (Degree Of Freedom) gripper and it is controllable by RS485 communication.

Figure. 1 Robotis' 3Finger robot

The force sensor is Interlink's FSR402, which is shown in Figure 2.

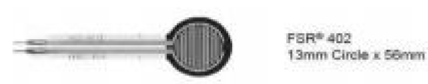

Figure. 2 Force sensor(FSR402)

The relationship between the characteristics and the output voltage is shown in Figure 3.

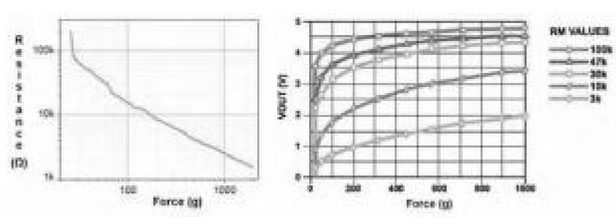

Figure. 3 sensor characteristics

The air pressure sensor uses BOSCH BMP180, and its shape is shown in Figure. 4 The pressure sensor has a measurement range of 300 ~ 1100hPa and has a high resolution of 0.01hPa.

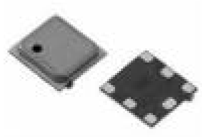

Figure. 4 Air pressure sensor(BMP180)

In order to insert the sensor for the test and seal the air, the existing fingertip was designed as shown in Figure. 5. The structure of the designed fingertip has holes for the insertion of three air pressure sensors, where three sensors are designed to determine at what point in the fingertip an object is gripped, such as by triangulation. The fingertip was made of rubber material with a thickness of 1 mm using a 3D printer.

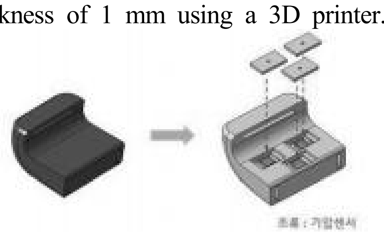

Figure. 5 designed fingertip

In this paper, only one air pressure sensor is used and the figure applied to the fingertip is shown on the left of Figure. 6. For the comparison of the force sensor and the air pressure sensor at the same time during the grip, a force sensor and an air pressure sensor were attached to both fingertips for holding the object and then the test was performed. Object used a cube of 45 grams of cube to get the same result in any direction.

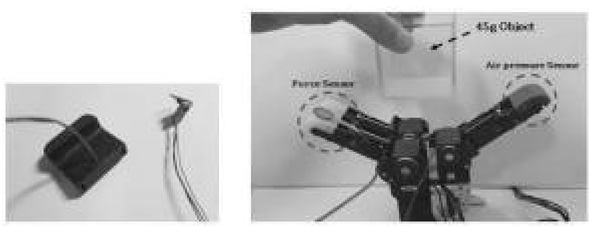

Figure. 6 produced shape and test environment

3. RESULT

In two cases (when gripping the object up, holding it sideways), we performed a comparison test with a force sensor. Figure. 7 shows the gripper holding up the object.

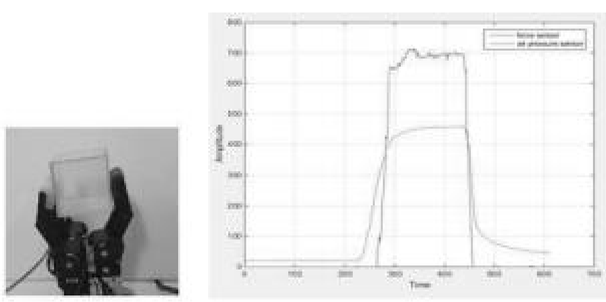

Figure. 7 Test results when holding up object

Figure. 8 shows the gripper holding the object sideways.

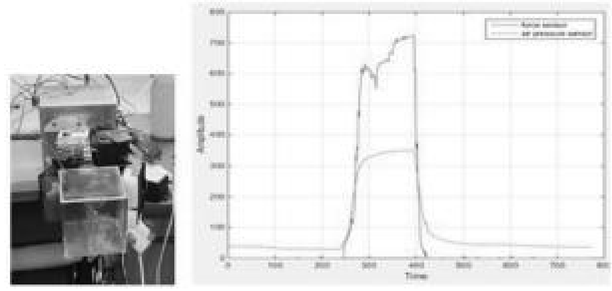

Figure. 8 Test results when holding the object sideways

4. CONCLUSION

Figure 7 and Figure 8 show the results.
As shown in Figure. 7, it can be confirmed that the sensing of the force sensor starts later than the application of the air pressure sensor at the time of gripping.
This is caused by the sensing dead zone due to the contact between the object and the force sensor.
On the other hand, in the case of the air pressure sensor, it can be confirmed that the sensor is flexible sensing when the object is set and released.

ACKNOWLEDGMENT

This research was supported by the MOTIE (Ministry of Trade, Industry & Energy), Korea, under the Industry Convergence Liaison Robotics Creative Graduates Education Program supervised by the KIAT (N0001126).

This research is based upon work supported by the Ministry of Trade, Industry & Energy(MOTIE, Korea) under Industrial Technology Innovation Program. (No.10073147)

REFERENCES

[1] J. Y. Han, J. K. Lee, S. Lee, K. C. Lee,"System of Tactile Sensor Signal Analysis for Grasping Control Algorithm " , the KSMPE Spring Conference 2016

[2] J. K. Lee, K. C. Lee, H. J. Kim, S. Lee, "Development of Robot Gripper System based on Tactile Sensor", Proceedings of the Korean Society of Precision Engineering Conference, 2014

[3] J. B. Baek, J. U. Jeong, S. U. Son, "The Case Study on Robot Gripper for Gripping Force Control Robot Gripper", Proceedings of the Korean Society of Precision Engineering Conference, 2015

[4] T. Y. Kim, S. Lee , K.C.Lee, “ Design of Gripper Control Algorithm Using Tactile Sensor”, Korea Institute of Machinery and Materials 2015 SpringSeminar
[5] Young-Jae Lee, “A Study On Slippage Sensing Algorithm of Manipulator for An Adaptive Control”, The Korea Institute of Information and Communication Engineering,1998
[6] An YoungLee, Soo Hyeon Kim and Young jin Choi “Development of Low Cost Gripper with Position/Force Control ” , Korea Robotics Society Annual Conference, 2014
[7] Young-Jun Jung, Yong-Hwan Oh, Sang-Rok Oh, Hyun-Seok Yang, “ Object Grasping Force Control by multi-fingered robotic hand” The KoreanInstituteofElectricalEngineers,2010
[8] Kim Seul Ki, Lee Seok, Lee Gyeongchang, “Analysis of Robot Gripper’s Slip detecting based on Tactile Sensor”, Institute of Control, Robotics and Systems 2014

2017 Changwon International Conference on Intelligent Robot and Convergence Industry (CICIRO 2017)
Nov. 30- Des. 1, 2017, Changwon Exhibition Convention Center(CECO), Changwon, Korea

Analysis of Traffic Sign Classification using Multiple Image Preprocessing Methods

Qing Tang[1] and Kang-Hyun Jo[2*]

The Graduate School of Electrical Engineering, University of Ulsan[1]

The School of Electrical Engineering, University of Ulsan, Ulsan 44610, Korea[2*]

Abstract: This paper presents a method for traffic sign classification using a 2-stage ConvNet. In this method, we compare different input which are RGB, grayscale, YUV images. Also we use histogram equalization to enhance contrast of input images. We also normalize every input image in the range (-1,1) as the preprocessing step. To increase robustness of classification model, we apply a dataset augmentation algorithm. Experimental results show that the method is effective in classifying traffic signs. Also the appropriate input images can improve classification model's performance well.

1. Introduction

Traffic sign plays a significant role in the regulating traffic behavior, ensuring the safety of the traffic and guiding the vehicles and pedestrians.

Generally, the traffic-sign recognition system includes two steps, which are detection and classification [7]. A number of research solve the detection and classification simultaneously [1]-[3]. Traffic sign recognition technology is regarded as a challenging task due to diversified backgrounds and various complexities, such as view point variations, lighting conditions, various types of sign and different resolution of the traffic sign input images [2, 3].

The model can classify 43 categories of traffic signs.

The model can classify 43 categories of traffic signs. To train and evaluate the proposed system, the GTSRB dataset [4] is utilized.

2. Image Preprocessing and Model Architecture

2.1 Color Space

The size of each image of GTSRB dataset is not the same, we resize all the image into 32x32x3, represented as [0, 255] integer values in RGB space. For choosing the better color space, we also transfer image from RGB to YUV color space. Classes of dataset are 43, such as, Speed limit, No entry and Keep left, etc.

2.2 Histogram Equalization and Normalization

In the real world, in order to be easily recognized and distinguished by the drivers, traffic sign are always designed in specific shapes and high saturated colors. We try to adapt histogram equalization to imput image to improve saturation, so the model can capture the high saturation region of traffic sign well.

And the second step is normalize image from (0, 255) to (-1, 1). Normalization can reduce the effect of illumination on image.

2.3 Dataset Augmentation

Dataset augmentation helps us generate additional training examples, also reduce the effect of dataset imbalance, which will lead bias toward the classes which have more samples and lead to misclassification. We use dataset augmentation algorithm [5] and we just change the brightness of input image.

2.4 Model Architecture

The architecture of neural network in this paper is a 2-stage ConvNet [5] which been proposed by Pierre Sermanet and Y. LeCun [6], and we change a little in S4 layer [5]. Also we add a Dropout module before the last layer of fully connection. The dropout probability is 0.5. Using the dropout unit can avoid over-fitting to improve validation accuracy.

3. Experiments

We focus on the German Traffic Sign Benchmarks (GTSRB) data set to evaluate the method in the paper, the GTSRB dataset consists of 43 classes of traffic sign. To evaluate the effectiveness of the different preprocessing method, we report the result of the experiment.

In Fig.1, 'Gray400_0.9367' means that the input are grayscale image, also if there are less than 400 samples in one class of GTSRB dataset, we will generate samples using dataset augmentation algorithm for that class until the number of sample reach 400, and the test accuracy of the Gary400 model is 0.9367. 'HE' means that the input are RGB image with histogram equalization step. 'RGB' means that the input are RGB image without histogram equalization step. 'YUV' means that the input are YUV image.

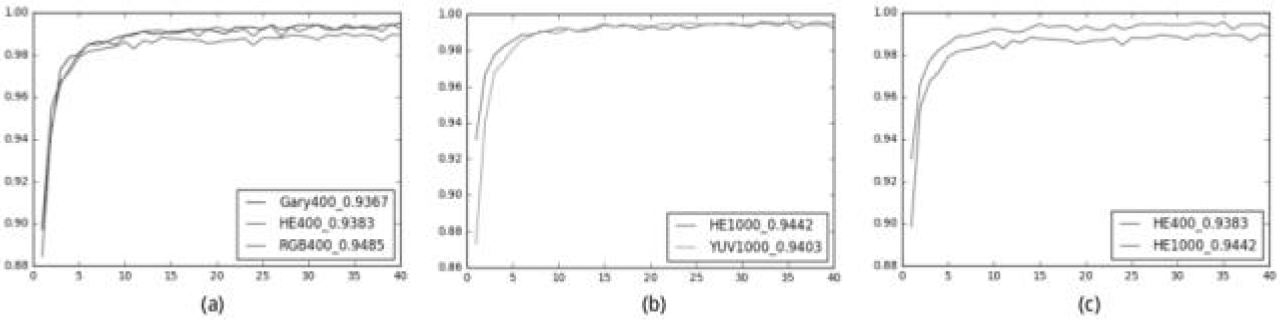

Fig.1 Accuracy of training and test step. The abscissa is epoch, the ordinate is validation accuracy. The number which behind the model name are the test accuracy of the model.

From Fig.1(a) we can see that using grayscale image to train the model can achieve better accuracy rather than test accuracy, also histogram equalization could not improve model performance in both validation and test step. In Fig.1(b), we compare these two methods which are using RGB image with histogram equalization and using YUV image as input. The experimental result shows that using RGB color channel can achieve better accuracy of the validation and test step. Compare with the model 'HE400', 'HE1000' generate more image for training using dataset augmentation algorithm. And the result show that dataset augmentation has a great help to performance.

4. Conclusion

We presented a traffic sign classification method based on Convolutional Neural Network architecture. We compare different preprocessing method for traffic sign classification model. In the future work, we will use RGB image to train the model. Also, we will try to use other neural networks to classify and compare with 2-stage ConvNet which we use in this paper.

REFERENCES

[1] C. Fang, C. Fuh, S. Chen, and P. Yen, "A road sign recognition system based on dynamic visual model," in The 2003 IEEE Computer Society Conf. Computer Vision and Pattern Recognition, Madison, Wisconsin, pp. 750-755 (2003).

[2] Miura, T. Kanda,mand Y.nShirai, "An active vision system for real-time traffic sign recognition," in 2000 IEEE Intelligent Transportation Systems, Dearborn, MI, USA, pp. 52-57 (2000).

[3] S. Vitabile, G. Pollaccia, G. Pilato, and F. Sorbello, "Road sign Recognition using a dynamic pixel aggregation technique in the HSV color space," in 11th Inter. Conf. Image Analysis and Processing, Palermo, Italy, pp. 572-577 (2011).

[4] Stallkamp, J, Schlipsing, M, Salmen, J, and Igel, C. "The German Traffic Sign Recognition Benchmark: A multi-class classification competition." In International Joint Conference on Neural Networks, (2011)

[5] Q. Tang, L. Kurnianggoro, K.H. Jo. "Traffic Sign Classification with Dataset Augmentation and Convolutional Neural Network." In 9thInternationalConferenceonGraphicandImage Processing,(2017).

[6] Pierre Sermanet and Yann LeCun. "Traffic Sign Recognition with Multi-Scale Convolutional Networks." In 2011 International Joint Conference on Neural Networks, IJCNN 2011 - Final Program, pp. 2809-2813 (2011)

[7] A. de la Escalera, J.M Armingol, M. Mata. "Traffic sign recognition and analysis for intelligent vehicles." Image and Vision Computing, vol. 11, n. 3, p. 247-258 (2003)

2017 Changwon International Conference on Intelligent Robot and Convergence Industry (CICIRO 2017)
Nov. 30- Des. 1, 2017, Changwon Exhibition Convention Center(CECO), Changwon, Korea

Exploiting Different Shape Features for Fall Action Classification

Sowmya Kasturi1 Kang-Hyun Jo2*

The Graduate School of Electrical Engineering, University of Ulsan1

The School of Electrical Engineering, University of Ulsan, Ulsan 44610, Korea2*

Abstract: The number of older people living alone has been increased over the past years. It is observed that fall and resulting injuries have become a major health problem among those older people. A vision based system for fall action classification from other actions would be of a great help in this case. But the inherent problem is the choice of features, which can distinguish a fall from non-fall action accurately. So, the proposed method exploits the bounding box and elliptical features over the human silhouette, separated from background. All the experiments are performed on top viewed Kinect depth images of UR fall detection dataset. Results showed that ellipse based features are superior to classic bounding box based features.

1. Introduction

Falls are one of the major cause for injuries and hospitalization of many older people. According to a study [1], 13% of 828 older Korean adults living in a community experienced falls during a period of one year. As the older people living alone are rapidly increasing in the society, in the absence of care taker, a fall event unattended could lead to a serious injury and hospitalization. Many automatic sensor based fall detection systems were developed to detect and alarm the caretaker in the occurrence of fall event. However, these systems often cause discomfort to wear all day around and easily prone to vibrations from surrounding environment causing false alarms. So the concentration has been shifted to develop RGB vision based systems to exploit the rich information offered by surveillance systems, but these are privacy intrusive and easily subjected to occlusion. In the proposed method, top viewed depth images has been considered to deal with the problems in the former one.

2. Theory

2.1 Shape features

Vision based systems uses a variety of features namely shape based, posture based, spatio- temporal, 3D head change and motion inactivity features [2]. The shape of the human varies drastically during a fall when compared to other non-fall actions like walking or standing. In [3], height, width, depth of a 3D bounding box features are used for fall classification. In the current method different bounding box and ellipse based shape features are exploited to choose features which are more helpful to classify a fall from a non-fall action. Seven bounding box features namely bounding box height and width, area, centroid, orientation, extent and eccentricity are extracted. The ellipse fitting based features considered are major and minor axis of the ellipse, area, centroid, orientation, extent and eccentricity. The area represents the number of pixels and eccentricity is the measure of aspect ratio and the extent is given by the ratio of number of pixels in the silhouette to the bounding box or ellipse.

$$Extent = \frac{N_s}{N_{be}}$$

The centroid, orientation of the ellipse changes greatly for fall and non-fall action and is calculated from the moments [4]

3. Results and Discussion

The experiments are conducted over 760 image frames from 5 videos of UR fall detection dataset [5]. Two classes are defined, fall and all the other negative samples as non-fall. The non-fall events considered are walking, standing and no human in the frame. A fixed background Fig. 1. (a) is manually selected and foreground is extracted from it by performing frame differencing with any current input frame (b). After the foreground extraction (c), the largest connected component is extracted which is the human silhouette (d). The bounding box and ellipse features are extracted from the silhouette and given as input to a binary SVM classifier. Two classes namely fall and no-fall are manually labelled for the training purpose and the classifier, classifies the action as one of these classes. One half of the dataset is used for training and the other for testing. Sample bounding box and ellipse fit results are shown in Fig.2 and Fig.3. The experimental results shows the supremacy of ellipse fit features over traditional bounding box features with an improved accuracy of almost 5% as shown in the Table 1. It is observed that the accuracy of the system is affected in the case where human body touches the nearby chair as shown in Fig.4

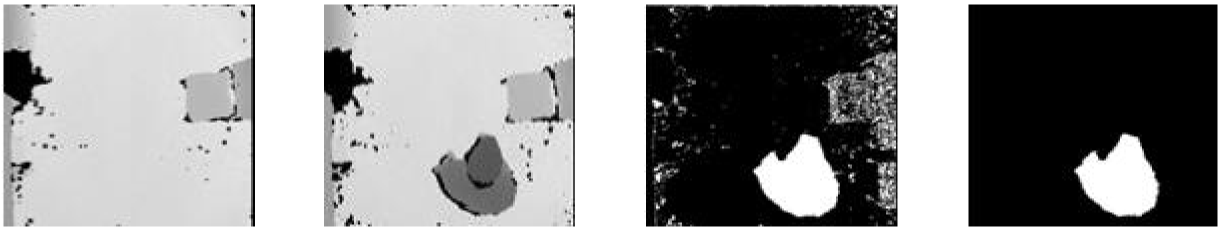

(a) (b) (c) (d)

Fig. 1. Human silhouette extraction

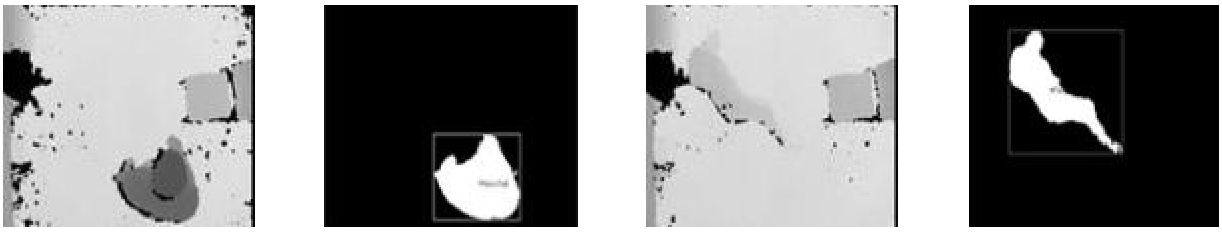

Fig. 2. Examples of bounding box results for a non-fall and fall action

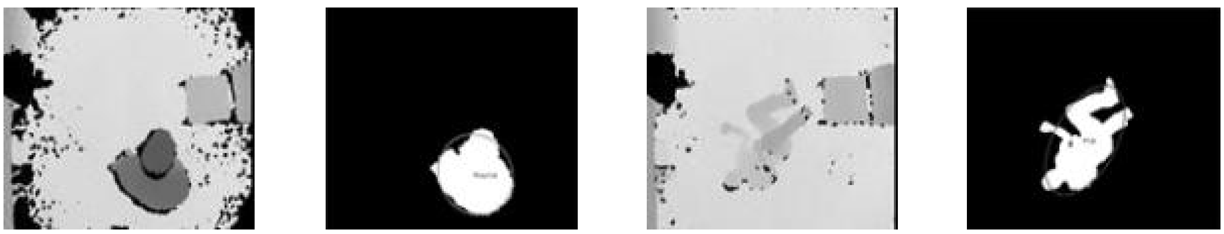

Fig.3. Examples of ellipse fit results for a non-fall and fall action

Features	Classification accuracy (%)	Sensitivity(%)
Bounding box	85.64	79.81
Ellipse fit	90.93	91.11

Table 1. Performance evaluation of different shape based features

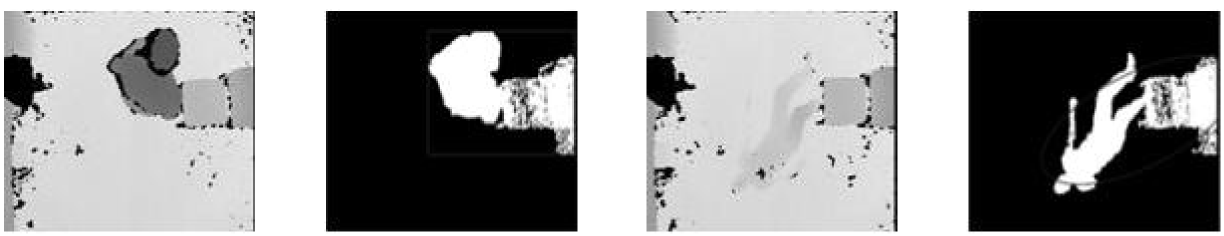

Fig.3. Examples of ellipse fit results for a non-fall and fall action

4. Conclusion

The paper exploits different bounding box and ellipse based shape features for the human fall action classification. The shaped based features are extracted from the separated human silhouette. A binary SVM classifier is fed with these features and classifies the event as fall or non-fall. The experimental results shows the robustness of ellipse fit features over traditional bounding box methods. In addition, both the features are observed to be insufficient for the action classification when the human silhouette is in touch with other objects in the environment.

REFERENCES

[1] Kim, Kwang-Il, "Evidence-based guideline for fall prevention in Korea," Journal of the Korean Geriatrics Society, Vol. 20, No. 1, pp. 1-28, 2016.

[2] Chung, Man Cheung, "A survey on fall detection: Principles and approaches," Neurocomputing , Vol.100, No. 100, pp.

144-152, 2013.
[3] Bevilacqua, Vitoantonio, "Fall detection in indoor environment with kinect sensor," Innovations in Intelligent Systems and Applications (INISTA) Proceedings2014 IEEE International Symposium on, pp. 319-324, 2014.
[4] J. Dongyao, V. Groza, L. XiaoHui, L. Xu, Z. Huaihua, and Q. Zeng, "A method of detecting human body falling action in a complex background," in Intelligent Engineering Systems (INES), 2016 IEEE 20th Jubilee International Conference on. IEEE, 2016, pp. 51-56.
[5] B. Kwolek and M. Kepski, "Human fall detection on embedded platform using depth maps and wireless accelerometer," Computer methods and programs in biomedicine, vol. 117, no. 3, pp. 489-501, 2014.

2017 Changwon International Conference on Intelligent Robot and Convergence Industry (CICIRO 2017)
Nov. 30 - Des.1, 2017, Changwon Exhibition Convention Center (CECO), Changwon, Korea

A Study on the Path Planning and Control of Robot Manipulator with Six Joint for Molding and Forging Process Automation

Min-Seong Kim[1], Geo-Seung Choi[2], Byung-Seuk Yoon[3], Jong-Bum Won[4] and Sung-Hyun Han[5]

[1] Department of Advanced Engineering., Kyungnam University, Changwon, 51767, Korea (E-mail : kms21018@naver.com)

[2] SAMHYUN CO. Ltd., Changwon, 51398, Korea (E-mail : gschoi@samhyun.co.kr)

[3] Dongmyeongjeong-gi Co., Ltd., Changwon, 51561, Korea (E-mail : bsyoon@naver.com)

[4] SMEC co., Ltd. Gimhae City, 50969, Korea (Tel : +82-10-4582-8264; E-mail :won@esmec.com)

[5] School of Mechanical Engineering, Kyungnam University, Changwon, 51767, Korea (Tel: +82-10-3585-5111; E-mail: shhan@kyungnam.ac.kr)

Abstract: In this study, we proposed robust control schemes for robot system which has the parametric uncertainties in forging process. In order to compensate these uncertainties, we use the neural control algorithm that has the capability to approximate any nonlinear model over the precise input space. In the proposed control schemes, it is not necessary to drive the linear formulation of robot dynamic equation and tune the parameters. We also suggest the robust adaptive control laws in all proposed schemes for decreasing the effect of approximation error. To reduce the number of neural of network, we consider the properties of robot dynamics and the decomposition of the uncertainty function. The proposed controllers are robust not only to the structured uncertainty such as payload parameter, but also to the unstructured one such as friction model and disturbance. The reliability of the control scheme is shown by computer simulations and experiment of robot manipulator with 6 axis in forging process.

Keywords: Robust control, decomposition, neural network, robot dynamics, uncertainty .

1. INTRODUCTION

To overcome these difficulties, in this paper we propose the adaptive control schemes which utilize a neural network as a compensator for any uncertainty. To reduce the error between the real uncertainty function and the compensator, we design simple and robust adaptive laws based on nonlinear stability method. In the proposed schemes, the compensator has to see many neural because uncertainties depend on all state variables. To overcome this problem, therefore, we introduce the control schemes in which the number of neural of the NN compensator can be reduced by using the properties of robot dynamics and uncertainties.

2. PATH PLANNING AND CONTROL

A robot manipulator is defined as an open kinematic chain of rigid links. Each degree of freedom of the manipulator is powered by independent torques. Using the Lagrangian formulation, the equations of motion of an -degree-of-freedom manipulator can be written as

$$D(q)\ddot{q} + C(q,\dot{q})\dot{q} + G(q) + F_r(\dot{q}) + \tau_d = \tau \quad (1)$$

where $q \in R^n$ is the generalized coordinates; $D(q) \in R^{n \times n}$ is the symmetric, bounded, positive-definite inertia matrix; vector $C(q,\dot{q})\dot{q} \in R^n$ presents the centripetal and Coriolis torques; $\tau_d \in R^n$, $G(q) \in R^n$, $F_r(\dot{q}) \in R^n$ and $\tau \in R^n$ represent the gravitational torques, friction, disturbance, and applied joint torques, respectively.
The robot model (2) is characterized by the following structural properties.

This property is utilized in this paper in order to reduce the number of neural in the neural network compensator.

The considered tracking problem is stated as follows: Knowing desired trajectories $q_d \in R^n$, $\dot{q}_d \in R^n$, with some or all the manipulator parameters unknown, determine a control law τ and a sliding surface $s = 0$ such that sliding mode occurs on the sliding surface, the tracking error $\tilde{q} = q - q_d$ has a prescribed transient response and it goes to zero asymptotically as $t \to \infty$.

A. Simple Adaptive Control Law

The sliding surface $s = 0$ is chosen as a hyperplane

$$s = \dot{\tilde{q}} + \Lambda\tilde{q} \quad (5)$$

where Λ is a positive-definite matrix whose eigenvalues are strictly in the right-half complex plane and $\tilde{q}$ is the tracking error vector.
If the sliding mode exists on $s = 0$, then from the theory of VSS, the sliding mode is governed by the following linear differential equation whose behavior is dictated by the sliding hyperplane design matrix Λ :

$$\dot{\tilde{q}} = -\Lambda\tilde{q} \quad (6)$$

Obviously, the tracking error transient response is then determined entirely by the eigenvector structure of the matrix Λ .
In order to derive the sliding mode control law, which forces the motion of the error to be along the sliding surface $s = 0$, a vector of self-defined reference variables is introduced for the succinct formula expression in the sequel, that is,

$$\dot{q}_r(t) = \dot{q}_d(t) - \Lambda\tilde{q}(t) \quad (7)$$

Consider now the uncertainties of robot manipulator, (1) can be rewritten as

$$D(q)\ddot{q}+C(q,\dot{q})\dot{q}+G(q)+F(q,\dot{q},t)=\tau \quad (8)$$

Where $F(q,\dot{q},t)=F_r(\dot{q})+\tau_d$. However, in this paper, this uncertainty function vector has to be replaced by $F(q,\dot{q},\ddot{q},t)$

So (9) can be rewritten as

$$D(q)\ddot{q}+C(q,\dot{q})\dot{q}+G(q)+F(q,\dot{q},\ddot{q},t)=\tau \quad (9)$$

we let a Lyapunov function candidate be

$$V(t)=\frac{1}{2}s^TDs+\sum_{i=1}^{n}\tilde{\theta}_i^T\Gamma_i\tilde{\theta}_i \quad (10)$$

Where $\tilde{\theta}_i=\theta_i^*-\theta_i$, θ^* is the j th column vector of the optimal parameter matrix θ^* and Γ_i is a strictly positive real constant.

Differentiating $V(t)$ with respect to time yields

$$\dot{V}(t)=s^TD\dot{s}+\frac{1}{2}s^T\dot{D}s+\sum_{i=1}^{n}\tilde{\theta}_i^T\Gamma_i\dot{\tilde{\theta}}_i$$

$$=-s^T(D\ddot{q}_r+C\dot{q}_r+G+F-\tau)+\sum_{i=1}^{n}\tilde{\theta}_i^T\Gamma_i\dot{\tilde{\theta}}_i \quad (11)$$

Where $F(q,\dot{q},\ddot{q},t)$ is a completely unknown nonlinear function vector. Therefore, we replace $F(q,\dot{q},\ddot{q},t)$ by a Neural network $\hat{F}(q,\dot{q},\ddot{q},\theta)$. Let us define the control law as

$$\tau=D(q)\ddot{q}_r+C(q,\dot{q})\dot{q}_r+G(q)+\hat{F}(q,\dot{q},\ddot{q},\theta)-K_Ds \quad (12)$$

Where $K_D=diag(k_i)$, $i=1,2,\ldots,n$.

3. EXPERIMENT AND RESULTS

We also apply real-time adaptive control based on neural network compensator to dual-arm robot shown in figs. 1. Because the characteristics of two arms are the same, so we show the results into one arm is enough.

Fig. 1. Experimental set-up

All the algorithm calculation is calculated by Matlab and Simulink matlab on host computer and push into dual-arm robot which is shown in the Fig. 2. The desired trajectories are $q_{1d}=q_{2d}=15\pi\sin(\frac{2\pi}{300\pi}t+\frac{2\pi}{3})$ and the results of robust adaptive control are shown below

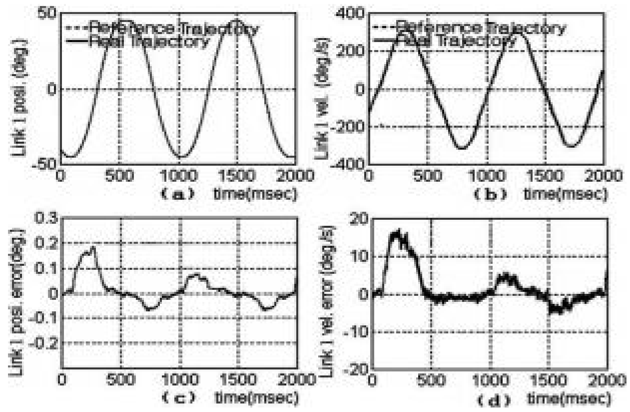

Fig. 2. (a)-(d) Experimental results for the position and velocity tracking of adaptive controller at the first joint.

4. CONCLUSIONS

In this paper, we have illustrated that the control objective is well accomplished and the neural network compensate the uncertainties. In addition, the proposed control technology needs to apply to robot manipulators include more joints, for forging process automation.

ACKNOWLEDGEMENT

This study was performed by project of the robot business belt construction enterprise..

REFERENCES

[1] J. E. Slotin and S. S. Sastry, “Tracking control of nonlinear systems using sliding surfaces, with application to robot manipulators,” Int. J. Contr., vol. 38, no. 2, pp. 465–492, 1983.

[2] J. J. E. Slotine and W. Li, Applied Nonlinear Control. Englewood Cliffs, NJ: Prentice-Hall, 1991.

[3] F. L. Lewis, C. T. Abdallah, and D. M. Dawson, Control of Robot Manipulators. London, U.K.: Macmillan, 1993.

[4] M. W. Spong, Robot Dynamics and Control. New York: Wiley, 1989.

[5] W. C. Ham, “Adaptive nonlinear control of one-link flexible arm,” in IEEE/RSJ Int. Conf. Intelligent Robots and Systems, vol. 1, Yokohama, Japan, 1993, pp. 3–7.

[6] “Adaptive control based on explicit model of robot manipulators,” IEEE Trans. Automat. Contr., vol. 38, pp. 654–658, 1993.

2017 Changwon International Conference on Intelligent Robot and Convergence Industry (CICIRO 2017)
Nov. 30- Des.1, 2017, Changwon Exhibition Convention Center(CECO), Changwon, Korea

Intelligent Control of Mobile-Manipulator Robot by Voice Command for Smart Factory

Yang-Keun Jeong[1*], Min-Seong Kim[2], Hui-Jin Kim[3], Woo-Song Lee[4], Yeon-Guk Noh[5], Geo-Seung Choi[6], In-Man Park[7] Jang-Sik Park[8] and Sung-Hyun Han[9]

[1] Shinla Information Technology Co., Ltd., Changwon, 51390, Korea (shintech@hanmail.net) * Corresponding author
[2] Department of Advanced Engineering, Graduate School Kyungnam University, Changwon, 51767, Korea (kms21018@naver.com)
3 Department of Mechanical engineering, Graduate School of Industry & Business administration Graduate School Kyungnam University, Changwon, 51767, Korea (jizhen79@nate.com)
[4] SUNJIN Technology co., Ltd., Changwon, 82331, Korea (elflws@hanmail.net)
[5] SFNT Co., Ltd., Changwon, 631-821, Korea (ykno1339@naver.com)
[6] SAMHYUN Co., Ltd, Changwon, 51398, Korea(gschoi@samhyun.co.kr)
[7] Intem Co., Ltd, 51565, Korea(intem237@hanmail.net)
[8] School of Electrical and Electronic Engineering, Kyungsung University, Pusan, 48434, Korea (jsipark@ks.ac.kr)
[9]Department of Mechanical Engineering, Kyungnam University, Changwon, 51767, Korea (shhan@kyungnam.ac.kr)

Abstract: Generally, it is possible to control the walking information based on the mobile robot's own postures, because a type of motion and gesture produces almost the same pattern of noise every time. In this paper, we describe a voice recognition control technology for mobile robot system which can robustly recognize voice by adults and children in noisy environments. We prove the performance of robot control system in a communication robot placed in a real noisy environment. Voice is captured using a wireless communication.

Keywords: Robust voice recognition, Side-lobe canceller, Navigation system

1. INTRODUCTION

Each kind of robot motion or gesture produces almost the same noises every time it is performed. By recording the motion and gesture noises in advance, the noises are easily estimated. By using this, we introduce a new method under robot motor noise. These methods can utilize pre-recorded noises as described later. Since each of these techniques has advantages and disadvantages, whether it is effective depends on the types of motion and gesture. The result of an experiment of isolated word recognition under a variety of motion and gesture noises suggested the effectiveness of this approach.

2. ROBOT SYSTEM

In this study, a sonar array composed of 16 ultrasonic sensors cannot be fired simultaneously due to cross talk. Instead, we adopt a scheduled firing method where sensors are activated in sequence of $\{s_1, s_{12}, s_2, s_{11} \ldots\}$. The arrangement of the ultrasonic sensors in upper layer and the sensors are marked as dots in the figure. The distances e_j $(j = 1, 2, \ldots 12)$ from the origin of the robot frame {R} to obstacles detected by the sensor s_j, can be defined as $e_j = ♎_j + R_r$. Here, R_r is the radius of the robot and the $♎_j$, is the range value measured by the sensor s_j .

$$u(t) ■ (v(t), ✎❑(t))_T ■ (v(t), w(t), Tms)_T \quad (1)$$

3. EXPERIMENT

The proposed robot has the maximum travel speed of 0.55 m/s and the maximum steering rate of 3.0rad/sec. Experiments are performed in an indoor with the first experiment for voice recognition without objects and second experiment for both of them: voice recognition and obstacles avoidance.

4. CONCLUSION

This paper proposed the integration of robust voice recognition and navigation system capable of performing autonomous navigation in unknown environments. In order to evaluate the performance of the overall system, a number of experiments have been undertaken in various environments.

REFERENCES

[1] M. Blanchet, J. Boudy, and P. Lockwood, "Environment adaptation for speech recognition in noise," in Proc. of EUSIPCO-92, vol. VI,1992, pp. 391–394.

2017 Changwon International Conference on Intelligent Robot and Convergence Industry (CICIRO 2017)
Nov. 30th~ Dec. 1st, 2017, Changwon Exhibition Convention Center(CECO), Changwon City, Korea

A Study on Robust Control of Robot Gripper Based on Pressure Sensors for Marking Automation Process

Min-Seong Kim1, Jeong-Seok Kang2, Jong-Dae Won3,
Sung-Hyun Han4 , Han-Sung Kim4

[1] Department of Advanced Engineering., Kyungnam University, Changwon, 51767, Korea
(E-mail : kms21018@naver.com)
[2] SMEC co., Ltd. Gimhae City, 50969, Korea
(E-mail : jskang@esmec.com)
[3] Young Chang Roboteck Co., Ltd., Gimhae City, 50969, Korea
(E-mail : wonjd@hanmail.net])
[4] School of Mechanmical Engineering, Kyungnam University, Changwon, 51767, Korea
(E-mail: shhan@kyungnam.ac.kr)
[4] School of Mechanmical Engineering, Kyungnam University, Changwon, 51767, Korea
(E-mail: hkim@kyungnam.ac.kr)

Abstract: In this study, we propose a new approach to control a robotic gripper based on the pressure sensor for application to the forging process automation. The increasing requirement for robotic grippers applications in limited environments such as forging process is motivating the need for flexible grippers which have the wide variety of objects encountered in 3D environments. The human hand is a very complex grasping tool that can handle objects of different sizes and shapes. Many researches have been carried out to develop artificial robot grippers with capabilities similar to the human hand. This gripper is the wide working space compared with its physical dimensions and the capability to deal with objects in working environment conditions. This tasks is achieved by using pressure sensor and by properly controlling and coordinating the gripper and the carrying arm. After a brief illustration of the gripper for forging process, the experimental activity is proposed and the results achieved are applied to the forging process.

Keywords: Robot Gripper, Flexible control, Wide working space, Force sensor, wide variety, forging process.

1. INTRODUCTION

At mechanical level study on dextrous grippers has mainly focused on the actuation and kinematics aspects. With very few exceptions, tendon actuated mechanisms, and their numerous variants, still represent an effective way to implement compact manipulators. Actuation of tendon based robot grippers poses various technical problems. Tendons coupling on one hand, friction and elasticity on the other, pose important problems for the control of tendon actuated mechanisms. However, the mechanical accuracy required to design a miniature dextrous gripper, is by far less than an equivalent design based on gears or other stiff transmission mechanism. Recently the tendency is to create robot hands more compact and high integrated sensors system, in order to increase the grasping capability and in order to reduce cabling through the finger, the palm and the arm. As a matter of fact, miniaturization and cabling harness represents a significant limitation to the design of small sized embedded sensor. [1]
The major contribution of this paper is to present the designofafullyintegrated tactileand3-axis forcesensor, with embedded electronics. The approach adopted has been that of using lowcost components available off-the-shelf, and to pursue a highly modular pressure sensor. The system is scalable and designed to be integrated on the supporting two joint.[2]

2. GRIPPER CONTROL

The mechanism of a flexible hand gripper requires the mass of the hand should be as low as possible. It is highly desirable that the hand weigh less than 1kg. Furthermore the low mass of the finger mechanism is desirable not only to achieve flexible motion but also for stable control.

Our philosophy about dynamic manipulation is maximization of the power and minimization of the mechanism. In particular four factors are important: (1) light weight, (2) high speed and high acceleration, (3) accuracy, (4) possibilities of flexible grasping. Fig. 1 shows the mechanical design of the hand, and Fig. 2 shows a scene of the Gripper control. We used three fingers, which is the minimum number to achieve a stable grasp. Each of fingers has 4 degrees of freedom (D.O.F); the hand system has 13 D.O.F included 1 D.O.F on the hand link. Note that the Joint 4 consists of the linear motor so that the finger tip can move as slide but other links just moving as rotate around a horizontal axis. In general a hand needs 9 D.O.F to move a target to any position and orientation. But our hand has 13 D.O.F so that the applications are very wide in the working environments, and the fingers are arranged so as to grasp the objects like circular and prismatic, etc. In order to achieve “lightning” high acceleration, we have developed a newactuator that allows a large current flow for a short time. Table 1 shows the specification for the actuator.
The finger has strain gauges at the joint 1 and joint 2 for force control. In addition a 6-axis force/torque sensor

and a tactile sensor are mounted on each fingertip. The flexible motion imposes a heavy load on the finger mechanism. For this reason a simple mechanism should be used for reduction gear, transmission, etc. In most traditional hand systems a wire-driven mechanism is used.Butthisisnotsuitableforalightweight mechanism, because it is large and complicated.

Early image processing is performed in order to achieve segmentation of the image, extraction of the target area, and computation of the image moments. Fromthese data, the position of the target is computed; each vision sensor is mounted on an active vision.

2.1 Pressure Sensor

Manipulation control requires in general some sort of feedback which could provide information about the interactions occurring during contact between the gripper and the grasped object. Assumptions must be made about the nature of the contact and, on the base of the selected contact models, it is possible to specify the nature of feedback required to properly control the interaction. Detailed contact mechanics models are in general too complex to be taken into account in real-time control applications.

The device consists of three strain sensitive thick-film resistors. A force applied to the interface stick produces a change of resistivity. Proper arrangement of the resistors in three Wheatstone bridges, and a simple decoupling amplifier, allow obtaining three voltages proportional to the applied force components. Digital potentiometers are used for self-calibration of the bridges and three instrument amplifiers provide appropriate signal conditioning beforesampling.

3. EXPERIMENTS

The main advantage of a multi-fingered hand is that itcangraspvariousobjectsbychangingitsshape.Several classifications of grasping have been proposed. In this proposal various grasps are classified into three large categories: a power grasp that passively resists arbitrary external forces exerted on the object, a precise grasp to manipulate the object, and an intermediate grasping which some fingers are used for a power grasp and the other fingers are used for a precise grasp.

We achieved these typical grasp types in our developed hand.Table.1 shows the specification of robot hand and fig. 2 is some examinations of flexible gasping objects.

Fig. 1. The scene of some objects catching test

Catching is one of the most important tasks for dynamic manipulation. In this section catching is shown using our flexible hand with a visual feedback controller. We used a rubber ball with radius of 5cm as a target, and we dropped it from about 1.2m in height. The speed of the falling ball is about 5.9m/s just before it hits the ground.

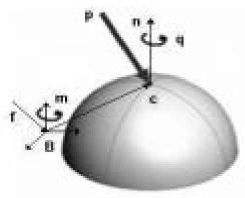

Fig. 2. Point of contact (**q**=0) and soft finger contact model.

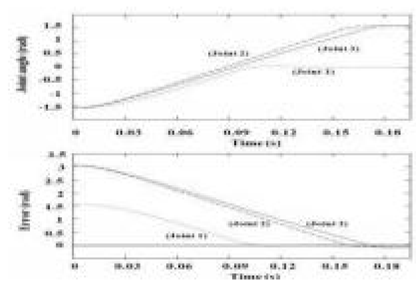

Fig. 3. Result of performance test for of gripper control

The success rate was more than 95% and tolerance of position error of the target was about ±1.5cm from the center of the palm.

Several types of failure modes were observed. The direction of a bounced ball depends on the coefficient of friction and restitution. It is difficult to know the accurate values of these parameters, but the errors in their measurement may be ignored if the speed of the fingertip is fast enough.

4. CONCLUSION

The sensor consists of a three components commercial force sensor and of a custom matrix tactile sensor based pressure sensitive conductive rubber. The joint used of both tactile and force information allows the direct solution of the point contact problem. A technique to compute the contact centroid and a quadratic approximation ofthe pressure distribution during contact has been proposed.

ACKNOWLEDGEMETN

This study was performed by project of the robot business belt construction enterprise.

REFERENCES

[1]T. Asfour, K. Berns and R. Dillmann, “The Humanoid Robot ARMAR”, Proc. of the Second International Symposium on Humanoid Robots (HURO´99), October 8- 9, 1999, Tokyo,Japan

[2] T. Asfour, K. Berns, J. Schelling and R. Dillmann, “Programming of Manipulation Tasks of the Humanoid Robot ARMAR”, The 9th International Conference on Advanced Robotics (ICAR'99), 25-27 October, Tokyo, Japan

2017 Changwon International Conference on Intelligent Robot and Convergence Industry (CICIRO 2017)
Nov. 30th~ Dec. 1st, 2017, Changwon Exhibition Convention Center(CECO), Changwon City, Korea

A Study on Accurate Motion Control of Mobile Robot with Dual-Arm

Yang-Geun Jeong[1], Gi-Su Shin[2], Min-Seong Kim[2], In-Man Park[3]and Sung-Hyun Han[4]

[1] Shinla Information Technology CO., Ltd., Changwon City, 51390, Korea (E-mail : shintech@hanmail.net)

[2] ANY TOY CO. Ltd., Kyungnam University, Changwon, 51767, Korea (E-mail : Shings@naver.com)

[2] Department of Advanced Engineering., Kyungnam University, Changwon, 51767, Korea (E-mail : kms21018@naver.com)

[3] Intem Co., Ltd., Changwon City, 51565, Korea (E-mail:intem237@hanmail.net)

[4] School of Mechanical Engineering, Kyungnam University, Changwon, 51767, Korea (E-mail: shhan@kyungnam.ac.kr)

Abstract: The main focus of this paper is obtaining a fuzzy perception of the environment in the design of each reactive behavior and solving the problem of behavior combination to implement a fuzzy behavior based control architecture. It should be remarked that, the proposed technique of the nonholonomic constraints are considered in the design ofeach behavior. Furthermore, inorder toimprove the capabilities ofthe intelligent control systemand its practical applicability, teleoperation and planned behaviors, together with their combination with reactive ones, have been considered.

Keywords: Real-Time control, Sensor, Intelligent Controller, Non-holonomic

1. INTRODUCTION

The real-time trajectory control is the process of determining and maintaining a path or trajectory to a goal destination. Autonomous mobile robots are required to navigate in more complex domains, where the environment is uncertain and dynamic. Autonomous navigation in these environments demands adaptation and perception capabilities. This paper describes improvements in the perception functions used in these kinds of robots. It should be noted that this is a nonholonomic vehicle with significant limitations in the reactive capabilities due to kinematic and dynamic constraints, and a few number of sensors and large blind sectors in between them, making autonomous navigation a nontrivial task. The methods presented in this paper have been conceived to deal with these limitations of conventional vehicles.

2. CONTROLSCHEME

The following considerations are based on a mobile robot with the three degrees of freedom of planar movement, x, y and θ. It is equipped with a ring of 12 ultrasonic sensors which are able to perceive vertical or nearlyverticalplanes.Thenumberofsensorsisirrelevant as long as there are no blind sectors between them. θ refers to the orientation of this ring of sensors and not to the orientation of the robot itself, which is of no importance for the wall following algorithm. With φ indicating the direction of movement the kinematics model of such a robot is described as follows:

$$dx = v\cos\varphi\, dt;\quad dy = -v\sin\varphi\, dt;\quad d\theta = \dot{\theta}\, dt \tag{1}$$

Since there is no modeling of the environment the absolute position of the robot does not matter. So there is no world frame used here and the kinematics model can be expressed instead as:

$$ds = v\,dt;\quad d\varphi = \dot{\varphi}\,dt;\quad d\theta = \dot{\theta}\,dt \tag{2}$$

The speed v, the angular speeds $\dot{\varphi}$ and $\dot{\theta}$ are used as control variables of the robot and generated by the fuzzy controller.

Perception of each ultrasonic sensor i of the mobile robot is assigned a vector ki. Its direction equals the orientation ofthe sensor´s axis and its length is a function of the distance di measured by this sensor:

$$k_i = \frac{d_{max} - d_i}{d_{max} - d_{min}} \tag{3}$$

where dmin and dmax designate the shortest and longest distance respectively at which an object may be positioned to be reliably detected. ki is limited to 0 and 1 respectively

Since a vehicle with nonholonomic constraints cannot move itself in any direction at every time instant, it is interesting to weight the different perceptions according with the direction where the obstacle was detected. In other words, an obstacle is less important if it is placed at a location that cannot be reached by the mobile robot, but it is more dangerous if it is on a reachable position.

where sat0,1(x) states for the saturation of x in the range [0, 1]. In this way, it is possible to assign different perceptions, i.e. different weights, to objects detected at the same distance relative to the mobile robot but at different directions. For example, perception function ki is obtained by using the nonlinear function

$$d_{\min}(\theta_i) = \frac{d_m(1-\alpha)}{(1-\alpha\cos\theta_i)},$$ and

$d_{\max} = n d_{\min}(\theta_i)$ (with n>1), in Eq. (4)

$$k_i = f(d_s, \theta_i) = sat_{0,1}\left[\frac{n d_m(1-\alpha) - d_s(1-\alpha\cos\theta_i)}{(n-1)d_m(1-\alpha)}\right] \quad (5)$$

Furthermore, it is interesting to stress that the perception vector implies a fuzzy high level description of the environment, being independent of the type of range sensor used. So, it is possible to use different perception functions from Eq. 4 for each kind of sensor (laser, ultrasonic, infrared). Thus, sensor data fusion can be reduced to compute different vectors from the sensor measurements and to combine them to obtain the perception vector.

The previous perception can be updated as follows: consider a robot of arbitrary shape equipped with proximity sensors. Any such sensor may be located at a position U, with its axis pointing to the direction s

A frame r represents the robots position and orientation, x and θ, respectively, with respect to the world reference system w. The velocity υ of the reference point and the angular velocity $\omega_{r/w}$ of the robot with respect to the fixed frame w, give the state of motion. Furthermore, the virtual perception coordinate system is assumed to be located at E, pointing to the direction of attention a1. Then, an object detected by a proximity sensor at a distance ds could be detected by a virtual sensor placed at E a distance d, and with an orientation θ with respect to the vehicle's direction of attention a1.

3. EXPERIMENTS

We have performed experimental results of the proposed methods to the mobile robot . The vehicle carries on-board a heterogeneous configuration of ultrasonic sensors. It is presented two kinds of experiment including general perception and application of fuzzy perception.

In this, instead of a typical ring of identical sonars, there are 12 sonars of three different types, placed at different locations. Six of them are large-range sensors (1.0–2.6m), four are mid-range (0.5–1.0m), and the other two are of short-range (0.1–0.5m). Furthermore, these ultrasonic sensors use a higher frequency and have a narrower sonar beam than the commonly used sonars in these kinds of applications. The sensors are arranged in a way that six of them cover the front part of the vehicle and the other four cover its lateral sides.

4. CONCLUSIONS

We propose a new approach to control of mobile robot of trajectory following and fuzzy perception concept with a nonholonomic mobile robot.

Experimental results, of an application to control the autonomous vehicle, demonstrate the robustness of the proposed method.

REFERENCES

[1] R. Braunstingl, "Improving reactive navigation using perception tracking", *Robotics and Manufacturing, Recent Trends in Research and Applications*, Vol.6, pp 25-30, New York,1996.

[2] J.J. Leonard, H.F. Durrant-Whyte, "Directed Sonar Sensing For Mobile Robot Navigation", Kluwer Academic Publishers, pp 147-155, 1992.

[3] A. Ollero, A. Garcia-Cerezo, J.L. Martinez, A. Mandow, "Fuzzy tracking methods for mobile robots", Prentice-Hall, pp 347-364, 1997.

[4] Ollero, G. Ulivi, F. Cuesta, "Fuzzy logic applications in mobile robotics", Kluwer Academic Publishers, pp. 301–324, 1999.

2017 Changwon International Conference on Intelligent Robot and Convergence Industry (CICIRO 2017)
Nov. 30th~ Dec. 1st, 2017, Changwon Exhibition Convention Center(CECO), Changwon City, Korea

A Real-Time Control for Precise Walking of Biped Robot

Jeong-Chul Moon1, In-Man Park2, and Sung-Hyun Han3

[1] Navy Shipyard, Changwon, Korea(thanggl@naver.com)
[2] Intem Co., Ltd., Changwon, 642-370, Korea (intem237@hanmail.net)
[3] School of Mechanical Engineering, Kyungnam University, Changwon, 51767, Korea (E-mail: shhan@kyungnam.ac.kr)

Abstract: This paper deals with the stable walking for a biped robot, on uneven terrain, A biped robot necessitates achieving posture stabilization since it has basic problems such as structural instability. In this paper, a stabilization algorithm is proposed using the ground reaction forces, which are measured using FSR (Force Sensing Resistor) sensors during walking, and the ground conditions are estimated from these data. From this information the robot selects the proper motion pattern and overcomes ground irregularities effectively. In order to generate the proper angel of the joint. The performance of the proposed algorithm is verified by simulation and walking experiments on a 24-DOFs biped robot.

Keywords: Force sensing resistor, fuzzy algorithm, biped robot, stabilization

1. INTRODUCTION

In this paper, a real-time walking stabilization method utilizing a fuzzy algorithm under uneven terrain is proposed. We focused most of our interest on landing phase. The ground reaction forces, measured by FSR sensors on the sole, are used to assess the ground condition and the robot posture. Simulation and experiment results for the proposed method are given in Section 3, followed by conclusions in the final section.

2. STABILIZATION

2.1 Walking pattern

Basically, a robot walks with the trajectory generated previously assuming even terrain. If different values from the expected sensor are measured during walking, the robot should be deployed using the stabilization algorithm. Fig.1 presents the walking algorithm.

When the robot is walking, it measures the ground reaction forces in real-time and utilizes them as inputs to the controller. When the control of the robot is interrupted by an unexpected situation or a unit step has ended, the new trajectory should be generated according to the changed situation. The newly verification based on the ZMP criterion. Once the stability of the trajectory is guaranteed, the robot becomes able to resume the walking.

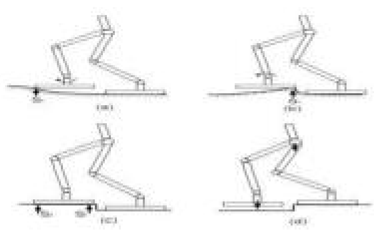

Fig. 1 The walking irregular ground condition.

2.2 Stabilization algorithm

In order to ensure that the robot walks stably, the motion should basically be stable and smooth. In addition, the robot must be able to detect approaching situations, and to control itself accordingly. When this control concept is applied, the robot is able to walk stably coping with unexpected external disturbances.

A robot can face unexpected situations during walking such as projecting ground, depressed ground, and projected ground as described in Fig.1.

3. STABILIZATION

3.1 Biped robot and sensor system

The second part consisting of the paper body must be edited in the double column format, with each column 80mm width and separated by 10mm. The top-level heading, usually called section, numbered in Arabic numerals, shall appear centered on the column with Times New Roman capital bold 11pt. The numbered level-two heading starts from the left in Times New Roman bold 10pt font. The main text uses Times New Roman 10pt font with single spacing. New paragraphs indent 4mm on the first line.

The simulation is based on a biped robot. The robot has a height of about 950mm, a weight of roughly 35kg, and 24 DOFs. The robot determines a walking pattern using the ground reaction forces measured from the sole.

The robot measures these forces using FSR sensors fixed at the sole, and the obtained data is employed as the input of the stabilization algorithm. FSR sensors are generally used for measuring the dynamic force by the variation of resistance in the force or pressure acting on the surface. FSR sensors are economical, thin, light, and easy to use. In addition, Moving-Average Filter is applied to reduced influence of the disturbance by sensor noise. Equation (1) shows the Moving-Average Filter.

$$R(n) \frac{\sum_{i=0}^{k} f(n-i)}{k}$$

The robot measures these forces using FSR sensors fixed at the sole, and the obtained data is employed as the input of the stabilization algorithm. FSR sensors are generally used for measuring the dynamic force by the variation of resistance in the force or pressure acting on the surface. FSR sensors are economical, thin, light, and easy to use. In addition, Moving-Average Filter is applied to reduced influence of the disturbance by sensor noise. Equation (1) shows the Moving-Average Filter.

In (1) k, and R(n) are the raw sensor data at n time, orders of filter, and filtered data, respectively.

Four sensors are equipped at 4 corners of each foot. In order to minimize impact and deformation, and also to distribute repulsive power, the sole is composed of a bakelite plate and a rubber plate. The sensors are fixed between the two plates.

The robot walks according to a basic trajectory. In basic walking, a stride is 0.12m, velocity is 0.04m/s, and the ground is regarded as being flat. The robot steps on projected ground of 11mm in height with the tie if the swing leg. When the control algorithm is not applied, the sensor data is presented as given in Fig.2, The robot pushes the ground continuously, and the heel does not contact until the end of the stride.

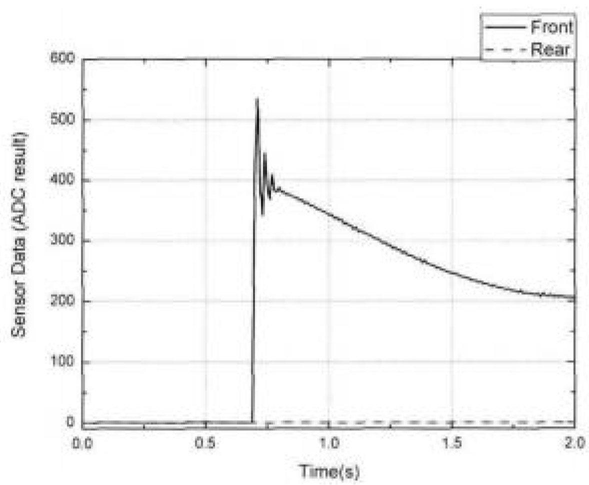

Fig. 2 FSR sensor data for uneven terrain

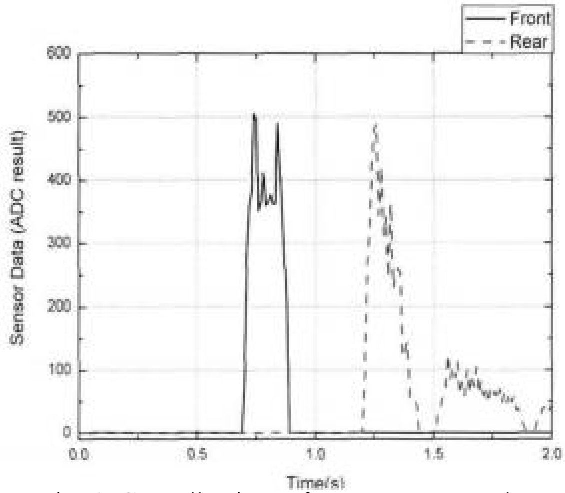

Fig. 3 Controller input for constant control.

4. CONCLUSION

This paper described a real-time control technology to implement the walking of a biped robot on uneven terrain. It was assumed that the ground condition on the basis of ground reaction forces measured sensors on the soles of the feet during walking. The robot could maintain balanced walking through control of the ankle joints using a fuzzy algorithm.

REFERENCES

[1] M. Vukobratovic and D. Juricic, "Contribution to the synthesis of biped gait," IEEE Trans. on Bio-Medical Engineering, vol. 16,pp. 1-6, 1969.

[2] K. Nishiwaki, S. Kagami, Y. Kuniyoshi, M. Inaba, and H. Inoue, "Online generation of humanoid walking motion based on a fast generation method of motion pattern that follows desired ZMP," *Proc. of IEEE/RSJ Int. Conf. on Intelligent Robots and System*, vol. 3, pp. 2684-2689,2002.

[3] D. Djoudi and C. Chevallereau, "Stability analysis of a walk of a biped with control of the ZMP," *Proc. of IEEE/RSJ Int. Conf. on Intelligent Robots and Systems*, pp. 2461-2467, 2005..

2017 Changwon International Conference on Intelligent Robot and Convergence Industry (CICIRO 2017)
Nov. 30th~ Dec. 1st, 2017, Changwon Exhibition Convention Center(CECO), Changwon City, Korea

A Robust Neural Network Control of Robot Manipulator for Industrial Application

Eun-Taek Ju[1], Woo-Song Lee[2], and Sung-Hyun Han[3]
[1] TESSCo., Ltd, Changwon, Korea (legna911@naver.com)
[2] SUNJIN Technology Co., Ltd., Changwon, 82331, Korea (elflws@nate.com)
[3] School of Mechanical Engineering, Kyungnam University, Changwon, 51767, Korea (shhan@kyungnam.ac.kr)

Abstract: In this paper, we present two kinds of robust control schemes for robot system which has the parametric uncertainties. In order to compensate these uncertainties, we use the neural network control system that has the capability to approximate any nonlinear function over the compact input space. In the proposed control schemes, we need not derive the linear formulation of robot dynamic equation and tune the parameters. We also suggest the robust adaptive control laws in all proposed schemes for decreasing the effect of approximation error. To reduce the number of neural of network, we consider the properties of robot dynamics and the decomposition of the uncertainty function. The proposed controllers are robust not only to the structured uncertainty such as payload parameter, but also to the unstructured one such as friction model and disturbance. The reliability of the control scheme is shown by computer simulations and experiment of robot manipulator with 8 axis.

Keywords: Tracking control, decomposition, neural network, robot dynamics, uncertainty

1. INTRODUCTION

In the recent decade, increasing attention has been given to the tracking control of robot manipulators. Tracking control is needed to make each joint track a desired trajectory. A lot of research has dealt with the tracking control problem: [1]–[4] were based on VSS (variable structure system) theory, [5]–[10] on adaptive theory, and [11]–[12] on Fuzzy logic. Robots have to face many uncertainties in their dynamics, in particular structured uncertainty, such as payload parameter, and unstructured one, such as friction and disturbance. It is difficult to obtain the desired control performance when the control algorithm is only based on the robot dynamic model. To overcome these difficulties, in this paper we propose the adaptive control schemes which utilize a neural network as a compensator for any uncertainty. To reduce the error between the real uncertainty function and the compensator, we design simple and robust adaptive laws based on Lyapunov stability theory. In the proposed control schemes, the NN compensator has to see many neural because uncertainties depend on all state variables. To overcome this problem, therefore, we introduce the control schemes in which the number of neural of the NN compensator can be reduced by using the properties of robot dynamics and uncertainties. By computer simulations, it is verified that the NN is capable to compensate the uncertainties of robot manipulator. This paper is organized as follows. Section 2 presents NN System. In Section 3, several properties of robot dynamics are introduced. In Section4, the adaptive control scheme is proposed, where the NN is utilized to compensate the uncertainties of the robot manipulator. The robust adaptive law is also designed. The algorithms that reduce the number of neural are proposed based on the properties of robot dynamics and uncertainties in Section 5. The decomposition algorithm of uncertainty function and results of computer simulations for the control scheme and experiment on dual-arm robot are also drawn in Section 6. In Section 7, we obtain the conclusions and discussion.

2. CONTROLLER DESIGN

2.1 Multiple Layers of Neurons

A network can have several layers. Each layer has a weight matrix ***W***, a bias vector ***b***, and an output vector ***a***. To distinguish between the weight matrices, output vectors, etc., for each of these layers in the figures, the number of the layer is appended as a superscript to the variable of interest. You can see the use of this layer notation in the three-layer network shown below, and in the equations at the bottom of the figure.

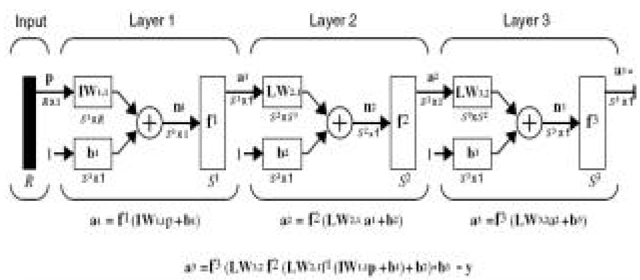

Fig. 1. MLP neural network

2.2 Dynamic, Nonlinear MLP Neural Network

This neural network consist of a number of layers and delay. The input and output of this network is dynamic and nonlinear.

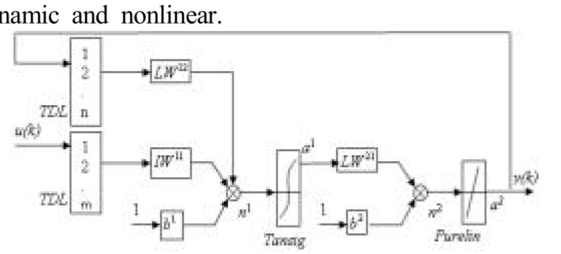

Fig. 2. Structure of dynamic, nonlinear neural network

To create adaptive characteristic for neural network controller, we design a neural network compensator following equation below:

$$y = \Theta^T \xi(x) \quad (1)$$

Where $\xi(x)$ is output of neural network and Θ is matrix of adaptive parameters

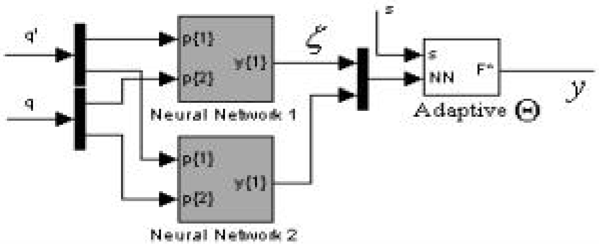

Fig. 3. The structure of adaptive neural network

3. DYNAMIC MODELING AND CONTROL OF ROBOT SYSTEM

A robot manipulator is defined as an open kinematic chain of rigid links. Each degree of freedom of the manipulator is powered by independent torques. Using the Lagrangian formulation, the equations of motion of an -degree-of-freedom manipulator can be written as

$$D(q)\ddot{q} + C(q,\dot{q})\dot{q} + G(q) + F_r(\dot{q}) + \tau_d = \tau \quad (2)$$

where $q \in R^n$ is the generalized coordinates; $D(q) \in R^{n \times n}$ is the symmetric, bounded, positive-definite inertia matrix; vector $C(q,\dot{q})\dot{q} \in R^n$ presents the centripetal and Coriolis torques; $\tau_d \in R^n$, $G(q) \in R^n$, $F_r(\dot{q}) \in R^n$ and $\tau \in R^n$ represent the gravitational torques, friction, disturbance, and applied joint torques, respectively.

The robot model (2) is characterized by the following structural properties.

Property 1: There exists a vector $\varphi \in R^m$ with components depending on manipulator parameters (masses, moments of inertia, etc.), such that

$$D(q)\ddot{q}_r + C(q,\dot{q})\dot{q}_r + G(q) + F_r(\dot{q}) + \tau_d = \Phi(q,\dot{q},\dot{q}_r,\ddot{q}_r)\varphi \quad (3)$$

where $\Phi(q,\dot{q},\dot{q}_r,\ddot{q}_r) \in R^{n \times m}$ is called the regressive matrix.

This property means that the dynamic equation can be linearized with respect to a specially selected set of manipulator parameters.

Property 2: Using a proper definition of matrix $C(q,\dot{q})$, both $C(q,\dot{q})$ and $D(q)$ are not independent and satisfy

$$x^T(\dot{D} - 2C)x = 0, \quad \forall x \in R^n \quad (4)$$

that is, $(\dot{D} - 2C)$ is a skew-symmetric matrix.

This property is simply a statement that the so-called fictitious forces, defined by $C(q,\dot{q})\dot{q}$, do not work on the system. This property is utilized in stability analysis.

Property 3: The friction in the dynamic equation (2) is of the form

$$F_r(\dot{q}) = F_v\dot{q} + F_d(\dot{q}) \quad (5)$$

with F_v the coefficient matrix of viscous friction and $F_d(\dot{q})$ a dynamic friction term. Since friction is a local effect, $F_r(\dot{q}) = F_v\dot{q} + F_d(\dot{q})$ is uncoupled among the joints. The friction is dependent on only angular velocity $\dot{q}$.

This property is utilized in this paper in order to reduce the number of neural in the neural network compensator.

The considered tracking problem is stated as follows: Knowing desired trajectories $q_d \in R^n$, $\dot{q}_d \in R^n$, with some or all the manipulator parameters unknown, determine a control law τ and a sliding surfaces $s = 0$ such that sliding mode occurs on the sliding surface, the tracking error $\tilde{q} = q - q_d$ has a prescribed transient response and it goes to zero asymptotically as $t \to \infty$.

A. Simple Adaptive Control Law

The sliding surfaces $s = 0$ is chosen as a hyperplane

$$s = \dot{\tilde{q}} + \Lambda\tilde{q} \quad (6)$$

where Λ is a positive-definite matrix whose eigenvalues are strictly in the right-half complex plane and $\tilde{q}$ is the tracking error vector.

If the sliding mode exists on $s = 0$, then from the theory of VSS, the sliding mode is governed by the following linear differential equation whose behavior is dictated by the sliding hyperplane design matrix Λ:

$$\dot{\tilde{q}} = -\Lambda\tilde{q} \quad (7)$$

Obviously, the tracking error transient response is then determined entirely by the eigenvector structure of the matrix Λ.

In order to derive the sliding mode control law, which forces the motion of the error to be along the sliding surface $s = 0$, a vector of self-defined reference variables is introduced for the succinct formula expression in the sequel, that is,

$$\dot{q}_r(t) = \dot{q}_d(t) - \Lambda\tilde{q}(t) \quad (8)$$

Consider now the uncertainties of robot manipulator, (2) can be rewritten as

$$D(q)\ddot{q} + C(q,\dot{q})\dot{q} + G(q) + F(q,\dot{q},t) = \tau \quad (9)$$

Where $F(q,\dot{q},t) = F_r(\dot{q}) + \tau_d$. However, in this paper, this uncertainty function vector has to be replaced by $F(q,\dot{q},t)$

So (9) can be rewritten as

$$D(q)\ddot{q} + C(q,\dot{q})\dot{q} + G(q) + F(q,\dot{q},\ddot{q};t) = \tau \quad (10)$$

we let a Lyapunov function candidate be

$$V(t) = \frac{1}{2}\left(s^T D s + \sum_{i=1}^{n} \tilde{\Theta}_i^T \Gamma_i^{-1} \tilde{\Theta}_i\right)$$

Where $\tilde{\Theta}_i = \Theta_i - \Theta_i^*$, Θ_i^* is the j th column vector of the optimal parameter matrix Θ^* and Γ_i is a strictly positive real constant.

Differentiating $V(t)$ with respect to time yields

$$\dot V(t) = s^T D\dot s + \frac{1}{2} s^T \dot D s + \sum_{i=1}^{n} \dot{\tilde\theta}_i^T \Gamma_i \tilde\theta_i$$

$$= -s^T (D\ddot q_r + C\dot q_r + G + F - \tau) + \sum_{i=1}^{n} \dot{\tilde\theta}_i^T \Gamma_i \tilde\theta_i \quad (12)$$

Where $F(q,\dot q,\ddot q,t)$ is a completely unknown nonlinear function vector. Therefore, we replace $F(q,\dot q,\ddot q,t)$ by a Neural network $\hat F(q,\dot q,\ddot q|\theta)$. Let us define the control law as

$$\tau = D(q)\ddot q_r + C(q,\dot q)\dot q_r + G(q) + \hat F(q,\dot q,\ddot q|\theta) - K_D s \quad (13)$$

Where $K_D = diag(K_i)$, $K_i > 0$, $i = 1,2,...,n$, and

$$\hat F(q,\dot q,\ddot q|\theta) = \begin{bmatrix} \theta_1^T \xi(q,\dot q,\ddot q) \\ \theta_2^T \xi(q,\dot q,\ddot q) \\ \dots \\ \dots \\ \theta_n^T \xi(q,\dot q,\ddot q) \end{bmatrix} \quad (14)$$

Letting the optimal parameter matrix of the NN, we can define the minimum approximation error vector

$$w = F(q,\dot q,\ddot q,t) - \hat F(q,\dot q,\ddot q|\theta^*). \quad (15)$$

Therefore,

$$\dot V = -s^T K_D s - s^T w + \sum_{i=1}^{n} \left(\tilde\theta_i^T \Gamma_i \dot{\tilde\theta}_i - s_i \tilde\theta_i^T \xi(q,\dot q,\ddot q) \right) \quad (16)$$

where $\tilde\theta_i = \theta_i^* - \theta_i$ and $\xi(q,\dot q,\ddot q)$ is a neural network basis function. Therefore, the adaptation laws are

$$\dot\theta_i = -\Gamma_i^{-1} s_i \xi(q,\dot q,\ddot q), \; i = 1,2,...,n \quad (17)$$

Then

$$\dot V(t) = -s^T K_D s - s^T w \quad (18)$$

Because the term $s^T w$ is of the order of the minimum approximation error and from the universal approximation theorem, it is expected that w should be very small, i.e., $w \to 0$, if not equal to zero in the adaptive neural network system. The proposed control scheme is shown in Fig. 4.

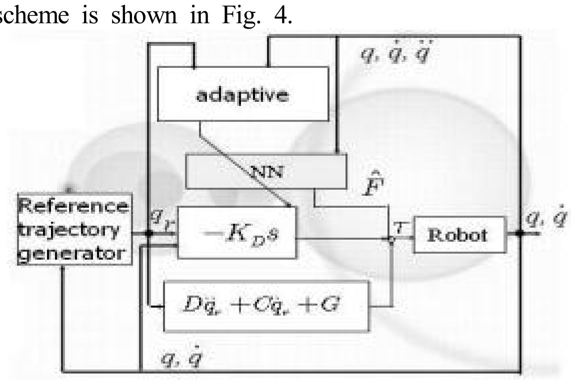

Fig. 4. the structure of the control systems

B. Robust Adaptive Control Law

Equation (16) contains the term $s^T w$; in this subsection, we propose the robust control law to reduce the approximation error. So we add a term to (13) as follows:

$$\tau = D(q)\ddot q_r + C(q,\dot q)\dot q_r + G(q) + \hat F(q,\dot q,\ddot q|\theta) - K_D s - W sign(s) \quad (19)$$

Where

$W = diag[w_{M1}, w_{M2}, w_{M3}, ..., w_{Mn}]$

$w_{Mi} \geq |w_i|$, $i = 1,2,....,n$

Now consider the Lyapunov candidate (11) as well as (17) and (19) and, after straightforward manipulation, we obtain the time derivative as follows:

$\dot V(t) = -s^T D s \leq 0$

A. Friction

From Section III, we can see that the friction is dependent on $\dot q$ and uncoupled among the joints.

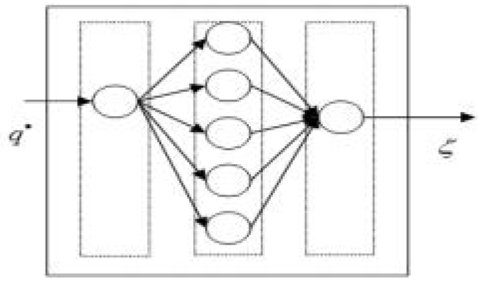

Fig. 5. The structure of a neural network as fiction compensator $\hat F(\dot q|\theta) = \theta^T \xi$

Simple Control Law:

$$\tau = D(q)\ddot q_r + C(q,\dot q)\dot q_r + G(q) + \hat F(\dot q|\theta) - K_D s \quad (20)$$

Robust Control Law:

$$\tau = D(q)\ddot q_r + C(q,\dot q)\dot q_r + G(q) + \hat F(\dot q|\theta) - K_D s - W sign(s) \quad (21)$$

Adaptive Law:

$$\dot\theta_i = -\Gamma_i^{-1} s_i \xi(\dot q), \; i = 1,2,...,n \quad (22)$$

B. Disturbance

From (7), considering only disturbance, $F(q,\dot q, \ddot q)$, the resulting control and adaptive laws are as follows.

Simple Control Law:

$$\tau = D(q)\ddot q_r + C(q,\dot q)\dot q_r + G(q) + \hat F(q,\dot q,\ddot q|\theta) - K_D s \quad (23)$$

Robust Control Law:

$$\tau = D(q)\ddot q_r + C(q,\dot q)\dot q_r + G(q) + \hat F(q,\dot q,\ddot q|\theta) - K_D s - W sign(s) \quad (24)$$

Adaptive Law:

$$\dot\theta_i = -\Gamma_i^{-1} s_i \xi(q,\dot q,\ddot q), \; i = 1,2,...,n \quad (25)$$

Therefore we use the structure of the neural network as friction, disturbance compensator following:

4. EXPERIMENT AND RESULTS

We also apply real-time adaptive control based on neural network compensator to dual-arm robot shown in figs. 6 – 8. Because the characteristics of two arms are the same, so we show the results into one arm is enough.

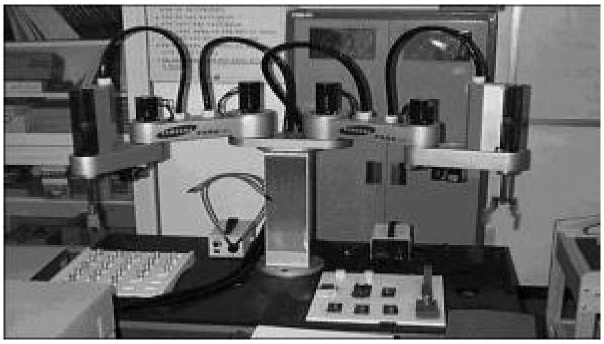

Fig. 6. Experimental set-up

All the algorithm calculation is calculated by Matlab and Simulink matlab on host computer and push into dual-arm robot which is shown in the Fig. 7. The desired trajectories are

$q_{1d} = q_{2d} = 15\pi \sin\left(\frac{2\pi}{300\pi} t - \frac{2\pi}{3}\right)$ and the

results of robust adaptive control are shown below

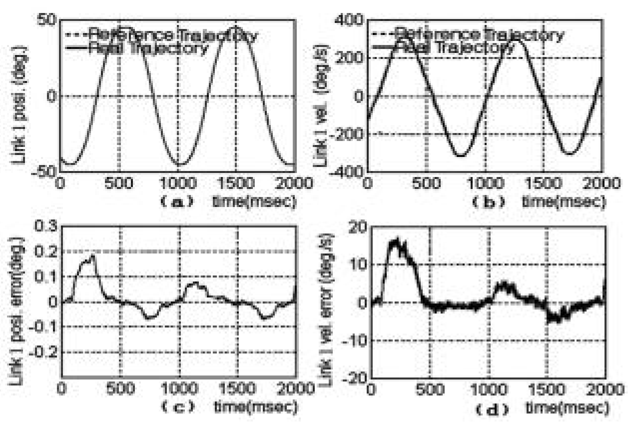

Fig. 7. (a)-(d) Experimental results for the position and velocity tracking of adaptive controller at the first joint.

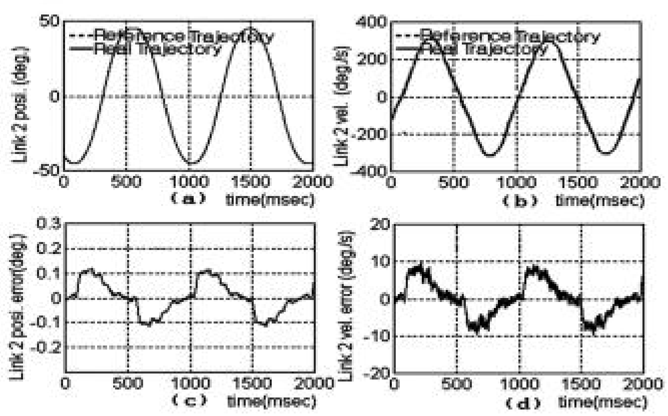

Fig. 8. (a)-(d) Experimental results for the position and velocity tracking of adaptive controller at the second joint.

7. CONCLUSIONS

In the results, we can see that the control objective is well accomplished and the neural network compensate the uncertainties. Especially, we observe that Fig. 10. is more better than Fig. 11. Because the robust control laws have the signum function $W\ \mathrm{sgn}(s)$. In all cases, robust control schemes are more effective than simple. The simulation and experimental results show that the neural network compensator - adaptive controller is robust to the payload variation, inertia parameter uncertainty and change of reference trajectory.

In addition, the proposed control technology needs to apply to robot manipulators include more joints, and degree of freedom. The research continues on the more general algorithms of the number and structure of neural network and it should be studied further for standard specification in manufacturing process.

REFERENCES

[1] G. Jumarie, "Tracking control of mechanical systems via sliding Lagrangian," J. Intell. Robotic Syst., vol. 13, pp. 181–199, 1995.

[2] C. Y. Su and T. P. Leung, "A sliding mode controller with bound estimation for robot manipulators," IEEE Trans. Robotics Automat., vol. 9, no. 2, pp. 208–214, 1993.

[3] J. E. Slotin and S. S. Sastry, "Tracking control of nonlinear systems using sliding surfaces, with application to robot manipulators," Int. J. Contr., vol. 38, no. 2, pp. 465–492, 1983.

[4] J. J. E. Slotine and W. Li, Applied Nonlinear Control. Englewood Cliffs, NJ: Prentice-Hall, 1991.

[5] F. L. Lewis, C. T. Abdallah, and D. M. Dawson, Control of Robot Manipulators. London, U.K.: Macmillan, 1993.

[6] M. W. Spong, Robot Dynamics and Control. New York: Wiley, 1989.

[7] W. C. Ham, "Adaptive nonlinear control of one-link flexible arm," in IEEE/RSJ Int. Conf. Intelligent Robots and Systems, vol. 1, Yokohama, Japan, 1993, pp. 3–7.

[8] "Adaptive control based on explicit model of robot manipulators," IEEE Trans. Automat. Contr., vol. 38, pp. 654–658, 1993.

[9] "Adaptive control based on speed gradient algorithm for robot manipulators," in Int. Conf. Industrial Electronics Control and Instrumentation, vol. 2, Bologna, Italy, 1994, pp. 776–781.

[10] B.K. Yoo, W.C. Ham "Adaptive Control of Robot Manipulator Using Fuzzy Compensator". IEEE transaction on Fuzzy System. VOL. 8. NO. 2. April 2000.

2017 Changwon International Conference on Intelligent Robot and Convergence Industry (CICIRO 2017)
Nov. 30th~ Dec. 1st, 2017, Changwon Exhibition Convention Center(CECO), Changwon City, Korea

A Study on Grasping Control of Hand Fingers 12 Joints

Jae-Jong Kim[1], In-Man Park[2], Hyun-Suk Sim[3]
and Sung-Hyun Han[4]

[1] Navy munitions situation,Changwon, Korea (1975kjj@hanmail.net)
[2] Intem Co., Ltd., Changwon, 642-370, Korea
(intem237@hanmail.net)
\[3] DongSan Tech Co., Ltd., Haman, 637-821, Korea
(hs8388@dscast.co.kr)
[4] School of Mechanical Engineering, Kyungnam University,
Changwon, 51767, Korea (shhan@kyungnam.ac.kr)

Abstract: Recently it is very important to control robot hands more compact and integrated sensors in order to increase compensate the grasping capability and to reduce cabling through the finger in the manipulator. As a matter of fact, the miniaturization and cabling harness represents a significant limitation to the design of small sized precise sensor. The main focus of this research is on a flexible grasping control of hand fingers, which consists of a flexible multi-fingered hand-arm system.

Keywords: Grasping Control, Hand Finger, Precise Sensing, Hand Design

1. INTRODUCTION

Recently Manipulation capability is important for a robot. Interaction between a robot hand and objects can be properly controlled only is suitable sensors are available. In particular, information about the forces applied at the contact, the contact location, other indirect measurements, e.g. estimate of mass object, its inertia ellipsoid, or even non mechanical measurements, may play a crucial role to implement secure grasp and safe manipulation tasks. In the past two decades several robot hands and dexterous grippers have been developed. The major goals have been on one hand that of studying and implement newer mechanical solutions in order to increase miniaturization and dexterity, and, on the other, to investigate manipulation models and control techniques. At mechanical level study on dextrous grippers has mainly focused on the actuation and kinematics aspects.

Actuation of tendon based robot grippers poses various technical problems. Tendons coupling on one hand, friction and elasticity on the other, pose important problems for the control of tendon actuated mechanisms. However, the mechanical accuracy required to design a miniature (e.g. human sized) dexterous gripper, is by far less than an equivalent design based on gears or other stiff transmission mechanism. Recently the tendency is to create robot hands more compact and high integrated sensors system, in order to increase the grasping capability and in order to reduce cabling through the finger, the palm and the arm. As a matter of fact, miniaturization and cabling harness represents a significant limitation to the design of small sized embedded sensor.

2. SYSTEM DESIGN

The mechanism of a flexible hand gripper requires the mass of the hand should be as low as possible. It is highly desirable that the hand weigh less than 1kg. Furthermore the low mass of the finger mechanism is desirable not only to achieve flexible motion but also for stable control.

Our philosophy about dynamic manipulation is maximization of the power and minimization of the mechanism. In particular four factors are important: (1)light weight, (2) high speed and high acceleration, (3) accuracy, (4) possibilities of flexible grasping.

The finger has strain gauges at the joint 1 and joint 2 for force control. In addition a 6-axis force/torque sensor and a tactile sensor are mounted on each fingertip.

The flexible motion imposes a heavy load on the finger mechanism. For this reason a simple mechanism should be used for reduction gear, transmission, etc. In most traditional hand systems a wire-driven mechanism is used. But this is not suitable for a lightweight mechanism, because it is large and complicated.

In our hand a newly developed small harmonic drive gear and a high-power mini actuator are fitted in each finger link and all of these parts are hidden in the plastic case. A harmonic drive gear has desirable properties for control such as no backlash and a high reduction rate.

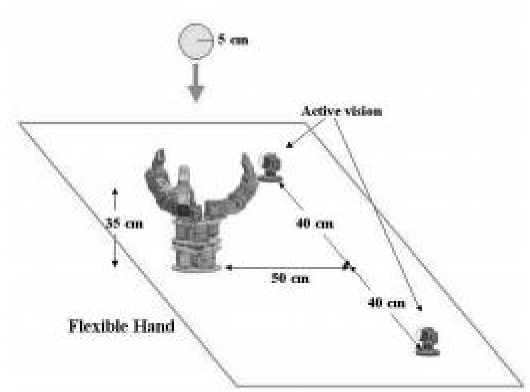

Fig. 1. Visual feedback control system

Following the purpose of this paper; we discus about the system set up in Fig. 1. Vision is with a massive parallel vision system called column-parallel high-speed vision system.

Early image processing is performed in order to achieve segmentation of the image, extraction of the target area, and computation of the image moments. From these data, the position of the target is computed; each vision sensor is mounted on an active vision.

The tactile transducer is a matrix of 64 electrodes covered by a layer of pressure sensitive conductive rubber (PCR Co. Ltd.). The electrodes are etched on a flexible PCB substrate in order to conform to a cylindrical surface. A thin elastic sheet covers the whole sensor and provides a mild preload useful to reduce noise. Pressure due to contacts produces changes of resistance among the electrodes. The geometry of the electrodes Fig. 1, has been defined with the goal of limiting the spurious currents that may occur across the various electrodes, and interfere with measurement, as discussed in.

Tactile data are sampled by the on-board MCU, with 10 bit resolution. Preliminary tests show an actual sensor resolution of 8 bit/taxel. Each tactile image consists of 64 taxels.

During contact, a number of adjacent taxels are subject to pressure. The analog output of the tactile sensor allows to measure the distribution of pressure over all the transducer. Therefore, we propose to compute the contact centroid , as

$$\hat{C} = \frac{\sum_{i=1}^{N}\sum_{j=1}^{N} x_{ij}.p(x_{ij})}{\sum_{i=1}^{N}\sum_{j=1}^{N} p(x_{ij})} \qquad (1)$$

where $\hat{\mathbf{C}}$ is the computed contact centroid, $\mathbf{x}_{ij}$ is the coordinate of the taxel and $p(\mathbf{x}_{ij})$ the weight of this. As a matter of fact further geometric information about the distribution of the pressure during contact could be useful, although not directly relevant to point contact model solution. To this aim the pressure distribution is approximated as an ellipsoid, as follows:

$$E = \frac{\sum_{i=1}^{N}\sum_{j=1}^{N}(x_{ij}-\hat{C})(x_{ij}-\hat{C})^{T}.p(x_{ij})}{\sum_{i=1}^{N}\sum_{j=1}^{N} p(x_{ij})} \qquad (2)$$

Where **E** is a symmetric matrix who represent the ellipsoid. The approach used to compute and the associated approximate ellipsoid, is strongly based on the availability of an analog tactile sensor.

3. EXPERIMENT

Catching is one of the most important tasks for dynamic manipulation. In this section catching is shown using our flexible hand with a visual feedback controller. We used a rubber ball with radius of 5cm as a target, and we dropped it from about 1.2m in height. The speed of the falling ball is about 5.9m/s just before it hits the ground.

Table. 1. The specification of robot hand.

Total D.O.F	12
Weight [g]	700
Max. Speed at a finger tip [m/s]	3.5
Max. force at a finger tip [N]	30
Joint resolution [deg]	0.4

The catching tasks for the ball are:
- Approaching (0~40ms)
- Locking (40~50ms)
- Rebounding (50~60ms)
- Holding (60ms~).

From various experimental trials, we have decided on the catching strategy shown in Fig. 2.

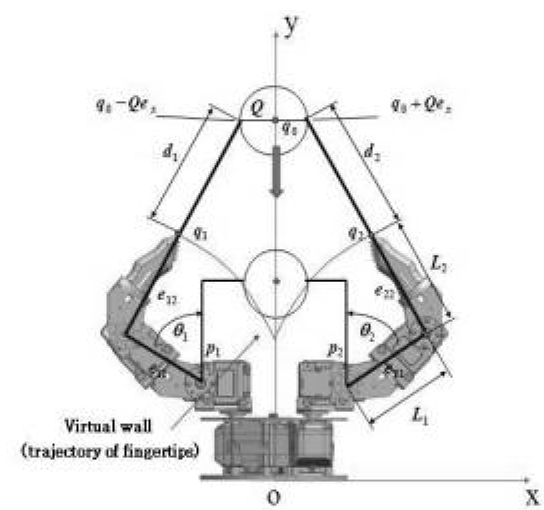

Fig. 2. The coordinates system for catching algorithm of grasping.

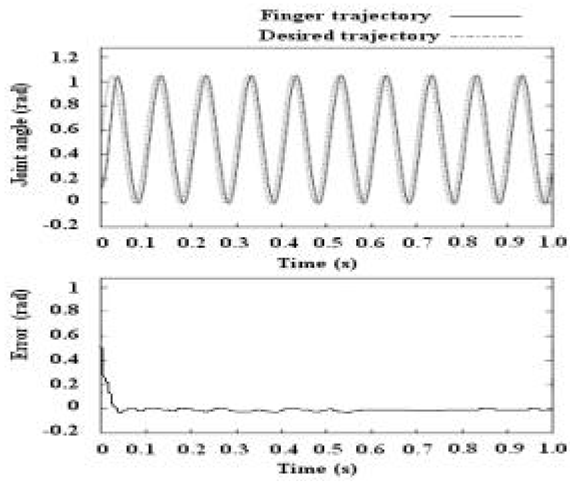

(a) Result for sine wave input trajectory

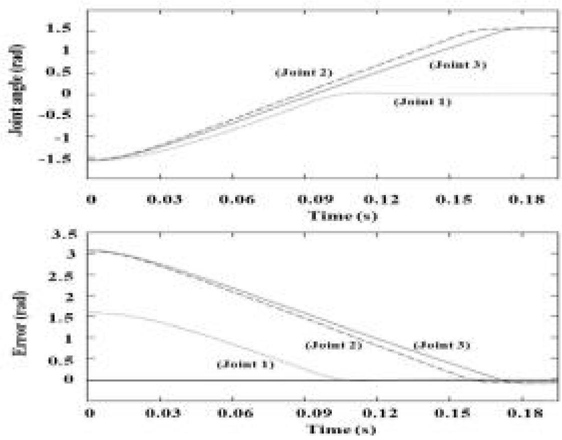

(b) Result for the step input trajectory

Fig. 3. Result of performance test for finger trajectory tracking

Fig. 3 shows the results when we changes the target position q_o and Fig. 8 when we changes the distance d1 and d2, (X-Y axis, q_o, d1 and d2 were defined in fig. 3.)

4. CONCLUSION

An integrated force and tactile sensor with embedded electronics has been presented in a lightweight flexible hand with 12 D.O.F, and the associated visual feedback control. The sensor consists of a three components commercial force sensor and of a custom matrix tactile sensor based pressure sensitive conductive rubber.

The need for a robotic hand that works in the real world is growing. And such a system should be able to adapt to changes in environment. We think that the concept of a flexible hand system with real-time control implementation will become an important issue in robotic research.

REFERENCES

[1] S.C.Jacobsen, E.K. Iversen, D.F. Knutti, R.T. Johnson andK.B. Biggers, “Design of the Utah/MIT dexterous hand”, Proc. IEEE Int. Conf. On Robotics and Automation, pp. 1520-1532, 1986

[2] Anotonio Bicchi, J. Kennedy Salisbury, David L. Brock ”Contact Sensing from Force Measurements” International Journal of Robotics Research. Vol. 12, No. 3, June 1993.

[3] S. Toyama, S. Hatae and S. Sugitani, “Multi-Degree of spherical ultrasonic motor”, Proc. ASME Japan/USA Sympo. Flexible Automation, 169, 1992

[4] Gongliang Guo, William A. Gruver, ”A new design for a dexterous robotic hand mechanism” IEEE Control Systems Magazine, v 12, n 4, Aug, 1992, p 35-38.

[5] Hideaki Hashimoto, Hideki Ogawa, Toshiya Umeda, Masao Obama Kyoichi Tatsuno, ”An Unilateral Master-Slave Hand System with a Forcecontrolled Slave Hand” IEEE International Conference o Robotics andAutomation 1995.

2017 Changwon International Conference on Intelligent Robot and Convergence Industry (CICIRO 2017)
Nov. 30- Des.1, 2017, Changwon Exhibition Convention Center(CECO), Changwon, Korea

A Study on Intelligent Control of Bipped Robot by Voice Command

Chang-Keun Oh[1], Woo-Song Lee [2] and Sung-Hyun Han[3]
[1] KyeongWon Industry Co., Ltd.,51402, Korea (ock38317@naver.com)
[2] SUNJIN Technology Co., Ltd., Changwon, 82331, Korea
(elflws@nate.com)
[3] School of Mechanical Engineering, Kyungnam University,
Changwon, 51767, Korea (shhan@kyungnam.ac.kr)

Abstract: Generally, it is possible to control the walking information based on the bipped robot's own postures, because a type of motion and gesture produces almost the same pattern of noise every time. In this paper, we describe an voice recognition control technology for bipped robot system which can robustly recognize voice by adults and children in noisy environments. We evaluate the performance of robot control system in a communication robot placed in a real noisy environment. Voice is captured using a wireless microphone. To suppress interference and noise and to attenuate reverberation, we implemented a multi-channel system consisting of an outlier-robust generalized side-lobe canceller technique and a feature-space noise suppression using criteria. Voice activity periods are detected based end-point detection

Key words: Robust voice recognition, Side-lobe canceller, navigation system

1. INTRODUCTION

To make human-robot communication natural, it is necessary for the robot to recognize voice even while it is moving and performing gestures. For example, a robot's gesture is considered to play a crucial role in natural human-robot communication [1-3]. In addition, robots are expected to perform tasks by physical actions to make a presentation. If the robot can recognize human interruption voice while it is executing physical actions or making a presentation with gestures, it would make the robot more useful.

Each kind of robot motion or gesture produces almost the same noises every time it is performed. By recording the motion and gesture noises in advance, the noises are easily estimated. By using this, we introduce a new method for VRCS under robot motor noise. Our method is based on three techniques, namely, multi-condition training, maximum-likelihood linear regression[5], and missing feature theory. These methods can utilize pre-recorded noises as described later. Since each of these techniques has advantages and disadvantages, whether it is effective depends on the types of motion and gesture. Thus, just combining these three techniques would not be effective for voice recognition under noises of all types of motion and gestures. The result of an experiment of isolated word recognition under a variety of motion and gesture noises suggested the effectiveness of this approach.

2. CONTROLSCHEME

The proposed robot system has three wheels; two driven wheels fixed at both sides of the mobile robot and one castor attached at the front and rear side of the robot. The ultrasonic sensors are mounted around of the mobile robot in middle layer for the detection of obstacles with various heights. In this study, a sonar array composed of 16 ultrasonic sensors cannot be fired simultaneously due to cross talk. Instead, we adopt a scheduled firing method where sensors are activated in sequence of $\{s_1, s_{12}, s_2, s_{11} \ldots\}$. The arrangement of the ultrasonic sensors in upper layer and the sensors are marked as dots in the figure. The distances e_j $(j = 1, 2, \ldots 12)$ from the origin of the robot frame {R} to obstacles detected by the sensor s_j, can be defined as $e_j = \square_j + R_r$. Here, R_r is the radius of the robot and the $\square_j$, is the range value measured by the sensor s_j .

A local map is introduced to record the sensory information provided by the 16 sonar sensors with respect to the mobile robot frame $\{R\}$. Sector map defined locally at the current mobile robot frame is introduced. Then, the obstacle position vector se'_j with respect to the frame $\{R\}'$ can be calculated by

$$Se'_j \square \begin{bmatrix} \cos\square & \sin\square & 0 & \square\sin\square / \square_p \\ \square\sin\square & \cos\square & 0 & (1\square\cos\square)/\square_p \\ 0 & 0 & 1 & 0 \\ 0 & 0 & 0 & 1 \end{bmatrix} \tag{1}$$

where se_j denotes the obstacle position vector defined at the frame $\{R\}$. When the mobile robot is located at a point $0'$. the distance value $se'_j = \| se'_j \|$ from the origin of the frame $\{R\}'$ to the obstacle and angle $s\varphi'$ can be calculated by Eq.(1) . Here, $\|.\|$ denotes Euclidean norm.

The local map defined at the frame $\{R\}'$ is newly constructed by using the previous local map defined at the frame $(R\}$ as follows:

$$Se_n \star Se'_{j,n} \square INT\left(\frac{se'_j}{e}\right) \square \frac{N}{2} ; \; j \square 1,2,\ldots, N \tag{2}$$

Where $\leftarrow$ and INT denote the updating operation and integer operation, respectively. Here, se_n, denotes the

distance value of n sector and N represents the number of the sector. If the range values obtained by sensors when the mobile robot is located at a point o' are e_j = (j = 1,2 ,... *12*) , the new local map is partially updated as follows :
$se_j \leftarrow e_j$, j = 1,2 .... *12.* The maximum range of the sonar sensor is set to be $\Omega_{max} = \Omega_{max} - R_r$. Any return range which is larger than is ignored.

The primitive behaviors may be divided as follows: goal-seeking behavior, ball-following behavior, keep-away behavior, free space explorer and emergency stop, etc. The output of a primitive behavior is defined by the vector.

$$u(t) = (v(t), \omega(t))^T = (v(t), w(t), T_{ms})^T \quad (3)$$

where t and T_{ms} denote the time step and the sampling time, respectively. Here, T denotes the transpose and $\omega(t)$ denotes the angular velocity of the robot.
We will divide the primitive behaviors into two basic: avoidance behavior and goal-seeking behavior.
The avoidance behavior is used to avoid the obstacles irrespective of the goal position, while the goal-seeking behavior is used to seek the goal position irrespective of obstacle location. Design of each behavior proceeds in following sequences;
(A) fuzzification of the input/output variables, (B) rule base construction through reinforcement learning, (C) reasoning process, (D) defuzzification of output variables.
In order for the mobile robot to arrive at the goal position without colliding with obstacles, we must control the mobile robot motion in consideration of the obstacle position X_{oi}, = (x_{oi}, y_{oi}) , the mobile robot position X = (x , y) and its heading angle θ with respect to the world coordinate frame {W} shown in Fig. 1.
In order to avoid the increase in the dimension of input space, the distance values d_i , (i = 1.2,3,4) are defined by

$$d_1 = \min(se_1, se_2, se_3)$$
$$d_2 = \min(se_4, se_5, se_6) \quad 4a$$
$$d_3 = \min(se_7, se_8, se_9) \quad 4b$$
$$d_4 = \min(se_{10}, se_{11}, se_{12})$$

θ_m([illegible]) denotes the orientation of a sector with the shortest range. We choose the input variables for avoidance behavior as θ_m and
$d_i = \|X_{0i} - X\|, (i = 1,2,3,4)$ for goal-seeking behavior as heading angle difference ψ and distance to goal $z = \|X_g - X\|$. The input linguistic variables d_i, ψ, θ_m and z are expressed by linguistic values (VN, NR, FR), (NB, NM, ZZ, PS, PM, PB), (LT, CT, RT) and (VN, NR, FR, VF), respectively Their membership functions are expressed .

3. EXPERIMENTS

The proposed robot has the maximum travel speed of 0.55 m/s and the maximum steering rate of 3.0rad/sec. Experiments are performed in an indoor with the first experiment for voice recognition without objects and second experiment for both of them: voice recognition and obstacles avoidance.
Through a series of the navigation experiments, it was observed that the heading angle error is a serious problem to the proposed robot depend on dead reckoning The large heading angle error almost resulted from the uncertain parameters when the mobile robot changes its direction Even if the wheel slippage occurs, the true position and heading angle of the mobile robot could be updated by two beacon pairs and consequently the mobile robot could arrive at the given goal position while avoiding the obstacles.

4. CONCLUSIONS

This paper proposed the integration of robust voice recognition and navigation system capable of performing autonomous navigation in unknown environments. In order to evaluate the performance of the overall system, a number of experiments have been undertaken in various environments.

REFERENCES

[1] M. Blanchet, J. Boudy, and P. Lockwood, “Environment adaptation for speech recognition in noise,” in Proc. of EUSIPCO-92, vol. VI,1992, pp. 391–394.

[2] R. P. Lippmann, E. A. Martin, and D. B. Paul, “Multi-style training for robust isolated-word speech recognition,” in Proc. of ICASSP-87. IEEE, 1987, pp. 705–708.

[3] J. Barker, M. Cooke, and P. Green, “Robust asr based on clean speech models: An evaluation of missing data techniques for connected digit recognition in noise,” in Proc. of Eurospeech-2001. ESCA, 2001, pp. 213–216.

[4] P. Renevey, R. Vetter, and J. Kraus, “Robust speech recognition using missing feature theory and vector quantization,” in Proc. Of Eurospeech-2001. ESCA, 2001, pp. 1107–1110.
S. Yamamoto, K. Nakadai, H. Tsujino, and H. Okuno, “Assessment of general applicability of robot audition system by recognizing three simultaneous speeches.” in Proc. of IEEE/RSJ International Conference on Intelligent Robots and Systems (IROS-2004). IEEE and RSJ, 2001, p. to appear.

2017 Changwon International Conference on Intelligent Robot and Convergence Industry (CICIRO 2017)
Nov. 30th~ Dec. 1st, 2017, Changwon Exhibition Convention Center(CECO), Changwon City, Korea

A Study on Real-Time Control of Intelligent Robot with Three Wheel

Moon-Kuen Cho[1], In-Man Park [2] and Sung-Hyun Han[3]

[1] HeeSu TechCo., Ltd, Korea (heesu0881@daum.net)
[2] Intem Co., Ltd., Changwon, 642-370, Korea
(intem237@hanmail.net)
[3] School of Mechanical Engineering, Kyungnam University, Changwon, 631-701, Korea
(Tel: +82-55-249-2624; E-mail: shhan@kyungnam.ac.kr)

Abstract: We propose a new approach to control of mobile robot of trajectory following and fuzzy perception concept with a nonholonomic mobile robot named ROBO-N. The main focus of this paper is obtaining a fuzzy perception of the environment in the design of each reactive behavior and solving the problem of behavior combination to implement a fuzzy behavior based control architecture. It should be remarked that, the proposed technique of the nonholonomic constraints are considered in the design of each behavior. Furthermore, in order to improve the capabilities of the intelligent control system and its practical applicability, teleoperation and planned behaviors, together with their combination with reactive ones, have been considered. Experimental results, of an application to control the ROBO-N Robot autonomous vehicle, demonstrate the robustness of the proposed method.

Keywords: Real-Time control, Ultrasonic Sensor, Fuzzy Controller, Non-holonomic Mobile Robot

1. INTRODUCTION

The real-time trajectory control is the process of determining and maintaining a path or trajectory to a goal destination. Autonomous mobile robots are required to navigate in more complex domains, where the environment is uncertain and dynamic. Autonomous navigation in these environments demands adaptation and perception capabilities. This paper describes improvements in the perception functions used in these kinds of robots. It should be noted that this is a nonholonomic vehicle with significant limitations in the reactive capabilities due to kinematic and dynamic constraints, and a few number of sensors and large blind sectors in between them, making autonomous navigation a nontrivial task. The methods presented in this paper have been conceived to deal with these limitations of conventional vehicles.

In addition, fuzzy perception can be used straightforward to perform the control of the mobile robot by means of fuzzy behavior-based scheme already presented in literature. The main differences of the proposed approach with respect to other behavior based methods are: 1 - The nonholonomic constraints are directly taken into account in the behaviors. 2 - The fuzzy perception itself can be used both in the design of each reactive behavior and to solve the problem of blending behaviors.

Hence, the fuzzy behavior-based control scheme presented in this research allows not only implement reactive behaviors but also teleoperation and planned behaviors, improving system capabilities and its practical application. Furthermore, in these behaviors, soft computing techniques play an important role to solve different problems.

2. ROBOT CONTROLTECHNOLOGY

The following considerations are based on a mobile robot with the three degrees of freedom of planar movement, x, y and θ. It is equipped with a ring of 12 ultrasonic sensors which are able to perceive vertical or nearly vertical planes. The number of sensors is irrelevant as long as there are no blind sectors between them. θ refers to the orientation of this ring of sensors and not to the orientation of the robot itself, which is of no importance for the wall following algorithm. With φ indicating the direction of movement the kinematics model of such a robot is described as follows:

$$dx = v\cos\varphi\, dt;\ dy = -v\sin\varphi\, dt;\ d\theta = \omega_\theta dt \qquad (1)$$

Since there is no modeling of the environment the absolute position of the robot does not matter. So there is no world frame used here and the kinematics model can be expressed instead as:

$$ds = v dt;\ d\varphi = \omega_\varphi dt;\ d\theta = \omega_\theta dt \qquad (2)$$

The speed v, the angular speeds ω_φ and ω_θ are used as control variables of the robot and generated by the fuzzy controller.

Perception of each ultrasonic sensor i of the mobile robot is assigned a vector ki. Its direction equals the orientation of the sensor´s axis and its length is a function of the distance di measured by this sensor:

$$k_i = \frac{d_{max} - d_i}{d_{max} - d_{min}} \qquad (3)$$

where dmin and dmax designate the shortest and longest distance respectively at which an object may be positioned to be reliably detected. ki is limited to 0 and

1 respectively

Since a vehicle with nonholonomic constraints cannot move itself in any direction at every time instant, it is interesting to weight the different perceptions according with the direction where the obstacle was detected. In other words, an obstacle is less important if it is placed at a location that cannot be reached by the mobile robot, but it is more dangerous if it is on a reachable position. This task can be accomplished by considering the perception angle (θ_i) in the computation of the perception function

$$k_i = f(d_s,\theta_i) = sat_{0,1}\left(\frac{d_{max}(\theta_i)-d_s}{d_{max}(\theta_i)-d_{min}(\theta_i)}\right) \tag{4}$$

where sat0,1(x) states for the saturation of x in the range [0, 1]. In this way, it is possible to assign different perceptions, i.e. different weights, to objects detected at the same distance relative to the mobile robot but at different directions. For example, perception function ki is obtained by using the nonlinear function

$d_{min}(\theta_i) = d_m(1+\delta)/(1+\delta\cos\theta_i)$, and $d_{max} = n d_{min}(\theta_i)$ (with n>1), in Eq. (4).

$$k_i = f(d_s,\theta_i) = sat_{0,1}\left(\frac{n d_m(1+\delta)-d_s(1+\delta\cos\theta_i)}{(n-1)d_m(1+\delta)}\right) \tag{5}$$

Furthermore, it is interesting to stress that the perception vector implies a fuzzy high level description of the environment, being independent of the type of range sensor used. So, it is possible to use different perception functions from Eq. 4 for each kind of sensor (laser, ultrasonic, infrared). Thus, sensor data fusion can be reduced to compute different vectors from the sensor measurements and to combine them to obtain the perception vector.

The previous perception can be updated as follows: consider a robot of arbitrary shape equipped with proximity sensors. Any such sensor may be located at a position U, with its axis pointing to the direction s

A frame r represents the robots position and orientation, x and θ, respectively, with respect to the world reference system w. The velocity υ of the reference point and the angular velocity $\omega_{r/w} = \dot{\theta}$ of the robot with respect to the fixed frame w, give the state of motion. Furthermore, the virtual perception coordinate system is assumed to be located at E, pointing to the direction of attention a1. Then, an object detected by a proximity sensor at a distance ds could be detected by a virtual sensor placed at E a distance d, and with an orientation θ with respect to the vehicle's direction of attention a1.

Now the virtual perception will be updated taking into account the robots motion as follows: considering a perception function k = f(d, θ) and the corresponding inverse perception function, d = g(k, θ), and carrying out some calculations, it can be shown that the derivatives of angle and length of the perception vector are given by (assuming g ≠ 0 and $\partial g/\partial k \neq 0$).

$$\dot{\theta} = \frac{1}{g}\left(\ldots\, \omega_{r/w}\, e\, r_1\cos(\ldots) - \ldots r_2\cos(\ldots)\right) - \omega_{r/w} - \omega_{a/r} \tag{6}$$

$$\dot{k} = \frac{1}{\partial g/\partial k}\left(\ldots\, \omega_{r/w}\, e\, r_1\cos(\ldots) - \ldots r_2\cos(\ldots) - \frac{\partial g}{\partial \theta}\dot{\theta}\right) \tag{7}$$

where $\omega_{r/w}$ is the angular velocity of the virtual perception coordinate system relative to the robot.

The wall following method described is not only useful to execute an explicit instruction such as "follow that wall". It's also used to avoid an unexpected obstacle in a predefined movement or mission. While the robot is moving, unexpected obstacles or walls can appear and avoiding them is desired and then continues executing the rest of the plan. Taking all that into account the problem of the obstacle avoidance could be reduced to three main aspects presented detail below.

This part has been simplified to the robot by the planner. The planner makes the calculations to obtain the minimum distance between each particular movement in the known environment. The avoidance begins when one sensor detects an object nearer than the distance given by the planner.

The avoidance of the obstacle consists of following the contour of the obstacle in the same way that has been explained before. The maximum speed of the following process will be the speed of the element movement (EM) that was in execution when the obstacle has been detected. That speed has been calculated as the maximum safe speed in the region of the environment by the planner.

That part of the avoidance is the most complex part because of the multiple possibilities of movements and reasons for the finishing.

The avoidance can finish:

a) When the robot gets back to one of the EMs of the plan. (main case).

b) When a long time has elapsed from the beginning of the avoidance. (The obstacle covers all the rest of mission).

c) If the robot is very far from the point of the beginning of the avoidance. (The robot could go very far from its goal in the mission).

The cases (b) and (c) are easy to detect but the case (a) depends on the types of the movements of the robot in the mission. It's important to know that all of the calculations to detect the end of the avoidance have to be made as fast as possible to get the maximum time free in the CPU for the rest of processes (Position control, radio communications, avoidance, etc.). Then all of the types of movements possible are reduced to segments of lines and circumference's arcs.

Perception vector can be considered by means of fuzzy logic yielding a fuzzy description of the environment. This description of the environment can be easily used as input to a fuzzy controller to perform reactive navigation. Furthermore, it is also possible to compute different perception vectors from the virtual perception, and to use them to implement fuzzy controllers or behaviors which perform specific tasks taking into account nonholonomic constraints. The combination of the different behaviors, in a cooperative scheme, can be also easily done by means of fuzzy logic. In the following, a detailed description of the perception based fuzzy control system is performed, including implementation and combination of behaviors.

3. EXPERIMENTS

We have performed experimental results of the proposed methods to the mobile robot ROBO-N. The vehicle carries on-board a heterogeneous configuration of ultrasonic sensors. It is presented two kinds of experiment including general perception and application of fuzzy perception. All the experiments have been implemented in the ROBO-N embed.

In this, instead of a typical ring of identical sonars, there are 12 sonars of three different types, placed at different locations. Six of them are large-range sensors (0.5–2.5m), four are mid-range (0.3–1.0m), and the other two are of short-range (0.06–0.5m). Furthermore, these ultrasonic sensors use a higher frequency and have a narrower sonar beam than the commonly used sonars in these kinds of applications. The sensors are arranged in a way that six of them cover the front part of the vehicle and the other four cover its lateral sides.

Experiments result is shown in where the robot has to navigate through a corridor which is partially obstructed by an obstacle. The robot starts at point A with corridor tracking behavior, since it has equal perception at both sides. As the robot moves on it detects free space to its left and changes its behavior smoothly to follow right wall. When entering the corridor it tries again to center itself in the corridor B.

4. CONCLUSIONS

This work describes the design and real implementation of wall following and fuzzy perception concept with a non-holonomic mobile robot named ROBO-N. The techniques to obtain a fuzzy perception of the environment in the design of each reactive behavior and solving the problem of behavior combination, to implement a fuzzy behavior based control architecture. It should be remarked that, at difference with other behavior based approaches, in the proposed technique the nonholonomic constraints are considered in the design of each behavior.

Furthermore, in order to improve the capabilities of the intelligent control system and its practical applicability, teleoperation and planned behaviors, together with their combination with reactive ones, have been considered. Experimental results, of an application to control the ROBO-N autonomous vehicle, demonstrate the robustness of the proposed method.

ACKNOWLEDGEMENT

This work was supported (National Robotics Research Center for Robot Intelligence Technology, Kyungnam University) by Ministry of Knowledge Economy under Human Resources Development Program for Convergence Robot Specialists.

REFERENCES

[1] R. Braunstingl, "Improving reactive navigation using perception tracking", *Robotics and Manufacturing, Recent Trends in Research and Applications*, Vol. 6, pp 25-30, NewYork, 1996.

[2] J.J. Leonard, H.F. Durrant-Whyte, "Directed Sonar Sensing For Mobile Robot Navigation", Kluwer Academic Publishers, pp 147-155, 1992.

[3] A. Ollero, A. Garcia-Cerezo, J.L. Martinez, A. Mandow, "Fuzzy tracking methods for mobile robots", Prentice-Hall, pp 347-364, 1997.

[4] Ollero, G. Ulivi, F. Cuesta, "Fuzzy logic applications in mobile robotics", Kluwer Academic Publishers, pp. 301–324, 1999.

2017 Changwon International Conference on Intelligent Robot and Convergence Industry (CICIRO 2017)
Nov. 30th~ Dec. 1st, 2017, Changwon Exhibition Convention Center(CECO), Changwon City, Korea

A Study on Robust Control of Robot Manipulator for Industrial Application

In-Kyun Yoon[1], Woo-Song Lee[2] and Sung-Hyun Han[3]
[1] Renault Samsung Motors Co., Ltd. Changwon, 641-808, Korea
(zoro3084@hanmail.net)
[2] SUNJIN Technology Co., Ltd., Changwon, 82331, Korea
(elflws@nate.com)
[3] School of Mechanical Engineering, Kyungnam University,
Changwon, 51767, Korea (shhan@kyungnam.ac.kr)

Abstract: In this paper, we present two kinds of robust control schemes for robot system which has the parametric uncertainties. In order to compensate these uncertainties, we use the neural network control system that has the capability to approximate any nonlinear function over the compact input space. In the proposed control schemes, we need not derive the linear formulation of robot dynamic equation and tune the parameters. We also suggest the robust adaptive control laws in all proposed schemes for decreasing the effect of approximation error. To reduce the number of neural of network, we consider the properties of robot dynamics and the decomposition of the uncertainty function. The proposed controllers are robust not only to the structured uncertainty such as payload parameter, but also to the unstructured one such as friction model and disturbance. The reliability of the control scheme is shown by computer simulations and experiment of robot manipulator with 7 axis.

Keywords: Robust control, decomposition, neural network, robot dynamics, uncertainty

1. INTRODUCTION

To overcome these difficulties, in this paper we propose the adaptive control schemes which utilize a neural network as a compensator for any uncertainty. To reduce the error between the real uncertainty function and the compensator, we design simple and robust adaptive laws based on Lyapunov stability theory. In the proposed control schemes, the NN compensator has to see many neural because uncertainties depend on all state variables. To overcome this problem, therefore, we introduce the control schemes in which the number of neural of the NN compensator can be reduced by using the properties of robot dynamics and uncertainties.

2. DYNAMIC MODELING AND CONTROL

A robot manipulator is defined as an open kinematic chain of rigid links. Each degree of freedom of the manipulator is powered by independent torques. Using the Lagrangian formulation, the equations of motion of an -degree-of-freedom manipulator can be written as

$$D(q)\ddot{q} + C(q,\dot{q})\dot{q} + G(q) + F_r(\dot{q}) + \tau_d = \tau \quad (2)$$

where $q \in R^n$ is the generalized coordinates; $D(q) \in R^{n \times n}$ is the symmetric, bounded, positive-definite inertia matrix; vector $C(q,\dot{q})\dot{q} \in R^n$ presents the centripetal and Coriolis torques; $\tau_d \in R^n$, $G(q) \in R^n$, $F_r(\dot{q}) \in R^n$ and $\tau \in R^n$ represent the gravitational torques, friction, disturbance, and applied joint torques, respectively.

The robot model (2) is characterized by the following structural properties.

Property 1: There exists a vector $\varphi \in R^m$ with components depending on manipulator parameters (masses, moments of inertia, etc.), such that

$$D(q)\ddot{q}_r + C(q,\dot{q})\dot{q}_r + G(q) + F_r(\dot{q}) = Y(q,\dot{q},\dot{q}_r,\ddot{q}_r)\varphi \quad (3)$$

where $Y(q,\dot{q},\dot{q}_r,\ddot{q}_r) \in R^{n \times m}$ is called the regressive matrix.

This property means that the dynamic equation can be linearized with respect to a specially selected set of manipulator parameters.

Property 2: Using a proper definition of matrix $C(q,\dot{q})$, both $C(q,\dot{q})$ and $D(q)$ are not independent and satisfy

$$x^T(\dot{D} - 2C)x = 0, \quad \forall x \in R^n \quad (4)$$

that is, $(\dot{D} - 2C)$ is a skew-symmetric matrix.

This property is simply a statement that the so-called fictitious forces, defined by $C(q,\dot{q})\dot{q}$, do not work on the system. This property is utilized in stability analysis.

Property 3: The friction in the dynamic equation (2) is of the form

$$F_r(\dot{q}) = F_v\dot{q} + F_d(\dot{q}) \quad (5)$$

with F_v the coefficient matrix of viscous friction and $F_d(\dot{q})$ a dynamic friction term. Since friction is a local effect, $F_r(\dot{q}) = F_v\dot{q} + F_d(\dot{q})$ is uncoupled among the joints. The friction is dependent on only angular velocity $\dot{q}$.

This property is utilized in this paper in order to reduce the number of neural in the neural network compensator.

The considered tracking problem is stated as follows: Knowing desired trajectories $q_d \in R^n$, $\dot{q}_d \in R^n$, with some or all the manipulator parameters unknown, determine a control law τ and a sliding surface $s = 0$ such that sliding mode occurs on the sliding surface, the tracking error $\tilde{q} = q - q_d$ has a prescribed transient response and it goes to zero asymptotically as $t \to \infty$.

A. Simple Adaptive Control Law

The sliding surface $s = 0$ is chosen as a hyperplane

$s = \dot{\tilde q} + \Lambda \tilde q$ (6)

where Λ is a positive-definite matrix whose eigenvalues are strictly in the right-half complex plane and $\tilde q$ is the tracking error vector.

If the sliding mode exists on $s = 0$, then from the theory of VSS, the sliding mode is governed by the following linear differential equation whose behavior is dictated by the sliding hyperplane design matrix Λ :

$\dot{\tilde q} = -\Lambda \tilde q$ (7)

Obviously, the tracking error transient response is then determined entirely by the eigenvector structure of the matrix Λ.

In order to derive the sliding mode control law, which forces the motion of the error to be along the sliding surface $s = 0$, a vector of self-defined reference variables is introduced for the succinct formula expression in the sequel, that is,

$\dot q_r(t) = \dot q_d(t) - \Lambda \tilde q(t)$ (8)

Consider now the uncertainties of robot manipulator, (2) can be rewritten as

$D(q)\ddot q + C(q,\dot q)\dot q + G(q) + F(q,\dot q,t) = \tau$ (9)

Where $F(q,\dot q,t) = F_r(\dot q) + \tau_d$. However, in this paper, this uncertainty function vector has to be replaced by $F(q,\ddot q,t)$

So (9) can be rewritten as

$D(q)\ddot q + C(q,\dot q)\dot q + G(q) + F(q,\dot q,\ddot q,t) = \tau$ (10)

we let a Lyapunov function candidate be

$V(t) = \frac{1}{2}\left(s^T D s + \sum_{i=1}^{n} \tilde\theta_i^T \gamma_i^{-1} \tilde\theta_i\right)$ (11)

Where $\tilde\theta_i = \theta_i^* - \theta_i$, θ^*_i is the j th column vector of the optimal parameter matrix θ^* and γ_i is a strictly positive real constant.

Differentiating $V(t)$ with respect to time yields

$\dot V(t) = s^T D\dot s + \frac{1}{2} s^T \dot D s + \sum_{i=1}^{n} \tilde\theta_i^T \gamma_i^{-1} \dot{\tilde\theta}_i$

$= -s^T(D\ddot q_r + C\dot q_r + G + F - \tau) + \sum_{i=1}^{n} \tilde\theta_i^T \gamma_i^{-1} \dot{\tilde\theta}_i$ (12)

Where $F(q,\dot q,\ddot q,t)$ is a completely unknown nonlinear function vector. Therefore, we replace $F(q,\dot q,\ddot q,t)$ by a Neural network $\hat F(q,\dot q,\ddot q,\theta)$ .Let us define the control law as

$\tau = D(q)\ddot q_r + C(q,\dot q)\dot q_r + G(q) + \hat F(q,\dot q,\ddot q,\theta) - K_D s$ (13)

Where $K_D = \mathrm{diag}(k_i)$, $i = 1,2,\dots,n$, and

$$\hat F(q,\dot q,\ddot q,\theta) = \begin{bmatrix} \theta_{1T}\,\xi(q,\dot q,\ddot q) \\ \theta_{2T}\,\xi(q,\dot q,\ddot q) \\ \vdots \\ \theta_{Tn}\,\xi(q,\dot q,\ddot q) \end{bmatrix} \quad (14)$$

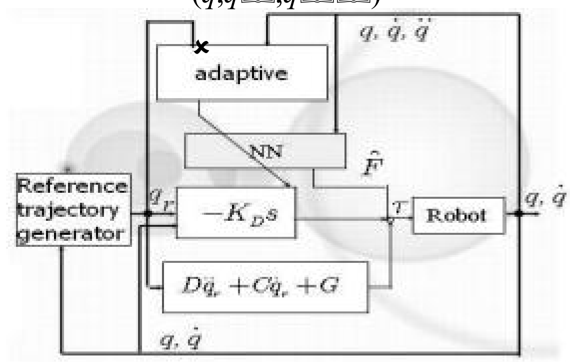

Fig. 4. the structure of the control systems

3. EXPERIMENT AND RESULTS

We also apply real-time adaptive control based on neural network compensator to dual-arm robot shown in figs. 6 – 8. Because the characteristics of two arms are the same, so we show the results into one arm is enough.

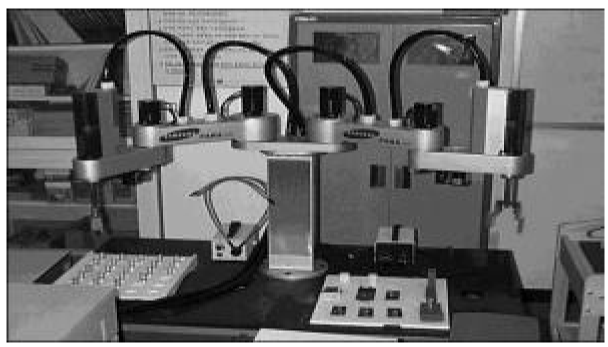

Fig. 6. Experimental set-up

All the algorithm calculation is calculated by Matlab and Simulink matlab on host computer and push into dual-arm robot which is shown in the Fig. 7. The desired trajectories are

$q_{1d} = q_{2d} = 15\pi \sin\left(\frac{2\pi}{300\pi}t - \frac{2\pi}{3}\right)$ and the results of robust adaptive control are shown below

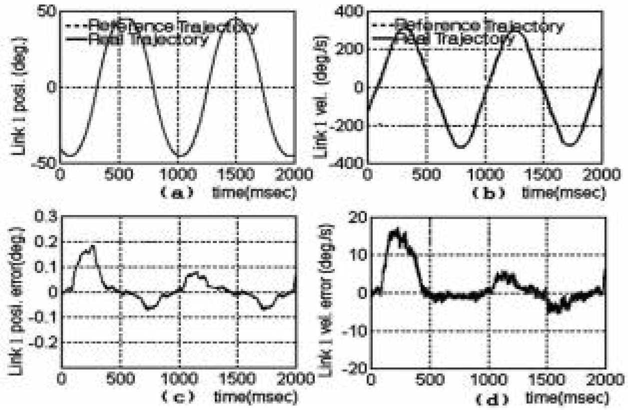

Fig. 7. (a)-(d) Experimental results for the position and velocity tracking of adaptive controller at the first joint.

4. CONCLUSIONS

In this paper, we have illustrated that the control objective is well accomplished and the neural network compensate the uncertainties. In addition, the proposed control technology needs to apply to robot manipulators include more joints, and degree of freedom.

REFERENCES

[1] J. E. Slotin and S. S. Sastry, “Tracking control of nonlinear systems using sliding surfaces, with application to robot manipulators,” Int. J. Contr., vol. 38, no. 2, pp. 465–492, 1983.

[2] J. J. E. Slotine and W. Li, Applied Nonlinear Control. Englewood Cliffs, NJ: Prentice-Hall, 1991.

[3] F. L. Lewis, C. T. Abdallah, and D. M. Dawson, Control of Robot Manipulators. London, U.K.: Macmillan, 1993.

[4] M. W. Spong, Robot Dynamics and Control. New York: Wiley, 1989.

[5] W. C. Ham, “Adaptive nonlinear control of one-link flexible arm,” in IEEE/RSJ Int. Conf. Intelligent Robots and Systems, vol. 1, Yokohama, Japan, 1993, pp. 3–7.

[6] “Adaptive control based on explicit model of robot manipulators,” IEEE Trans. Automat. Contr., vol. 38, pp. 654–658, 1993.

[7] “Adaptive control based on speed gradient algorithm for robot manipulators,” in Int. Conf. Industrial Electronics Control and Instrumentation, vol. 2, Bologna, Italy, 1994, pp. 776–781.

[8] B.K. Yoo, W.C. Ham “Adaptive Control of Robot Manipulator Using Fuzzy Compensator”. IEEE transaction on Fuzzy System. VOL. 8. NO. 2. April 2000.

2017 Changwon International Conference on Intelligent Robot and Convergence Industry (CICIRO 2017)
Nov. 30th~ Dec. 1st, 2017, Changwon Exhibition Convention Center(CECO), Changwon City, Korea

A Study on Robust Motion Control of Humanoid Type Robot for Cooperative Working

Ki-Young Ko[1], Eun-Tae Ha[2] and Sung-Hyun Han[3]

[1] Doosan Heavy Industries & Construction Co., Ltd., Changwon, 51711, Korea
(kiyoung.ko@doosan.com)
[2] Future Technology Institute Co., Ltd, Changwon, 642-939, Korea
(E-mail: euntha@hanmail.net)
[3] School of Mechanical Engineering, Kyungnam University,
Changwon, 631-701, Korea (E-mail: shhan@kyungnam.ac.kr)

Abstract: We present a new technology for real-time walking of a humanoid robot. A humanoid robot necessitates achieving stabilization for real time walking since it has basic problems such as structural stability. In this paper, a robust control algorithm for stable walking is proposed based the ground reaction forces, which are measured using force sensors during walking, and the environmental conditions are estimated from these situation. From this information the robot selects the proper motion and overcomes ground irregularities effectively. In order to generate the proper angel of the joint. The performance of the proposed algorithm is verified by simulation and experiments for a 20-DOFs humanoid robot.

Keywords: Stable Walking, Control Algorithm, Humanoid Robot, Robust Walking

1. INTRODUCTION

This paper proposes an obstacle avoidance architecture allowing walking humanoid robots to walk safely around in factory and home environment.

For a wheeled robot, many solutions on this subject have been presented in the literature using ultrasonic sensors or laser range finders and they mainly detect walls and relatively large obstacles around the robot. But solving the problem of obstacle avoidance for a humanoid robot in an unstructured environment is a big challenge, because the robot can easily lose its stability or fall down if it hits or steps on an obstacle.

Our strategy focuses on floor estimation, because in our view information about the floor is most important for a humanoid robot while walking. For this purpose, we developed a stereo-vision system and detect the floor plane using a randomized version of the hough transform. The aim of this proposition is to establish a new industry involving autonomous robots and artificial intelligence.

A main technological target of the proposed robot (Model:V-HUR) is to autonomously explore and wander around in home environments as well as to communicate with humans.

2. SYSTEM MODELING

The V-HUR consists of 2 microphones for speech recognition and sound localization utilizing as well as speech synthesis play a big role in the communication capabilities of Robot. Audio and visual recognition results are memorized in a system that reflects the current environment. The stereo-vision system consists of 2 cameras as the robot's eyes and a module for stereo processing in the robot's head. Using its stereo camera V-HUR can compute distance to objects, extract a floor plane and generate a path for walking around obstacles.

V-HUR is able to communicate with network computers by utilizing its wireless lan.

The V-HUR consists of 40 joints of the intelligent servo actuators. In real time, it enables V-HUR to walk adaptively on inclined and irregular terrain and allows the robot to re-stabilize immediately even when external forces affect its balance. Furthermore, a sub-system for real time step pattern generation realizes various walking patterns ranging from active and stable humanoid walking to moving flexibility.

Base on the height of V-HUR, the Robot's structure and the main applications for the stereo system, the distant between 2 color CCD cameras is 4cm. This distant allows for reliable floor estimation up to a range of 3m and reliable distance estimation of other objects in the range of 20cm to 4m.

The system consists of an 8-bit micro processor with two 16Mbyte SDRAM units and a flash ROM. The stereo-vision module computes disparity between 2 CCD cameras by using block matching receives a pair of images from them. The main board of the CPU receives the resulting disparity image as a digital video signal. The stereo control parameters can be set between the main CPU and the 8bit CPU on board through a special serial communication link (see fig. 1).

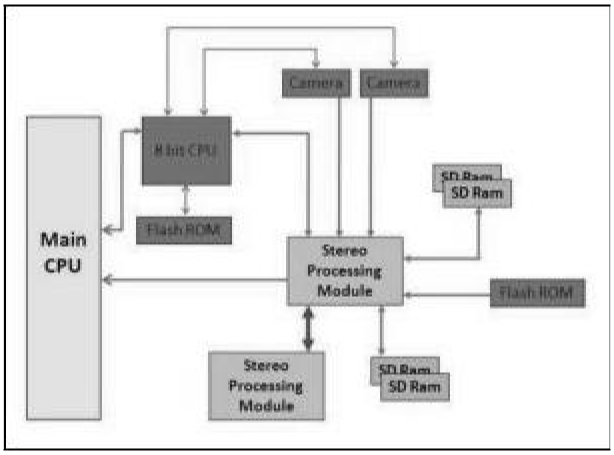

Fig. 1. System's hardware

The system's software briefly describes each module below (see Fig. 1).

The important point of this module is that to deliver disparity images with the corresponding kinematic transformations to the *3D Range Transfer* module. This module receives image data from the stereo-vision system and joint angle sensor data from each actuator.

This module aims at to convert all the 3D measurements to the floor coordinate system. The disparity image obtained from stereo-vision is first converted into 3D range data using parameters from stereo calibration. Then a transformed data is applied for finding planes in the 3D data.

It integrates information into a 2D grid configuration of size 3.5x3.5m around the robot. Image source: receiving either from the *3D Range Transfer* or odometer information from the Receiver module.

Control mechanism where the behavior of the robot is determined autonomously according to internal states and external observations. A part of *Operation Planning Controller* is a *planning pioneer* that, given a goal point, computes a collision-free path leading to the destination. The *planning pioneer* system then generates walk and head motion commands which are sent to the *Source Distribution* which in turn send them to the *Motion preparing* and the *Actuator.*

The vision system (mentioned above) receives image from the two CCD cameras. These parameters are useful for computing 3D range data. The disparity is calculated for each pixel in the left image by searching for the corresponding pixel in the right image. An additional reliability image is calculated following criteria to reject results on above conditions. After block matching has been carried out, the matching score is calculated by interpolating scores near the highest peak. The sharpness of this peak corresponds to the available texture around this pixel and thus can be used as a reliability value for the disparity calculation. If there are other peaks with similar matching scores then the disparity computation is ambiguous and the reliability is set to a low value. (The matching score is compared with neighboring scores).

3. EXPERIMENT

Firstly, the disparity is converted into 3D range data using the parameters from camera calibration and then a Hough transformation is applied to all data points. Apply the *randomized Hough transformation* selects sets of data points from which the surface parameters can be directly computed and records the result in a table. If many data sets yield the same parameters, a high score for these parameters is obtained.

The details of this method are showed in the flow chart in the Fig. 2 below.

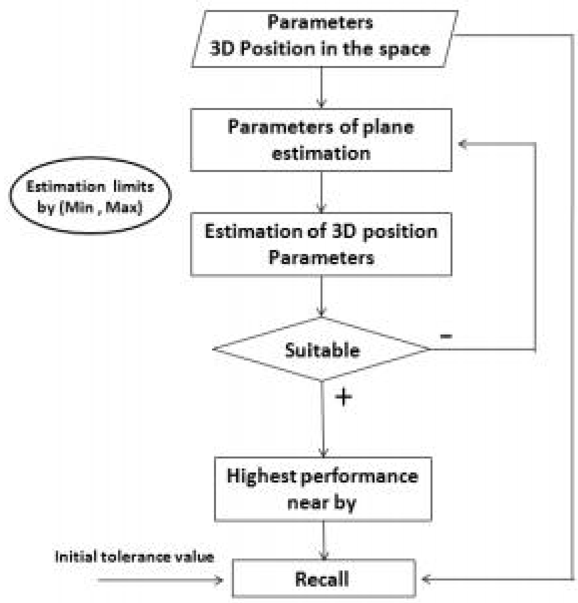

Fig 2. Flow chart of plane extraction

Although applying floor detection methods, obstacles and regions the robot can walk on can be found. However, in general it is difficult to decide from a single observation with a limited field of view, the action the robot should carry out next. We follow this notion and introduce a terrain map where all observations and motions are integrated.

The terrain map is a 2-dimensional occupancy grid centered on the current position of the robot (egocentric coordinate system). We maintain the (global) robot orientation and a small relative (x y) location of the robot within the cell at the center of the grid. Initially, all cells are set to a probability of 1.0 and time 0. Each grid cell contains the probability that an obstacle covers the cell and the time the cell was last updated.

The robot motion is defined as a coordinate transformation from one foot to the other whenever the robot performs a step. From this transformation a displacement and a change in orientation can be derived and applied to the position and orientation of the robot in the grid.

In our implementation shifting the grid is actually performed by changing an offset into the grid data array so that no data has to be moved physically. After shifting the coordinate system of the occupancy grid, new cells at the border are initialized.

Define: the cell size Sc, the robot position (Rx, Ry) inside the grid, and the moving displacement (Mx, My), we obtain:

$$(Ax,\ Ay) = \left(\left\lfloor \frac{Rx + Mx}{Sc} \right\rfloor, \left\lfloor \frac{Ry + My}{Sc} \right\rfloor \right) \quad (1)$$

The new robot position inside the grid becomes as follows:

$$(Mx - Sc \cdot Ax, My - Sc \cdot Ay) \rightarrow (Rx, Ry) \ . \quad (2)$$

The change in orientation _a is simply added to the global orientation of the robot .

In an additional, searching for shortcuts along the found path, a smooth walking trajectory is realized.

The robot can find a path to a destination point by using the occupancy grid reflects the terrain around. The definition of each cell of the occupancy grid is a node connecting to neighboring cells and defines the path planning problem as a search problem on this graph.

4. CONCLUSION.

The autonomous mobility for the humanoid robot V-HUR in the home environment is realized base on the development of a small stereo vision system, the recognition of floor and obstacles using plane extraction.

The terrain is represented in a robot centric coordinate system without making any structural assumptions about the surrounding world. And the representation of a terrain map based on these observations, robot motion, and the generation of a walking path on the terrain map. We therefore believe, our approach is well suited for many different a home environment where no a priori information about the environment is given. The limitation of our system is that the terrain has to contain enough texture in order to obtain reliable stereo data.

REFERENCES

[1] D. Pagac, E. Nebot and H. Durrant-Whyte, “An evidential approach to map-building for autonomous vehicles,” *IEEE Transactions on Robotics and Automation*, 14(4), 623-629, 1998.

[2] Ole Wijk, ”Triangulation Based Fusion of Sonar Data with Application in Mobile Robot Mapping and Localization,” *PhD thesis*, Royal Institute of Technology, Stockholm, Sweden, 2001.

[3] Y. Kuroki, T. Ishida, J. Yamaguchi, M. Fujita and T.T. Doi, “A Small Biped Entertainment Robot,” in *Proc. Int. Conf. on Humanoid Robots*, pp.181-186, 2001.

[4] M. Fujita and K. Kageyama, “An Open Architecture for Robot Entertainment,” in *Proc. Inernational Conference on Autonomous Agents*, pp. 435-440, 1997.

[5] M. Fujita and H. Kitano, “Development of an Quadruped Robot for Robot Entertainment,” *Autonomous Robots*, vol. 5, pp.7-8, Kluwer Academic, 1998.

2017 Changwon International Conference on Intelligent Robot and Convergence Industry (CICIRO 2017)
Nov. 30th~ Dec. 1st, 2017, Changwon Exhibition Convention Center(CECO), Changwon City, Korea

A Study on Stable Control of Intelligent Robot with Dual Arm for Cooperation working

Ho-Young Bae[1], Yang-Keun Jeong[2], Woo-Song Lee[3], In-Man Park[4] and Sung-Hyun Han[5]

[1] V-Mac Company Co., Ltd. Changwon, 50850, Korea (sswq1r@hanmail.net)
[2] Shinla Information Technology Co., Ltd., Changwon, 641-465, Korea (shintech@hanmail.net))
[3] Sungsanam Deco Co.,Ltd., Changwon, 630-500 Korea (elflws@nate.com)
[4] Intem Co., Ltd., Changwon, 642-370, Korea (intem237@hanmail.net)
[5] School of Mechanical Engineering, Kyungnam University, Changwon, 51767, Korea (shhan@kyungnam.ac.kr)

Abstract: The autonomous mobility for the biped robot V-HUR in the home environment is realized base on the development of a small stereo vision system, the recognition of floor and obstacles using plane extraction. The terrain is represented in a robot centric coordinate system without making any structural assumptions about the surrounding world. And the representation of a terrain map based on these observations, robot motion, and the generation of a walking path on the terrain map.

Keywords: Stable Walking, Control Algorithm, Biped Robot, Robust Walking

1. INTRODUCTION

This paper proposes an obstacle avoidance architecture allowing walking humanoid robots to walk safely around in factory and home environment.

Our strategy focuses on floor estimation, because in our view information about the floor is most important for a humanoid robot while walking. For this purpose, we developed a stereo-vision system and detect the floor plane using a randomized version of the hough transform. The aim of this proposition is to establish a new industry involving autonomous robots and artificial intelligence.

A main technological target of the proposed robot is to autonomously explore and wander around in home environments as well as to communicate with humans.

2. SYSTEM MODELING

The robot consists of 2 microphones for speech recognition and sound localization utilizing as well as speech synthesis play a big role in the communication capabilities of Robot. Audio and visual recognition results are memorized in a system that reflects the current environment. The stereo-vision system consists of 2 cameras as the robot's eyes and a module for stereo processing in the robot's head. Using its stereo camera V-HUR can compute distance to objects, extract a floor plane and generate a path for walking around obstacles.

robot is able to communicate with network computers by utilizing its wireless lan.

The robot consists of 40 joints of the intelligent servo actuators. In real time, it enables V-HUR to walk adaptively on inclined and irregular terrain and allows the robot to re-stabilize immediately even when external forces affect its balance. Furthermore, a sub-system for real time step pattern generation realizes various walking patterns ranging from active and stable biped walking to moving flexibility.

The important point of this module is that to deliver disparity images with the corresponding kinematic transformations to the *3D Range Transfer* module. This module receives image data from the stereo-vision system and joint angle sensor data from each actuator.
This module aims at to convert all the 3D measurements to the floor coordinate system. The disparity image obtained from stereo-vision is first converted into 3D range data using parameters from stereo calibration. Then a transformed data is applied for finding planes in the 3D data.
It integrates information into a 2D grid configuration of size 3.5x3.5m around the robot. Image source: receiving either from the *3D Range Transfer* or odometer information from the Receiver module.
Control mechanism where the behavior of the robot is determined autonomously according to internal states and external observations. A part of *Operation Planning Controller* is a *planning pioneer* that, given a goal point, computes a collision-free path leading to the destination. The *planning pioneer* system then generates walk and head motion commands which are sent to the *Source Distribution* which in turn send them to the *Motion preparing* and the *Actuator.*

The vision system (mentioned above) receives image from the two CCD cameras. These parameters are useful for computing 3D range data. The disparity is calculated for each pixel in the left image by searching for the corresponding pixel in the right image. An additional reliability image is calculated following criteria to reject results on above conditions. After block matching has been carried out, the matching score is calculated by interpolating scores near the highest peak. The sharpness of this peak corresponds to the available texture around this pixel and thus can be used as a reliability value for the disparity calculation. If there are other peaks with similar matching scores then the disparity computation is ambiguous and the reliability is set to a low value. (The matching score is compared with neighboring scores).

3. EXPERIMENT

Firstly, the disparity is converted into 3D range data using the parameters from camera calibration and then a Hough transformation is applied to all data points. Apply the *randomized Hough transformation* selects sets of data points from which the surface parameters can be directly computed and records the result in a table. If many data sets yield the same parameters, a high score for these parameters is obtained.

Although applying floor detection methods, obstacles and regions the robot can walk on can be found. However, in general it is difficult to decide from a single observation with a limited field of view, the action the robot should carry out next. We follow this notion and introduce a terrain map where all observations and motions are integrated.

The terrain map is a 2-dimensional occupancy grid centered on the current position of the robot (egocentric coordinate system). We maintain the (global) robot orientation and a small relative (x y) location of the robot within the cell at the center of the grid. Initially, all cells are set to a probability of 1.0 and time 0. Each grid cell contains the probability that an obstacle covers the cell and the time the cell was last updated.

The robot motion is defined as a coordinate transformation from one foot to the other whenever the robot performs a step. From this transformation a displacement and a change in orientation can be derived and applied to the position and orientation of the robot in the grid.

In our implementation shifting the grid is actually performed by changing an offset into the grid data array so that no data has to be moved physically. After shifting the coordinate system of the occupancy grid, new cells at the border are initialized.

Define: the cell size Sc, the robot position (Rx, Ry) inside the grid, and the moving displacement (Mx, My), we obtain:

$$(Ax,\ Ay) = \left(\frac{Rx + Mx}{Sc},\ \frac{Ry + My}{Sc} \right) \qquad (1)$$

The new robot position inside the grid becomes as follows:

$$(Mx - Sc \cdot Ax, My - Sc \cdot Ay) \rightarrow (Rx, Ry)\ . \qquad (2)$$

The change in orientation *_a* is simply added to the global orientation of the robot .

In an additional, searching for shortcuts along the found path, a smooth walking trajectory is realized.

The robot can find a path to a destination point by using the occupancy grid reflects the terrain around. The definition of each cell of the occupancy grid is a node connecting to neighboring cells and defines the path planning problem as a search problem on this graph.

4. CONCLUSION.

We present a new technology for real-time walking of a biped robot. A biped robot necessitates achieving stabilization for real time walking since it has basic problems such as structural stability. In this paper, a robust control algorithm for stable walking is proposed based the ground reaction forces, which are measured using force sensors during walking, and the environmental conditions are estimated from these situation. From this information the robot selects the proper motion and overcomes ground irregularities effectively. In order to generate the proper angel of the joint. The performance of the proposed algorithm is verified by simulation and experiments for a 22-DOFs humanoid robot.

The limitation of our system is that the terrain has to contain enough texture in order to obtain reliable stereo data.

REFERENCES

[1] T. Ishida, Y. Kuroki, J. Yamaguchi, M. Fujita and T.T. Doi, "Motion Entertainment by a Small Humanoid Robot Based on OPEN-R," in *Int. Conf. on Intelligent Robots and Systems (IROS-01),* pp.1079-1086, 2001.

[2] M. Fujita and H. Kitano, "Development of an Quadruped Robot for Robot Entertainment," *Autonomous Robots*, vol. 5, pp.7-8, Kluwer Academic, 1998.

[3] M. Fujita and K. Kageyama, "An Open Architecture for Robot Entertainment," in *Proc.*

Inernational Conference on Autonomous Agents, pp. 435-440, 1997.
[4] Y. Kuroki, T. Ishida, J. Yamaguchi, M. Fujita and T.T. Doi, “A Small Biped Entertainment Robot,” in *Proc. Int. Conf. on Humanoid Robots*, pp.181-186, 2001.
[5] Ole Wijk, ”Triangulation Based Fusion of Sonar Data with Application in Mobile Robot Mapping and Localization,” *PhD thesis*, Royal Institute of Technology, Stockholm, Sweden, 2001.
[6] D. Pagac, E. Nebot and H. Durrant-Whyte, “An evidential approach to map-building for autonomous vehicles,” *IEEE Transactions on Robotics and Automation*, 14(4), 623-629, 1998.

2017 Changwon International Conference on Intelligent Robot and Convergence Industry (CICIRO 2017)
Nov. 30th~ Dec. 1st, 2017, Changwon Exhibition Convention Center(CECO), Changwon City, Korea

A Study on Travelling Control of Humanoid Type Mobile Robot with Three Wheel

Se-Bin Park[1], In-Man Park [2] and Sung-Hyun Han[3]

[1] Navy, Changwon, Korea (3bin99@naver.com)
[2] Intem Co., Ltd., Changwon, 642-370, Korea
(intem237@hanmail.net)
[3] School of Mechanical Engineering, Kyungnam University, Changwon, 51767, Korea
(shhan@kyungnam.ac.kr)

Abstract: The main focus of this paper is obtaining a fuzzy perception of the environment in the design of each reactive behavior and solving the problem of behavior combination to implement a fuzzy behavior based control architecture. It should be remarked that, the proposed technique of the nonholonomic constraints are considered in the design of each behavior. Furthermore, in order to improve the capabilities of the intelligent control system and its practical applicability, teleoperation and planned behaviors, together with their combination with reactive ones, have been considered.

Keywords: Real-Time control, Sensor, Fuzzy Controller, Non-holonomic

1. INTRODUCTION

The real-time trajectory control is the process of determining and maintaining a path or trajectory to a goal destination. Autonomous mobile robots are required to navigate in more complex domains, where the environment is uncertain and dynamic. Autonomous navigation in these environments demands adaptation and perception capabilities. This paper describes improvements in the perception functions used in these kinds of robots. It should be noted that this is a nonholonomic vehicle with significant limitations in the reactive capabilities due to kinematic and dynamic constraints, and a few number of sensors and large blind sectors in between them, making autonomous navigation a nontrivial task. The methods presented in this paper have been conceived to deal with these limitations of conventional vehicles.

2. CONTROLSCHEME

The following considerations are based on a mobile robot with the three degrees of freedom of planar movement, x, y and θ. It is equipped with a ring of 12 ultrasonic sensors which are able to perceive vertical or nearly vertical planes. The number of sensors is irrelevant as long as there are no blind sectors between them. θ refers to the orientation of this ring of sensors and not to the orientation of the robot itself, which is of no importance for the wall following algorithm. With $\dot\varphi$ indicating the direction of movement the kinematics model of such a robot is described as follows:

$$dx = v\cos\varphi\,dt;\quad dy = -v\sin\varphi\,dt;\quad d\theta = \dot\theta\,dt \tag{1}$$

Since there is no modeling of the environment the absolute position of the robot does not matter. So there is no world frame used here and the kinematics model can be expressed instead as:

$$ds = v\,dt;\quad d\varphi = \dot\varphi\,dt;\quad d\theta = \dot\theta\,dt \tag{2}$$

The speed v, the angular speeds $\dot\varphi$ and $\dot\theta$ are used as control variables of the robot and generated by the fuzzy controller.

Perception of each ultrasonic sensor i of the mobile robot is assigned a vector ki. Its direction equals the orientation of the sensor´s axis and its length is a function of the distance di measured by this sensor:

$$k_i = \frac{d_{max} - d_i}{d_{max} - d_{min}} \tag{3}$$

where dmin and dmax designate the shortest and longest distance respectively at which an object may be positioned to be reliably detected. ki is limited to 0 and 1 respectively

Since a vehicle with nonholonomic constraints cannot move itself in any direction at every time instant, it is interesting to weight the different perceptions according with the direction where the obstacle was detected. In other words, an obstacle is less important if it is placed at a location that cannot be reached by the mobile robot, but it is more dangerous if it is on a reachable position. This task can be accomplished by considering the perception angle (θi) in the computation of the perception function

$$k_i = f(d_s,\theta_i) = sat_{0,1}\left(\frac{d_{max}(\theta_i) - d_s}{d_{max}(\theta_i) - d_{min}(\theta_i)}\right) \tag{4}$$

where sat0,1(x) states for the saturation of x in the range [0, 1]. In this way, it is possible to assign different perceptions, i.e. different weights, to objects detected at the same distance relative to the mobile robot but at different directions. For example, perception function ki is obtained by using the nonlinear function

$d_{\min}(\theta_i) = \frac{d_m(1-\epsilon)}{(1-\epsilon\cos\theta_i)}$, and $d_{\max} = nd_{\min}(\theta_i)$ (with n>1), in Eq. (4).

$$k_i = f(d_s,\theta_i) = sat_{0,1}\left(\frac{nd_m(1-\epsilon)-d_s(1-\epsilon\cos\theta_i)}{(n-1)d_m(1-\epsilon)}\right) \quad (5)$$

Furthermore, it is interesting to stress that the perception vector implies a fuzzy high level description of the environment, being independent of the type of range sensor used. So, it is possible to use different perception functions from Eq. 4 for each kind of sensor (laser, ultrasonic, infrared). Thus, sensor data fusion can be reduced to compute different vectors from the sensor measurements and to combine them to obtain the perception vector.

The previous perception can be updated as follows: consider a robot of arbitrary shape equipped with proximity sensors. Any such sensor may be located at a position U, with its axis pointing to the direction s

A frame r represents the robots position and orientation, x and θ, respectively, with respect to the world reference system w. The velocity υ of the reference point and the angular velocity $\omega_{r/w} = e_r$ of the robot with respect to the fixed frame w, give the state of motion. Furthermore, the virtual perception coordinate system is assumed to be located at E, pointing to the direction of attention a1. Then, an object detected by a proximity sensor at a distance ds could be detected by a virtual sensor placed at E a distance d, and with an orientation θ with respect to the vehicle's direction of attention a1.

Now the virtual perception will be updated taking into account the robots motion as follows: considering a perception function k = f(d, θ) and the corresponding inverse perception function, d = g(k, θ), and carrying out some calculations, it can be shown that the derivatives of angle and length of the perception vector are given by (assuming g $\neq$ 0 and $\frac{\partial g}{\partial k} \neq 0$).

$$\dot{\theta} = \frac{1}{g}\left(x \cdot (\omega_{r/w} \times e)\, r_1 \cos\theta - \ldots r_2 \cos\theta\right) - \omega_{r/w} - \omega_{a/r} \quad (6)$$

$$\dot{k} = \frac{1}{\partial g/\partial k}\left(x \cdot (\omega_{r/w} \times e)\, r_1 \cos\theta - \ldots r_2 \cos\theta - \frac{\partial g}{\partial \theta}\dot{\theta}\right) \quad (7)$$

where $\omega_{r/w} = \dot{\theta}$ is the angular velocity of the virtual perception coordinate system relative to the robot.

3. EXPERIMENTS

We have performed experimental results of the proposed methods to the mobile robot ROBO-N. The vehicle carries on-board a heterogeneous configuration of ultrasonic sensors. It is presented two kinds of experiment including general perception and application of fuzzy perception. All the experiments have been implemented in the ROBO-N embed.

In this, instead of a typical ring of identical sonars, there are 12 sonars of three different types, placed at different locations. Six of them are large-range sensors (0.5–2.5m), four are mid-range (0.3–1.0m), and the other two are of short-range (0.06–0.5m). Furthermore, these ultrasonic sensors use a higher frequency and have a narrower sonar beam than the commonly used sonars in these kinds of applications. The sensors are arranged in a way that six of them cover the front part of the vehicle and the other four cover its lateral sides.

Experiments result is shown in where the robot has to navigate through a corridor which is partially obstructed by an obstacle. The robot starts at point A with corridor tracking behavior, since it has equal perception at both sides. As the robot moves on it detects free space to its left and changes its behavior smoothly to follow right wall. When entering the corridor it tries again to center itself in the corridor B.

4. CONCLUSIONS

We propose a new approach to control of mobile robot of trajectory following and fuzzy perception concept with a nonholonomic mobile robot.

Experimental results, of an application to control the autonomous vehicle, demonstrate the robustness of the proposed method.

REFERENCES

[1] R. Braunstingl, "Improving reactive navigation using perception tracking", *Robotics and Manufacturing, Recent Trends in Research and*

Applications, Vol. 6, pp 25-30, NewYork, 1996.

[2] J.J. Leonard, H.F. Durrant-Whyte, “Directed Sonar Sensing For Mobile Robot Navigation”, Kluwer Academic Publishers, pp 147-155, 1992.

[3] A. Ollero, A. Garcia-Cerezo, J.L. Martinez, A. Mandow, “Fuzzy tracking methods for mobile robots”, Prentice-Hall, pp 347-364, 1997.

[4] Ollero, G. Ulivi, F. Cuesta, “Fuzzy logic applications in mobile robotics”, Kluwer Academic Publishers, pp. 301–324, 1999.

2017 Changwon International Conference on Intelligent Robot and Convergence Industry (CICIRO 2017)
Nov. 30th~ Dec. 1st, 2017, Changwon Exhibition Convention Center(CECO), Changwon City, Korea

A Travelling Control of Mobile Robot Based on Sonar Sensors

Jae-Sang Kim[1], Yang-Keun Jeong[2], Jong Bum Won[3], and Sung-Hyun Han[4]

[1] Hanwha Techwin Co., Ltd., Changwon, 51542, Korea (Jaesangkim70@gmail.com)
[2] Shinla Information Technology Co., Ltd., Changwon, 641-465, Korea (shintech@hanmail.net)
[3] Smec Co., Ltd., Changwon, 621-184, Korea (won@esmec.com)
[4] School of Mechanical Engineering, Kyungnam University, Changwon, 51767, Korea (shhan@kyungnam.ac.kr)

Abstract: This paper describes the design and real implementation of wall following and fuzzy perception concept with a non-holonomic mobile robot named KHAN-Robo. The main focus of this paper is obtaining a fuzzy perception of the environment in the design of each reactive behavior and solving the problem of behavior combination to implement a fuzzy behavior based control architecture. It should be remarked that, the proposed technique of the nonholonomic constraints are considered in the design of each behavior. Furthermore, in order to improve the capabilities of the intelligent control system and its practical applicability, teleoperation and planned behaviors, together with their combination with reactive ones, have been considered. Experimental results, of an application to control the KHAN-Robo autonomous vehicle, demonstrate the robustness of the proposed method.

Keywords: Robot Navigation, Ultrasonic Sensor, Fuzzy Controller, Non-holonomic Mobile Robot.

1. INTRODUCTION

This paper describes improvements in the perception functions used in these kinds of robots. It should be noted that this is a nonholonomic vehicle with significant limitations in the reactive capabilities due to kinematic and dynamic constraints, and to the few number of sensors and large blind sectors in between them, making autonomous navigation a nontrivial task. The methods presented in this paper have been conceived to deal with these limitations of conventional vehicles.

2. OBSTACLEAVOIDANCE

2.1 Start to avoid an unexpected obstacle

This part has been simplified to the robot by the planner. The planner makes the calculations to obtain the minimum distance between each particular movement in the known environment. The avoidance begins when one sensor detects an object nearer than the distance given by the planner.

How to avoid the obstacle: The avoidance of the obstacle consists of following the contour of the obstacle in the same way that has been explained before. The maximum speed of the following process will be the speed of the element movement (EM) that was in execution when the obstacle has been detected. That speed has been calculated as the maximum safe speed in the region of the environment by the planner.

2.2 Finish the avoidance of the obstacle

That part of the avoidance is the most complex part because of the multiple possibilities of movements and reasons for the finishing.

The avoidance can finish:

a) When the robot gets back to one of the EMs of the plan. (main case).

b) When a long time has elapsed from the beginning of the avoidance. (The obstacle covers all the rest of mission).

c) If the robot is very far from the point of the beginning of the avoidance. (The robot could go very far from its goal in the mission).

The cases (b) and (c) are easy to detect but the case (a) depends on the types of the movements of the robot in the mission. It's important to know that all of the calculations to detect the end of the avoidance have to be made as fast as possible to get the maximum time free in the CPU for the rest of processes (Position control, radio communications, avoidance, etc.). Then all of the types of movements possible are reduced to segments of lines and circumference's arcs.

3. CONTROLLER

Perception vector can be considered by means of fuzzy logic yielding a fuzzy description of the environment. This description of the environment can be easily used as input to a fuzzy controller to perform reactive navigation. Furthermore, it is also possible to compute different perception vectors from the virtual perception, and to use them to implement fuzzy controllers or behaviors which perform specific tasks taking into account nonholonomic constraints. The combination of the different behaviors, in a cooperative scheme, can be also easily done by means of fuzzy logic. In the following, a detailed description of the perception based fuzzy control system is performed, including implementation and combination of behaviors.

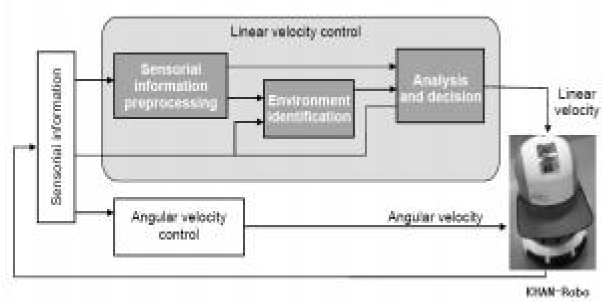

Fig.1 Block diagram of control system

4. EXPERIMENTALRESULTS

This section presents some experimental results of the proposed methods to the non-holonomic mobile robot KHAN¬-Robo. The vehicle carries on-board a heterogeneous configuration of ultrasonic sensors. It is presented two kinds of experiment including general perception and application of fuzzy perception. All the experiments have been implemented in the KHAN-Robo embed.

In this, instead of a typical ring of identical sonars, there are 12 sonars of three different types, placed at different locations. Six of them are large-range sensors (0.6–3.0 m), four are mid-range (0.2–1.0 m), and the other two are of short-range (0.06‐ 0.3 m). Furthermore, these ultrasonic sensors use a higher frequency and have a narrower sonar beam than the commonly used sonars in these kinds of applications. The sensors are arranged in a way that six of them cover the front part of the vehicle and the other four cover its lateral sides.

In these experiments, the virtual perception system was placed at the center of the robot's rear axle and the direction of attention a1 was kept parallel to the front wheel.

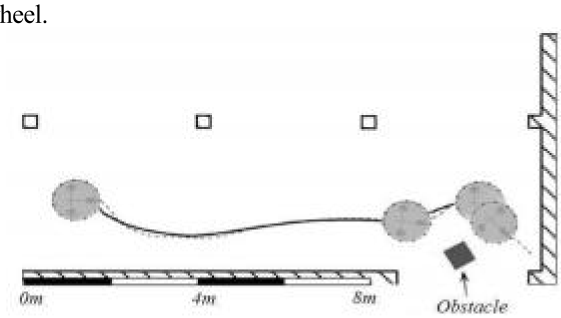

(a)Loss of perception while turning right

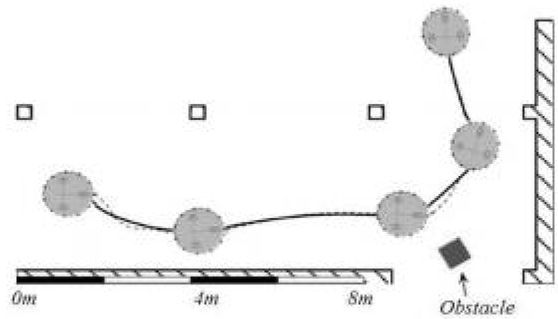

(b)With perception memory

Fig. 2 The differences result of perception's type

Fig. 2 shows an experiment with the same conditions but it was applied with differential perceptions.

Experiments result is shown in Fig. 3 where the robot has to navigate through a corridor which is partially obstructed by an obstacle. The robot starts at point A with corridor tracking behavior, since it has equal perception at both sides. As the robot moves on it detects free space to its left and changes its behavior smoothly to follow right wall. When entering the corridor it tries again to center itself in the corridor B until it encounters the obstacle at C and the obstacle avoidance behavior becomes dominant. The corridor is wide enough, i.e. the perception at both sides is sufficiently low that the turnaround behavior is not activated, so the robot tries to round the obstacle and, indeed, detects the passage between the obstacle and the wall. From this point on the robot is again guided mainly by the corridor tracking behavior until D.

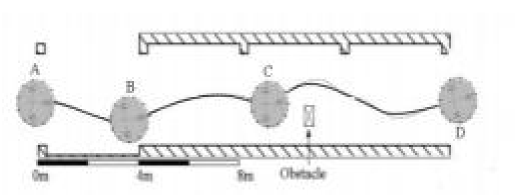

Fig. 3 Reactive behavior navigation of KHAN-Robo

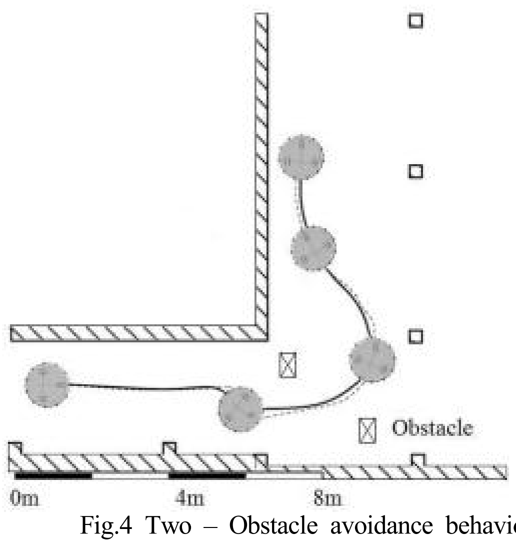

Fig.4 Two – Obstacle avoidance behaviors

5. CONCLUSIONS

This work describes the design and real implementation of wall following and fuzzy perception concept with a non-holonomic mobile robot named KHAN-Robo. The techniques to obtain a fuzzy perception of the environment in the design of each reactive behavior and solving the problem of behavior combination, to implement a fuzzy behavior based control architecture. It should be remarked that, at difference with other behavior based approaches, in the proposed technique the nonholonomic constraints are considered in the design of each behavior.
Furthermore, in order to improve the capabilities of the intelligent control system and its practical applicability, teleoperation and planned behaviors, together with their combination with reactive ones, have been considered. Experimental results, of an application to control the KHAN-Robo autonomous vehicle, demonstrate the robustness of the proposed method.

REFERENCES

[1] G.A. Bekey, “Localization, Navigation, and Mapping”, Autonomous Robots: From Biological Inspiration to Implementation and Control, The MIT press, pp 473-507, 2005.

[2] R.C. Luo, T.M. Chen, “Autonomous mobile target tracking system based on grey-fuzzy control algorithm,” IEEE Trans. Ind. Electron. Vol. 47, No. 4, pp 920–931, 2000.

[3] J. Gasos, A. Rosetti, “Uncertainty representation for mobile robots: perception, modeling and navigation in unknown environments”, J. of Fuzzy Sets and Systems, Vol. 107, No. 1, pp 1–24, 1999.

[4]] A. Ollero, B.C. Arrue, J. Ferruz, G. Heredia, F. Cuesta, F. Lopez-Pichaco, C. Nogales, “Control and perception components for autonomous vehicle guidance. Application to the ROMEO vehicles”, Control Engineering Practice, Vol. 7, No. 10, pp 1291-1299, 1999..

2017 Changwon International Conference on Intelligent Robot and Convergence Industry (CICIRO 2017)
Nov. 30th~ Dec. 1st, 2017, Changwon Exhibition Convention Center(CECO), Changwon City, Korea

A Precise Position Control of Robot Manipulator with Eight Joints

Taek-Jong Nam[1] Yang-Keun Jeong[2], Jong Bum Won[3], Hyun-Cheol Lee[4] and Sung-Hyun Han[5]

[1] S&T Dynamics Co., Ltd., Changwon, 51534, Korea(namtj1004@hanmail.net)
[2] Shinla Information Technology Co., Ltd., Changwon, 641-465, Korea (shintech@hanmail.net)
[3] Smec Co., Ltd., Changwon, 621-184, Korea (won@esmec.com)
[4] SG Servo Co., Ltd. Changwon, 641-846, Korea (rnd@sgservo.co.kr)
[5] School of Mechanical Engineering, Kyungnam University, Changwon, 51767, Korea (shhan@kyungnam.ac.kr)

Abstract: We describe a new approach to the design and real-time implementation of an adaptive controller for robotic manipulator based on digital signal processors in this paper. The Texas Instruments DSPs(TMS320C80) chips are used in implementing real-time adaptive control algorithms to provide enhanced motion control performance for dual-arm robotic manipulators. In the proposed scheme, adaptation laws are derived from model reference adaptive control principle based on the improved direct Lyapunov method. The proposed adaptive controller consists of an adaptive feed-forward and feedback controller and time-varying auxiliary controller elements. The proposed control scheme is simple in structure, fast in computation, and suitable for real-time control. Moreover, this scheme does not require any accurate dynamic modeling, nor values of manipulator parameters and payload. Performance of the proposed adaptive controller is illustrated by simulation and experimental results for robot manipulator consisting of dual arm with four degrees of freedom at the joint space and cartesian space.

Keywords: Adaptive Control, Dual-Arm Robot, Real Time Control, Real-Time Implementation

1. INTRODUCTION

This paper describes a new approach to the design of adaptive control system and real-time implementation using digital signal processors for robotic manipulators to achieve the improvement of speedness, repeating precision, and tracking performance at the joint and cartesian space.

2. MODELING

The dynamic model of a manipulator-plus-payload is derived and the tracking control problem is stated in this section.

Let us consider a nonredundant joint robotic manipulator in which the n×1 generalized joint torque vector $\tau(t)$ is related to the n×1 generalized joint coordinate vector q(t) by the following nonlinear dynamic equation of motion

$$D(q)\ddot{q} + N(q, \dot{q}) + G(q) = \tau(t) \tag{1}$$

where $D(q)$ is the n×n symmetric positive-definite inertia matrix, $N(q, \dot{q})$ is the n×1 coriolis and centrifugal torque vector, and $G(q)$ is the n×1 gravitational loading vector.

Equation (1) describes the manipulator dynamics without any payload. Now, let the n×1 vector X represent the end-effector position and orientation coordinates in a fixed task-related cartesian frame of reference. The cartesian position, velocity, and acceleration vectors of the end-effector are related to the joint variables by

$$\begin{aligned} X(t) &= \Phi(q) \\ \dot{X}(t) &= J(q)\,\dot{q}(t) \\ \ddot{X}(t) &= \dot{J}(q, \dot{q})\,\dot{q}(t) + J(q)\,\ddot{q}(t) \end{aligned} \tag{2}$$

where $\Phi(q)$ is the n×1 vector representing the forward kinematics and $J(q) = [\partial \Phi(q)/\partial q]$ is the n×n Jacobian matrix of the manipulator.

Let us now consider payload in the manipulator dynamics. Suppose that the manipulator end-effector is firmly grasping a payload represented by the point mass M_p. For the payload to move with acceleration $\ddot{X}(t)$ in the gravity field, the end-effector must apply the n×1 force vector $T(t)$ given by

$$T(t) = M_p [\ddot{X}(t) + g] \tag{3}$$

where g is the n×1 gravitational acceleration vector. The end-effector requires the additional joint torque

$$\tau_f(t) = J(q)^T T(t) \tag{4}$$

where superscript T denotes transposition. Hence, the total joint torque vector can be obtained by combining equations (1) and (4) as

$$J(q)^T T(t) = D(q)\ddot{q} + N(q,\dot{q}) + G(q) + \tau(t) \quad (5)$$

Substituting equations (2) and (3) into equation (5) yields

$$\Delta M_p J(q)^T [J(q)\ddot{q} + \dot{J}(q,\dot{q})\dot{q} - g] + D(q)\ddot{q} + N(q,\dot{q}) + G(q) + \tau(t) \quad (6)$$

Equation (6) shows explicity the effect of payload mass ΔM_p on the manipulator dynamics. This equation can be written as

$$[D(q)+\Delta M_p J(q)^T J(q)]\ddot{q} + [N(q,\dot{q}) + \Delta M_p J(q)^T \dot{J}(q,\dot{q})\dot{q}] + [G(q) - \Delta M_p J(q)^T g] + \tau(t) \quad (7)$$

where the modified inertia matrix $[D(q)+\Delta M_p J(q)^T J(q)]$ is symmetric and positive-definite. Equation (7) constitutes a nonlinear mathematical model of the manipulator-plus-payload dynamics.

3.ADAPTIVE CONTROLSCHEME

The manipulator control problem is to develop a control scheme which ensures that the joint angle vector q(t) tracks any desired reference trajectory $q_r(t)$, where $q_r(t)$ is an n×1 vector of arbitrary time functions. It is reasonable to assume that these functions are twice differentiable, that is, desired angular velocity $\dot{q}_r(t)$ and angular acceleration $\ddot{q}_r(t)$ exist and are directly available without requiring further differentiation of $q_r(t)$. It is desirable for the manipulator control system to achieve trajectory tracking irrespective of payload mass ΔM_p.

The controllers designed by the classical linear control scheme are effective in fine motion control of the manipulator in the neighborhood of a nominal operating point P_o. During the gross motion of the manipulator, operating point P_o and consequently the linearized model parameters vary substantially with time. Thus it is essential to adapt the gains of the feedforward, feedback, and PI controllers to varying operating points and payloads so as to ensure stability and trajectory tracking by the total control laws. The required adaptation laws are developed in this section.

4. SIMULATIONAND EXPERIMENT

4.1 Simulation

This section represents the simulation results of the position and velocity control of a four-link robotic manipulator by the proposed adaptive control algorithm, as shown in Fig.1, and discusses the advantages of using joint controller based-on DSPs for motion control of a dual-arm robot. The adaptive scheme developed in this paper will be applied to the control of a dual-arm robot with eighth axes. Fig.1 represents link coordinates of the dual-arm robot.

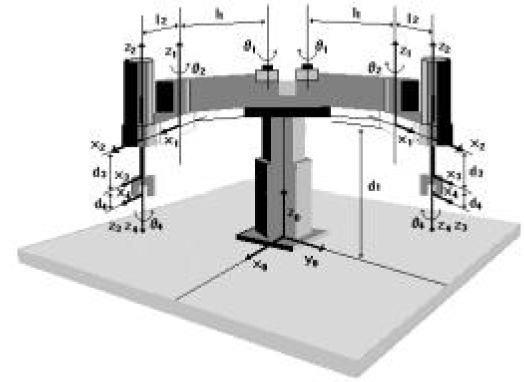

Fig.1. Link coordinates of dual-arm robot

Table 1 Link parameters of robot.

Mass of link(kg)		Length of link(kg)		Inertia of link(kg)		Gear ratio of link	
m1	15.0067	I1	0.35	I1	0.1538	r1	1/100
m2	8.994	I2	0.3	I2	0.0674	r2	1/80
m3	3.0	I3	0.175	I3	0.045	r3	1/200
m4	1.0	I4	0.007	I4	0.0016	r4	1/75
m5	15.067	I5	0.35	I5	0.1538	r5	1/100
m6	8.994	I6	0.3	I6	0.0674	r6	1/80
m7	3.0	I7	0.175	I7	0.045	r7	1/200
m8	1.0	I8	0.007	I8	0.0016	r8	1/75

Table 2 Motor parameters of robot

Rotor inertia ($kg \cdot m^2$)		Torque constant (K m/a)		Backemf constant (V s/rad)		Amaturewinding resistance(oh	
Jm1	5.0031×10^{-5}	Ka1	21.4839×10^{-2}	Kb1	214.8592 ×	Ra1	1.5
Jm2	1.3734×10^{-5}	Ka2	20.0124×10^{-2}	Kb2	200.5352 ×	Ra2	4.2
Jm3	0.8829×10^{-5}	Ka3	20.0124×10^{-2}	Kb3	200.5352 ×	Ra3	9
Jm4	0.2256×10^{-5}	Ka4	17.6580×10^{-2}	Kb4	176.6620 ×	Ra4	20
Jm5	5.0031×10^{-5}	Ka5	21.4839×10^{-2}	Kb5	214.8592 ×	Ra5	1.5
Jm6	1.3734×10^{-5}	Ka6	20.0124×10^{-2}	Kb6	200.5352 ×	Ra6	4.2
Jm7	0.8829×10^{-5}	Ka7	20.0124×10^{-2}	Kb7	200.5352 ×	Ra7	9
Jm8	0.2256×10^{-5}	Ka8	17.6580×10^{-2}	Kb8	176.6620 ×	Ra8	20

4.2 Experiment

The performance test of the proposed adaptive controller has been performed for the dual-arm robot at the joint space and cartesian space. At the cartesian space, it has been tested for the peg-in-hole tasks, repeating precision tasks, and trajectory tracking for B-shaped reference trajector. At the joint space, it has been tested for the trajectory tracking of angular position and velocity for a dual-arm robot made in Samsung Electronics Company in Korea. Fig. 4 represents the schematic diagram of control system of dual-arm robot. And Fig. 5 represents the block diagram of the interface between the PC, DSP, and dual-arm robot.

The performance test in the joint space is performed to evaluate the position and velocity control performance of the four joints under the condition of payload variation, inertia parameter uncertainty, and change of reference trajectory.

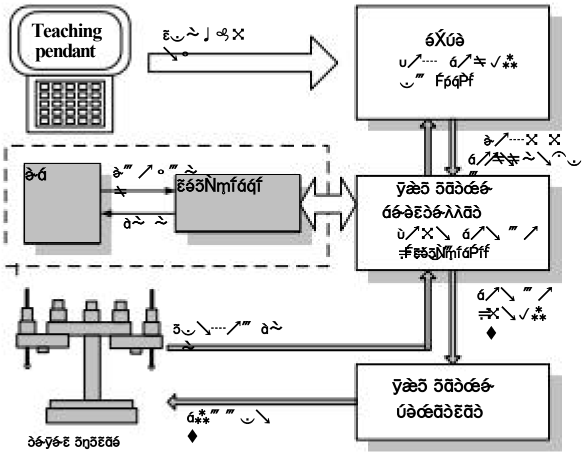

Fig. 4. The block diagram of the interface between the PC. DSP, and dual-arm robot.

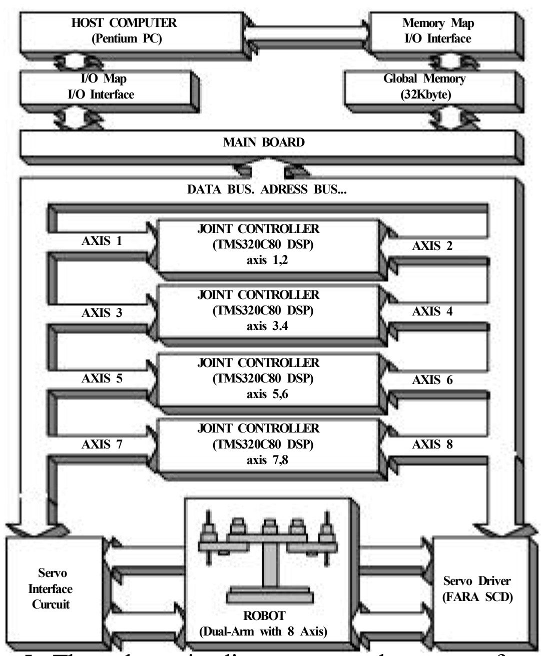

Fig. 5. The schematic diagram control system of dual-arm robot.

Fig. 6 shows the experimental results of the position and velocity control at the first joint with payload 4 kg and the change of reference trajectory

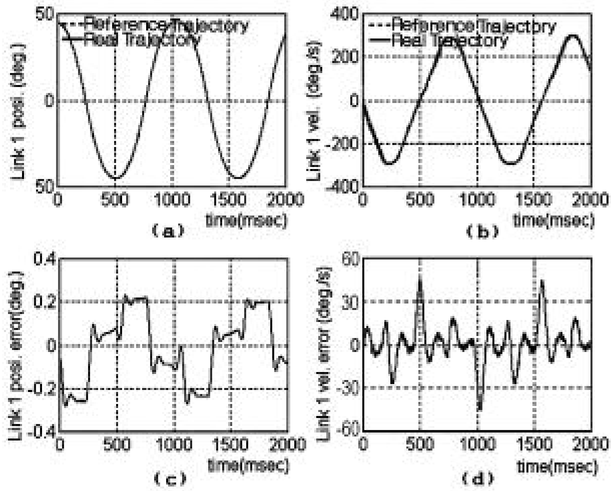

Fig. 6. (a)-(d) Experimental results for the position and velocity tracking of adaptive controller at the first joint with 4kg payload.

5. CONCLUSIONS

The proposed DSP-based adaptive controllers have several advantages over the analog control and the micro-computer based control. This allows instructions and data to be simultaneously fetched for processing. Moreover, most of the DSP instructions, including multiplications, are performed in one instruction cycle. The DSP tremendously increase speed of the controller and reduce computational delay, which allows for faster sampling operation. It is illustrated that DSPs can be used for the implementation of complex digital control algorithms, such as our adaptive control for robot systems.

REFERENCES

[1] P.C.V. Parks, July 1966, "Lyapunov Redesign of Model Reference Adaptive Control System," IEEE Trans. Auto. Contr., Vol. AC-11, No. 3, pp. 362-267.

[2] Y.K. Choi, M.J. Chang, and Z. Bien, 1986, "An Adaptive Control Scheme for Robot Manipulators." IEEE Trans. Auto. Contr., Vol. 44, No. 4, pp. 1185-1191.

[3] Y.M. Yoshhiko, June 1995, "Model Reference Adaptive Control for Nonlinear System with unknown Degrees, "In the proceeding of American Control Conference, pp.2505-2514, Seatle.

[4] S. Dubowsky, and D.T. DesForges, 1979, "The Application of Model Reference Adaptation Control to Robot Manipulators," ASME J. Dyn. Syst., Meas., Contr., Vol. 101, pp. 193-200.

2017 Changwon International Conference on Intelligent Robot and Convergence Industry (CICIRO 2017)
Nov. 30th~ Dec. 1st, 2017, Changwon Exhibition Convention Center(CECO), Changwon City, Korea

A Stable Control of Legged Robot Based on Ultrasonic Sensor

Seong-Gyu Park[1], Eun-Tae Ha[2] and Sung-Hyun Han[3]

[1] GMB Korea Corp. Co., Ltd., Changwon, 51557, Korea (paksung9@hanmail.net)

[2] Future Technology Institute Co., Ltd, Changwon, 642-939, Korea (euntha@hanmail.net)

[3] School of Mechanical Engineering, Kyungnam University, Changwon, 51767, Korea (shhan@kyungnam.ac.kr)

Abstract: This paper discusses the implementation of a binaural sensory pod using an ultrasonic emitter and two receivers on a mobile robot that employs legged-style locomotion. A series of obstacle avoidance behavior programmed onto a micro-controller allows the robot is to successfully navigate a cluttered environment both Semi-Autonomous and Automatically. Inspired by insects and other animals, robots have been designed with physical antennae and tactile sensors to navigate their environment. While insects have compliant, articulated antennae to sense their environment, mechanical antennae for mobile robots are usually less compliant and can possibly impede the robot while it is navigating difficult terrain. The use of non-contact sensors based on biological hearing can alleviate this problem. Inspired by the intramural time difference method of sound location, as used by larger animals, and using a self generated sound pulse, as in the echo location of bats, a binaural sensor pod was created using ultrasonic sensors.

Keywords: Force sensing resistor, Legged Robot, Ultrasonic Sensor, stabilization.

1. INTRODUCTION

Animals and insects use sensory systems such as hearing, and tactile inputs to move automatically through their environment the crickets and other small animals like the small brown bat have binaural hearing that relies on intensity, or level differences in the sounds received by each hearing sensor. Intensity measurement is used since the separation of the hearing organs is very small.

While insects have compliant, articulated antennae to sense their environment, mechanical antennae for mobile robots are usually less compliant and can possibly impede the robot while it is navigating difficult terrain. The use of non-contact sensors based on binaural ultrasonic sensor can alleviate this problem.

To locate objects and navigate away from them, two obstacles detection and avoidance behaviors were created.

The first behavior allowed Semi-Autonomous operation of the robot and used a simple method of detecting objects within one of three zones: left, center, and right. Objects sensed in the left or right zones caused the robot to steer away in the opposite direction. Centrally located obstacles stopped the robot's forward progress and required an operator to reverse direction and choose a new heading.

The second behavior provided the robot with full autonomy. It used a 2m sensor range and determined the azimuth of obstacles using interaural time differences. Once the location of an object was calculated, steering and drive speed were adjusted proportionately based on position and distance of the object.

The new experiments were conducted in a similar manner with a tube (1.6m long, 0.3m diameter) at various positions in front of the sensor pod. The purposes of these additional experiments were then performed to determine the new xy-plane sensor envelope for the binaural ultrasonic sensor pod. The left and right sensor envelopes mirrored one another and expanded the detection angle near the pod from 90 degrees to about 110 degrees (Fig. 1) for a distance of about 2.5m. Beyond 3m the combined envelope detected objects in a 7.5m wide path out to a range of 8.2m.

The emitter cannot send ultrasonic pulses over a range of 135 degrees while the receivers are capable of detecting echoes from angles of ±45 degrees (the full possible sensory range of two receivers angled 45 degrees apart). As a result, the sensor envelope for the binaural sensor pod is limited to 110 degrees

Using two receivers at a splayed angle created three sensory zones. There are two outer zones where only a single sensor can detect an object (colored areas of Fig. 3), and a central zone where both sensors receive echoes from the same target (white area of Fig. 1).

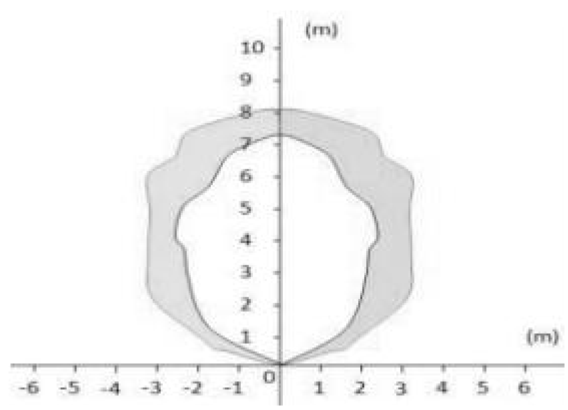

Fig. 1. Sensor envelope for the binaural ultrasonic sensor pod with a single emitter with angled dual receivers.

2. CONTROLALGORITHMS

The robot was programmed by two separate behaviors are as follows.

- Semi-Autonomous mode
- Autonomous operation mode

The microcontroller interpreted radio control commands from the receiver as initiated by the operator. The binaural sensor pod detected obstacles and corrected the robot' s course and/or speed, overriding the operator' s commands (an operator drove the robot).

Based on the detection of sensed obstacles, the three channels that control speed, steering, and the body flexion joint were all interpreted by the microcontroller and then modified.

ased on the detection of sensed obstacles, the three channels that control speed, steering, and the body flexion joint were all interpreted by the microcontroller and then modified.

Set an obstacle warning distance of 60cm as a software threshold for when the avoidance behavior would take action, the actual distance at which actions were taken varied with the angle the obstacle face had with the mid-sagittal plane. The more acute the angle, the closer the robot came to the obstacle before an automatic action was taken. In two cases, the angle of the wall with the mid-sagittal plane was very small (less than 20 degrees) and glancing impacts occurred. If an obstacle appeared in the left field, the robot would turn to the right to avoid a collision. This was accomplished by replacing the operator's intended steering control value and creating a full right turn signal to be sent to the steering servo motors instead. The operator's intended signal was still interpreted by the Microcontroller, but then ignored in favor of the behavior's control signal. Once the object was no longer detected within range, the operator's signal was once again sent to the steering servo motors. Similarly, obstacles appearing in the right field would cause the robot to steer to the left until the obstacle was no longer detected. If both left and right ultrasonic receivers detected an obstacle, indicating the presence of something in the center field, forward motion was stopped. In this case the operator could fully steer the robot between the left and right extremes, but could only drive in reverse.

This avoidance behavior created the ability for the robot to follow a wall. If the operator drove the robot forward while steering it toward a wall, the robot would approach the wall until a potential collision was detected. Then, the obstacle avoidance behavior would steer the robot away from the wall while it still moved forward. When the wall was no longer in range, the operator's steering command would resume and the robot would once again head toward the wall.

3. EXPERIMENT

The mounting placed of the emitter is approximately 12cm from the ground and the mountings of the receivers from the ground are 17cm. The binaural ultrasonic sensor pod was mounted to the front of the Walking Robot where it had an unobstructed view of the area ahead of the robot.

In some cases, the operator driving and steering was used in the obstacle course scenario when an obstacle was detected in the center field of view. During these cases, the operator controlled the robot to drive in reverse until the obstacle was no longer in range and chose a new heading when resuming forward motion.

This behavior experiments were conducted as follows. Wall-following: the operator drove the robot forward while steering toward either the left or right wall.

For the second set of trials one run was performed in each of two unique obstacle courses.

Fig. 2 (a) shows the actual path taken by the blue line. Short red lines indicate times when the operator directed the robot toward the wall but the obstacle avoidance behavior steered away from the impending collision. Five autonomous course corrections were made by the behavior and no wall collisions occurred. For these trials, 28 of 30 collisions with the wall were avoided.

Fig. 2 (b) shows semi-autonomous runs through obstacle courses. The obstacle avoidance behavior avoided 19 out of 20 collisions. In the first obstacle course the robot collided with the wall and required operator action to correct the situation. The obstacle avoidance behavior performed the correct steering action, however, the robot was too close to the wall when it was detected and it was too late to prevent the collision. There were no collisions with walls or other obstacles during the second obstacle course.

Thirty eight experiments were conducted with the Autonomous operation: 28 wall-following trials, and 10 obstacle avoidance trials.

In case of the robot was placed near a wall and activated. If the robot was close enough to the wall it approached the wall and steered away such that the angle with the wall became increasingly shallow. Also, as the robot came closer to the wall the speed decreased.

The robot continued to follow the wall until it found a corner, at which time it stopped since there was no path it could take according to the programmed behavior.

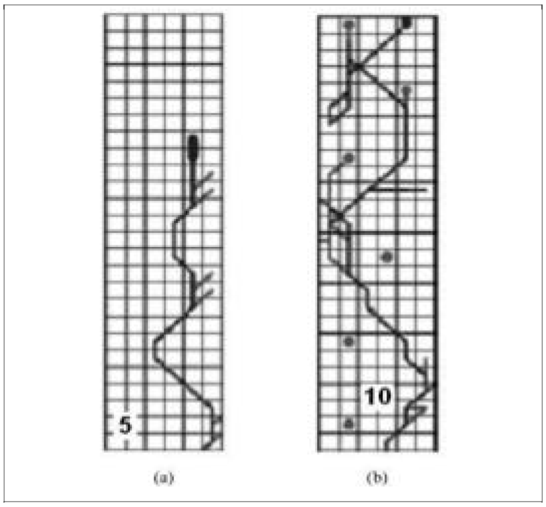

Fig. 2. The Trajectories of Mobile Robot.

- The robot moved from bottom to top.
- Red lines show the commanded path that wasn't chosen.
- Robot paths for wall following (left) and two unique obstacle courses (right).
- Numbers indicate times that an autonomous course correction was made due to a sensed obstacle.

4. CONCLUSIONS

We have discussed the implementation of a binaural sensory pod using an ultrasonic emitter and two receivers on a mobile robot that employs legged-style locomotion.

The binaural ultrasonic sensor pod and programmed avoidance behavior has proven itself useful as a mobile robot navigation aid. By using the modular design implemented for these experiments, the sensor pods could be integrated with other mobile robots to provide non-contact sensing and navigation for them as well.

REFERENCES

[1] M. Fujita and K. Kageyama, "An Open Architecture for Robot Entertainment," Proc. Inernational Conference on Autonomous Agents, pp. 435-440, 1997.

[2] M. Fujita and H. Kitano, "Development of an Quadruped Robot for Robot Entertainment," Autonomous Robots, vol. 5, pp.7-8, Kluwer Academic, 1998

[3] T. Ishida, Y. Kuroki, J. Yamaguchi, M. Fujita and T.T. Doi, "Motion Entertainment by a Small Humanoid Robot Based on OPEN-R," Int. Conf. on Intelligent Robots and Systems (IROS-01), pp.1079-1086, 2001.

[4] Y. Kuroki, T. Ishida, J. Yamaguchi, M. Fujita and T.T. Doi, "A Small Biped Entertainment Robot," Proc. Int. Conf. on Humanoid Robots, pp.181-186, 2001.

[5] William A. Lewinger, Michael S. Watson and Roger D. Quinn, "Obstacle Avoidance Behavior for a Biologically-inspired Mobile Robot Using Binaural Ultrasonic Sensors," Int. Conf. on Intelligent Robots and Systems (IROS-06), Beijing, 2006.

2017 Changwon International Conference on Intelligent Robot and Convergence Industry (CICIRO 2017)
Nov. 30th~ Dec. 1st, 2017, Changwon Exhibition Convention Center(CECO), Changwon City, Korea

A Study on Grasping Control of Robot Hand with 12 Joints

Chang-Young Lee[1], Yang-Keun Jeong[2] and Sung-Hyun Han[3]

[1] Navy Shipyard, Changwon, Korea (leecy93@hanmail.net)
[2] Shinla Information Technology Co., Ltd., Changwon, 641-465, Korea (shintech@hanmail.net)
[3] School of Mechanical Engineering, Kyungnam University, Changwon, 51767, Korea (shhan@kyungnam.ac.kr)

Abstract: Recently it is very important to control robot hands more compact and integrated sensors in order to increase compensate the grasping capability and to reduce cabling through the finger in the manipulator. As a matter of fact, the miniaturization and cabling harness represents a significant limitation to the design of small sized precise sensor. The main focus of this research is on a flexible grasping control of hand fingers, which consists of a flexible multi-fingered hand-arm system.

Keywords: Grasping Control, Hand Finger, Precise Sensing, Real Time Control

1. INTRODUCTION

The mechanical level design of robot hands is on the actuation and motion control aspects. With very few exception([1]-[2]), tendon actuated mechanisms, and their numerous variants, still represent an effective way to implement compact manipulators. Actuation of tendon based robot grippers poses various technical problems. Tendons coupling on one hand, friction and elasticity on the other, pose important problems for the control of tendon actuated mechanisms. However, the mechanical accuracy required to design a miniature (e.g. human sized) dexterous gripper, is by far less than an equivalent design based on gears or other stiff transmission mechanism. Recently the tendency is to create robot hands more compact and high integrated sensors system, in order to increase the grasping capability and in order to reduce cabling through the finger, the palm and the arm. As a matter of fact, miniaturization and cabling harness represents a significant limitation to the design of small sized embedded sensor([3]). The major contribution of this paper is to present the design of a fully integrated tactile and 3-axis force sensor, with embedded electronics. The approach adopted has been that of using low cost components available off-the-shelf, and to pursue a highly modular sensor design.

2. HAND DESIGN

The mechanism of a flexible hand gripper requires the mass of the hand should be as low as possible. It is highly desirable that the hand weigh less than 1kg. Furthermore the low mass of the finger mechanism is desirable not only to achieve flexible motion but also for stable control.

Our study about dynamic manipulation is maximization of the power and minimization of the mechanism. In particular four factors are important: (1)light weight, (2) high speed and high acceleration, (3) accuracy, possibilities of flexible grasping. The Fig. 1 shows the mechanical design of the hand, and Fig. 2 shows a scene of the Gripper control. We used three fingers, which is the minimum number to achieve a stable grasp. Each of fingers has 4 degrees of freedom (D.O.F); the hand system has 12 D.O.F included 1 D.O.F on the hand link. Note that the Joint 4 consists of the linear motor so that the finger tip can move as slide but other links just moving as rotate around a horizontal axis. In general a hand needs 9 D.O.F to move a target to any position and orientation. But our hand has 12 D.O.F so that the applications are very wide in the working environments, and the fingers are arranged so as to grasp the objects like circular and prismatic, etc. In order to achieve high acceleration, we have developed a new actuator that allows a large current flow for a short time. Table 1 shows the specification for the actuator.

The finger has strain gauges at the joint 1 and joint 2 for force control. In addition a 6-axis force/torque sensor and a tactile sensor are mounted on each fingertip.

The flexible motion imposes a heavy load on the finger mechanism. For this reason a simple mechanism should be used for reduction gear, transmission, etc. In most traditional hand systems a wire-driven mechanism is used. But this is not suitable for a lightweight mechanism, because it is large and complicated.

In our hand a newly developed small harmonic drive gear and a high-power mini actuator are fitted in each finger link and all of these parts are hidden in the plastic case. A harmonic drive gear has desirable properties for control such as no backlash and a high reduction rate.

Vision is with a massive parallel vision system called column-parallel high-speed vision system [2].
Early image processing is performed in order to achieve segmentation of the image, extraction of the target area, and computation of the image moments. From these data, the position of the target is computed; each vision sensor is mounted on an active vision.

Manipulation control requires in general some sort of feedback which could provide information about the interactions occurring during contact between the gripper and the grasped object. Assumptions must be made about the nature of the contact and, on the base of the selected contact models, it is possible to specify the nature of feedback required to properly control the interaction. Detailed contact mechanics models are in general too complex to be taken into account in real-time control applications. In practice, simplified lumped parameter models are usually considered [3]. In the soft finger model it is assumed that also a torque, aligned with the normal to the surfaces in contact, arises. The model equations for these models are:

$$\begin{cases} f = p \\ m = q + c \times p \end{cases} \quad (1)$$

Where **p** and **q** are the contact force and torque (for soft finger models only), **c** is the contact location, and **f** and **m** are the measured force and torque. Bicchi and Salisbury, [3], proposed procedures for computing **p** and **q** on the base of the measurements **f** and **m**. However a precise geometric model of the pressure (the robot finger) is required, and, except the case of simple geometries, the method is computationally intensive and critical for real-time implementation.

A direct solution to the contact problem would be obviously possible if the contact location c would be directly measured. Therefore the availability of a direct force measurement and of the contact location allows directly solving the point contact problem.

At system level the goal is to develop to an integrated tactile/force sensors with embedded electronics to be placed on the phalanges of three fingers. The relevant problems considered have been: choice of appropriate force transducers, pressure transducers for contact measurements, integrated electronic design.

The tactile transducer is a matrix of 64 electrodes covered by a layer of pressure sensitive conductive rubber (PCR Co. Ltd.). The electrodes are etched on a flexible PCB substrate in order to conform to a cylindrical surface. A thin elastic sheet covers the whole sensor and provides a mild preload useful to reduce noise. Pressure due to contacts produces changes of resistance among the electrodes. The geometry of the electrodes Fig. 2, has been defined with the goal of limiting the spurious currents that may occur across the various electrodes, and interfere with measurement, as discussed in [3].

Tactile data are sampled by the on-board MCU, with 10 bit resolution. Preliminary tests show an actual sensor resolution of 8 bit/taxel. Each tactile image consists of 64 taxels.

During contact, a number of adjacent taxels are subject to pressure. The analog output of the tactile sensor allows to measure the distribution of pressure over all the transducer. Therefore, we propose to compute the contact centroid [3], as

$$\hat{C} = \frac{\sum_{i=1}^{N}\sum_{j=1}^{N} x_{ij}.p(x_{ij})}{\sum_{i=1}^{N}\sum_{j=1}^{N} p(x_{ij})} \quad (2)$$

where $\hat{C}$ is the computed contact centroid, $\mathbf{x}_{ij}$ is the coordinate of the taxel and $p(\mathbf{x}_{ij})$ the weight of this. As a matter of fact further geometric information about the distribution of the pressure during contact could be useful, although not directly relevant to point contact model solution. To this aim the pressure distribution is approximated as an ellipsoid, as follows:

$$E = \frac{\sum_{i=1}^{N}\sum_{j=1}^{N} (x_{ij} - \hat{C})(x_{ij} - \hat{C})^{T}.p(x_{ij})}{\sum_{i=1}^{N}\sum_{j=1}^{N} p(x_{ij})} \quad (3)$$

Where **E** is a symmetric matrix who represent the ellipsoid. The approach used to compute and the associated approximate ellipsoid, is strongly based on the availability of an analog tactile sensor.

3. EXPERIMENT

The main advantage of a multi-fingered hand is that it can grasp various objects by changing its shape. Several classifications of grasping have been proposed. In this proposal various grasps are classified into three large categories: a power grasp that passively resists arbitrary external forces exerted on the object, a precise grasp to manipulate the object, and an intermediate grasping which some fingers are used for a power grasp and the other fingers are used for a precise grasp.

We achieved these typical grasp types in our developed hand. Table1 shows the specification of robot hand.

Catching is one of the most important tasks for dynamic manipulation. In this section catching is shown using our flexible hand with a visual feedback controller. We used a rubber ball with radius of 5cm as a target, and we dropped it from about 1.2m in height. The speed of the falling ball is about 5.9m/s just before it hits the ground.

Table. 1. The specification of robot hand.

Total D.O.F	12
Weight [g]	600
Max. Speed at a finger tip [m/s]	3.3
Max. force at a finger tip [N]	27
Joint resolution [deg]	0.36

From various experimental trials, we have decided on the catching strategy shown in Fig. 1.

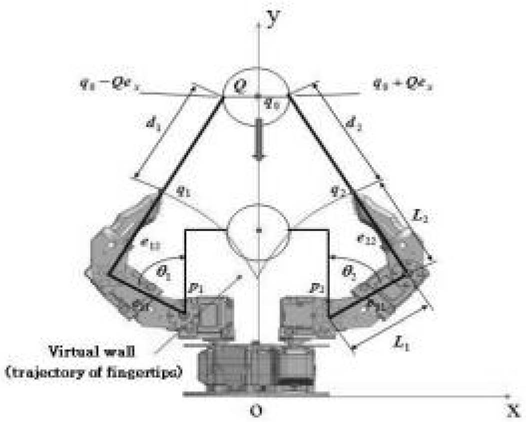

Fig. 1. The coordinates system for catching algorithm of grasping.

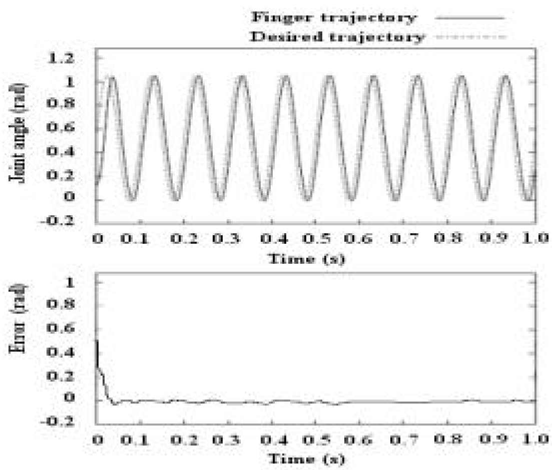

Fig. 2. Results of performance experiment for trajectory control.

when we changes the distance d1 and d2, X-Y axis, q_o, d1 and d2 were defined in Fig. 1 and Fig. 2 shows the results when we changes the target position q_o.

4. CONCLUSION

An integrated force and tactile sensor with embedded electronics has been presented in a lightweight flexible hand with 12 D.O.F, and the associated visual feedback control. The sensor consists of a three components commercial force sensor and of a custom matrix tactile sensor based pressure sensitive conductive rubber. The joint used of both tactile and force information allows the direct solution of the point contact problem. A technique to compute the contact centroid and a quadratic approximation of the pressure distribution during contact has been proposed. Ongoing work is focusing on a flexible manipulation system, which consists of a dual flexible multi-fingered hand-arm system, and a dual active vision system. In the future this new hand-arm system will be used for multi tasks.

The need for a robotic hand that works in the real world is growing. And such a system should be able to adapt to changes in environment. We think that the concept of a flexible hand system with real-time control implementation will become an important issue in robotic research.

ACKNOWLEDGEMENT

This work was supported (National Robotics Research Center for Robot Intelligence Technology, Kyungnam University) by Ministry of Knowledge Economy under Human Resources Development Program for Convergence Robot Specialists.

REFERENCES

[1] S. Toyama, S. Hatae and S. Sugitani, “Multi-Degree of spherical ultrasonic motor”, Proc. ASME Japan/USA Sympo. Flexible Automation, 169, 1992

[2] Anotonio Bicchi, J. Kennedy Salisbury, David L. Brock ”Contact Sensing from Force Measurements” International Journal of Robotics Research. Vol. 12, No. 3, June 1993.

[3] S.C.Jacobsen, E.K. Iversen, D.F. Knutti, R.T. Johnson andK.B. Biggers, “Design of the Utah/MIT dexterous hand”, Proc. IEEE Int. Conf. On Robotics and Automation, pp. 1520-1532, 1986

2017 Changwon International Conference on Intelligent Robot and Convergence Industry (CICIRO 2017)
Nov. 30th~ Dec. 1st, 2017, Changwon Exhibition Convention Center(CECO), Changwon City, Korea

A Study on Intelligent Control of Humanoid Robot with Voice recognition

Min-Hwan Lee[1], Woo-Song Lee [2] and Sung-Hyun Han[3]
[1] SUNGJIN PRECISION Co., Ltd., Haman, 52027, Korea (minhwanlee01@naver.com)
[2] SUNJIN Technology Co., Ltd., Changwon, 82331, Korea
(elflws@nate.com)
[3] School of Mechanical Engineering, Kyungnam University,
Changwon, 51767, Korea (shhan@kyungnam.ac.kr)

Abstract: Generally, it is possible to control the motion by using information on the robot's own postures, because a type of motion and gesture produces almost the same pattern of noise every time. In this paper, we describe an voice recognition control system for robot system which can robustly recognize voice by adults and children in noisy environments. We evaluate the performance of robot control system in a communication robot placed in a real noisy environment. Voice is captured using a wireless microphone. To suppress interference and noise and to attenuate reverberation, we implemented a multi-channel system consisting of an outlier-robust generalized side-lobe canceller technique and a feature-space noise suppression using criteria. Voice activity periods are detected based end-point detection

Key words: Robust voice recognition, Side-lobe canceller, navigation system

1. INTRODUCTION

To make human-robot communication natural, it is necessary for the robot to recognize voice even while it is moving and performing gestures. For example, a robot's gesture is considered to play a crucial role in natural human-robot communication [1-4]. In addition, robots are expected to perform tasks by physical actions to make a presentation. If the robot can recognize human interruption voice while it is executing physical actions or making a presentation with gestures, it would make the robot more useful.

Each kind of robot motion or gesture produces almost the same noises every time it is performed. By recording the motion and gesture noises in advance, the noises are easily estimated. By using this, we introduce a new method for VRCS under robot motor noise. Our method is based on three techniques, namely, multi-condition training, maximum-likelihood linear regression[5], and missing feature theory. These methods can utilize pre-recorded noises as described later. Since each of these techniques has advantages and disadvantages, whether it is effective depends on the types of motion and gesture. Thus, just combining these three techniques would not be effective for voice recognition under noises of all types of motion and gestures. The result of an experiment of isolated word recognition under a variety of motion and gesture noises suggested the effectiveness of this approach. In what follows, Section 2 discusses the design of voice recognition system, and Section 3 explains our method for avoid the obstacles by navigation strategy. Section 4 describes the recognition, navigation experiments, and the results, before conclusion and mentioning future work in Section 5.

2. CONTROLSCHEME

Accounting for the two problems (caused by noisy environments and differences on speaker age) described in Section I, we developed an RVR system to be robust on background noise and speakers of different ages. The first block is a front-end processing. It contains a microphone wireless transmitter. The real-time wireless microphone system for suppressing interference and noise and for attenuating reverberation consists of an outlier-robust generalized side-lobe canceller and feature-space noise suppression. In the second block, there are two decoders depending on the age of the speaker (adult or child); each decoder works using gender-dependent acoustic models. Noise-suppressed voice at the first block is recognized using these two decoders, and one hypothesis is selected based on posterior probability.

The proposed robot system has three wheels; two driven wheels fixed at both sides of the mobile robot and one castor attached at the front and rear side of the robot. The ultrasonic sensors are mounted around of the mobile robot in middle layer for the detection of obstacles with various heights. In this study, a sonar array composed of 16 ultrasonic sensors cannot be fired simultaneously due to cross talk. Instead, we adopt a scheduled firing method where sensors are activated in sequence of $\{s_1, s_{12}, s_2, s_{11} \ldots\}$. The arrangement of the ultrasonic sensors in upper layer and the sensors are marked as dots in the figure. The distances e_j $(j = 1, 2, \ldots 12)$ from the origin of the robot frame {R} to obstacles detected by the sensor s_j, can be defined as $e_j = \underline{\Omega}_j + R_r$. Here, R_r is the radius of the robot and the $\underline{\Omega}_j$, is the range value measured by the sensor s_j .

A local map is introduced to record the sensory information provided by the 16 sonar sensors with respect to the mobile robot frame $\{R\}$. Sector map defined locally at the current mobile robot frame is introduced. Then, the obstacle position vector se'_j with respect to the frame $\{R\}'$ can be calculated by

$$Se_j = \begin{bmatrix} \cos\delta\theta & \sin\delta\theta & 0 & -\sin\delta\theta/\rho_p \\ -\sin\delta\theta & \cos\delta\theta & 0 & (1-\cos\delta\theta)/\rho_p \\ 0 & 0 & 1 & 0 \\ 0 & 0 & 0 & 1 \end{bmatrix} \quad (1)$$

where se_j denotes the obstacle position vector defined at the frame $\{R\}$. When the mobile robot is located at a point $0'$. the distance value $se'_j = \| se'_j \|$ from the origin of the frame $\{R\}'$ to the obstacle and angle $s\varphi'$ can be calculated by Eq.(1) . Here, $\|.\|$ denotes Euclidean norm.

The local map defined at the frame $\{R\}'$ is newly constructed by using the previous local map defined at the frame $(R\}$ as follows:

$$Se_n \leftarrow Se_{j,n} = INT\left(\frac{s\varphi'_j N}{\pi} + \frac{1}{2}\right); \; j = 1,2,..., N \quad (2)$$

Where $\leftarrow$ and INT denote the updating operation and integer operation, respectively. Here, se_n, denotes the distance value of n sector and N represents the number of the sector. If the range values obtained by sensors when the mobile robot is located at a point o' are e_j = (j = 1,2 ,... 12) , the new local map is partially updated as follows :
$se_j \leftarrow e_j$, j = 1,2 .... $12.$ The maximum range of the sonar sensor is set to be $\rho_{max} = \rho_{max} - R_r$. Any return range which is larger than is ignored.

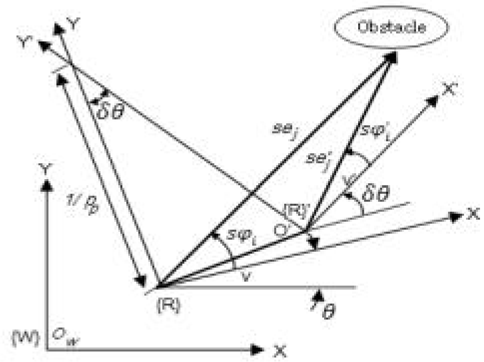

Fig. 1 The coordinate transformation for updating the local map

The primitive behaviors may be divided as follows: goal-seeking behavior, ball-following behavior, keep-away behavior, free space explorer and emergency stop, etc. The output of a primitive behavior is defined by the vector.

$$u(t) = (v(t), \omega(t))^T = (v(t), w(t), Tms)^T \quad (3)$$

where t and T_{ms} denote the time step and the sampling time, respectively. Here, T denotes the transpose and $\omega(t)$ denotes the angular velocity of the robot.
We will divide the primitive behaviors into two basic: avoidance behavior and goal-seeking behavior.
The avoidance behavior is used to avoid the obstacles irrespective of the goal position, while the goal-seeking behavior is used to seek the goal position irrespective of obstacle location. Design of each behavior proceeds in following sequences;
(A) fuzzification of the input/output variables, (B) rule base construction through reinforcement learning, (C) reasoning process, (D) defuzzification of output variables.
In order for the mobile robot to arrive at the goal position without colliding with obstacles, we must control the mobile robot motion in consideration of the obstacle position X_{oi}, = (x_{oi}, y_{oi}) , the mobile robot position $X = (x , y)$ and its heading angle θ with respect to the world coordinate frame $\{W\}$ shown in Fig. 1.

In order to avoid the increase in the dimension of input space, the distance values d_i , (i = 1.2,3,4) are defined by

$$d_1 = \min(se_1, se_2, se_3)$$
$$d_2 = \min(se_4, se_5, se_6) \quad 4a$$
$$d_3 = \min(se_7, se_8, se_9) \quad 4b$$
$$d_4 = \min(se_{10}, se_{11}, se_{12})$$

$\phi_m(-\pi \leq \phi_m \leq \pi)$ denotes the orientation of a sector with the shortest range. We choose the input variables for avoidance behavior as ϕ_m and $d_i = \| X_{0i} - X \|, (i = 1,2,3,4)$ for goal-seeking behavior as heading angle difference ψ and distance to goal $z = \| X_g - X \|$. The input linguistic variables d_i, ψ, ϕ_m and z are expressed by linguistic values (VN, NR, FR), (NB, NM, ZZ, PS, PM, PB), (LT, CT, RT) and (VN, NR, FR, VF), respectively Their membership functions are expressed .

3. EXPERIMENTS

All the parameters used in the navigation experiments are given in Table 1. The proposed robot has the maximum travel speed of 0.52 m/s and the maximum steering rate of 2.0rad/sec. Experiments are performed in an indoor with the first experiment for voice recognition without objects and second experiment for both of them: voice recognition and obstacles avoidance.

Through a series of the navigation experiments, it was observed that the heading angle error is a serious problem to the proposed robot depend on dead reckoning The large heading angle error almost resulted from the uncertain parameters when the mobile robot changes its direction Even if the wheel slippage occurs, the true position and heading angle of the mobile robot could be updated by two beacon pairs and consequently the mobile robot could arrive at the given goal position while avoiding the obstacles.

4. CONCLUSIONS

We have proposed the integration of robust voice recognition and navigation system capable of performing autonomous navigation in unknown environments. In order to evaluate the performance of the overall system, a number of experiments have been undertaken in various environments. The experimental results show that the mobile robot with the complete voice recognition and navigation system can arrive at the goal position according to the desire of speaker even if the wheel slip occurs. From the developed of voice recognition and navigation system, it was observed that the mobile robot can successfully arrive at the desired position through the unknown environments without colliding with obstacles.

ACKNOWLEDGEMENT

This work was supported (National Robotics Research Center for Robot Intelligence Technology, Kyungnam University) by Ministry of Knowledge Economy under Human Resources Development Program for Convergence Robot Specialists.

REFERENCES

[1] S. Yamamoto, K. Nakadai, H. Tsujino, and H. Okuno, “Assessment of general applicability of robot audition system by recognizing three simultaneous speeches.” in Proc. of IEEE/RSJ International Conference on Intelligent Robots and Systems (IROS-2004). IEEE and RSJ, 2001, p. to appear.

[2] P. Renevey, R. Vetter, and J. Kraus, “Robust speech recognition using missing feature theory and vector quantization,” in Proc. Of Eurospeech-2001. ESCA, 2001, pp. 1107–1110.

[3] J. Barker, M. Cooke, and P. Green, “Robust asr based on clean speech models: An evaluation of missing data techniques for connected digit recognition in noise,” in Proc. of Eurospeech-2001. ESCA, 2001, pp. 213–216.

[4] R. P. Lippmann, E. A. Martin, and D. B. Paul, “Multi-style training for robust isolated-word speech recognition,” in Proc. of ICASSP-87. IEEE, 1987, pp. 705–708.

[5] M. Blanchet, J. Boudy, and P. Lockwood, “Environment adaptation for speech recognition in noise,” in Proc. of EUSIPCO-92, vol. VI,1992, pp. 391–394.

2017 Changwon International Conference on Intelligent Robot and Convergence Industry (CICIRO 2017)
Nov. 30th~ Dec. 1st, 2017, Changwon Exhibition Convention Center(CECO), Changwon City, Korea

A Study on Robust Control of Articulated Robot Arm with Seven Joints

Hee-Jin Kim[1], Sung-Cheol Jang[2], and Sung-Hyun Han[3]

[1] M.S Course, Manigement & Industry
Graduate School Kyungnam University, 51767,
Korea (E-mail : jizhen79@nate.com)
[2] Dept. of Aviation Mechatronics, Korea Aviation Polytechnic College,
Sacheon, 664-708, Korea (scjang@kopo.ac.kr)
[3] School of Mechanmical Engineering, Kyungnam University,
Changwon, 51767, Korea (shhan@kyungnam.ac.kr)

Abstract: In this paper, we present two kinds of robust control schemes for robot system which has the parametric uncertainties. In order to compensate these uncertainties, we use the neural network control system that has the capability to approximate any nonlinear function over the compact input space. In the proposed control schemes, we need not derive the linear formulation of robot dynamic equation and tune the parameters. We also suggest the robust adaptive control laws in all proposed schemes for decreasing the effect of approximation error. To reduce the number of neural of network, we consider the properties of robot dynamics and the decomposition of the uncertainty function. The proposed controllers are robust not only to the structured uncertainty such as payload parameter, but also to the unstructured one such as friction model and disturbance. The reliability of the control scheme is shown by computer simulations and experiment of robot manipulator with 7 axis.

Keywords: Robust control, decomposition, neural network, robot dynamics, uncertainty

1. INTRODUCTION

To overcome these difficulties, in this paper we propose the adaptive control schemes which utilize a neural network as a compensator for any uncertainty. To reduce the error between the real uncertainty function and the compensator, we design simple and robust adaptive laws based on Lyapunov stability theory. In the proposed control schemes, the NN compensator has to see many neural because uncertainties depend on all state variables. To overcome this problem, therefore, we introduce the control schemes in which the number of neural of the NN compensator can be reduced by using the properties of robot dynamics and uncertainties.

2. DYNAMIC MODELING

A robot manipulator is defined as an open kinematic chain of rigid links. Each degree of freedom of the manipulator is powered by independent torques. Using the Lagrangian formulation, the equations of motion of an -degree-of-freedom manipulator can be written as

$$D(q)\ddot{q} + C(q,\dot{q})\dot{q} + G(q) + F_r(\dot{q}) + \tau_d = \tau \quad (1)$$

where $q \in R^n$ is the generalized coordinates; $D(q) \in R^{n\times n}$ is the symmetric, bounded, positive-definite inertia matrix; vector $C(q,\dot{q})\dot{q} \in R^n$ presents the centripetal and Coriolis torques; $\tau_d \in R^n$, $G(q) \in R^n$, $F_r(\dot{q}) \in R^n$ and $\tau \in R^n$ represent the gravitational torques, friction, disturbance, and applied joint torques, respectively.

The robot model (1) is characterized by the following structural properties.

Property 1: There exists a vector $\theta \in R^m$ with components depending on manipulator parameters (masses, moments of inertia, etc.), such that

$$D(q)\ddot{q}_r + C(q,\dot{q})\dot{q}_r + G(q) + F_r(\dot{q}) + \tau_d = Y(q,\dot{q},\ddot{q})\theta \quad (2)$$

where $Y(q,\dot{q},\ddot{q}) \in R^{n\times m}$ is called the regressive matrix.

This property means that the dynamic equation can be linearized with respect to a specially selected set of manipulator parameters.

Property 2: Using a proper definition of matrix $C(q,\dot{q})$, both $C(q,\dot{q})$ and $D(q)$ are not independent and satisfy

$$x^T(\dot{D} - 2C)x = 0, \quad \forall x \in R^n \quad (3)$$

that is, $(\dot{D} - 2C)$ is a skew-symmetric matrix.

This property is simply a statement that the so-called fictitious forces, defined by $C(q,\dot{q})\dot{q}$, do not work on the system. This property is utilized in stability analysis.

Property 3: The friction in the dynamic equation (1) is of the form

$$F_r(\dot{q}) = F_v\dot{q} + F_d(\dot{q}) \quad (4)$$

with F_v the coefficient matrix of viscous friction and $F_d(\dot q)$ a dynamic friction term. Since friction is a local effect, $F_r(\dot q) = F_v \dot q + F_d(\dot q)$ is uncoupled among the joints. The friction is dependent on only angular velocity $\dot q$.

This property is utilized in this paper in order to reduce the number of neural in the neural network compensator.

The considered tracking problem is stated as follows: Knowing desired trajectories $q_d \in R^n$, $\dot q_d \in R^n$, with some or all the manipulator parameters unknown, determine a control law τ and a sliding surface $s = 0$ such that sliding mode occurs on the sliding surface, the tracking error $\tilde q = q - q_d$ has a prescribed transient response and it goes to zero asymptotically as $t \to \infty$.

A. Simple Adaptive Control Law

The sliding surfaces $s = 0$ is chosen as a hyperplane

$$s = \dot{\tilde q} + \Lambda \tilde q \quad (5)$$

where Λ is a positive-definite matrix whose eigenvalues are strictly in the right-half complex plane and $\tilde q$ is the tracking error vector.

If the sliding mode exists on $s = 0$, then from the theory of VSS, the sliding mode is governed by the following linear differential equation whose behavior is dictated by the sliding hyperplane design matrix Λ :

$$\dot{\tilde q} = -\Lambda \tilde q \qquad (6)$$

Obviously, the tracking error transient response is then determined entirely by the eigenvector structure of the matrix Λ.

In order to derive the sliding mode control law, which forces the motion of the error to be along the sliding surface $s = 0$, a vector of self-defined reference variables is introduced for the succinct formula expression in the sequel, that is,

$$\dot q_r(t) = \dot q_d(t) - \Lambda \tilde q(t) \quad (7)$$

Consider now the uncertainties of robot manipulator, (1) can be rewritten as

$$D(q)\ddot q + C(q,\dot q)\dot q + G(q) + F(q,\dot q,t) = \tau \qquad (8)$$

Where $F(q,\dot q,t) = F_r(\dot q) + \tau_d$. However, in this paper, this uncertainty function vector has to be replaced by $F(q,\dot q,\ddot q,t)$.

So (8) can be rewritten as

$$D(q)\ddot q + C(q,\dot q)\dot q + G(q) + F(q,\dot q,\ddot q,t) = \tau \quad (9)$$

we let a Lyapunov function candidate be

$$V(t) = \frac{1}{2}\left(s^T D s + \sum_{i=1}^{n} \tilde\theta_i^T \Gamma_i \tilde\theta_i\right) \qquad (10)$$

Where $\tilde\theta_i = \theta_i^* - \theta_i$ is the j th column vector of the optimal parameter matrix θ^* and Γ_i is a strictly positive real constant.

Differentiating $V(t)$ with respect to time yields

$$\dot V(t) = s^T D \dot s + \frac{1}{2} s^T \dot D s + \sum_{i=1}^{n} \tilde\theta_i^T \Gamma_i \dot{\tilde\theta}_i$$

$$= -s^T (D\ddot q_r + C\dot q_r + G + F - \tau) + \sum_{i=1}^{n} \tilde\theta_i^T \Gamma_i \dot{\tilde\theta}_i \qquad (11)$$

Where $F(q,\dot q,\ddot q,t)$ is a completely unknown nonlinear function vector. Therefore, we replace $F(q,\dot q,\ddot q,t)$ by a Neural network $\hat F(q,\dot q,\ddot q|\theta)$. Let us define the control law as

$$\tau = D(q)\ddot q_r + C(q,\dot q)\dot q_r + G(q) + \hat F(q,\dot q,\ddot q|\theta) - K_D s \quad (12)$$

Where $K_D = \mathrm{diag} K_i$, $i = 1,2,...,n$, and

$$\hat F(q,\dot q,\ddot q|\theta) = \begin{bmatrix} \theta_1^T \xi(q,\dot q,\ddot q) \\ \theta_2^T \xi(q,\dot q,\ddot q) \\ \vdots \\ \theta_n^T \xi(q,\dot q,\ddot q) \end{bmatrix} \qquad (13)$$

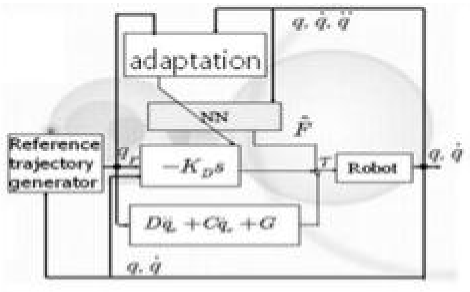

Fig. 1. the structure of the control systems

3. EXPERIMENT AND RESULTS

We also apply real-time adaptive control based on neural network compensator to dual-arm robot shown in figs. 2 – 3. Because the characteristics of two arms are the same, so we show the results into one arm is enough.

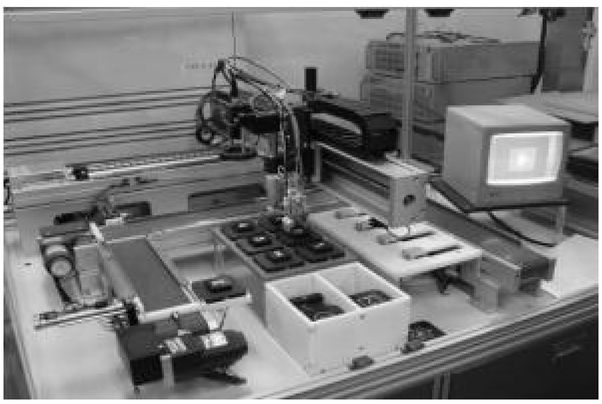

Fig. 2. Experimental set-up

All the algorithm calculation is calculated by Matlab and Simulink matlab on host computer and push into dual-arm robot which is shown in the Fig. 3. The desired trajectories are

$q_{1d} = q_{2d} = 15^{\circ} \sin(\frac{2\pi}{300} t + \frac{2\pi}{3})$ and the

results of robust adaptive control are shown below

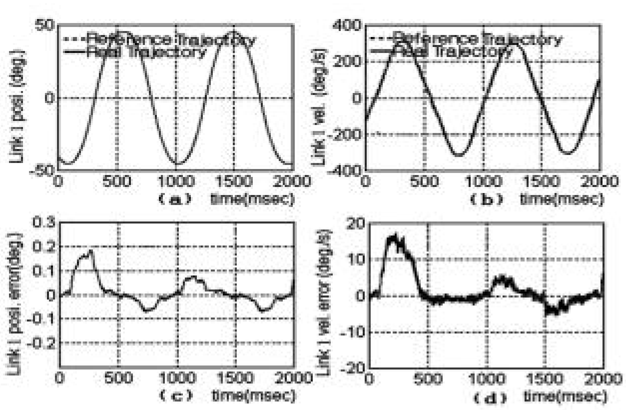

Fig. 3. (a)-(d) Experimental results for the position and velocity tracking of adaptive controller at the first joint.

4. CONCLUSIONS

In this paper, we have illustrated that the control objective is well accomplished and the neural network compensate the uncertainties. In addition, the proposed control technology needs to apply to robot manipulators include more joints, and degree of freedom.

ACKNOWLEDGEMENT

This work was supported by the Technology Innovation Program, 10045252, Development of robot task intelligence technology, funded by the Ministry of Trade, Industry & Energy (MOTIE, Korea).

REFERENCES

[1] J. E. Slotin and S. S. Sastry, “Tracking control of nonlinear systems using sliding surfaces, with application to robot manipulators,” Int. J. Contr., vol. 38, no. 2, pp. 465–492, 1983.

[2] J. J. E. Slotine and W. Li, Applied Nonlinear Control. Englewood Cliffs, NJ: Prentice-Hall, 1991.

[3] F. L. Lewis, C. T. Abdallah, and D. M. Dawson, Control of Robot Manipulators. London, U.K.: Macmillan, 1993.

[4] M. W. Spong, Robot Dynamics and Control. New York: Wiley, 1989.

[5] W. C. Ham, “Adaptive nonlinear control of one-link flexible arm,” in IEEE/RSJ Int. Conf. Intelligent Robots and Systems, vol. 1, Yokohama, Japan, 1993, pp. 3–7.

[6] “Adaptive control based on explicit model of robot manipulators,” IEEE Trans. Automat. Contr., vol. 38, pp. 654–658, 1993.

[7] “Adaptive control based on speed gradient algorithm for robot manipulators,” in Int. Conf. Industrial Electronics Control and Instrumentation, vol. 2, Bologna, Italy, 1994, pp. 776–781.

[8] B.K. Yoo, W.C. Ham “Adaptive Control of Robot Manipulator Using Fuzzy Compensator”. IEEE transaction on Fuzzy System. VOL. 8. NO. 2. April 2000.

2017 Changwon International Conference on Intelligent Robot and Convergence Industry (CICIRO 2017)
Nov. 30th~ Dec. 1st, 2017, Changwon Exhibition Convention Center(CECO), Changwon City, Korea

A Study on Robust Control of Robotic Hand with 14 Joints for cooperate Working

Young-Tae Back[1], Yang-Keun Jeong[2] and Sung-Hyun Han[3]

[1] S&T Dynamics Co., Ltd., Changwon, 51534, Korea(younhtb7@naver.com)
[2] Shinla Information Technology Co., Ltd., Changwon, 641-465, Korea (shintech@hanmail.net)
[3] School of Mechanical Engineering, Kyungnam University, Changwon, 51767, Korea (shhan@kyungnam.ac.kr)

Abstract: Recently it is very important to control robot hands more compact and integrated sensors in order to increase compensate the grasping capability and to reduce cabling through the finger in the manipulator. As a matter of fact, the miniaturization and cabling harness represents a significant limitation to the design of small sized precise sensor. The main focus of this research is on a flexible grasping control of hand fingers, which consists of a flexible multi-fingered hand-arm system.

Keywords: Grasping Control, Hand Finger, Precise Sensing, Real Time Control

1. INTRODUCTION

Actuation of tendon based robot grippers poses various technical problems. Tendons coupling on one hand, friction and elasticity on the other, pose important problems for the control of tendon actuated mechanisms. However, the mechanical accuracy required to design a miniature (e.g. human sized) dexterous gripper, is by far less than an equivalent design based on gears or other stiff transmission mechanism. Recently the tendency is to create robot hands more compact and high integrated sensors system, in order to increase the grasping capability and in order to reduce cabling through the finger, the palm and the arm. As a matter of fact, miniaturization and cabling harness represents a significant limitation to the design of small sized embedded sensor.

2. SYSTEM DESIGN

The mechanism of a flexible hand gripper requires the mass of the hand should be as low as possible. It is highly desirable that the hand weigh less than 1kg. Furthermore the low mass of the finger mechanism is desirable not only to achieve flexible motion but also for stable control.

Our study about dynamic manipulation is maximization of the power and minimization of the mechanism. In particular four factors are important: (1)light weight, (2) high speed and high acceleration, (3) accuracy, possibilities of flexible grasping.

The flexible motion imposes a heavy load on the finger mechanism. For this reason a simple mechanism should be used for reduction gear, transmission, etc. In most traditional hand systems a wire-driven mechanism is used. But this is not suitable for a lightweight mechanism, because it is large and complicated.

In our hand a newly developed small harmonic drive gear and a high-power mini actuator are fitted in each finger link and all of these parts are hidden in the plastic case. A harmonic drive gear has desirable properties for control such as no backlash and a high reduction rate.

Vision is with a massive parallel vision system called column-parallel high-speed vision system [2].
Early image processing is performed in order to achieve segmentation of the image, extraction of the target area, and computation of the image moments. From these data, the position of the target is computed; each vision sensor is mounted on an active vision.

Manipulation control requires in general some sort of feedback which could provide information about the interactions occurring during contact between the gripper and the grasped object. Assumptions must be made about the nature of the contact and, on the base of the selected contact models, it is possible to specify the nature of feedback required to properly control the interaction. Detailed contact mechanics models are in general too complex to be taken into account in real-time control applications. In practice, simplified lumped parameter models are usually considered [3]. In the soft finger model it is assumed that also a torque, aligned with the normal to the surfaces in contact, arises. The model equations for these models are:

$$\begin{cases} f = p \\ m = q + c \times p \end{cases} \qquad (1)$$

Where **p** and **q** are the contact force and torque (for soft finger models only), **c** is the contact location, and **f** and **m** are the measured force and torque. Bicchi and Salisbury, [3], proposed procedures for computing **p** and **q** on the base of the measurements **f** and **m**. However a precise geometric model of the pressure (the robot finger) is required, and, except the case of simple geometries, the method is computationally intensive and critical for real-time implementation.

A direct solution to the contact problem would be obviously possible if the contact location c would be directly measured. Therefore the availability of a direct force measurement and of the contact location allows directly solving the point contact problem.

At system level the goal is to develop to an integrated tactile/force sensors with embedded electronics to be placed on the phalanges of three fingers. The relevant problems considered have been: choice of appropriate force transducers, pressure transducers for contact measurements, integrated electronic design.

The tactile transducer is a matrix of 64 electrodes covered by a layer of pressure sensitive conductive rubber (PCR Co. Ltd.). The electrodes are etched on a flexible PCB substrate in order to conform to a cylindrical surface. A thin elastic sheet covers the whole sensor and provides a mild preload useful to reduce noise. Pressure due to contacts produces changes of resistance among the electrodes. The geometry of the electrodes Fig. 2, has been defined with the goal of limiting the spurious currents that may occur across the various electrodes, and interfere with measurement, as discussed in [3].

Tactile data are sampled by the on-board MCU, with 10 bit resolution. Preliminary tests show an actual sensor resolution of 8 bit/taxel. Each tactile image consists of 64 taxels.

During contact, a number of adjacent taxels are subject to pressure. The analog output of the tactile sensor allows to measure the distribution of pressure over all the transducer. Therefore, we propose to compute the contact centroid [3], as

$$\hat{C} = \frac{\sum_{i=1}^{N}\sum_{j=1}^{N} x_{ij} . p(x_{ij})}{\sum_{i=1}^{N}\sum_{j=1}^{N} p(x_{ij})} \tag{2}$$

where $\hat{C}$ is the computed contact centroid, $\mathbf{x}_{ij}$ is the coordinate of the taxel and $p(\mathbf{x}_{ij})$ the weight of this. As a matter of fact further geometric information about the distribution of the pressure during contact could be useful, although not directly relevant to point contact model solution. To this aim the pressure distribution is approximated as an ellipsoid, as follows:

$$E = \frac{\sum_{i=1}^{N}\sum_{j=1}^{N} (x_{ij} - \hat{C})(x_{ij} - \hat{C})^{T} . p(x_{ij})}{\sum_{i=1}^{N}\sum_{j=1}^{N} p(x_{ij})} \tag{3}$$

Where **E** is a symmetric matrix who represent the ellipsoid. The approach used to compute and the associated approximate ellipsoid, is strongly based on the availability of an analog tactile sensor.

3. EXPERIMENT

Catching is one of the most important tasks for dynamic manipulation. In this section catching is shown using our flexible hand with a visual feedback controller. We used a rubber ball with radius of 5cm as a target, and we dropped it from about 1.2m in height. The speed of the falling ball is about 5.9m/s just before it hits the ground.

Table. 1. The specification of robot hand.

Total D.O.F	14
Weight [g]	700
Max. Speed at a finger tip [m/s]	3.5
Max. force at a finger tip [N]	30
Joint resolution [deg]	0.4

From various experimental trials, we have decided on the catching strategy shown in Fig. 1.

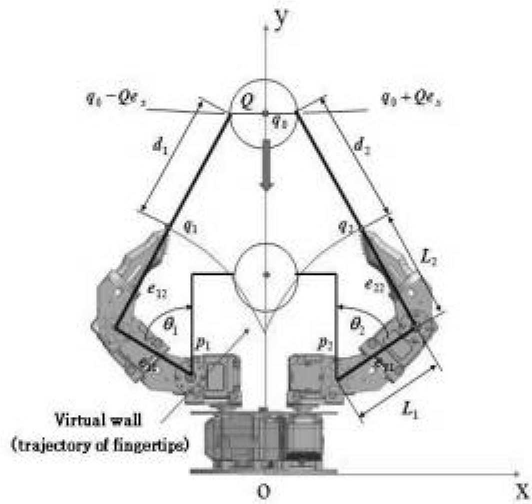

Fig. 1. The coordinates system for catching algorithm of grasping.

4. CONCLUSION

An integrated force and tactile sensor with embedded electronics has been presented in a lightweight flexible hand with 14 D.O.F, and the associated visual feedback control. The sensor consists of a three components commercial force sensor and of a custom matrix tactile sensor based pressure sensitive conductive rubber.

The need for a robotic hand that works in the real world is growing. And such a system should be able to adapt to changes in environment. We think that the concept of a flexible hand system with real-time control implementation will become an important issue in robotic research.

REFERENCES

[1] S.C.Jacobsen, E.K. Iversen, D.F. Knutti, R.T. Johnson andK.B. Biggers, “Design of the Utah/MIT dexterous hand”, Proc. IEEE Int. Conf. On Robotics andAutomation, pp. 1520-1532, 1986

[2] Anotonio Bicchi, J. Kennedy Salisbury, David L. Brock ”Contact Sensing from Force Measurements” International Journal of Robotics Research. Vol. 12, No. 3, June 1993.

[3] S. Toyama, S. Hatae and S. Sugitani, “Multi-Degree of spherical ultrasonic motor”, Proc. ASME Japan/USASympo. Flexible Automation, 169, 1992

2017 Changwon International Conference on Intelligent Robot and Convergence Industry (CICIRO 2017)
Nov. 30th~ Dec. 1st, 2017, Changwon Exhibition Convention Center(CECO), Changwon City, Korea

A Study on Robust Voice Control of Biped Robot for Cooperate working

Seong-Ju Choi[1], Jong-Dae Won[2], Woo-Song Lee [3], and Sung-Hyun Han[4]
[1] PST CAMTOSS, Changwon, Korea (pstcsj@hanmail.net)
[2]Youngchang Tools Co.,Ltd., Changwon, 641-847 Korea
(wonjd27@young-chang.com)
[3] SUNJIN Technology Co., Ltd., Changwon, 82331, Korea (elflws@nate.com)
[4] School of Mechanical Engineering, Kyungnam University,
Changwon, 631-701, Korea (shhan@kyungnam.ac.kr)

Abstract: Generally, it is possible to control the motion by using information on the robot's own postures, because a type of motion and gesture produces almost the same pattern of noise every time. In this paper, we describe an voice recognition control system for robot system which can robustly recognize voice by adults and children in noisy environments. We evaluate the performance of robot control system in a communication robot placed in a real noisy environment. Voice is captured using a wireless microphone. To suppress interference and noise and to attenuate reverberation, we implemented a multi-channel system consisting of an outlier-robust generalized side-lobe canceller technique and a feature-space noise suppression using criteria. Voice activity periods are detected based end-point detection

Key words: Robust voice recognition, Side-lobe canceller, navigation system

1. INTRODUCTION

To make human-robot communication natural, it is necessary for the robot to recognize voice even while it is moving and performing gestures. For example, a robot's gesture is considered to play a crucial role in natural human-robot communication [1-4]. In addition, robots are expected to perform tasks by physical actions to make a presentation. If the robot can recognize human interruption voice while it is executing physical actions or making a presentation with gestures, it would make the robot more useful.

Each kind of robot motion or gesture produces almost the same noises every time it is performed. By recording the motion and gesture noises in advance, the noises are easily estimated. By using this, we introduce a new method for VRCS under robot motor noise. Our method is based on three techniques, namely, multi-condition training, maximum-likelihood linear regression[5], and missing feature theory. These methods can utilize pre-recorded noises as described later. Since each of these techniques has advantages and disadvantages, whether it is effective depends on the types of motion and gesture. Thus, just combining these three techniques would not be effective for voice recognition under noises of all types of motion and gestures. The result of an experiment of isolated word recognition under a variety of motion and gesture noises suggested the effectiveness of this approach. In what follows, Section 2 discusses the design of voice recognition system, and Section 3 explains our method for avoid the obstacles by navigation strategy. Section 4 describes the recognition, navigation experiments, and the results, before conclusion and mentioning future work in Section 5.

2. CONTROLSCHEME

Accounting for the two problems (caused by noisy environments and differences on speaker age) described in Section I, we developed an RVR system to be robust on background noise and speakers of different ages. The first block is a front-end processing. It contains a microphone wireless transmitter. The real-time wireless microphone system for suppressing interference and noise and for attenuating reverberation consists of an outlier-robust generalized side-lobe canceller and feature-space noise suppression. In the second block, there are two decoders depending on the age of the speaker (adult or child); each decoder works using gender-dependent acoustic models. Noise-suppressed voice at the first block is recognized using these two decoders, and one hypothesis is selected based on posterior probability.

The proposed robot system has three wheels; two driven wheels fixed at both sides of the mobile robot and one castor attached at the front and rear side of the robot. The ultrasonic sensors are mounted around of the mobile robot in middle layer for the detection of obstacles with various heights. In this study, a sonar array composed of 16 ultrasonic sensors cannot be fired simultaneously due to cross talk. Instead, we adopt a scheduled firing method where sensors are activated in sequence of $\{s_1, s_{12}, s_2, s_{11} \ldots\}$. The arrangement of the ultrasonic sensors in upper layer and the sensors are marked as dots in the figure. The distances e_j $(j = 1, 2,\ldots 12)$ from the origin of the robot frame {R} to obstacles detected by the sensor s_j, can be defined as $e_j=$ ♎$_j$ + R_r . Here, R_r is the radius of the robot and the ♎$_j$, is the range value measured by the sensor s_j .

A local map is introduced to record the sensory information provided by the 16 sonar sensors with respect to the mobile robot frame $\{R\}$. Sector map defined locally at the current mobile robot frame is introduced. Then, the obstacle position vector se'_j with respect to the frame $\{R\}'$ can be calculated by

$$Se_j = \begin{bmatrix} \cos\delta\theta & \sin\delta\theta & 0 & -\sin\delta\theta/\rho_p \\ -\sin\delta\theta & \cos\delta\theta & 0 & (1-\cos\delta\theta)/\rho_p \\ 0 & 0 & 1 & 0 \\ 0 & 0 & 0 & 1 \end{bmatrix} \quad (1)$$

where se_j denotes the obstacle position vector defined at the frame $\{R\}$. When the mobile robot is located at a point $0'$. the distance value $se'_j = \| se'_j \|$ from the origin of the frame $\{R\}'$ to the obstacle and angle $s\varphi'$ can be calculated by Eq.(1) . Here, ‖.‖ denotes Euclidean norm.

The local map defined at the frame $\{R\}'$ is newly constructed by using the previous local map defined at the frame $(R\}$ as follows:

$$Se_n \leftarrow Se_{j,n} = INT\left(\frac{s\varphi'_j}{\varphi}\frac{N}{2}\right);\ j = 1,2,...,\ N \quad (2)$$

Where $\leftarrow$ and INT denote the updating operation and integer operation, respectively. Here, se_n, denotes the distance value of n sector and N represents the number of the sector. If the range values obtained by sensors when the mobile robot is located at a point o' are e_j = (j = 1,2 ,... 12) , the new local map is partially updated as follows :

$se_j \leftarrow e_j$, j = 1,2 .... 12. The maximum range of the sonar sensor is set to be $\Omega_{max} = \Omega_{max} - R_r$. Any return range which is larger than is ignored.

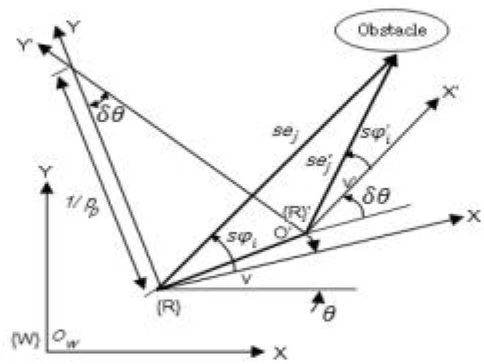

Fig. 1 The coordinate transformation for updating the local map

The primitive behaviors may be divided as follows: goal-seeking behavior, ball-following behavior, keep-away behavior, free space explorer and emergency stop, etc. The output of a primitive behavior is defined by the vector.

$$u(t) = (v(t),\omega(t))^T = (v(t),w(t),T_{ms})^T \quad (3)$$

where t and T_{ms} denote the time step and the sampling time, respectively. Here, T denotes the transpose and $\omega(t)$ denotes the angular velocity of the robot.

We will divide the primitive behaviors into two basic: avoidance behavior and goal-seeking behavior.

The avoidance behavior is used to avoid the obstacles irrespective of the goal position, while the goal-seeking behavior is used to seek the goal position irrespective of obstacle location. Design of each behavior proceeds in following sequences;

(A) fuzzification of the input/output variables, (B) rule base construction through reinforcement learning, (C) reasoning process, (D) defuzzification of output variables.

In order for the mobile robot to arrive at the goal position without colliding with obstacles, we must control the mobile robot motion in consideration of the obstacle position X_{oi}, = (x_{oi}, y_{oi}) , the mobile robot position $X = (x\ ,\ y\ )$ and its heading angle θ with respect to the world coordinate frame $\{W\}$ shown in Fig. 1.

In order to avoid the increase in the dimension of input space, the distance values d_i , (i = 1.2,3,4) are defined by

$$d_1 = \min(se_1,se_2,se_3)$$

$$d_2 = \min(se_4,se_5,se_6) \quad 4a$$

$$d_3 = \min(se_7,se_8,se_9) \quad 4b$$

$$d_4 = \min(se_{10},se_{11},se_{12})$$

$\varphi_m(-\pi \le \varphi_m \le \pi)$ denotes the orientation of a sector with the shortest range. We choose the input variables for avoidance behavior as φ_m and $d_i = \|X_{0i} - X\|, (i = 1,2,3,4)$ for goal-seeking behavior as heading angle difference ψ and distance to goal $z = \|X_g - X\|$. The input linguistic variables d_i, ψ, φ_m and z are expressed by linguistic values (VN, NR, FR), (NB, NM, ZZ, PS, PM, PB), (LT, CT, RT) and (VN, NR, FR, VF), respectively Their membership functions are expressed .

3. EXPERIMENTS

All the parameters used in the navigation experiments are given in Table 1. The proposed robot has the maximum travel speed of 0.52 m/s and the maximum steering rate of 2.0rad/sec. Experiments are performed in an indoor with the first experiment for voice recognition without objects and second experiment for both of them: voice recognition and obstacles avoidance.

Through a series of the navigation experiments, it was observed that the heading angle error is a serious problem to the proposed robot depend on dead reckoning The large heading angle error almost resulted from the uncertain parameters when the mobile robot changes its direction Even if the wheel slippage occurs, the true position and heading angle of the mobile robot could be updated by two beacon pairs and consequently the mobile robot could arrive at the given goal position while avoiding the obstacles.

4. CONCLUSIONS

We have proposed the integration of robust voice recognition and navigation system capable of performing autonomous navigation in unknown environments. In order to evaluate the performance of the overall system, a number of experiments have been undertaken in various environments. The experimental results show that the mobile robot with the complete voice recognition and navigation system can arrive at the goal position according to the desire of speaker even if the wheel slip occurs. From the developed of voice recognition and navigation system, it was observed that the mobile robot can successfully arrive at the desired position through the unknown environments without colliding with obstacles.

REFERENCES

[1] S. Yamamoto, K. Nakadai, H. Tsujino, and H. Okuno, “Assessment of general applicability of robot audition system by recognizing three simultaneous speeches.” in Proc. of IEEE/RSJ International Conference on Intelligent Robots and Systems (IROS-2004). IEEE and RSJ, 2001, p. to appear.

[2] P. Renevey, R. Vetter, and J. Kraus, “Robust speech recognition using missing feature theory and vector quantization,” in Proc. Of Eurospeech-2001. ESCA, 2001, pp. 1107–1110.

[3] J. Barker, M. Cooke, and P. Green, “Robust asr based on clean speech models: An evaluation of missing data techniques for connected digit recognition in noise,” in Proc. of Eurospeech-2001. ESCA, 2001, pp. 213–216.

[4] R. P. Lippmann, E. A. Martin, and D. B. Paul, “Multi-style training for robust isolated-word speech recognition,” in Proc. of ICASSP-87. IEEE, 1987, pp. 705–708.

[5] M. Blanchet, J. Boudy, and P. Lockwood, “Environment adaptation for speech recognition in noise,” in Proc. of EUSIPCO-92, vol. VI,1992, pp. 391–394.

2017 Changwon International Conference on Intelligent Robot and Convergence Industry (CICIRO 2017)
Nov. 30th~ Dec. 1st, 2017, Changwon Exhibition Convention Center(CECO), Changwon City, Korea

A Study on Stable Walking Control of Mobile Robot with Dual Arm

Hyung-Tae Lee[1], Yang-Keun Jeong[2],
Woo-Song Lee[3], In-Man Park[4], and Sung-Hyun Han[5]

[1] DONGYANG VOCATIONAL INSTITUE, Changwon, Korea (sucutzzang@daum.net)
[2] Shinla Information Technology Co., Ltd., Changwon, 641-465, Korea
(shintech@hanmail.net)
[3] SUNJIN Technology Co., Ltd., Changwon, 82331, Korea
(elflws@nate.com)
[4] Intem Co., Ltd., Changwon, 642-370, Korea
(intem237@hanmail.net)
[5] School of Mechanical Engineering, Kyungnam University, Changwon, 631-701, Korea
(shhan@kyungnam.ac.kr)

Abstract: We present a new technology for real-time walking of a biped robot. A biped robot necessitates achieving stabilization for real time walking since it has basic problems such as structural stability. In this paper, a robust control algorithm for stable walking is proposed based the ground reaction forces, which are measured using force sensors during walking, and the environmental conditions are estimated from these situation. From this information the robot selects the proper motion and overcomes ground irregularities effectively. In order to generate the proper angel of the joint. The performance of the proposed algorithm is verified by simulation and experiments for a 20-DOFs humanoid robot.

Keywords: Stable Walking, Control Algorithm, Biped Robot, Robust Walking

1. INTRODUCTION

This paper proposes an obstacle avoidance architecture allowing walking humanoid robots to walk safely around in factory and home environment.

For a wheeled robot, many solutions on this subject have been presented in the literature using ultrasonic sensors or laser range finders and they mainly detect walls and relatively large obstacles around the robot. But solving the problem of obstacle avoidance for a humanoid robot in an unstructured environment is a big challenge, because the robot can easily lose its stability or fall down if it hits or steps on an obstacle.

Our strategy focuses on floor estimation, because in our view information about the floor is most important for a humanoid robot while walking. For this purpose, we developed a stereo-vision system and detect the floor plane using a randomized version of the hough transform. The aim of this proposition is to establish a new industry involving autonomous robots and artificial intelligence.

A main technological target of the proposed robot (Model:V-HUR) is to autonomously explore and wander around in home environments as well as to communicate with humans.

2. SYSTEM MODELING

The V-HUR consists of 2 microphones for speech recognition and sound localization utilizing as well as speech synthesis play a big role in the communication capabilities of Robot. Audio and visual recognition results are memorized in a system that reflects the current environment. The stereo-vision system consists of 2 cameras as the robot's eyes and a module for stereo processing in the robot's head. Using its stereo camera V-HUR can compute distance to objects, extract a floor plane and generate a path for walking around obstacles.

V-HUR is able to communicate with network computers by utilizing its wireless lan.

The V-HUR consists of 40 joints of the intelligent servo actuators. In real time, it enables V-HUR to walk adaptively on inclined and irregular terrain and allows the robot to re-stabilize immediately even when external forces affect its balance. Furthermore, a sub-system for real time step pattern generation realizes various walking patterns ranging from active and stable biped walking to moving flexibility.

Base on the height of V-HUR, the Robot's structure and the main applications for the stereo system, the distant between 2 color CCD cameras is 4cm. This distant allows for reliable floor estimation up to a range of 3m and reliable distance estimation of other objects in the range of 20cm to 4m.

The system consists of an 8-bit micro processor with two 16Mbyte SDRAM units and a flash ROM. The stereo-vision module computes disparity between 2 CCD cameras by using block matching receives a pair of images from them. The main board of the CPU receives the resulting disparity image as a digital video signal. The stereo control parameters can be set between the main CPU and the 8bit CPU on board through a special serial communication link (see fig. 1).

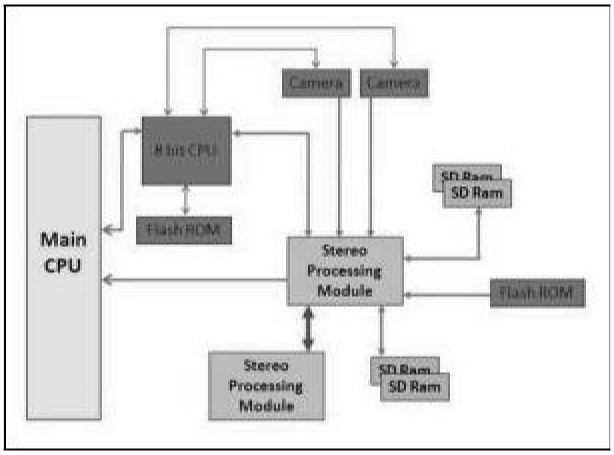

Fig. 1. System's hardware

The system's software briefly describes each module below (see Fig. 1).

The important point of this module is that to deliver disparity images with the corresponding kinematic transformations to the *3D Range Transfer* module. This module receives image data from the stereo-vision system and joint angle sensor data from each actuator.

This module aims at to convert all the 3D measurements to the floor coordinate system. The disparity image obtained from stereo-vision is first converted into 3D range data using parameters from stereo calibration. Then a transformed data is applied for finding planes in the 3D data.

It integrates information into a 2D grid configuration of size 3.5x3.5m around the robot. Image source: receiving either from the *3D Range Transfer* or odometer information from the Receiver module.

Control mechanism where the behavior of the robot is determined autonomously according to internal states and external observations. A part of *Operation Planning Controller* is a *planning pioneer* that, given a goal point, computes a collision-free path leading to the destination. The *planning pioneer* system then generates walk and head motion commands which are sent to the *Source Distribution* which in turn send them to the *Motion preparing* and the *Actuator.*

The vision system (mentioned above) receives image from the two CCD cameras. These parameters are useful for computing 3D range data. The disparity is calculated for each pixel in the left image by searching for the corresponding pixel in the right image. An additional reliability image is calculated following criteria to reject results on above conditions. After block matching has been carried out, the matching score is calculated by interpolating scores near the highest peak. The sharpness of this peak corresponds to the available texture around this pixel and thus can be used as a reliability value for the disparity calculation. If there are other peaks with similar matching scores then the disparity computation is ambiguous and the reliability is set to a low value. (The matching score is compared with neighboring scores).

3. EXPERIMENT

Firstly, the disparity is converted into 3D range data using the parameters from camera calibration and then a Hough transformation is applied to all data points. Apply the *randomized Hough transformation* selects sets of data points from which the surface parameters can be directly computed and records the result in a table. If many data sets yield the same parameters, a high score for these parameters is obtained.

The details of this method are showed in the flow chart in the Fig. 2 below.

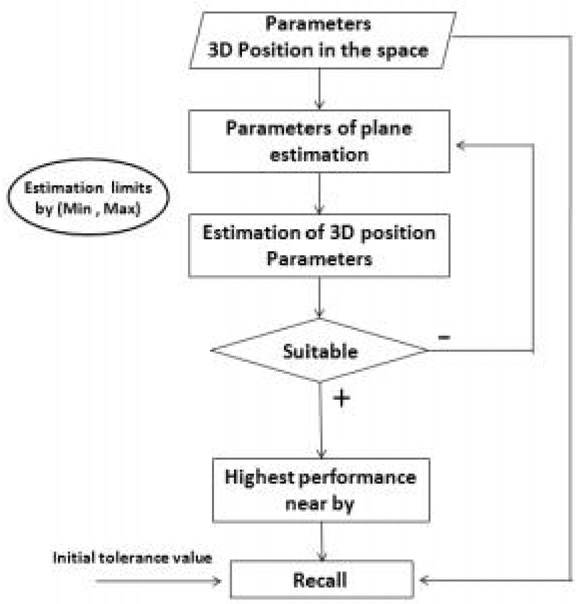

Fig 2. Flow chart of plane extraction

Although applying floor detection methods, obstacles and regions the robot can walk on can be found. However, in general it is difficult to decide from a single observation with a limited field of view, the action the robot should carry out next. We follow this notion and introduce a terrain map where all observations and motions are integrated.

The terrain map is a 2-dimensional occupancy grid centered on the current position of the robot (egocentric coordinate system). We maintain the (global) robot orientation and a small relative (x y) location of the robot within the cell at the center of the grid. Initially, all cells are set to a probability of 1.0 and time 0. Each grid cell contains the probability that an obstacle covers the cell and the time the cell was last updated.

The robot motion is defined as a coordinate transformation from one foot to the other whenever the robot performs a step. From this transformation a displacement and a change in orientation can be derived and applied to the position and orientation of the robot in the grid.

In our implementation shifting the grid is actually performed by changing an offset into the grid data array so that no data has to be moved physically. After shifting the coordinate system of the occupancy grid, new cells at the border are initialized.

Define: the cell size Sc, the robot position (Rx, Ry) inside the grid, and the moving displacement (Mx, My), we obtain:

$$(Ax,\ Ay) = \left(\left\lfloor \frac{Rx + Mx}{Sc} \right\rfloor, \left\lfloor \frac{Ry + My}{Sc} \right\rfloor \right) \quad (1)$$

The new robot position inside the grid becomes as follows:

$$(Mx - Sc \cdot Ax, My - Sc \cdot Ay) \rightarrow (Rx, Ry) \ . \quad (2)$$

The change in orientation _a is simply added to the global orientation of the robot .

In an additional, searching for shortcuts along the found path, a smooth walking trajectory is realized.

The robot can find a path to a destination point by using the occupancy grid reflects the terrain around. The definition of each cell of the occupancy grid is a node connecting to neighboring cells and defines the path planning problem as a search problem on this graph.

4. CONCLUSION.

The autonomous mobility for the biped robot V-HUR in the home environment is realized base on the development of a small stereo vision system, the recognition of floor and obstacles using plane extraction.

The terrain is represented in a robot centric coordinate system without making any structural assumptions about the surrounding world. And the representation of a terrain map based on these observations, robot motion, and the generation of a walking path on the terrain map. We therefore believe, our approach is well suited for many different a home environment where no a priori information about the environment is given. The limitation of our system is that the terrain has to contain enough texture in order to obtain reliable stereo data.

ACKNOWLEDGEMENT

This work was supported (National Robotics Research Center for Robot Intelligence Technology, Kyungnam University) by Ministry of Knowledge Economy under Human Resources Development Program for Convergence Robot Specialists.

REFERENCES

[1] D. Pagac, E. Nebot and H. Durrant-Whyte, “An evidential approach to map-building for autonomous vehicles,” *IEEE Transactions on Robotics and Automation*, 14(4), 623-629, 1998.

[2] Ole Wijk, ”Triangulation Based Fusion of Sonar Data with Application in Mobile Robot Mapping and Localization,” *PhD thesis*, Royal Institute of Technology, Stockholm, Sweden, 2001.

[3] Y. Kuroki, T. Ishida, J. Yamaguchi, M. Fujita and T.T. Doi, “A Small Biped Entertainment Robot,” in *Proc. Int. Conf. on Humanoid Robots*, pp.181-186, 2001.

[4] M. Fujita and K. Kageyama, “An Open Architecture for Robot Entertainment,” in *Proc. Inernational Conference on Autonomous Agents*, pp. 435-440, 1997.

[5] M. Fujita and H. Kitano, “Development of an Quadruped Robot for Robot Entertainment,” *Autonomous Robots*, vol. 5, pp.7-8, Kluwer Academic, 1998.

[6] T. Ishida, Y. Kuroki, J. Yamaguchi, M. Fujita and T.T. Doi, “Motion Entertainment by a Small Humanoid Robot Based on OPEN-R,” in *Int. Conf. on Intelligent Robots and Systems (IROS-01),* pp.1079-1086, 2001.

2017 Changwon International Conference on Intelligent Robot and Convergence Industry (CICIRO 2017)
Nov. 30th~ Dec. 1st, 2017, Changwon Exhibition Convention Center(CECO), Changwon City, Korea

A Study on Visual Feedback Control of Articulated Robot Arm with Seven Joints

Ki-Hyun Kim[1], Hyun-Suk Sim[2] and Sung-Hyun Han[3]

[1] Doosan Heavy Industries & Construction Co., Ltd., Changwon, 51711, Korea
(E-mail: kihyeon.kim@doosan.com)
[2] DongSan Tech Co., Ltd., Haman, 637-821, Korea
(hs8388@dscast.co.kr)
[3] School of Mechanical Engineering, Kyungnam University,
Changwon, 51767, Korea (shhan@kyungnam.ac.kr)

Abstract: This paper presents how it is effective to use many features for improving the accuracy of the visual servoing control for SCARA robot. Some rank conditions, which relate the image Jacobian, and the control performance are derived. It is also proven that the accuracy is improved by increasing the number of features. Effectiveness of the redundant features is verified by the real time experiments on a Dual-Arm Robot manipulator system.

Keywords: Visual Feedback Control, Redundant Feature, Feature-Based Visual Tracking, Real-Time Control

1. INTRODUCTION

There are mainly two ways to put the visual feedback into practice. One is called look-and-move and the other is visual feedback. Visual feedback is the fusion of results from many elemental areas including high-speed image processing, kinematics, dynamics, control theory, and real-time computing.

This paper presents a method to solve this problem by using a binocular stereo vision. The use of stereo vision can lead to an exact image Jacobian not only at around a desired location but also at the other locations. The suggested technique places a robot manipulator to the desired location without giving such prior knowledge as the relative distance to the desired location or the model of an object even if the initial positioning error is large. This paper deals with modeling of stereo vision and how to generate feedback commands. The performance of the proposed visual feedback system was evaluated by the simulations and experiments and obtained results were compared with the conventional case for a SCARA type dual-armrobot.

2. VISUALFEEDBACK CONTROL

The origin of the world frame is located at a certain point in the world.

Now let ${}^l p = ({}^l x, {}^l y)$ and ${}^r p = ({}^r x, {}^r y)$ be the projections onto the left and right images of a point p in the environment, which is expressed as ${}^c p = ({}^c x\ {}^c y\ {}^c z)$ in the camera frame. Then the following equation is obtained (see Fig. 1).

$$ {}^l x\,{}^c z = f({}^c x + 0.5d) \quad (1\text{-a})$$

$$ {}^r x\,{}^c z = f({}^c x - 0.5d) \quad (1\text{-b})$$

$$ {}^l y\,{}^c z = f\,{}^c y \quad (1\text{-c})$$

$$ {}^r y\,{}^c z = f\,{}^c y \quad (1\text{-d})$$

Suppose that the stereo correspondence of feature points between the left and right images is found. In the visual feedback, we need to know the precise relation between the moving velocity of camera and the velocity of feature points in the image, because we generate a feedback command of the manipulator based on the velocity of feature points in the image.

This relation can be expressed in a matrix form which is called the image Jacobian. Let us consider n feature points $p_k (k = 1, \cdots, n)$ on the object and the coordinates in the left and right images are ${}^l p_k({}^l x_k, {}^l y_k)$ and ${}^r p_k({}^r x_k, {}^r y_k)$, respectively. Also define the current location of the feature points in the image ${}^I p$ as

$$ {}^I p = ({}^l x_1\ {}^r x_1\ {}^l y_1\ {}^r y_1 \cdots {}^l x_n\ {}^r x_n\ {}^l y_n\ {}^r y_n)^T \quad (2)$$

where each element is expressed with respect to the virtual image frame Σ_p.

First, to make it simple, let us consider a case when the number of the feature points is one. The relation between the velocity of feature point in image ${}^I \dot{p}$ and the velocity of camera frame ${}^c \dot{p}$ is given as

$$ {}^I \dot{p} = {}^I J_c\, {}^c \dot{p} \quad (3)$$

where ${}^I J_c$ is the Jacobian matrix which relates the two frames. Now let the translational velocity components of camera be v_x, v_y and v_z and the rotational velocity components be w_x, w_y, w_z then we can express the camera velocity V as

$$ V = [v_x\ v_y\ v_z\ w_x\ w_y\ w_z]^T = [{}^c v\ {}^c w_c]^T \quad (4)$$

Then the velocity of the feature point seen from the camera frame ${}^c\dot{p}$ can be written

$$
\begin{aligned}
{}^c\dot{p} &= \frac{d\,{}^cp}{dt} \\
&= \frac{d}{dt}\,{}^cR_w({}^wp - {}^wp_c) \\
&= {}^cR_w\{-{}^w\omega_c \times ({}^wp - {}^wp_c)\} + {}^cR_w({}^w\dot{p} - {}^w\dot{p}_c)
\end{aligned} \tag{5}
$$

where ${}^cR_w$ is the rotation matrix from the camera frame to the world frame and ${}^wp_c$ is the location of the origin of the camera frame written in the world frame. As the object is assumed to be fixed into the world frame, ${}^w\dot{p} = 0$. The relation between ${}^c\dot{p}$ and V is

$$
\begin{aligned}
{}^c\dot{p} &= {}^cR_w\{-{}^w\omega_c \times ({}^wp - {}^wp_c)\} - {}^cR_w\,{}^w\dot{p}_c \\
&= -{}^c\omega_c \times {}^cp - {}^c\dot{p}_c \\
&= \begin{bmatrix} -\omega_y\,{}^cz + \omega_z\,{}^cy - v_x \\ -\omega_z\,{}^cx + \omega_x\,{}^cz - v_y \\ -\omega_x\,{}^cy + \omega_y\,{}^cx - v_z \end{bmatrix}
\end{aligned} \tag{6}
$$

Therefore, substituting Eq. (6) into Eq. (3), we have the following equation.

$$
\begin{aligned}
{}^I\dot{p} &= {}^IJ_c\,{}^c\dot{p} \\
&= JV
\end{aligned} \tag{7}
$$

In Eq. (7) matrix J which expresses the relation between velocity ${}^I\dot{p}$ of the feature point in the image and moving velocity V of the camera is called the image jacobian.

From the model of the stereo vision Eq. (1), the following equation can be obtained.

$$2\,{}^cx({}^lx - {}^rx) = d({}^lx + {}^rx) \tag{8}$$

$${}^cy({}^lx - {}^rx) = {}^ly\,d = {}^ry\,d \tag{9}$$

$${}^cz({}^lx - {}^rx) = f\,d \tag{10}$$

Above discussion is based on the case of one feature point. In practical situation, however, the visual feedback is realized by using plural feature points. When we use n feature points, image Jacobian $J_1, \cdots, J_n$ are given from the coordinates of feature points in the image. By combining them, we express the image Jacobian (J_{im}) as

$$J_{im} = [J_1 \cdots J_n]^T \tag{11}$$

Then, it is possible to express the relation of the moving velocity of the camera and the velocity of the feature points even in the case of plural feature points, that is,

$${}^I\dot{p} = J_{im}V \tag{12}$$

where we suppose that the stereo and temporal correspondence of the feature points are found.

In the case of the monocular, the image Jacobian J has the following form.

$$
J = f\begin{bmatrix} -\frac{1}{{}^cz} & 0 & \frac{{}^cx}{{}^cz^2} & \frac{{}^cx\,{}^cy}{{}^cz^2} & -\left(1 + \frac{{}^cx^2}{{}^cz^2}\right) & \frac{{}^cy}{{}^cz} \\ 0 & -\frac{1}{{}^cz} & \frac{{}^cy}{{}^cz^2} & 1 + \frac{{}^cy^2}{{}^cz^2} & -\frac{{}^cx\,{}^cy}{{}^cz^2} & -\frac{{}^cx}{{}^cz} \end{bmatrix} \tag{13}
$$

The x, y and z axes of the coordinate frames are shown in Fig. 1.

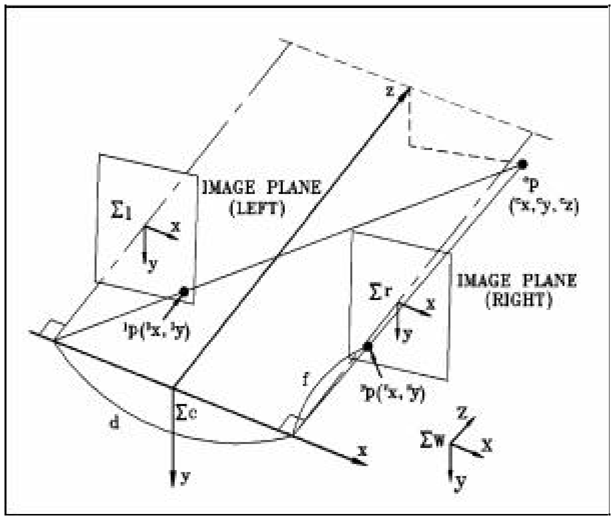

Fig. 1 The coordinates system of vision model.

3. EXPERIMENTS

We have compared the visual feedback using the monocular vision with that using the stereo vision by the experiment.

The error between the desired location and the current location of the feature points in cases of the monocular and stereo visions are shown in Fig. 2.

Next, we will show the results for the change of the way to choose the feature points and set the initial error image.

Two stereo images were taken and transformed to the binary images in the real time and in parallel by two image input devices and the coordinate of the gravitational center of each feature point was calculated in parallel by two transporters. We gave the stereo correspondence of the feature point in the first sampling. However, the stereo and temporal correspondence of the feature points in the succeeding sampling was found automatically by searching a nearby area where there were the feature points in the previous sampling frame. The coordinates of the feature points were sent to a transporter for motion control and it calculated a feedback command for the robot. The result was sent to the robot controller by using RS-232C, and the robot was controlled by a velocity servo systemin the controller.

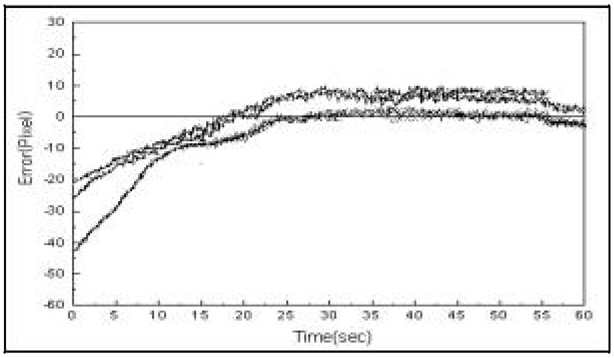

(a) Left image

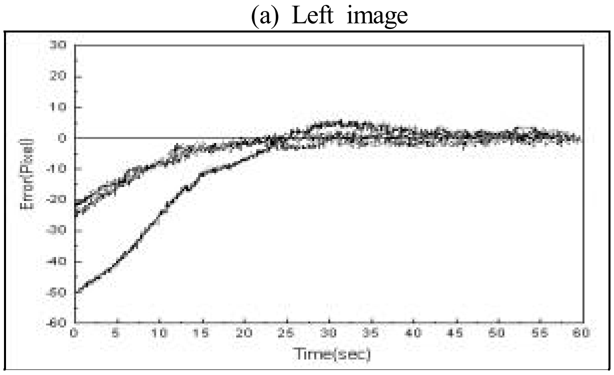

(b) Right image

Fig. 2. Position error in x and y axes.

The sampling period of visual feedback was about 50*m*sec . Details were 16*m*sec for taking a stereo image, about 1*m*sec for calculating the coordinates of the feature points, 3*m*sec for calculating feedback command, about 16*m*sec for communicating with the robot controller. If we send a feedback input to the robot controller without using RS-232C, the faster visual feedback can be realized.

The desired location was (0,0,550) *mm* and the desired orientation in Euler angle, (✗,❑,◩) ■ (0,0,0) degree and the initial error was (55,55,55) *mm* for translation. The other parameters were the same as in the simulation. The error of current and desired location of the feature points are shown in Fig. 5. From these experimental results, we can see that the manipulator converges toward a desired location even if the calibration is not precise.

4. CONCLUSION

We have proposed a new technical of visual feedback with the stereo vision to control the position and orientation of an assembling robot with respect to an object. The method overcomes the several problems associated with the visual feedback with the monocular vision. By using the stereo vision, the image Jacobian can be calculated at any position. So neither shape information nor desired distance of the target object is required. Also the stability of visual feedback is illustrated even when the initial error is very large.

REFERENCES

[1] Chaumette, F., Rives, P., and Espiau, B., “Positioning of a robot with respoect to an object, tracking it and estimating its velocity by visual servoing,” In *Proceedings of the IEEE International Conference on Robotics and Automation*, pp. 2248-2253, 1991.

[2] Bernard, E., Francois, C., and Patrick, R., “A new approach to visual servoing in robotics,” *IEEE Transactions on Robotics and Automation*, pp. 313-326, 1992.

[3] Weiss, L. E., Sanderson, A. C., and Neuman, C. P., “Dynamic sensor-based control of robots with visual feedback,” *IEEE Journal of Robotics and Automation*, pp. 404-417, 1987.

[4] Hashimoto, K., Kimoto, T. Edbine, T., and Kimura, H., “Manipulator control with image-based visual servo,” In *Proceedings of IEEE International Conference on Robotics and Automation*, pp. 2267-2272, 1991.

[5] Hashimoto, K., Edbine, T., and Kimura, H., “Dynamic visual feedback control for a hand-eye manipulator,” In *Proceedings of the IEEE/RSJ International Conference on Intelligent Robots and Systems*, pp. 1863-1868, 1992.

[6] G. Hager, S. Hutchinson, and P. I. Corke. “A tutorial on visual servo control,” *IEEE Trans. Robotics & Automation*, Vol. 12, No. 5, pp. 651-670, 1996.